ARTMENT OF COMMERCE ● NATIONAL OCEANIC AND ATMOSPHERIC ADMINISTRATION

NATIONAL OCEAN SURVEY

NATIONAL DATA BUOY CENTER

EXPERIMENTAL AND ANALYTICAL STUDIES OF BUOY HULL MOTIONS IN WAVES

APRIL 1972

EXPERIMENTAL AND ANALYTICAL STUDIES OF BUOY HULL MOTIONS IN WAVES

by

Paul Kaplan, Alfred I. Raff

and

Theodore P. Sargent

of

Oceanics, Incorporated

Prepared for

NATIONAL DATA BUOY CENTER
Contract NAS8-26879

APRIL 1972

TABLE OF CONTENTS

NOMENCLATURE

$a_{11'\ldots 39}$ = coefficients of equations of buoy motion

a_w = wave amplitude, ft.

A'_{33} = local cross-section vertical added mass, slugs/ft.

$\overline{A}_H$ = radiated wave amplitude ratio for two-dimensional vertical oscillation

A_p = projected frontal underwater area of buoy hull, ft.^{2}

B^* = local cross-section waterline breadth, ft.

c = wave celerity ($c=g/\omega$), ft./sec.

C_D = current (longitudinal) drag coefficient

C_S = local cross-section area coefficient

d' = draft of disc or spar buoy, ft.

f_{dh} = three-dimensional heave damping factor

f_{dp} = three-dimensional pitch damping factor

f_I = three-dimensional added moment of inertia factor

g = acceleration of gravity, ft./sec.^{2}

$\overline{GB}$ = $\overline{KG}-\overline{KB}$, ft.

$\overline{h}$ = average draft of cross-section, ft.

H = local cross-section draft, ft.

H_z = moment damping coefficient of disc buoy (from Kim)

I_y = mass moment of inertia of buoy, slugs-ft.^{2}

I_z = added moment of inertia coefficient of disc buoy (from Kim)

J_1 = Bessel Function of order 1

J_3 = Bessel Function of order 3

k = wave number ($k = \omega^2/g = 2\pi/\lambda$), ft.$^{-1}$

k_1 = longitudinal (surge) added mass coefficient

k_3 = vertical (heave) added mass coefficient

k_e = encounter frequency wave number ($k_e = \omega_e^2/g$), ft.$^{-1}$

$\overline{KB}$ = vertical height of center of buoyancy of buoy, ft.

$\overline{KG}$ = vertical height of center of gravity of buoy, ft.

m = mass of buoy, slugs.

M_w = pitch wave moment, lb.-ft.

M_y = vertical added mass coefficient of disc buoy (from Kim)

N_y = vertical damping coefficient of disc buoy (from Kim)

N'_z = local cross-section vertical damping coefficient, lb.-sec. ft.$^{-2}$

P = catamaran separation distance between hull centerline and overall vessel centerline, ft.

P_i, Q_i = integral functions of spar buoy geometry, defined in text

R_a = average underwater radius of disc buoy, ft.

R_w = waterplane radius of disc buoy, ft.

S = cross-section area (underwater), ft.^{2}

S_o = waterplane area of spar buoy, ft.^{2}

t = time, sec.

T = cross-section draft, ft.

V_c = current speed at surface, ft./sec.

x = surge; longitudinal coordinate in buoy axes system, positive to bow, ft.

X_w = longitudinal wave force, lb.

z = heave; vertical coordinate in buoy axes system, positive downwards, ft.

z_G = vertical center of gravity, of spar buoy, ft.

Z_w = vertical wave force, lb.

γ = frequency parameter ($\gamma = 2 R_w/\lambda$)

ε_H = phase angle of radiated wave for two-dimensional vertical oscillation

ε_s = phase angle of radiated wave for two-dimensional horizontal oscillation

η = wave elevation, ft.

θ = pitch angle of buoy, positive bow upwards

λ = wavelength, ft.

ρ = mass density of water, slugs/ft.^{3}

Δ = displacement of buoy (Δ=gm), lb.

ω = wave frequency [$\omega = (2\pi g/\lambda)^{1/2}$], rad./sec.

ω_e = encounter frequency of buoy oscillation, rad./sec.

EXPERIMENTAL AND ANALYTICAL STUDIES OF BUOY HULL MOTIONS IN WAVES

INTRODUCTION

In the development of the National Data Buoy System it is necessary to evolve particular types of configurations of moored buoy systems that would provide suitable performance to enhance the measurement capabilities of each individual moored buoy element. These buoys and their associated payloads are planned for use over large ocean regions to provide a network of environmental reporting stations that will yield continuous data on the important properties of the ocean and atmosphere for use in weather forecasting and other technologies dependent on air-ocean interaction. The effective design and engineering development of such systems requires an ability to predict the buoy (and hence the transmitting antenna) oscillatory motions and structural acceleration loadings in various seaways; the determination of the tensions along the cable under various operating conditions; etc. Knowledge of such results will greatly enhance the design of handling equipment for both launching and retrieving of buoys at sea, and will also provide basic information on system survivability under extreme environmental conditions.

In order to carry out the prediction of the motion characteristics of a moored buoy system, a computer simulation technique based upon a mathematical model will be used. This procedure, which is generally based upon the results given in [1], makes use of buoy hull forces, motions, etc. in conjunction with those of the mooring. The computer simulation of the

complete system response is being treated in [2] and [3], where information on the buoy hull hydrodynamics is an integral component. The mathematical model used for this complete system analysis involves theoretical representation of various hydrodynamic and hydrostatic forces acting on the buoy hulls, and hence it is then important to have a measure of validity of these representations for use in the computer simulation studies of the complete buoy-mooring system. The present study is intended to carry out experimental model tests of the motion of various buoy hulls in waves, together with an attendant theoretical analysis that developes the various hydrodynamic forces acting on the buoy hull and also establishes the equations of motion of the hull per se in various wave systems. A comparison of the experimental data with theoretical predictions will indicate the capability of the theory to predict the various aspects of forces, moments, equation coefficients, etc. that enter into the analysis used to predict complete system performance.

The main assumption in the work described in [1]-[3] is that of linearity, when considering the dynamic problem of response to waves. In that case it is then necessary to determine if buoy motions per se are linear with respect to wave amplitude, and also whether the concept of linear superposition can be applied to determine the response of the various buoy hulls in irregular waves. This capability would then allow generalization (of all system responses in the computer simulation work) by means of application of spectral analysis techniques for determining statistical measures of the

different system response characteristics of interest for the moored system. Thus it is necessary to determine the response characteristics of buoy hulls alone in both regular and irregular waves in order to evaluate whether they provide such a performance as well as to determine the capability of theoretical representations of the resulting forces, motions, etc. of the hulls for use in the complete system response analysis.

The present report describes the various buoy hull forms considered; the model test program carried out; the theoretical analysis of buoy motions; and comparisons between theory and experiment. A description and detailing of these various items is provided in the report, together with the assumptions underlying the work as well as the conclusions obtained from the investigations. This work was carried out for Sperry Systems Management Division (SSMD), in its role as Systems Engineering Contractor for the National Data Buoy Project Office, under Sperry (SSMD) Purchase Order No. 138666A.

MODEL DESCRIPTION

Four buoy models were designed and built for the test program. Each is representative of a different generic buoy shape, as follows: disc, boat, catamaran and spar types. The designs were based on satisfying requirements that were appropriate to the full scale sizes of the proposed "high capability buoy" for the National Data Buoy Project (total flotation volume corresponding to 120,000 lb. and reserve buoyancy of 65,000 lb.) The disc hull shape is similar in proportion to the ONR/Convair "Monster" buoy. The boat hull shape is similar in proportion to the USN "NOMAD" buoy. The catamaran hull shape was developed from the boat hull. Each catamaran hull was made with half the width of the boat hull, all other dimensions (length and depth) being the same. Thus, all the hydrostatic functions in the longitudinal plane are the same for the boat and catamaran buoys. The separation distance between catamaran hulls was selected so that the total breadth of the catamaran was twice that of the boat hull; that is, the clear space between catamaran hulls was twice the width of each hull. The spar hull shape was determined in an effort to be representative of various spar buoys, and also of reasonable proportions for ease of testing. The largest depth and smallest diameter, in practical terms, led to a depth/diameter ratio of 15 which is considered representative of a spar hull type buoy.

The lines drawings which show the details of shape and size for the four models are shown in Figures 1 to 4. The buoy models were made as large as possible within the practical constraints of the experimental facility (to be discusses in a

later section), and they corresponded, more or less, to a scale ratio of the order of 1:6. The model test inertial and geometric conditions for each buoy are given in Table 1. The center of gravity and pitch gyradius were based on estimated average values for other buoys of similar type.

Table 1

Model Test Inertial and Geometric Conditions of Buoys

Buoy Type	Disc	Boat	Catamaran	Spar
Draft, Ft.	0.375	1.25	1.25	7.5
Trim	0.0	0.0	0.0	0.0
Displacement, lbs.	198.7	309.8	309.8	91.02
KG, above base-line, ft.	0.45	1.23	1.23	3.03
LCG, fwd. of ⊠, ft.	0.0	-0.246	-0.246	0.0
Pitch gyradius, ft.	1.80	1.31	1.31	2.55

The hydrostatic characteristics were computed for each buoy type, at model scale, and are plotted in Figures 5 to 7. The hydrostatic curves show, as a function of buoy hull draft, the displacement, center of buoyancy (vertical and longitudinal, where appropriate), metacentric radius height (in longitudinal plane), pounds per inch immersion and longitudinal center of floatation, where appropriate. In addition, the pitch righting moment coefficient (pitch moment per unit pitch angle) is shown in Figures 8 to 10.

MODEL TEST CONDITIONS

The model tests for the four different buoy hull shapes were carried out with the models oriented such that their longest dimension would be parallel to the direction of propagation of the waves for all hull forms (except for the spar). As a result the test conditions corresponded to essentially head seas for the boat shape and the catamaran hull, while the circular symmetry of the disc and spar buoy hull forms allows equivalent orientation in any direction for those buoys. The tests were conducted in this manner since the entire analysis corresponding to the buoy-mooring combination is that of co-planar motion. Thus, for test purposes, the conditions corresponded to those discussed in the basic theoretical development in [1], where the presence of a current in the model test was essentially represented by means of a model towed at a particular forward speed. This particular procedure is only appropriate to the case of testing alone, with different considerations applied to the case corresponding to that of a current and a wave system acting together as a measure of the real situation at sea (as discussed in [1] and [2]).

The model tests in regular waves were designed to cover approximately 8 wavelengths, 2-3 wave amplitudes, and 2-3 speeds for each particular hull form. This would result in a total number of runs of the order of 200 for the regular wave tests. The irregular wave tests included 2 wave spectra for each hull form, with the possibility of tests at 2 different speeds. One of the speeds is zero, while the possibility of testing at a

forward speed in irregular seas was also investigated (discussion concerning the results of that type of test is presented in a later section).

The tests were carried out in a model wave tank at the Offshore Technology Corporation in Escondido, Calif. This particular test facility was selected for the present program due to its dimensions, that would reduce difficulties associated with wall reflections. The dimensions of the wave basin were 120 ft. long, 48 ft. wide, and with a water depth of 15 ft. The importance of elimination of wall interference effects is very significant for the present case of buoy motions, which occur primarily at zero speed or for conditions corresponding to very low speeds in tank model test studies. The tank at Offshore Technology Corp. has a hydraulically operated wavemaker which can generate waves whose period extends from 0.3 sec. up to 4 sec. A small towing speed, up to 4 ft./sec. is also possible in that facility.

The wave generation is obtained from a signal coming from a finely tuned electronic oscillator at the desired wave period, which then drives the hydraulic wavemaker mechanism. For the case of irregular waves, 6 different oscillators are set to the particular frequencies desired, with their output signal summed and used to drive the hydraulic wavemaker. The amplitude of each of these frequency components is selected in order to provide a distribution of wave amplitude and hence wave energy in the particular irregular wave system. This type of wave system generation is essentially equivalent to that of a sum of sinusoidal waves with frequencies that are not commensurate

in their values, and the sum produces an irregular wave form. While this system is not random, it nevertheless is a practical means of simulating a realistic random sea by virtue of a finite number of sinusoidal waves. The consequences of this type of representation of the irregular wave system in regard to the analysis of the records of motion, wave amplitudes, etc. are discussed in a later section of this report.

The instrumentation system used for measurement of the motions of the different buoy hull forms was made up of two separate types of support, viz. one system that was applicable to the boat, catamaran, and disc hull, with another special system that was only used for the spar buoy hull. The particular measuring apparatus used for the majority of the tests had the hull form supported at some point about which the model could pivot in its pitch degree of freedom, and this pitch motion was indicated by the deflections of a particular RVDT (Rotational Variable Displacement Transducer). The model rotated in pitch about the bottom of a vertical rod which in turn was supported by a square plate made of light material (plexiglas), as shown in Figure 11a. The square plexiglas plate was in turn attached to a series of horizontal rods, with the attachments supported by 8 universal joints, with additional rods with varying degrees of stiffness and orientation, i.e. either flat vertically or horizontally (as required) in order to provide a measure of the deflections corresponding to the motions of heave and surge. Particular RVDTs that would indicate the heave and surge displacements were attached at the ends of the horizontal rods on a large metal plate, which

was then secured to the towing carriage. Additional support was provided by horizontal beams and further metal elements, as shown in Figure 11a. Some minor restraint in surge was imposed by virtue of very soft springs that were attached in the horizontal direction, as shown in Figure 11a. The purpose of these particular springs was to only allow oscillatory motion in surge and to eliminate any drift effects that would occur in that particular mode of motion. It also provided some means of stabilizing the surge equilibrium position about which the oscillations took place when the model was towed at a forward speed.

The instrumentation system for the spar buoy is shown in Figure 11b. In that particular case the spar model was supported at its center of gravity (CG) as well as a point above, so that appropriate measurements of heave, pitch and surge were directly obtained for that particular method of support. The restraining springs in surge were somewhat stiffer for this configuration, especially in the case when the spar buoy was towed at forward speed (different springs were used for surge restraint at zero speed and for conditions at speed in view of the greater forces necessary to restrict drifting effects at speed for all models and all instrument support systems). As shown in Figure 11b, the heave and surge RVDTs also function as universal joint axes, and they were combined together in one large element that was covered by a rubberized outer boundary that provided the necessary waterproofing.

In the case of each instrumentation system for each particular buoy hull model, appropriate calibrations were made

in order to determine the signal levels that corresponded to particular deflections in heave, pitch,and surge. Similarly calibrations were made for the wave height probe, which was based on a capacitance measuring system, that was located closer to one side of the tank in line with the location of the CG of each model for the zero speed case. These calibration signal levels were recorded on optical oscillograph paper, as well as on magnetic tape, with these same recording systems used for recording all of the motion time histories obtained in the tests.

The measurements obtained for the case of the spar buoy are directly the heave, pitch, and surge of the model relative to the CG. In the case of the other three hull forms, the pitch and heave motions obtained from the outputs of the measuring system corresponded to that of the particular hull relative to the CG reference. However, the surge motion measured for each of the hulls would not correspond to that of the CG reference, since it contained an influence of the pitch motion. As a result, it is necessary to either correct the measured motions to refer surge relative to the CG, or in the case of comparisons between theory and experiment to provide a corrected surge that would correspond to the measurement position in order to have a direct correlation between the measured "surge" motion and that predicted by theory (a discussion of this procedure and the results obtained will be presented in a later section of this report).

ANALYSIS OF TEST DATA

The model tests were initially run in regular waves for each hull, with tests run for the boat hull, disc hull, and catamaran hull (with the appropriate apparatus) in that order. After completion of the regular wave tests for the catamaran hull, tests were then carried out in random seas for that particular craft, followed by random sea tests for the boat hull and the disc hull. This was done in order to obtain all regular wave information for each craft initially, in order to determine the characteristics under those conditions, as well as for convenience in establishing the required random wave spectra for use with all the models. The tests for the spar buoy, with its own particular instrumentation system (as illustrated in Figure 11b), were then carried out in both regular and irregular seas.

For each case, an initial transient response at zero speed was obtained in order to determine the natural frequencies in heave and pitch for the model under those conditions. The tests in regular waves were run over a range of wavelengths that would characterize the model response, within the restrictions of the particular tank size, so that the observed responses would extend up to frequencies sufficiently large that the motion responses were quite small. The low frequency end of the tests were waves sufficiently long that the asymptotic conditions of heave and pitch response ratios of 1.0 (for heave per unit wave amplitude and the ratio of pitch angle to wave slope) would be approached. The response information examined and presented in this report is the heave and surge amplitude

responses per unit wave amplitude ($\frac{|z|}{a_w}$ and $\frac{|x|}{a_w}$) and the ratio of pitch amplitude to wave slope ($\frac{|\theta|}{ka_w}$), where $k = \frac{2\pi}{\lambda}$, a_w = wave amplitude, λ = wavelength.

The wave amplitudes in the tests were selected to be relatively small initially and then increased, with a larger number of variations in amplitude for a particular wavelength considered in the tests for conditions where large responses (near resonant conditions) were experienced. In that particular case a variation of the response per unit amplitude was obtained in sufficient detail to indicate if there were any significant nonlinearities in the response. For those cases where different ratios of the responses with respect to variation in wave amplitudes were indicated in the test results, plots of these variations as a function of wave amplitude were prepared and a determination of the mean value was made. Examples of such results for each buoy type tested, and for the case with the largest number of variations in wave amplitude, are given in Figure 12. If there was any particular trend with regard to increasing amplitude where the presence of nonlinearity was indicated, this would be portrayed by such plots. In most cases except for a small region near resonance conditions (where the differences were still not large nor definitely indicative of a nonlinear trend), the results were sufficiently linear so that the mean values are properly representative of the magnitude of the observed data point.

The tests were carried out at forward speed in order to simulate current conditions and also as a possible means of

obtaining data that would not be affected by wall reflection interference. Such wall reflection interference arises from the waves generated by the model hull oscillations in response to the oncoming ambient wave system, and a forward speed condition would reduce the possibility of such interferences affecting the measured responses (e.g. see [4]). The use of a wide wave tank would also tend to reduce the prospect of wall reflections since a sufficient amount of motion time history due to the ambient wave forcing action could be recorded before the reflected wave interference would occur, even at zero speed (that was the main reason for selecting the particular test facility in this investigation). Examination of the recorded motion responses, wave measurements, etc. showed that the wave reflections due to wall interference were discernible in some cases, but the number of oscillations in the records were more than sufficient to obtain the desired response information before any influence of wall reflection was manifested in the data even for zero speed. This was certainly true for the case of regular waves, while there was a possibility of some influence to be present in the case of tests in random waves due to the longer test time. The method of analysis of random wave responses, and the manner of elimination of consideration of any wall reflection interference in that case, is discussed later in this section of the report.

For the case of the boat hull, the tests were carried out at model speeds of zero and 1.96 ft./sec. This forward speed

condition corresponds roughly to a current of 3 kt. for a scale ratio of 1:6. The model data are presented as a function of wave frequency, for the case of zero speed in Figures 13-15, while for the case of forward speed in Figures 16-18. The resonant periods in heave and pitch for the boat hull model at zero speed were found to be in the range of 1.1-1.2 sec. The general pattern of the responses at zero speed, in regard to the occurrence of some type of resonant response in heave and pitch, correlates with that value of natural period, and the associated shift in the occurrence of a resonant response at the higher speed condition to a lower wave frequency value is also consistently illustrated in these results.

For the case of the disc hull, the responses are presented as a function of wave frequency in Figures 19-21, for V = 0. Results obtained for V = 2.3 ft./sec. for the disc hull are given in Figures 22-24, with some limited response information obtained for an intermediate speed of 1.5 ft./sec. given in Figures 25-27. The maximum speed of 2.3 ft./sec. was limited to that particular value since there was a very large steady-state wave disturbance associated with the translation of the disc hull form through the water, which arises due to the relatively large "bluntness" associated with such a form. There may be some questions in regard to the influence of this steady disturbance since it could possibly alter the form of the hull relative to the water surface that is assumed to be responsible for different forces, coefficients in equations of motion, etc. The intermediate speed is selected in order

to determine whether such effects due to forward speed would also manifest themselves to the same degree at a somewhat lower speed.

Examination of the results for V = 0 in Figures 19-21 does not exhibit any discernible resonant type of response in either heave and pitch. Transient responses in heave and pitch indicated periods of the order of 1.0 sec., with attendant difficulties in determining the values of the natural period due to the very large damping associated with this particular hull form in those modes of motion. Comparison with the results obtained at forward speed shows that there is an indication of some type of resonant response for those conditions, at a frequency value that would correlate with the observed natural period after allowance for the influence of forward speed on the frequency of encounter. The frequency of encounter in this case of head seas is defined by

$$f_e = f + \frac{2\pi V}{g} f^2 \qquad (1)$$

where f is the wave frequency (in Hz.), V is the forward speed, and g is the acceleration due to gravity. This relation shows that a particular encounter frequency is associated with a lower value of wave frequency, so that resonance corresponding to a particular natural frequency would be indicated at a lower wave frequency value than the actual natural frequency value.

The lack of any significant response at the indicated resonant frequencies at zero speed could possibly be due to the smaller

value of wavelength associated with that condition relative to the diameter of the disc hull. This is due to the dependence of the wave excitation forces and moments on wavelength, which is different than in the case of ordinary mechanical systems. If the wavelength is very small compared to the disc diameter, the wave excitation becomes very small since the wave is spacially averaged over the disc, while waves very long compared to the disc diameter act as if a single local point value of the wave terms (displacement, velocity, acceleration, etc.) produces the wave excitation input. At intermediate wavelengths between these extremes there are different values of the excitation terms, and the wavelength condition corresponding to this present natural frequency is about 5 ft. With the disc diameter of 4 ft. in this case, a small excitation input would then be generally expected, and large response magnitudes are thus not exhibited. There was some variation in the response ratio (with respect to wave amplitude) near such resonant frequencies, but this was not sufficient to imply any significant nonlinear behavior in that region.

For the catamaran hull, transient responses in heave and pitch resulted in the following model natural periods; 0.9 sec. for heave and 1.12 sec. for pitch. The test data, in the form of amplitude response ratios, for V = 0 are given in Figures 28-30. Data obtained from tests at V = 2.0 ft./sec. are given in Figures 31-33, while some further data at an intermediate speed of V = 1.5 ft./sec. are given in Figures 34-36. Variations of wave amplitude in the regions near resonance

were made in order to determine the possible influence of nonlinearity or significant sensitivity to changes of parameters in this region, as shown in the figures for the catamaran hull. The measured response data indicated very large resonances and sharply tuned responses for these motions, especially at forward speed, with the non-dimensional response ratios extending up to magnitudes of about 3.5. The sharply tuned experimental responses do not precisely correspond to the period values indicated from transient response tests, but are still sufficiently close to indicate a fair degree of agreement. The shift of the resonant peak to lower values of wave frequency as the forward speed increases is generally proper and consistent with simple reasoning with regard to the influence of frequency of encounter. The large amplitudes of motion associated with the large response ratios required a limitation of the wave amplitude in the tests, so that the maximum amplitude tested was 1.65 in. (The maximum wave amplitude for the other buoy hulls, as well as all of the wave amplitudes and measured data used in the tests, is tabulated in the Appendix.)

During the tests there was noticeable wave generation between the hulls, with the appearance of wave systems that were propagating forward between the hulls. This situation occurred for conditions that appeared to be close to those that produce the relation $\frac{\omega_e V}{g} = 0.25$, which is a critical condition with regard to wave generation (see [5] and [6]). Large wave disturbance and propagation of waves in a forward direction (as well as also laterally) for an oscillating and translating

body are associated with that particular critical value, and the presence of the "boundaries" created by the two catamaran hulls would also act to focus the disturbances, as in a channel.

The test data presented in the figures are assumed to be appropriate to a constant value of forward speed, but the tests actually covered a range of speeds that average about this value (e.g. for V = 2.0 ft./sec. the test speeds range from 1.9 ft./sec. to 2.06 ft./sec., while for the nominal speed condition of V = 1.5 ft./sec. the speed range is 1.47 ft./sec. up to 1.61 ft./sec.). Because of the sharp resonant response characteristic, some deviation in the results would generally be expected, but that would not be significant in affecting the main results of the test program.

The spar buoy hull model was tested with its own special instrumentation system, as described previously, and the same type of measurements carried out as for the other hulls. Transient tests at zero speed showed the natural period of heave to be 2.8 sec., and the natural period of pitch to be 3.73-3.8 sec. The spar buoy tests were carried out in a series of waves that had generally longer periods than those corresponding to the other hull forms, in view of the known long natural period of spar buoys. The results obtained in the tests for V = 0 are shown in Figures 37-39, while the results at V = 1.0 ft./sec. are shown in Figures 40-42. The characteristic large response ratios as the frequencies approach resonance for these speeds are indicated in these figures, and in only one case did it appear that data was obtained for conditions at frequencies lower than

resonance so that the curve would provide a greater characterization of the response form (see Figure 40.) With regard to the surge motions, it appears that the surge motion response at zero speed is generally smaller than that at forward speed, which is somewhat at variance with a simple analysis that would consider more damping to be present for the case at forward speed. There does not appear to be any specific reason for this result at this time, and further discussion with regard to this result will be provided when considering comparison between theory and experiment.

The analysis of the irregular wave responses was carried out in a particular manner that recognized the irregular waves to be made up of a sum of various sinusoidal waves of different frequencies, with different amplitudes associated with each frequency. Two different sea states were represented in the form of a distribution of wave amplitude at different frequencies, which were defined as Sea Condition No. 1 and Sea Condition No. 2. Their characteristics are tabulated below, in the form of the particular frequency and the nominal wave amplitude associated with that frequency that was designated for establishment of such waves. These nominal values were used in order to set the expected amplitude from the wavemaker, but they would not be necessarily precise. However, the important information is the actual amplitude of the waves that is present in the total wave record signal, and that is determined by analysis of the recorded irregular wave records.

Table 2

Wave Content of Irregular Seas

Sea Condition No. 1

Frequency, cps.	Height, in.
0.4	0.65
0.53	1.0
0.65	2.0
0.75	1.7
0.89	1.0
1.05	0.65

Sea Condition No. 2

Frequency, cps.	Height, in.
0.45	0.5
0.58	1.5
0.71	2.0
0.86	1.2
0.97	0.8
1.09	0.4

Since the irregular waves contain various components at specific frequencies, the wave records and the resulting responses of heave, pitch and surge of the various buoy hull forms will contain the same frequency content (assuming linearity). It is only necessary then to filter each record in order to determine the signal at the particular frequency of interest, and then apply the results to determine the desired motion

amplitude ratios at each particular frequency for each hull response. This information can then be compared to the results obtained in regular sinusoidal wave tests, and will indicate whether the same characteristics are obtained from the irregular sea content as in the case of single sinusoidal waves, i.e. a definite test for the consequences of linear superposition in an irregular sea.

With all the measured data on magnetic tape, the technique for filter analysis was carried out using an analog computer. The type of filter chosen for determining the response at a particular frequency was a very sharply tuned filter known as an exact staggered triple filter, as described in [7]. The procedure used here is to initially analyze the wave record at the particular frequencies that are listed for a specific sea condition, as given in Table 2. Then the individual motion records are analyzed at each frequency selected, and the filtered data in all cases was then displayed on an oscillograph recorder. The amplitudes of the motion responses and the wave motion amplitudes at each particular frequency were then measured on the oscillograph record, using the known calibration factors appropriately converted to account for the various analysis instruments, etc. and the required amplitude ratios were directly determined. Another important test to apply to the data is the determination if any response values were present at intermediate frequencies between the frequencies that were specified in each selected irregular sea. The lack of any significant magnitude of response signal at

these intermediate frequencies (since some small value may be present due to imperfect filter action with the analog computer system) is also necessary to verify linear superposition, since nonlinear interaction would provide significant responses in a large band of frequencies that would encompass the intermediate frequencies investigated in this manner.

Another possible influence on the results obtained by this method of analysis is that due to the possible effects of wall reflections. Examination of the filtered output signals on the oscillograph recorder would indicate whether any change in the pattern of the signal had occurred at each frequency that could be interpreted as an influence of wall reflection. The data analyzed for this series of tests showed fairly uniform amplitudes of the outputs at each frequency, for a sufficient length of time that would allow determination of the amplitude corresponding to that frequency. In any case where there was discernible influence that started to appear, it was after a sufficient length of time for the filtered record to provide the information required. Hence the possible influence of wall reflection was not included in the determination of the necessary response ratios used in the analysis of the irregular wave test data.

This procedure was carried out for tests at zero speed for the different hull forms considered in the test program, where Sea Condition No. 1 was analyzed for all four hull forms, and Sea Condition No. 2 was analyzed for the spar and the disc. This would provide a sufficient basis for determining whether

linear superposition is valid for the various motion responses of these buoy hull forms in the irregular wave system testing at zero speed.

The results obtained for the response ratios by this filter analysis of the irregular wave records are compared with the experimental data from regular wave tests for the case of the disc hull at zero speed in Figures 43-45. The irregular sea analysis shown in these figures is obtained from data in both irregular sea conditions that were established in the tests, and it can be seen that sufficiently good agreement between the experimentally determined results if found by these two test methods. Separate analysis of frequencies intermediate between the values tabulated in Table 2 showed very small responses that would not indicate any interaction between the various frequency components. Thus it appears that linear superposition is a valid procedure to use for further analysis of motions of this particular buoy form in irregular seas. A similar demonstration of the frequency response characteristics obtained from analysis of irregular sea records for the case of the spar buoy at zero speed, using data from the two sea conditions, is shown in Figures 46-48. The results also validate the assumption of linear superposition.

The comparison for the case of the catamaran hull, in regard to the frequency response from the irregular sea records with those obtained from regular wave tests, is shown in Figures 49-51 for zero speed. In that particular case the agreement is also sufficient to indicate the validity of linear superposition. The same type of comparison was made for the case of the boat

hull, with the results shown in Figures 52-54. In that particular case the general pattern of the frequency response obtained from the irregular sea record analysis is very similar to that found from regular wave tests. However, for all three modes of motion, the results obtained from the irregular sea analysis were consistently lower than those obtained from the regular wave tests. Examining the schedule and time records of the test program, it was seen that the test records analyzed for this case of the boat hull were made in the start of a test day in the tank after completing tests of another hull the previous day. No special calibration checks were made at that time (or at least no special calibration record was found), and the motion calibrations used in the regular wave tests were then applied in the analysis of the irregular wave responses. It is therefore conceivable that use of improper calibration data for the motion responses could account for this difference, which is nevertheless still not that significant.

No analysis was applied to the case of tests in irregular waves when the model had forward speed. In that case, the ideal situation would assume the encounter frequencies would be influenced by the particular constant forward speed, and the encounter frequency values corresponding to the fixed frequencies in a stationary wave record would then be the components present in the motion responses. Simple calculations to determine these effective encounter frequencies would be carried out and the motion responses analyzed in exactly the same manner as in the case of zero speed. However there were difficulties associated with that procedure that are due to both the

test technique as well as the limitations of the test facility.

All tests were carried with the model free to surge, and as a result there would not be a constant forward speed. The actual speed would "hunt" about some average condition and the relatively large excursions in the speed (relative to the average surge) would not allow proper determination of the encounter frequencies that would have to be used in the filtering process. Since the filters are sharply tuned filters that require the precise value of the frequency they are examining, this type of analysis could not be properly applied to the present case where the surge degree of freedom was allowed. In addition, the model was towed by a sprocket-chain tow line that did not provide a precisely uniform speed, even if there were no surging present. As a result it would not be feasible to obtain an adequate test of linear superposition at forward speed under the conditions used for the testing.

Since the main purposes of testing at forward speed were to assist in eliminating wall effects, as well as simulating the influence of a current, the importance of analysis of these forward speed tests is thereby minimized. This is due to the exhibited lack of influence of wall reflections on the measured data as analyzed, even at zero speed, as well as the fact that there would not necessarily be such an influence as an altered frequency of encounter when a current is present together with a wave system in the actual open sea. The influence of the forward speed on a frequency of encounter change is only appropriate to the specific type of testing that

has been carried out, but is not a proper analog of the effect that occurs for a moored buoy system at sea.

The overall conclusions to be obtained from all of the comparisons at zero speed, for all four hulls tested, is a verification that linear superposition is satisfied by the motion responses (and also the wave records as well). This allows application of techniques of spectral analysis (e.g. as in [8]) for these responses for determining statistical characertistics of the hull motion per se, or any combination with a cable to provide such information for particular responses of the coupled linear buoy-mooring system treated in [2].

An estimate of the accuracy of the experimental data can be obtained by comparative analysis of those tests in regular waves which were repeated with the same (within 5%) wave amplitude. Nine such comparisons can be made from the data shown in the Appendix, and "average experimental errors" in the measured buoy hull responses from those comparisons obtained. This yielded average errors as follows: 7.5% for heave, 13% for surge and 8.5% for pitch. The surge error is higher because the surge response is smaller with respect to the absolute precision with which the response is measured. This experimental error estimate does not account for systematic errors, such as calibration errors, which are not believed to be present.

THEORETICAL ANALYSIS

The calculation of the buoy motions in waves follows fairly closely the exposition given in [1]. A strictly linear theory is used and only the motions in the longitudinal plane are considered. The variation of hydrodynamic forces with frequency of oscillation is taken into account, since all calculations are done in the frequency domain, rather than the time domain. Differences between the present treatment, which has been incorporated in the computer program [3], and the previous work [1] are given in detail here. However, the results in [1] serve as a basis for this study and should be referenced where appropriate.

The equations of motion are formulated relative to an axes system whose origin is located at the center of gravity of the buoy. The axes are initially fixed in the buoy, with the x-axis position toward the bow (in the direction of the oncoming current) and the z-axes positive downwards. The angular displacement in pitch of the buoy is then positive bow upwards.

The linear equations of motion, for all the various types of buoys to be considered, are written in general coupled form as:

$$a_{11}\ddot{x} + a_{12}\dot{x} + a_{13}x + a_{14}\ddot{z} + a_{15}\dot{z} + a_{16}z + a_{17}\ddot{\theta} + a_{18}\dot{\theta} + a_{19}\theta = X_w$$

$$a_{21}\ddot{x} + a_{22}\dot{x} + a_{23}x + a_{24}\ddot{z} + a_{25}\dot{z} + a_{26}z + a_{27}\ddot{\theta} + a_{28}\dot{\theta} + a_{29}\theta = Z_w \quad (2)$$

$$a_{31}\ddot{x} + a_{32}\dot{x} + a_{33}x + a_{34}\ddot{z} + a_{35}\dot{z} + a_{36}z + a_{37}\ddot{\theta} + a_{38}\dot{\theta} + a_{39}\theta = M_w$$

where x = surge, positive forwards

z = heave, positive downwards

θ = pitch, positive bow up

X_w, Z_w, M_w = wave excitation forces and moments

a_{ij} = coefficients in linear equations of motion

From physical considerations many of the coefficients in (2) are taken to be zero, which gives:

$$a_{11}\ddot{x} + a_{12}\dot{x} \qquad\qquad a_{17}\ddot{\theta} + a_{18}\dot{\theta} \qquad = X_w$$

$$a_{24}\ddot{z} + a_{25}\dot{z} + a_{26}z + a_{27}\ddot{\theta} + a_{28}\dot{\theta} + a_{29}\theta = Z_w$$

$$a_{31}\ddot{x} + a_{32}\dot{x} + a_{34}\ddot{z} + a_{35}\dot{z} + a_{36}z + a_{37}\ddot{\theta} + a_{38}\dot{\theta} + a_{39}\theta = M_w$$

The considerations leading to the form of Equation (3) are the lack of any coupling between the translatory motions of heave and surge, within the limits of linear theory, the lack of any spring-like terms in the surge mode, and the symmetry of the x-force with respect to the pitch angle θ. There is only coupling in the longitudinal plane between pitch and surge, which is analogous to the coupling between roll and sway in the lateral plane.

The particular coefficients and wave excitation for each buoy shape are given in the subsections to follow. Where these differ from the work in [1], the derivation and justification are indicated herein.

Boat Hull

The analysis for the boat shaped buoy follows that given in [1]. In addition, with the change in axis system convention in the present study, the analysis corresponds to that presented for conventional ship forms in [9] for the heave and pitch degrees of freedom. The analysis uses the strip method, in which

each cross-section of the hull is treated in a two-dimensional manner, and the results integrated on the hull length. However, since buoys are not quite as slender as ships (wider relative to length) three-dimensional effects become more significant. Therefore, a correction due to three-dimensional effects has been added to the pitch added moment of inertia (which as a more significant dependence on slenderness ratio than vertical added mass) and also to the damping in heave and pitch. The damping corrections were derived by Havelock [10] for submerged spheroids, and are used herein as the best guidance available.

The surge damping term includes the small axial wave damping contribution. This is in addition to the linear approximation of viscous drag. It is derived on the basis of an "expanding" two-dimensional section, where the expansion is proportional to $\frac{dB^*}{dx}$, the longitudinal rate of change of the ship local beam. The two-dimensional section damping form used is that derived in [11], which is based on thin-strip theory.

The non-zero coefficients are as follows:

$$a_{11} = m(1 + k_1)$$

$$a_{12} = C_D A_p V_c + \rho\omega_e \int \left|\frac{dB^*}{dx}\right|^2 \left|\frac{1-e^{-k_e H}(k_e H-1)}{k_e{}^2 H}\right|^2 dx$$

$$a_{17} = k_1 m \overline{GB}$$

$$a_{18} = a_{12} \overline{GB}$$

$$a_{31} = a_{17}$$

$$a_{32} = a_{18}$$

$$a_{24} = m + \int A'_{33}dx \qquad a_{25} = f_{dh}\int N'_z dx - V_c\int d(A'_{33})$$

$$a_{26} = \rho g\int B^* dx \qquad a_{27} = a_{34} = -\int A'_{33}xdx \qquad (4)$$

$$a_{28} = -\int N'_z xdx + 2V_c\int A'_{33}dx + V_c\int xd(A'_{33})$$

$$a_{29} = -\rho g\int B^* xdx + V_c a_{25} \qquad a_{37} = I_y + f_I\int A'_{33}x^2dx$$

$$a_{38} = f_{dp}\int N'_z x^2dx = 2V_c\int A'_{33}xdx - V_c\int x^2 d(A'_{33})$$

$$a_{39} = \rho g\int B^* x\,dx + V_c a_{35} - gm\overline{GB} \qquad a_{35} = -\int N'_z xdx + V_c\int xd(A'_{33})$$

$$a_{36} = -\rho g\int B^* xdx$$

where m = mass of buoy

k_1 = longitudinal added mass coefficient

C_D = current (viscous) drag coefficient

A_p = projected frontal underwater area

V_c = current speed

$\overline{GB} = \overline{KG} - \overline{KB}$

I_y = mass moment of inertia of buoy

H = local section draft

ω_e = wave encounter frequency

ρ = mass density of water

g = acceleration of gravity

k_e = wave number (encounter) $k_e = \frac{\omega_e^2}{g}$

A'_{33} = local cross-section vertical added mass

N'_z = local cross-section vertical damping coefficient

B^* = local cross-section waterline breadth

f_I = three-dimensional added moment of inertia factor (0.4 used in the present case of Nomad buoy)

f_{dh} = three-dimensional heave damping factor

f_{dp} = three-dimensional pitch damping factor

The wave excitation is as follows:

$$X_w = \int \frac{dX_w}{dx}\, dx$$

$$\frac{dX_w}{dx} = -a_w e^{-k\bar{h}} k\rho g S \cdot \cos(kx + \omega_e t) \qquad (5)$$

$$Z_w = \int \frac{dZ_w}{dx}\, dx$$

$$M_w = -\int \frac{dZ_w}{dx}\, x\, dx \qquad (6)$$

$$\frac{dZ_w}{dx} = -a_w e^{-k\bar{h}} \left\{ \left[(\rho g B^* - A'_{33} kg) \sin(kx) + kc \left(N'_z - V_c \frac{dA'_{33}}{dx} \right) \cos(kx) \right] \cos \omega_e t + \left[(\rho g B^* - A'_{33} kg) \cos(kx) - kc \left(N'_z - V_c \frac{dA'_{33}}{dx} \right) \sin(kx) \right] \sin \omega_e t \right\} \qquad (7)$$

where a_w = wave amplitude

S = cross-section underwater area

$k = \frac{2\pi}{\lambda}$, wave number

c = wave celerity

The value of $\bar{h}$ is approximated by:

$$\bar{h} = HC_s$$

where C_s = local section area coefficient

All of the integrations indicated above in equations (4), (5) and (6) are over the length of the buoy hull. They are carried out numerically since the hull cross-section shape has an arbitrary lengthwise variation. Simple trapezoidal integration is considered appropriate and applied in [3].

The three-dimensional factors for heave and pitch damping f_{dh} and f_{dp} were developed by Havelock [10] for a submerged spheroid and are applied here, in a_{25} and a_{38} above, as the best possible approach. In Havelock's notation, we have:

$$f_{dh} = \frac{E_H}{E_{HS}} = \frac{15}{8} k_o a (1 + k_2)^2 \int_0^{\frac{\pi}{2}} \frac{J^2_{3/2}(k_o ae \cos\theta)}{(k_o ae \cos\theta)^3} d\theta \qquad (8)$$

$$f_{dp} = \frac{E_p}{E_{ps}} = \frac{105}{8} k_o ae^2 \left[1+(2\zeta_o^2-1)^2 k^1\right]^2 \int_o^{\frac{\pi}{2}} \frac{J^2_{5/2}(k_o ae \cos\theta)}{(k_o ae \cos\theta)^3} d\theta \qquad (9)$$

where E_H = rate of energy loss for heaving calculated from three-dimensional flow

E_{HS} = rate of energy loss for heaving calculated from the strip method

E_p = rate of energy loss for pitching calculated from three-dimensional flow

E_{ps} = rate of energy loss for pitching calculated from the strip method

k_o = wave number = $\omega^2 g^{-1}$, ft.$^{-1}$

a = half-length of body, ft.

e = eccentricity of body

k_2 = added inertia coefficient, for transverse oscillation

ζ_o = e^{-1}

k^1 = added moment of inertia coefficient

J = Bessel function.

From Lamb [12], we have:

$$\left.\begin{aligned} e &= (a^2-b^2)^{1/2}\, a^{-1} \\ k_2 &= \beta_o(2-\beta_o)^{-1} \\ k^1 &= \frac{e^4(\beta_o-\alpha_o)}{(2-e^2)\left\{2e^2-(2-e^2)(\beta_o-\alpha_o)\right\}} \\ \alpha_o &= \frac{2(1-e^2)}{e^3}\left(\frac{1}{2}\log\frac{1+e}{1-e}-e\right) \\ \beta_o &= \frac{1}{e^2}-\frac{1-e^2}{2e^3}\log\frac{1+e}{1-e} \end{aligned}\right\} \quad (10)$$

where b = half-breadth of body (radius of spheroid), ft.

In addition, we obtain the longitudinal added inertia coefficient, k_1, from Lamb [12], as:

$$k_1 = \frac{\alpha_o}{2-\alpha_o} \quad (11)$$

The Bessel functions are defined in terms of trigonometric functions, from McLachlan [13], by:

$$\left.\begin{aligned} J_{3/2}(z) &= (2/\pi z)^{\frac{1}{2}}\left[(\sin z)/z - \cos z\right] \\ J_{5/2}(z) &= (2/\pi z)^{\frac{1}{2}}\left[(3z^{-2}-1)\sin z - 3z^{-1}\cos z\right] \end{aligned}\right\} \quad (12)$$

The integrals indicated above are carried out numerically using 2.5° increments.

The particular three-dimensional added inertia factor, f_I, is generally found from a tabulation of such factors that are available in [12] for spheroids. The actual value is found as a function of the diameter-length ratio for an equivalent spheroid that would represent the submerged portion of the hull

form. This is a general procedure applicable to any hull form for which three-dimensional flow influences are anticipated, and is based upon the assumption that this factor, as presented in [12], is equivalent to the ratio of the actual three-dimensional added inertia to the value obtained by integrating the weighted two-dimensional added mass values (which define the added inertia in the strip theory approach).

Disc Hull

The coefficients in the equations of motion for the disc shaped buoy are based on the results of Kim [14] with polynomial curve fits to his numerical results. These curve fits were as follows:

$$M_y = 2.65-1.3258(k_eR_a)+0.6254(k_eR_a)^2-0.1542(k_eR_a)^3+0.01458(k_eR_a)^4$$

$$I_z = 0.266+0.08017(k_eR_a)-0.07483(k_eR_a)^2+0.01933(k_eR_a^3-0.00167(k_eR_a)^4$$

$$H_z = -0.00166(k_eR_w)+0.10502(k_eR_w)^2-0.06863(k_eR_w)^3+0.01671(k_eR_w)^4 -0.00144(k_eR_w)^5$$

for $0 \leq k_eR_a \leq 4.0$, and

$$N_y = 3.6008(k_eR_w)-4.5184(k_eR_w)^2+2.5304(k_eR_w)^3-0.6674(k_eR_w)^4 +0.06694(k_eR_w)^5$$

for $0 \leq k_eR_w \leq 3.0$, and

$N_y = 1.125-0.157(k_eR_w)$ for $3.0<k_eR_w\leq4.0$.

where M_y = vertical added mass coefficient

I_z = added moment of inertia coefficient

H_z = moment damping coefficient

N_y = vertical damping coefficient

k_e = encounter wave number ($k_e = \frac{\omega_e^2}{g}$)

R_a = average underwater radius

R_w = waterline radius

Extrapolations beyond the above frequency range were incorporated in order to allow computations to proceed at high frequencies. The buoy motions become negligible in this range so that simple linear extrapolation proved adequate, as follows:

$$\left.\begin{aligned} M_y &= 1.62-0.1(k_e R_a) \\ I_z &= 0.264-0.015(k_e R_a) \\ N_y &= 0.73-0.05(k_e R_w) \\ H_z &= 0.11-0.006(k_e R_w) \\ &\text{for } 4.0 < k_e R_{a_w} \leq 14.0 \end{aligned}\right\} \quad (14)$$

The part of the coupling terms between surge and pitch that are based on the approximate representation as viscous drag forces and moments were not employed here.

The wave excitation forces and moments were expanded beyond the simple hydrostatic terms given in [1]. The added mass and damping forces in the wave excitation were incorporated into the total expression by assuming reasonable analytic distributions of these terms over the buoy length. The distribution of added mass and damping force was assumed constant over the buoy length for derivation of the vertical wave excitation force. A more refined distribution, varying as the beam, was used to develop the pitch moment wave excitation since moments are more sensitive

to the exact nature of the force distributions. The wave force integrations were then carried out to give closed form expressions for the excitation. This resulted in:

$$Z_w = a_w \sin \omega_e t \left[-\rho g \pi R_w^2 \left(\frac{2J_1(\gamma)}{\gamma} \right) + \omega^2 \rho R_a^3 M_y \left(\frac{\sin \gamma}{\gamma} \right) \right]$$

$$+ a_w \cos \omega_e t \left[-\omega \left(\rho R_w^3 \omega_e N_y \right) \left(\frac{\sin \gamma}{\gamma} \right) \right]$$

$$M_w = a_w \sin \omega_e t \left[-\omega R_w \left(\rho R_w^3 \omega_e N_y \right) \frac{\pi}{8} \left(J_1(\gamma) - J_3(\gamma) \right) \right] \qquad (15)$$

$$+ a_w \cos \omega_e t \left[\rho g \pi R_w^3 \left(\frac{J_1(\gamma) - J_3(\gamma)}{2} \right) + \left(\rho R_a^3 M_y \right) \frac{g\pi\gamma}{8} \left(J_1(\gamma) - J_3(\gamma) \right) \right]$$

$$X_w = a_w \cos \omega_e t \left[-2\rho g \pi d' R_w J_1(\gamma) \right]$$

where ω = wave frequency

$J_{1,3}$ = Bessel Functions

d' = draft of buoy

$\gamma = \frac{2\pi R_w}{\lambda}$,

with λ = wavelength

The list of non-zero coefficients is expressed as follows:

$$a_{11} = m(1+k_1) \qquad a_{31} = a_{17}$$

$$a_{12} = C_D \rho A_p V_c \qquad a_{37} = I_y + \rho R_a^5 I_z$$

$$a_{17} = k_1 m\overline{GB} \qquad a_{38} = \rho R_w^5 \omega_e H_z \qquad (16)$$

$$a_{24} = m + \rho R_a^3 M_y \qquad a_{39} = g\frac{\pi}{4} R_w^4 - gm\overline{GB}$$

$$a_{25} = \rho R_w^3 \omega_e N_y$$

$$a_{26} = \rho g \pi R_w^2$$

There are no coupled damping coefficients proportional to forward speed (or current) in these equations, as they have been assumed to be zero (in distinction to the existence of such terms suggested in [1], based on the analog of the normal surface ship case, as in [9]). A check on the original derivation of such terms (in [15]) was made for a configuration considered closer to the disc-type buoy. The results in [15] were derived for a long slender prolate spheroid, and a more appropriate form for the present disc buoy would be an oblate spheroid. Actual evaluations were made for a hemisphere shape, for analytical simplicity, and it was shown that no coupling terms would occur in that case. These results were applied in establishing the disc buoy equations with forward speed, in analogy to the procedures whereby the results of [15] were adapted toward ordinary long slender surface ships.

Catamaran Hull

This buoy shape is not treated in [1]. The approach employed herein is to consider the catamaran in the same manner as a single boat shaped hull (strip method), but to fully account for hull interaction terms in the calculations of the two-dimensional hydrodynamic forces (due to added mass and damping). In addition, since each of the catamaran hulls is generally more slender, as in standard ships, the three-dimensional corrections are not ordinarily used, and the factors are taken as 1.0. For the present case the slenderness ratio is still not that small to preclude any three-dimensional influence, but the particular type of three-dimensional correction is not known for a catamaran since the hydrodynamic forces are

strongly affected by interactions between the separate hulls.

The interaction effect is represented by Ohkusu [16] in general terms for symmetrical two-dimensional catamaran sections. Simplifying the results for symmetrical sections (both for each hull and the total catamaran) leads to:

$$A'_{33cat} = 2A'_{33} + \frac{2P}{k_e^2} R_e \left[\frac{i\bar{A}_H^2 \, e^{i2(\varepsilon_H - k_e P)}}{1 - i\, H^+ \, e^{-i2k_e P}} \right] \tag{17}$$

$$H^+ = ie^{i\varepsilon_H}\cos\varepsilon_H - e^{i\varepsilon_s} \sin\varepsilon_s \tag{18}$$

$$N'_{zcat} = \frac{\rho g}{\omega_e^3} \bar{A}^2_{Hcat} \tag{19}$$

$$\bar{A}^2_{Hcat} = 2\bar{A}_H^2 - 2\, I_m \left[\frac{i\bar{A}_H^2 \, e^{i2(\varepsilon_H - k_e P)}}{1 - i\, H^+ \, e^{i2k_e P}} \right]$$

where $\bar{A}_H$ = radiated wave amplitude ratio for two-dimensional vertical oscillation

ε_H = phase angle of radiated wave for two-dimensional vertical oscillation

ε_s = phase angle of radiated wave for two-dimensional horizontal oscillation

P = catamaran separation distance between hull centerline and overall vessel centerline

The above equations indicate how the two-dimensional results for added mass and damping of one hull section are applied to determine the results for catamaran sections. It should be noted that the radiated wave phase angle for horizontal (sway) motion is required to obtain the vertical motion characteristics.

This approach to catamaran motion calculations was applied by Ohkusu and Takaki [17] and compared satisfactorily

with their experimental results. They used catamarans where each hull was relatively slender, with a length-beam ratio of 11.1. Their comparisons covered two hull separation distances, zero and a forward speed, and head and beam seas.

An essentially similar approach is proposed by Nordenstrom, Faltinsen and Pedersen [18], but only for zero speed. However, they employ an extension of the "close-fit" method, for calculation of the two-dimensional properties, including catamaran interaction effects, rather than the Lewis form method of Ohkusu [16]. Otherwise, their approach, via the strip method, etc., is the same, and they demonstrate an agreement with some two-dimensional sectional results of Ohkusu. In general, it has been shown that in most cases the much simpler Lewis form approach is adequate for moderate section shapes. In addition, it appears that the comparison with experimental data by Nordenstrom, et al, [18], is not as satisfactory as that shown by Ohkusu and Takaki [17].

Spar Hull

The analysis follows that shown in [1], based on the work of Newman [19]. In addition, the viscous drag terms which represent the current influence are included, as appropriate. This method was also applied by Adee and Bai [20] where the (generally small) vertical added mass was considered. To summarize, the coefficients and wave excitation are represented as follows, using notation similar to that in [19] and [20].

$$a_{11} = m$$

$$a_{12} = \frac{m^2 k_e{}^3 \omega_e}{4\rho} Q_o{}^2 + C_D \rho A_p V_c$$

$$
\left.
\begin{aligned}
a_{17} &= -\frac{m}{2} P_1 \\
a_{18} &= \frac{m^2 k_e{}^3 \omega_e}{4\rho} Q_o Q_1 + C_D \rho A_p V_c \overline{GB} \\
a_{24} &= m\ (1 + k_e) \\
a_{25} &= \frac{\rho \omega_e}{2m} S_o{}^2 (m k_e Q_o - \rho S_o) \\
a_{26} &= \rho g S_o \\
a_{31} &= -m P_1 \\
a_{32} &= -\frac{m^2 k_e{}^3 \omega_e}{2\rho} Q_o Q_1 + C_D \rho A_p V_c \overline{GB} \\
a_{37} &= I_y + m P_2 \\
a_{38} &= \frac{m^2 k_e{}^3 \omega_e}{2\rho} Q_1{}^2 \\
a_{39} &= g m P_1
\end{aligned}
\right\} \quad (20)
$$

$$
\left.
\begin{aligned}
&\text{and } P_i = \frac{\rho}{m} \int_{d'}^{o} (z_G - z)^i S(z) dz \quad (i = 1,2) \\
Q_i &= \frac{\rho}{m} \int_{d'}^{o} e^{-k_e z} (z_G - z)^i S(z) dz \quad (i = 0,1)
\end{aligned}
\right\} \quad (21)
$$

where S = cross-section area (horizontal plane).

$$
\left.
\begin{aligned}
Z_w &= -a_w \sin\omega_e t\ (\rho g S_o - g m k Q_o') \\
M_w &= -a_w \cos\omega_e t\ (2\omega^2 m Q_1') \\
X_w &= a_w \cos\omega_e t (\omega^2 m Q_o')
\end{aligned}
\right\} \quad (22)
$$

where S_o = waterplane area and the Q_i' are defined as in Equation (21) with k_e replaced by k.

The vertical added mass coefficient k_3 is found from values listed for spheroids in [12], using the slenderness ratio of the submerged portion of the spar buoy as the reference value for the equivalent spheroid. The value of k_3, as used here, is the longitudinal added mass coefficient presented in [12], and denoted as k, in that listing.

COMPARISON OF THEORY AND EXPERIMENT

The comparison between the available theoretical results, as represented by the equations in the preceding section, was obtained by computer implementation of the equations using numerical values appropriate to the various hull forms and the conditions for the tests (speed, wavelength, etc.). As a result of the analysis of the model tests for all four hull forms, in both regular and irregular seas, the various motion responses were found to be linear with respect to wave amplitude. All the theoretical developments of the four hulls of interest are also linear with respect to wave amplitudes, thereby allowing a direct comparison with regard to aspects such as frequency response, influence of forward speed, etc. which can be directly demonstrated using the presently available experimental data. This set of comparisons serves as a means of validating the available theories for application to other possible buoy hull forms, of different relative proportions, shapes, etc. that may be used in various conceptual designs of moored buoy systems. The use of a valid theory is directly applicable in the computer simulation studies described in [2], which is then a method for predicting performance of various moored buoy systems prior to actual construction, placement, and full scale performance evaluation at sea.

The first hull form that was considered was the boat hull. The results of comparison of theory and experiment, for the case of zero forward speed, are shown in Figures 55-57a. In these figures the response ratios of the motions of heave, pitch

and surge are represented in frequency response form, and the computer responses are shown together with the experimental data. The theoretical computations were carried out for the boat hull buoy, which had a length-beam ratio of 2.11, which is quite small compared to that of normal ships. As a result the necessary corrections for added inertia and the heave and pitch damping terms were made, as described in the preceding section. The results of the comparison are only fair in this particular case, with some significant deviation in regard to the heave amplitude somewhere near resonance, together with a fairly poor representation of the surge motion response. As mentioned previously, the surge motion as measured is not exactly the surge motion with respect to the center of gravity which is the quantity desired for use in the buoy-mooring simulation, and which is also the quantity represented in the equations. The inclusion of the influence of pitch, as it affects the measured surge, is represented by the following relation:

$$\text{surge measured} = x + h\theta \tag{23}$$

where x = surge motion with respect to CG

h = z-coordinate of surge measurement point, with respect to CG

The use of the three-dimensional correction factors applied to considerations of added inertia and damping is not generally the practice used in theoretical studies of ship motions, but these results are applied in the present case because it is expected that the physical situation demands some influence of three-dimensionality for this case. Whether the particular forms

chosen for the three-dimensional influence (i.e. those taken from (10)) are the most appropriate is generally a subject for more advanced consideration, and the results presented for heave and pitch in Figures 55-56 represent the best possible type of agreement between the available theory and the experimental data, when considering various combinations and forms of such factors. Since this procedure is somewhat subjective and only limited considerations are available for any three-dimensional treatment for a ship-like form, the techniques applied represent the state of the art appropriate to this type of hull form configuration.

The motivation for the use of the three-dimensional damping factors was the very small length-beam ratio, together with the discovery that the usual ship motion computations based on the work in [9] showed small responses relative to the experimental measurements, indicating an overdamped response. The numerical values of the three-dimensional factors based on the theory of [10], as applied to the present case of length-beam ratio of 2.11, are shown in Figure 57b as functions of frequency (the same values are used in treating the conditions tested at forward speed, using the appropriate value of frequency of encounter). These factors have their greatest influence at low frequencies and it is known that they tend to approach a value near unity in the higher frequency range of practical interest (the actual limit of 1.0 is approached for long spheroids, with a limit at high frequency dependent on the actual length-beam ratio). Thus the expected behavior of the validity of a two-dimensional strip theory

to be more valid at higher frequencies is indicated by these general results.

The comparison given in Figures 58-60 for the boat hull at forward speed (V=1.96 ft./sec.) exhibits some type of improvement with regard to the prediction capability of theory, which could possibly be associated with the increased frequency associated with wave encounter at speed (see discussion above concerning range of applicability of strip theory). Nevertheless there appears to be some small variation with regard to the cccurrence of the resonant condition, as well as the degree of response amplitude near resonance, and it can be seen that these factors are significantly influenced by the assumptions associated with the fluid inertial forces (added mass and added inertia) and the hydrodynamic damping, all of which will exhibit significant three-dimensional effects. It appears that, as a result of the comparison of available theory with these experimental results, that further theoretical effort has to be devoted to consideration of response evaluation for boat hull forms with small length-beam ratios.

For the case of the disc hull the comparison between theory and experiment for the responses due to waves is shown for zero speed in Figures 61-63. In that case it can be seen that there is generally good agreement between theory and experiment for the heave and pitch motions, except for some small reduction of the experimental data in a portion of the low frequency range. The comparison for the case of surge also shows a deviation in This particular range, but the comparison might be improved somewhat if the actual surge relative to the CG was considered as a final measured value that could be compared directly with the

theoretical estimate. The present method of comparison, which is applied to the case of the boat and catamaran hulls also, involves computed values that place a great degree of reliance on proper phasing, etc. in order to provide a valid representation of the measured surge. It is possible that the more direct comparison of the motion would provide a better result, but that was not cnnsidered to any extent in the type of comparison that has been presented in this report.

The disc hull results at a forward speed of V = 2.3 ft./sec. are shown in Figures 64-66, and for the speed V = 1.5 ft./sec. the comparison between theory and experiment is shown in Figures 67-69. Examining these results shows that there is fairly good agreement for the pitch and surge motion responses, but the agreement is not as good in the case of heave motion for the disc. These computed results are based upon the theory for the disc hull described in the preceding section. These are no speed-dependent coupling terms in these equations, as discussed previously, but some early computations were carrie out using such terms, as listed in [1] and based upon the analogy to ordinary surface ships (see [9]). The computed results were quite erratic in comparison to the experimental values when such speed-dependent terms were included, and the constituent force terms were very large compared to other terms in the equations. This result led to further analysis of the basic derivation of such terms in ship motion theory (see [15]) which ultimately resulted in the determination that such terms were not appropriate (or had small values) for the case of the disc hull. The occurrence of a resonant frequency

for the disc at a value that would not coincide with the natural period observed in zero speed transient tests has been discussed in an earlier section, and that difference is evident in the comparison exhibited in Figures 64 and 67. Only a small difference between theory and experiment, in regard to the occurrence of the resonant condition, is indicated in the case of pitch motion. One possible influence that could cause such a difference is due to the steady state wave pattern associated with this particular hull when it is moving at forward speed, and it can easily be seen that the magnitude of the restoring forces, added mass, etc. could attain different values due to the nature of the underwater form of the disc hull relative to the water surface. A more detailed study of this possibility would involve a series of tests whereby constituent forces were measured, which would be beyond the scope of the present investigation. The theoretical results obtained here nevertheless represent information based on the generally available hydrodynamic data associated with such hull forms, which are only approximated as a flat disc on the surface. These theoretical results, except for the small difference in the magnitude of the heave resonant frequency, (see later discussion on theoretical evaluation of natural frequencies for all buoy hulls tested), are sufficiently useful for application to prediction of motion of disc-like hull forms in waves, and hence can be used in the complete buoy-mooring computer simulation work in [2].

The comparison between theory and experiment for the motion responses of the catamaran hull are shown in Figures 70-72 for zero speed, in Figures 73-75 for V = 1.5 ft./sec., and in Figures 76-78 for the case V = 2.0 ft./sec. The agreement between theory and experiment in regard to the determination of the natural periods is fairly good for all cases, but the agreement in regard to magnitudes near the resonant condition is not very good for the case of zero speed. The degree of agreement improved significantly as the forward speed increased, as can be seen by examination of Figures 76-78 for the larger speed condition of V = 2.0 ft./sec. (which is also associated with larger frequencies where strip theory is more valid). The lack of agreement in regard to the amplitude values at the lower speeds can be more or less ascribed to the effect of damping near these resonant conditions, since the theoretical computed responses are very sharply tuned, as is the case for the experimental results as well. The degree of validity of the theoretical computations of the two-dimensional added mass and damping values for a twin hull catamaran, as based upon the results in [16], have not been established completely and the sensitivity of the values of these force terms may be large with respect to small changes in governing parameters. An illustration of the sensitivity of the damping values, in regard to their influence on the resulting motion frequency response characteristics, is shown in Figures 79-82. These figures illustrate the difference in the responses in heave and pitch for zero speed and V = 1.5 ft./sec., as the distance between the hull is varied somewhat.

Another factor that has not been considered in the theoretical representation of the catamaran responses is due to three-dimensionality. The length-beam ratio of the catamaran hull form, i.e. for each separate single hull, has a value of 4.2 which is still smaller than that of a normal surface ship. However, it is not known what type of three-dimensional factor should be used in the case of the catamaran, where wave interference effects are paramount, since the three-dimensional factor for the case of a single boat hull has not been fully established. The theoretical results presented here in comparison with the experimental data do show a trend toward good agreement as the speed increases. The theoretical techniques represent the present state of the art in regard to catamaran hulls, which are not usually considered for such low speeds, and hence they represent the most useful techniques to be used for this case. Thus they can be applied to the computer simulation work in [2], with particular care exercised in investigating contributions that arise due to the hull motions at a condition of very low current speed.

The results for the spar hull at zero speed are given in Figures 83-85, and the comparison between theory and experiment for the case where V = 1.0 ft./sec. are given in Figures 86-88. An examination of all these responses shows a small difference between theory and experiment in regard to the heave resonant frequency, as well as for the case of pitch resonant frequency. The sharply tuned response characteristics in these modes, due to small damping, are also exhibited in the figures for both theory and experiment. The difference in the natural period in

heave could possibly be explained by the influence of the support system, as shown in Figure 11b. Discussions with personnel at Offshore Technology Corp. sometime after the tests were completed indicated that there was a possible vertical spring restoring influence in the measuring system itself. This could possibly be provided by the rubber coating at the lower submerged support position of the spar instrument system, where this coating contained the surge and heave RVDTs. The stiffness obtained from such a system is relatively small but it would have significant influence on the total restoring effect of the spar hull, since this particular model itself has such a small restoration effect in comparison to those of the other hull forms tested. A spring-like action of the support system, which could correspond to a stiffness of the order of 1 lb./ft. in heave would probably be present in this system, which some additional check tests of this prospect have indicated (private communication with personnel at Offshore Technology Corp.). With the effective hydrostatic restoring force rate of the spar buoy itself of the order of 12 lb./ft., it can be seen that there is a possible 5% difference in the natural frequency indicated by the experimental data (larger natural frequency for the experiments) as compared to the theoretical prediction. A similar influence could possibly be expected to occur in the case of pitch motion also, which could possibly account for that difference as well.

The general agreement for the spar buoy in regard to frequency response characteristics, as well as the evaluation of

the natural resonance frequencies (when accounting for the influence of the instrumentation system) is quite good for the case of the heave and pitch motions. However, there appears to be some difference in the surge response, as compared to theory, for the case of zero speed. Much better agreement is indicated by the results at forward speed in regard to surge. It is possible that the instrumentation system that provided the surge measurement at zero speed could have an effect on the surge measurement also. This type of influence would not necessarily occur when the system had forward speed since the steady drag force would tend to move the spar buoy relative to the support system so that its deflections would be more easily attained under those conditions. This possibility has not been investigated in detail, but since this type of motion may not be too important for a spar buoy, limited consideration has been given to the lack of agreement that is exhibited in surge at zero speed. The other motions can generally be predicted quite well, and hence the theory can be readily adapted for application in the computer simulation studies of complete moored buoy systems.

In order to provide further documentation with regard to the capabilities of theory in estimating the natural periods of heave and pitch for the various buoy hulls, a tabulation of the results obtained from theory and experiment (at zero speed) is provided below. The theoretical expressions for the heave and pitch natural periods are given by:

$$T_{heave} = 2\pi \sqrt{\frac{a_{24}}{a_{26}}} \qquad (24)$$

$$T_{pitch} = 2\pi \sqrt{\frac{a_{37}}{a_{39}}} \quad , \qquad (25)$$

and in the case of all of the hulls, with the exception of the spar, it is necessary to carry out an iterative computation in order to arrive at the values of the natural periods. This is necessitated by the fact that the added mass in heave and the added pitch inertia are themselves functions of frequency so that the precise value corresponding to the natural period found from such repeated computations. The values obtained from the theoretical expressions in Eq. (24) and (25) are tabulated below in Table 3, together with the experimental values. The experimental values are found from analysis of transient responses, which are obtained from reading oscillograph tape records. In some cases the natural periods were difficult to discern too well (due to overdamped responses, etc.) and only a general approximate range is given in such cases.

Table 3

Comparison of Theoretical and Experimental Natural Periods

	Heave Period, sec.		Pitch Period, sec.	
Hull	Theory	Experiment	Theory	Experiment
Boat	1.13	1.1-1.2	1.15	1.1-1.2
Disc	0.99	∿1.0	0.85	∿1.0
Catamaran	0.98	0.9	1.13	1.12
Spar	3.02	2.8	4.33	3.8

It can be seen that there is generally quite good agreement for all cases, with the possible exception of the spar buoy results in pitch. The possible influence of the stiffness inherent

in the test apparatus, which would reflect itself in pitch as well, is the main cause for such a deviation, which was discussed above. Nevertheless, a general statement can be made that the present theory is capable of adequately predicting the natural periods in heave and pitch for the various hulls considered in this program.

CONCLUSIONS

As a result of the present study, both experimental and theoretical, of buoy motions in waves certain conclusions have been reached, as summarized below. These results are especially pertinent to the subsequent application of the theory in calculations which simulate the combined buoy-cable moored system in the presence of current and waves.

1) The buoy motions in waves are linear with respect to wave amplitude. This conclusion was demonstrated in the regular wave tests conducted at various wave heights, up to a maximum of about 1/20th the wavelength.
2) The principle of linear superposition applies to buoy motions in irregular waves. This was verified in the irregular wave tests and their comparison with the regular wave test results.
3) Theoretical calculations of buoy motions in waves are not in perfect agreement with experimental results, but are sufficient for engineering application in buoy-cable dynamic calculations. The theoretical results indicate the major characteristic of the motion responses, and have been developed on the basis of the present state of the art of buoy hull dynamic analysis. While some areas where the theoretical approach needs advancement are evident, in general the computer results both at speed (simulating a current) and at zero speed, are in fairly good agreement with the experimental data, taking into consideration some possible defects in the comparison process. The major defect in present theory

is the lack of a precise manner of accounting for three-dimensional flow effects on hull forms that are not slender, i.e. for small length-beam ratio buoy hulls.

Another point with regard to the theoretical calculations is worth noting at this point. That is, that the determination of the response of the complete buoy-cable system, with the mooring line attached to the buoy and interacting with it, may not be very sensitive to differences in some hydrodynamic and hydrostatic coefficients. The total system sensitivity may not be as severe as for the simply coupled buoy hull system. This is a subject for determination when exercising the computer program developed in [3].

REFERENCES

1. Kaplan, P. and Raff, A.I.: "Development of a Mathematical Model for a Moored Buoy System", Oceanics, Inc. Report No. 69-61, April 1969.

2. Goodman, T.R.; Kaplan, P.; Sargent, T.P.; and Bentson, J.: "Static and Dynamic Analysis of a Moored Buoy System", Oceanics, Inc. Report No. 72-87, January 1972.

3. Sargent, T.P.; Raff, A.I.; and Bentson,J.: "Buoy-Cable Dynamics Program", Oceanics, Inc. Report No. 72-88, January 1972.

4. Vossers, G. and Swaan, W.A.: "Some Seakeeping Tests with a Victory Model", Int. Shipbuilding Prog. Vol. 7, May 1960.

5. Kaplan, P.: "The Waves Generated by the Forward Motion of Oscillatory Pressure Distributions", Proc.Fifth Midwestern Conf. on Fluid Mech., University of Michigan, 1957.

6. Brard, R.: "Introduction a l'etude theorique du tangage en march," Bulletin de L'Assoc. Tech. Maritime et Aeronaut., Vol. 47, 1948, pp. 455-479.

7. Bates, M.R.; Bock, D.H. and Powell, F.D.: "Analog Computer Applications in Prediction Design", Reprint from IRE Transactions on Electronic Computers, Vol. EC-6, No. 3, September 1957.

8. St. Denis, M. and Pierson, W.J.: "On the Motions of Ships in Confused Seas", Transactions of SNAME, 1953.

9. Kaplan, P. and Raff, A.I.: "Evaluation and Verification of Computer Calculations of Wave-Induced Ship Structural Loads", Oceanics, Inc. Report No. 70-77, November 1970.

10. Havelock, T.H.: "The Damping of Heave and Pitch: A Comparison of Two-Dimensional and Three-Dimensional Calculations", Transactions, Royal Institution of Naval Architects, Vol. 98, 1956.

11. Kaplan, P. and Jacobs, W.R.: "Two-Dimensional Damping Coefficients from Thin Strip Theory", Davidson Lab. Note 586, April 1960.

12. Lamb, H.: "Hydrodynamics", Sixth Edition, Dover Publications New York, 1945.

13. McLachlan, N.W.: "Bessel Functions for Engineers", Second Edition, Oxford University Press, London, 1961.

14. Kim, W.D.: "On the Forced Oscillations of Shallow-Draft Ships:, Journal of Ship Research, Vol. 7, No. 2, October 1963.

15. Havelock, T.H.: "The Coupling of Heave and Pitch Due to Speed of Advance", Transactions, Royal Inst. of Naval Arch., Vol. 97, 1955.

16. Ohkusu, M.: "On the Motion of Multihull Ships in Waves (I)", Reports of Research Institute for Applied Mechanics, Kyushu University, Vol. XVIII, No. 60, 1970.

17. Ohkusu, M. and Takaki, M.: "On the Motions of Multihull Ships in Waves (II)", Reports of Research Institute for Applied Mechanics, Vol. XIX, No. 62, 1971.

18. Nordenstrom, N; Faltinsen, O.; and Pedersen, B.: "Prediction of Wave-Induced Motions and Loads for Catamarans", Reprint, Third Annual Offshore Technology Conf. (OTC1418), Houston, 1971.

19. Newman, J.N.: "The Motions of a Spar Buoy in Regular Waves", DTMB Report 1499, May 1963.

20. Adee, B.H. and Bai, K.J.: "Experimental Studies of the Behavior of Spar Type Stable Platforms in Waves", College of Engineering, U. of California, Report No. NA-70-4, 1970.

NDBP

Scale Model Test Program

DISC TYPE MODEL

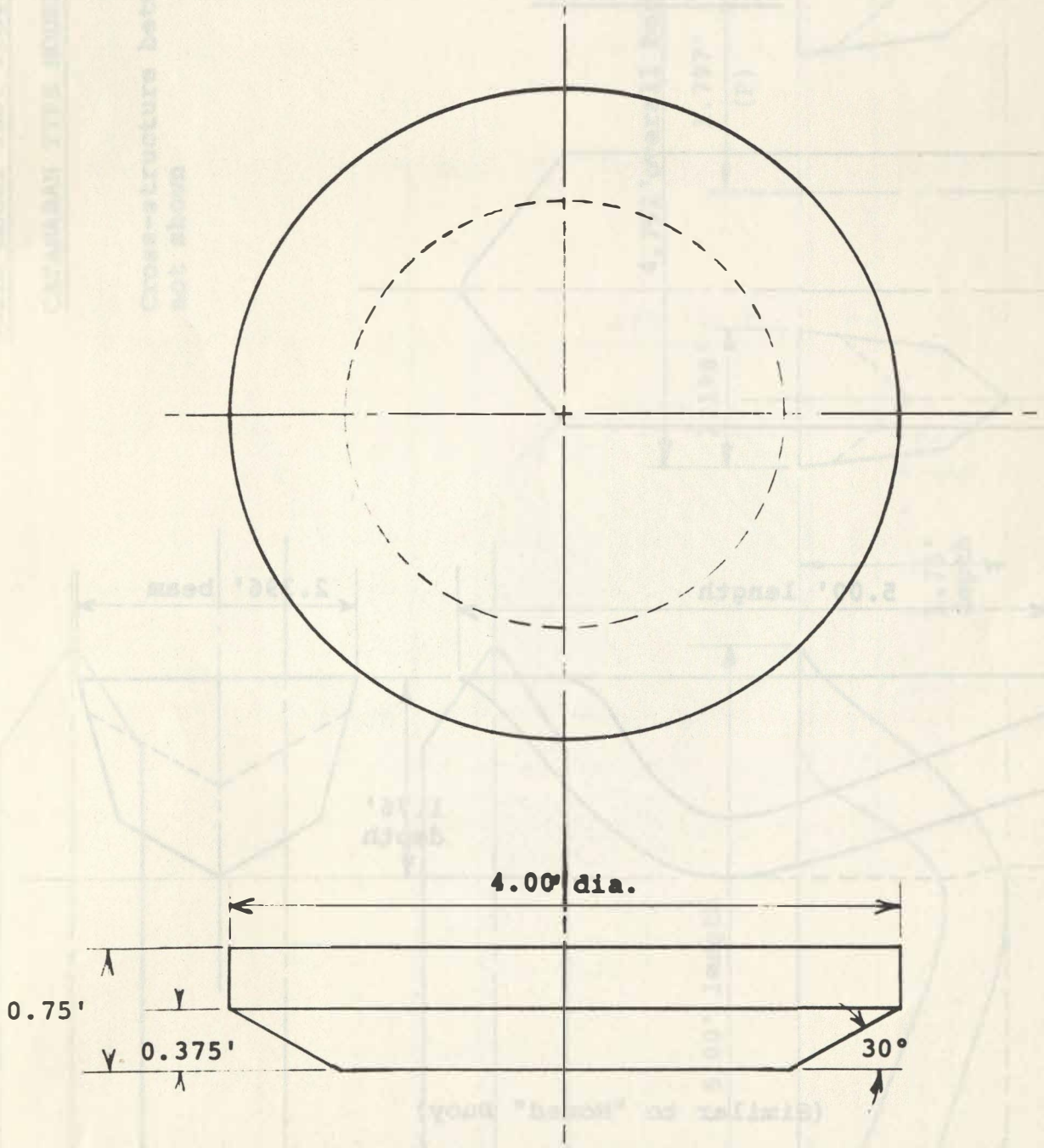

(Similar to "Monster" Buoy)

Fig. 1 Lines Sketch - Disc Buoy

NDBP

Scale Model Test Program

BOAT TYPE MODEL

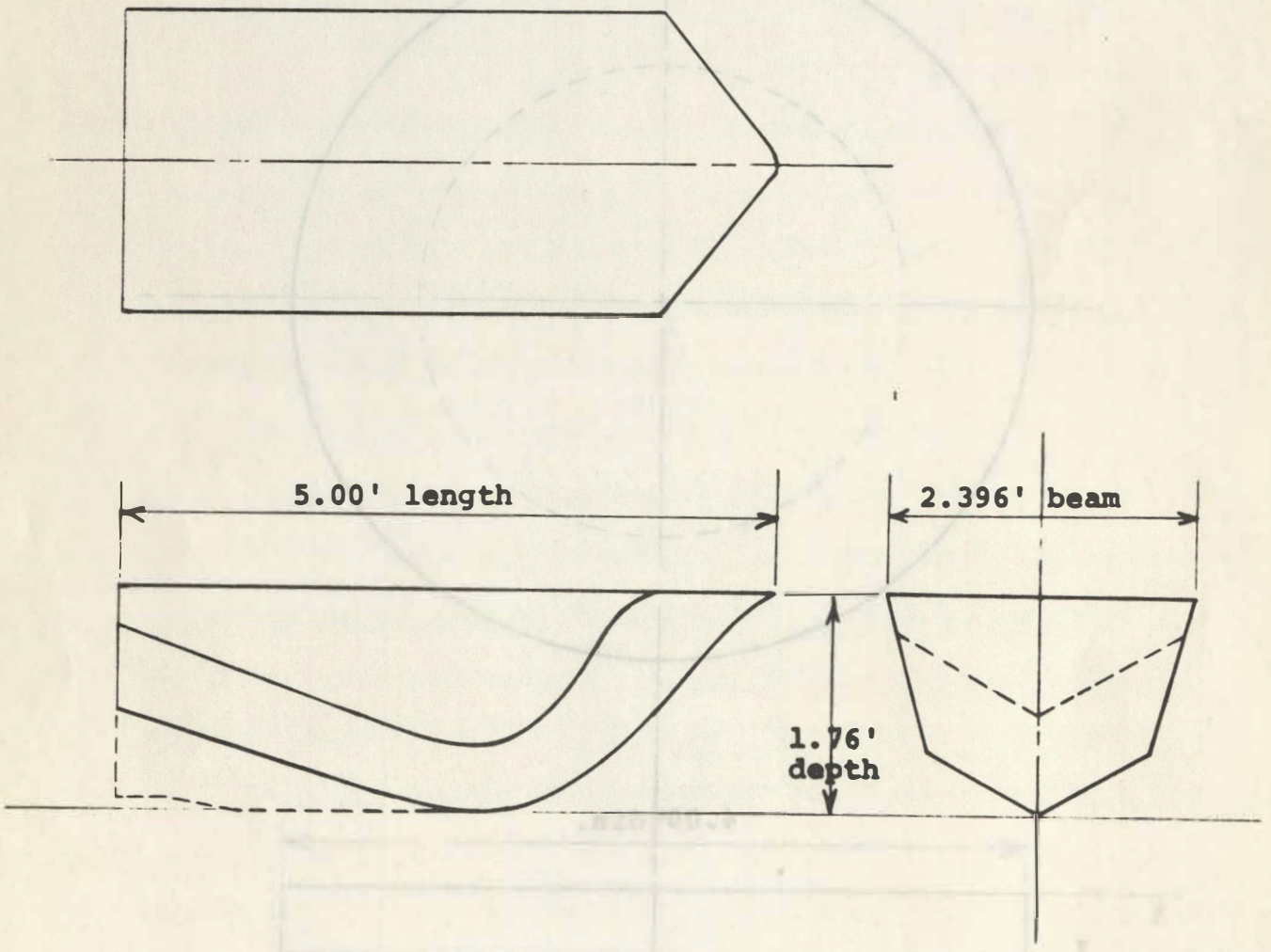

(Similar to "Nomad" Buoy)

Fig. 2 Lines Sketch - Boat Buoy

NDBP

Scale Model Test Program

CATAMARAN TYPE MODEL

Cross-structure between hulls not shown

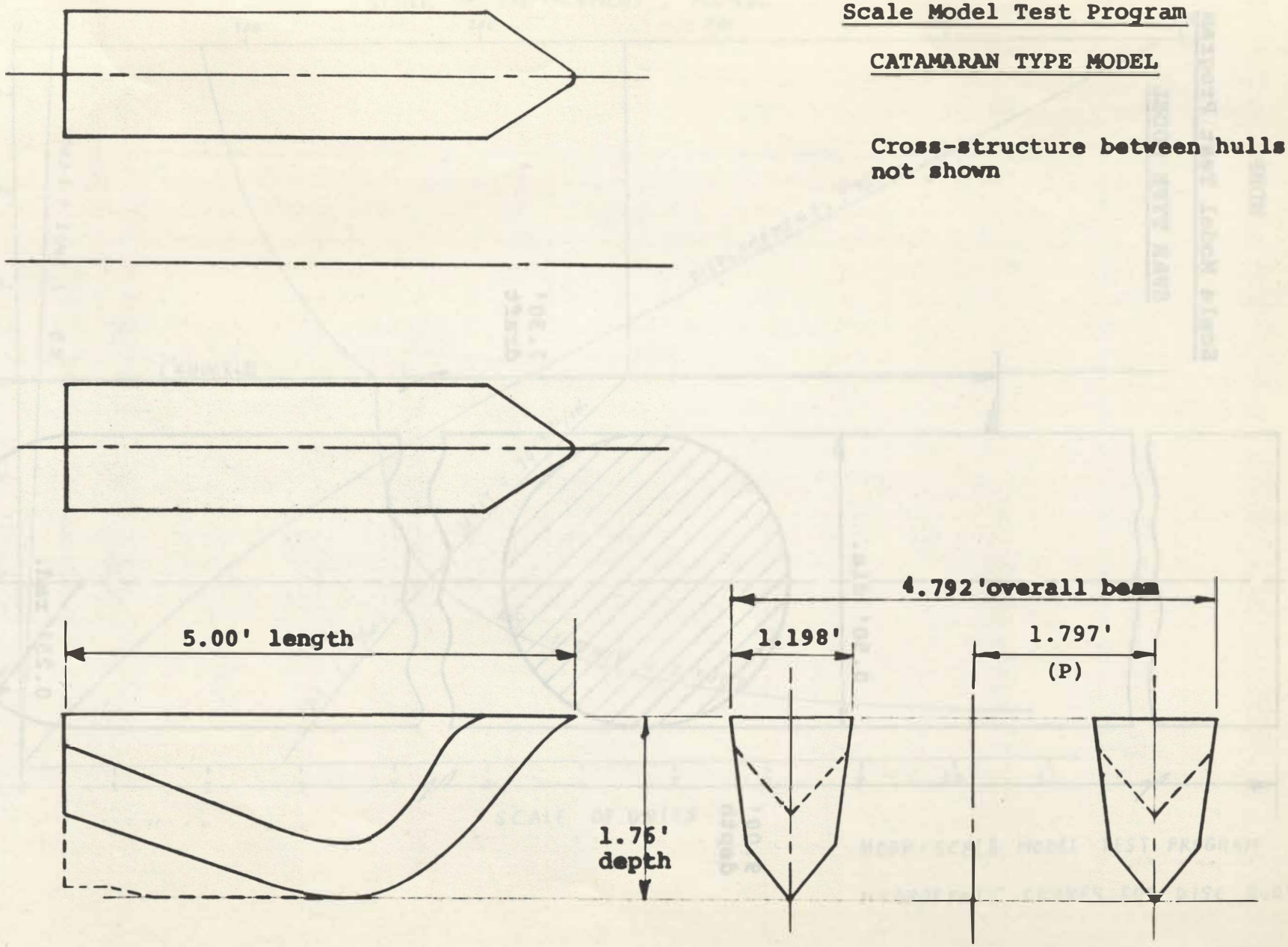

Fig. 3 Lines Sketch - Catamaran Buoy

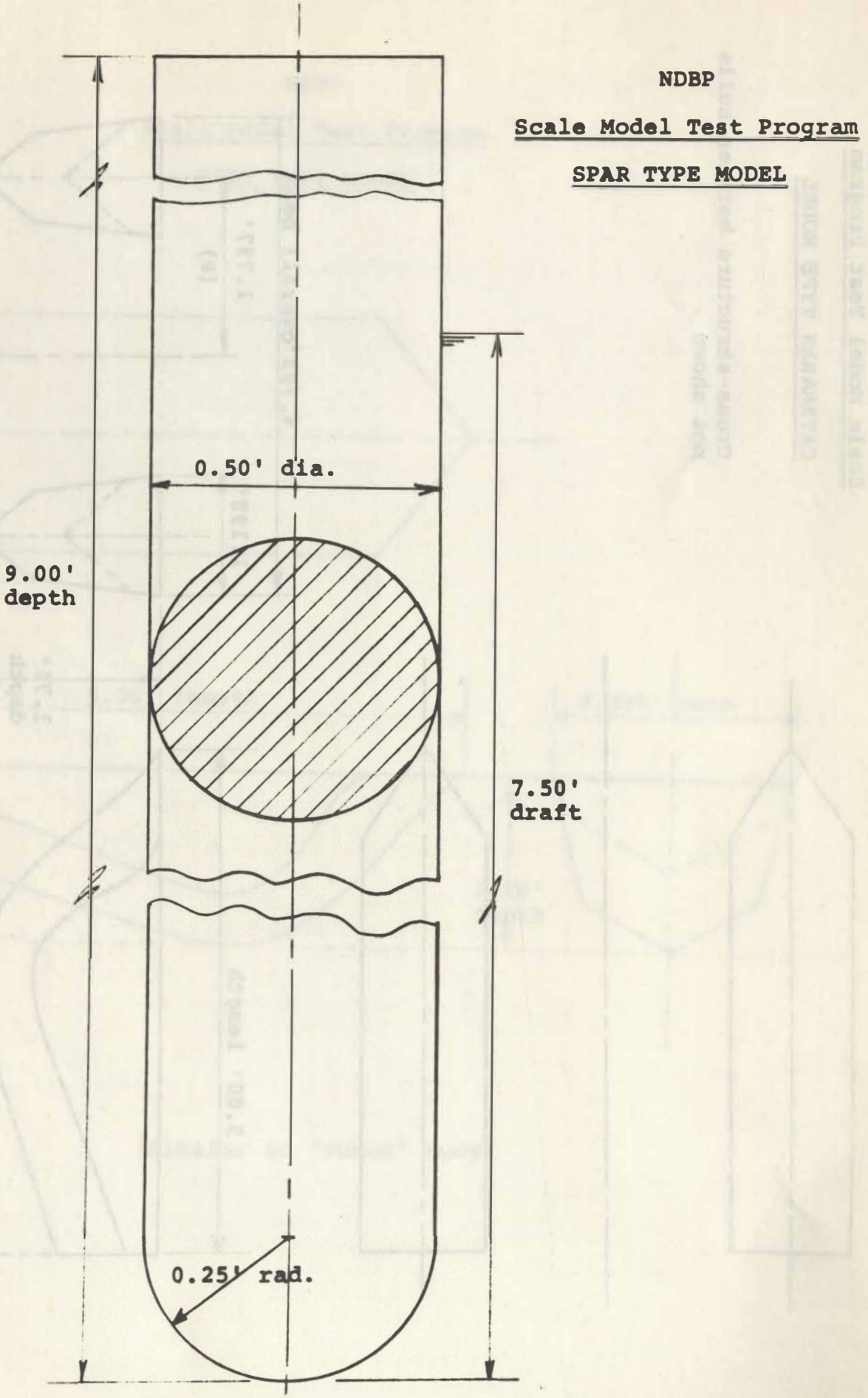

Fig. 4 Lines Sketch - Spar Buoy

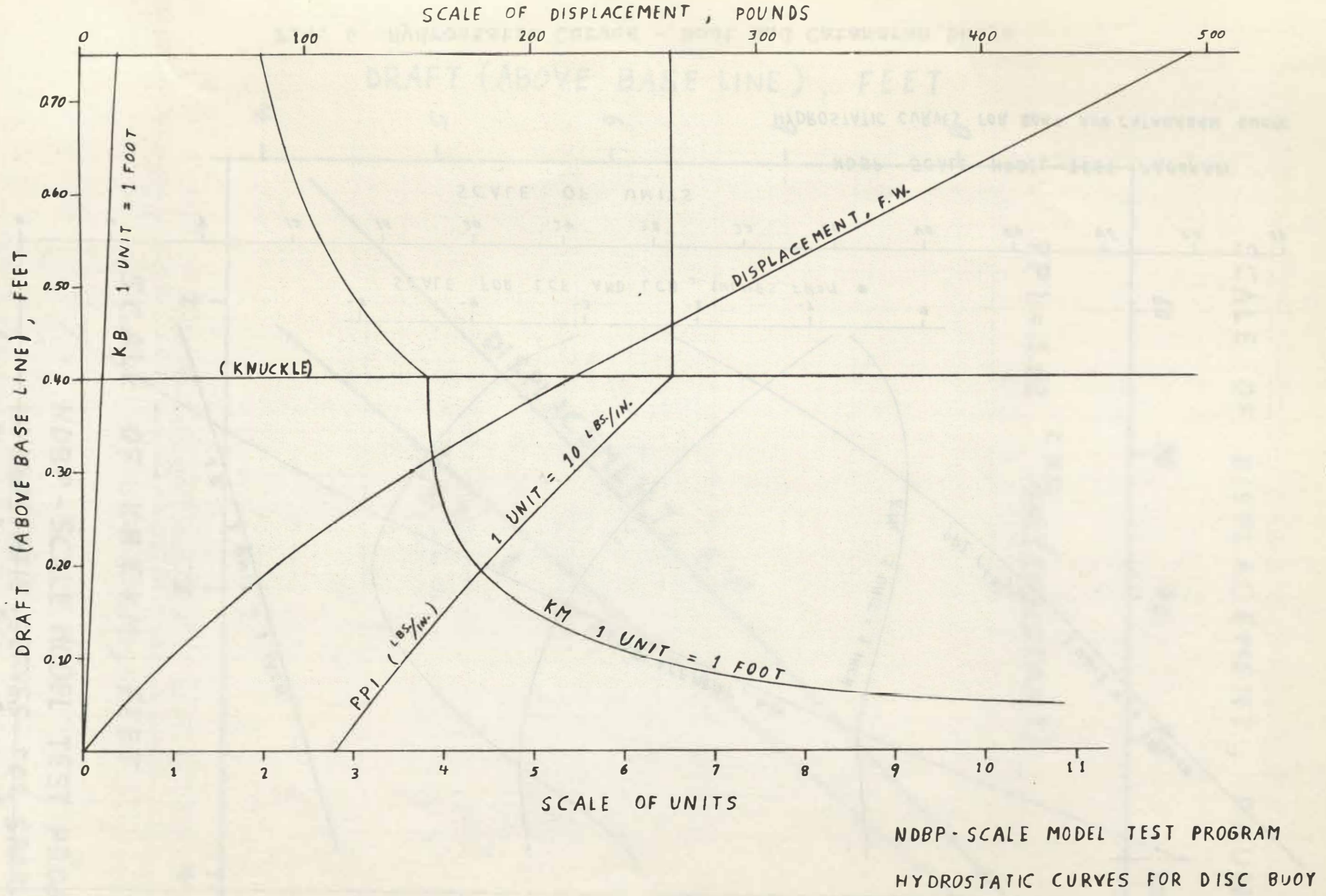

Fig. 5 Hydrostatic Curves - Disc Buoy

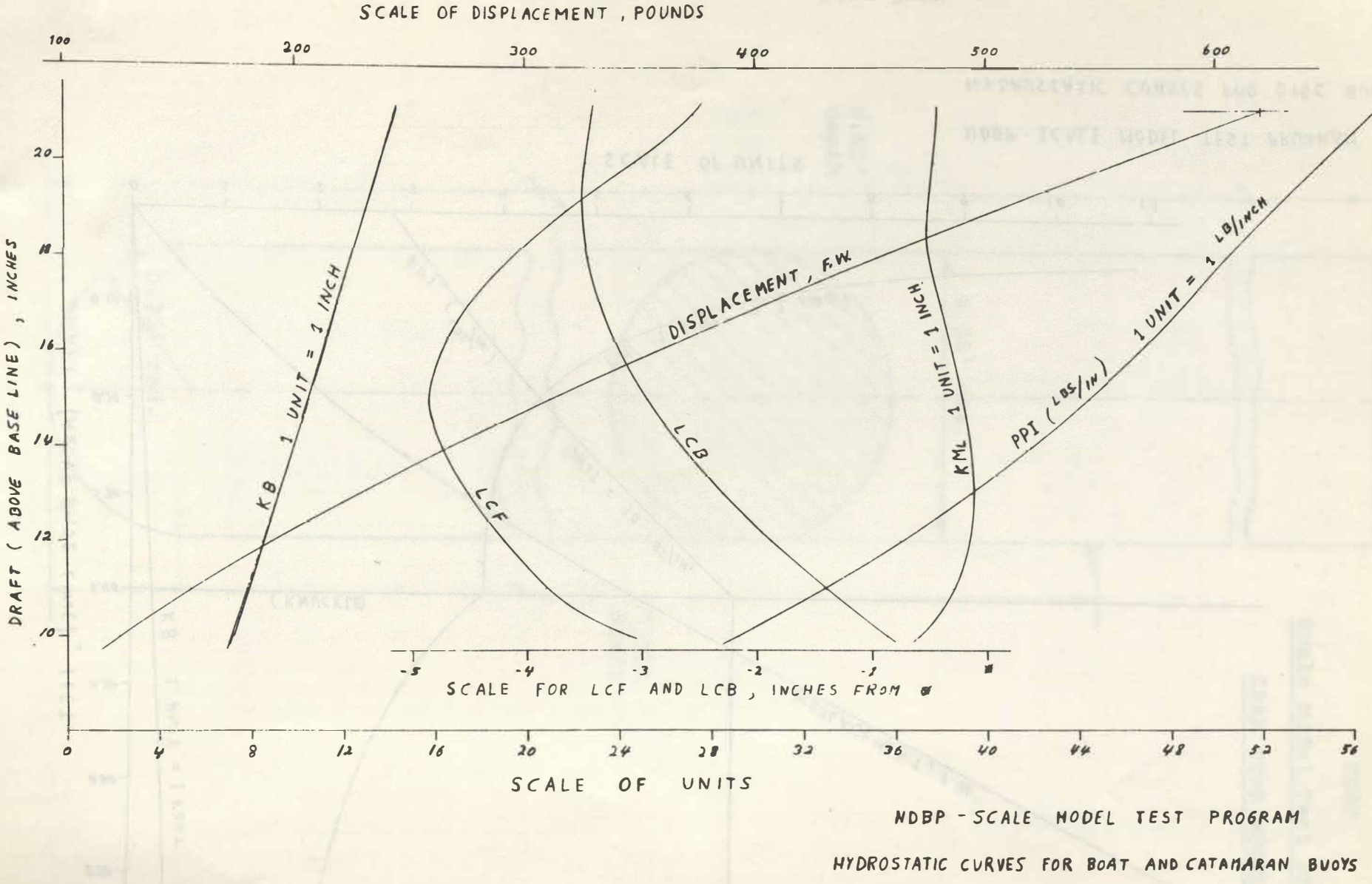

Fig. 6 Hydrostatic Curves - Boat and Catamaran Buoys

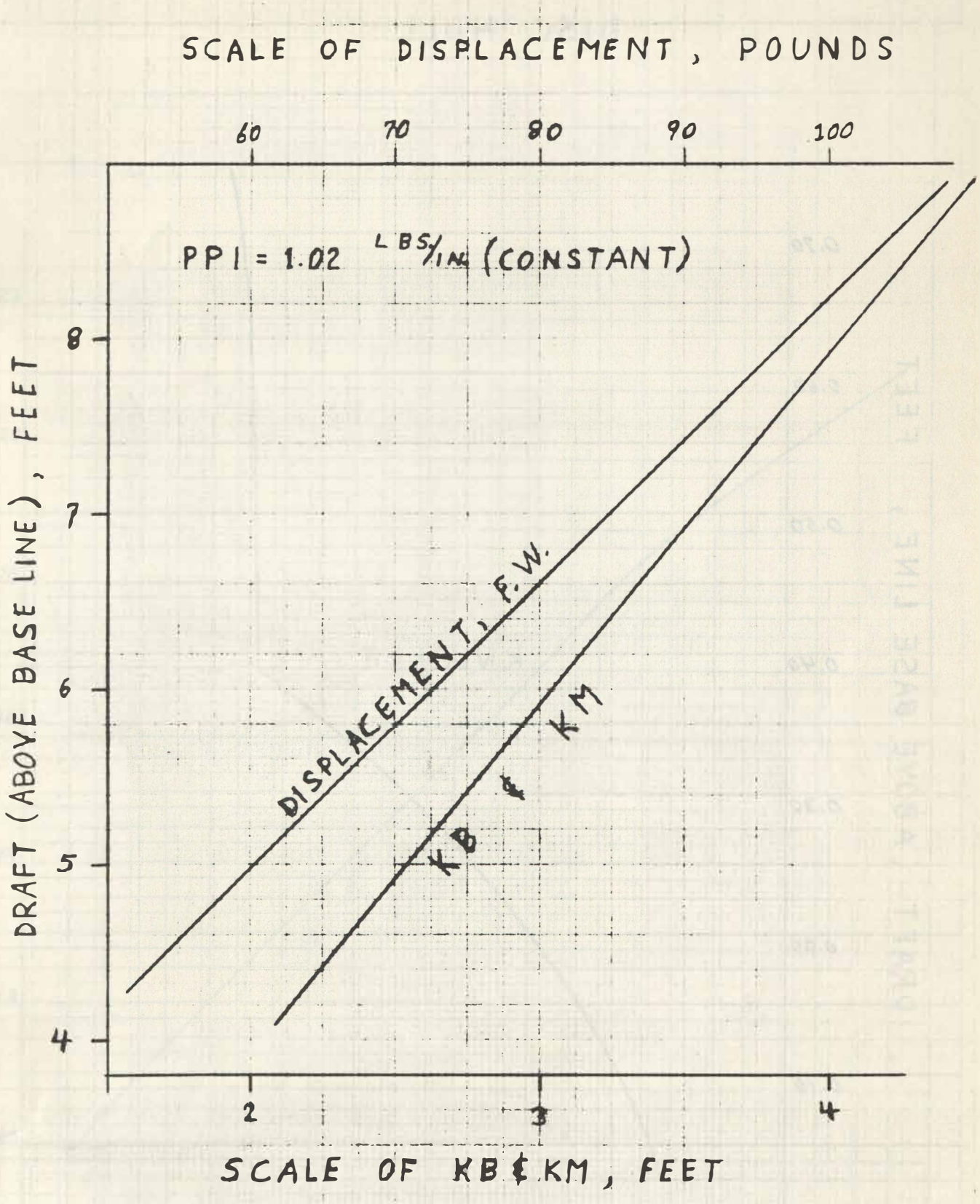

Fig. 7 Hydrostatic Curves - Spar Buoy

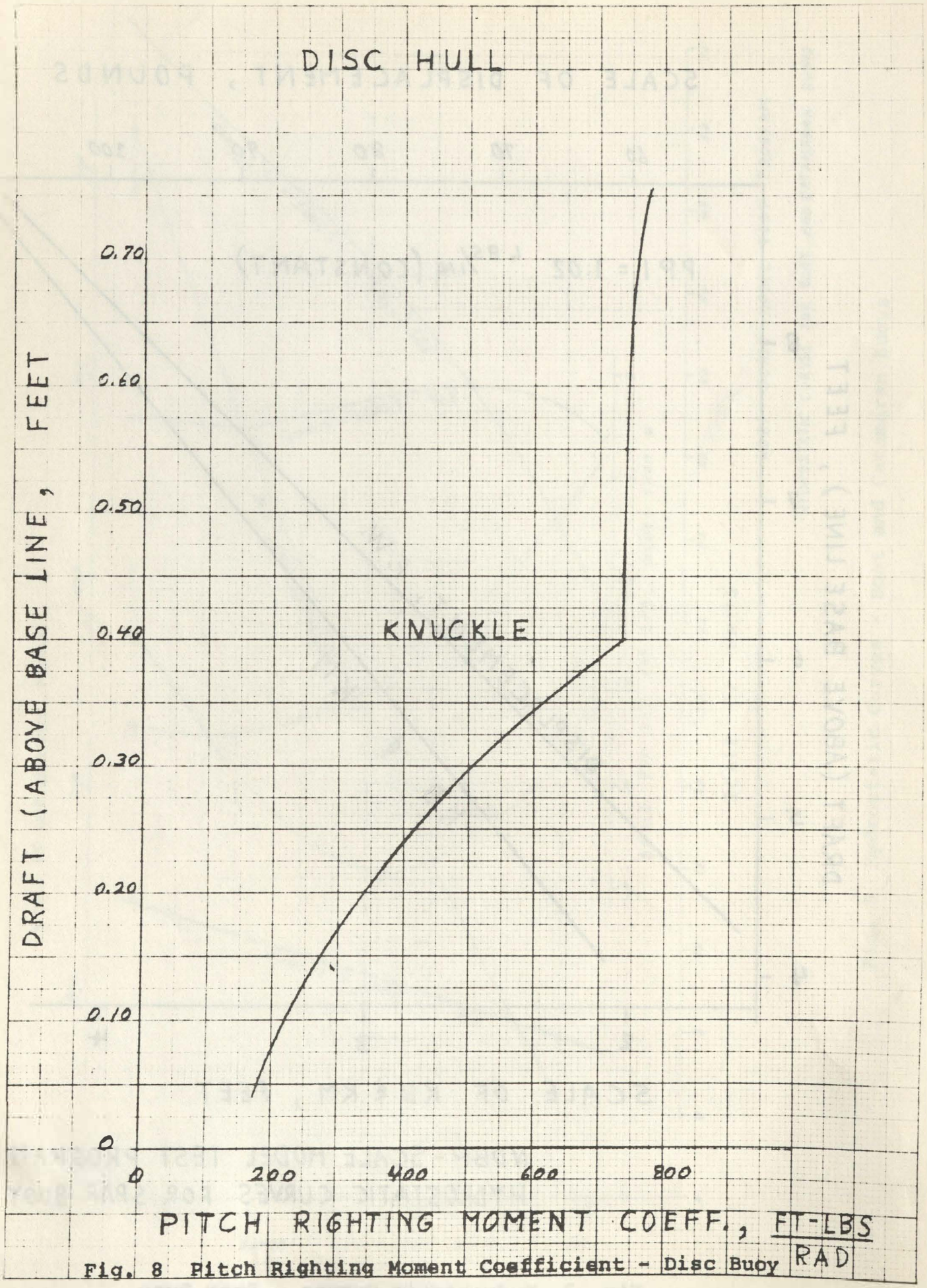

Fig. 8 Pitch Righting Moment Coefficient - Disc Buoy

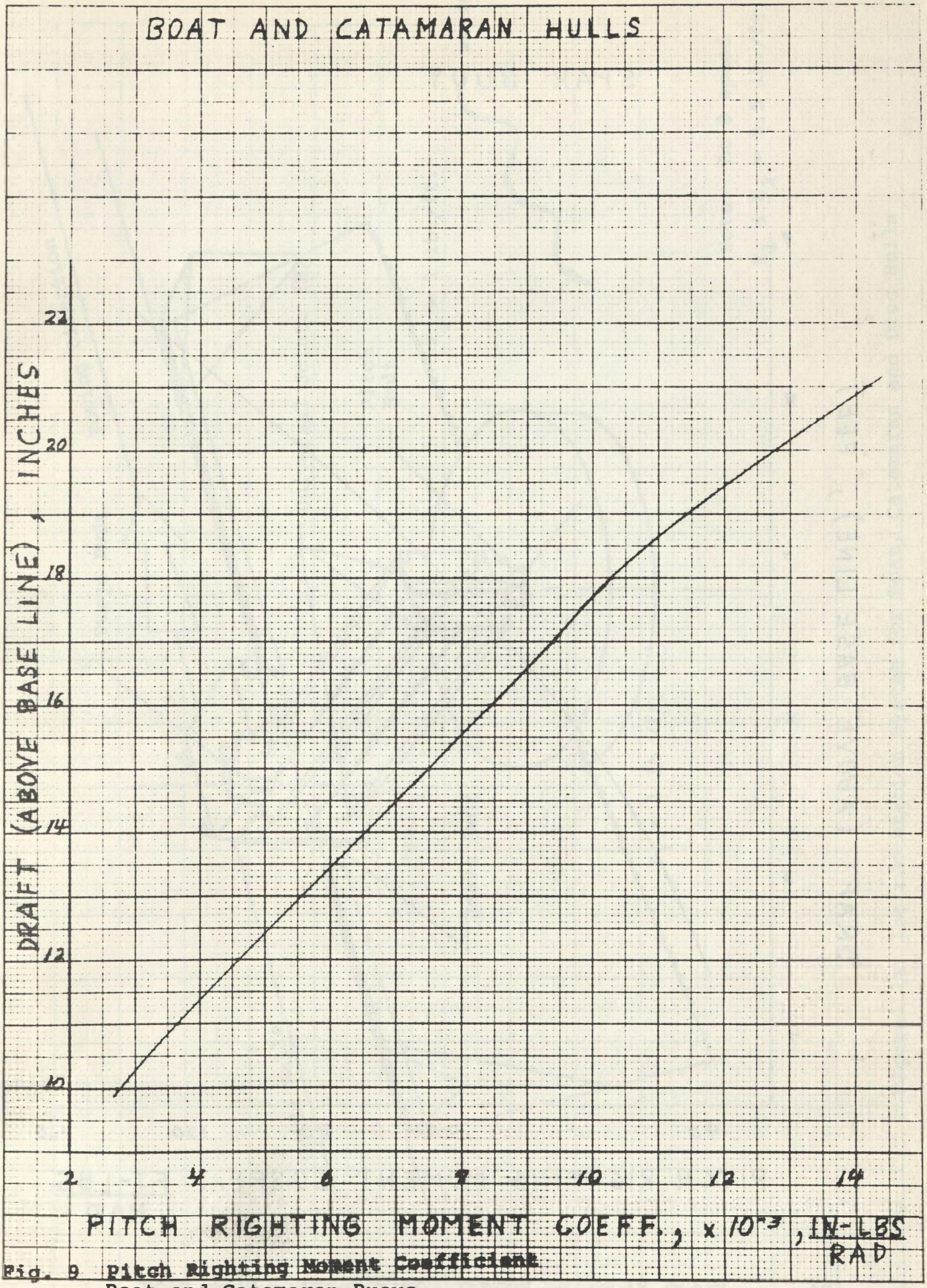

Fig. 9 Pitch Righting Moment Coefficient
Boat and Catamaran Buoys

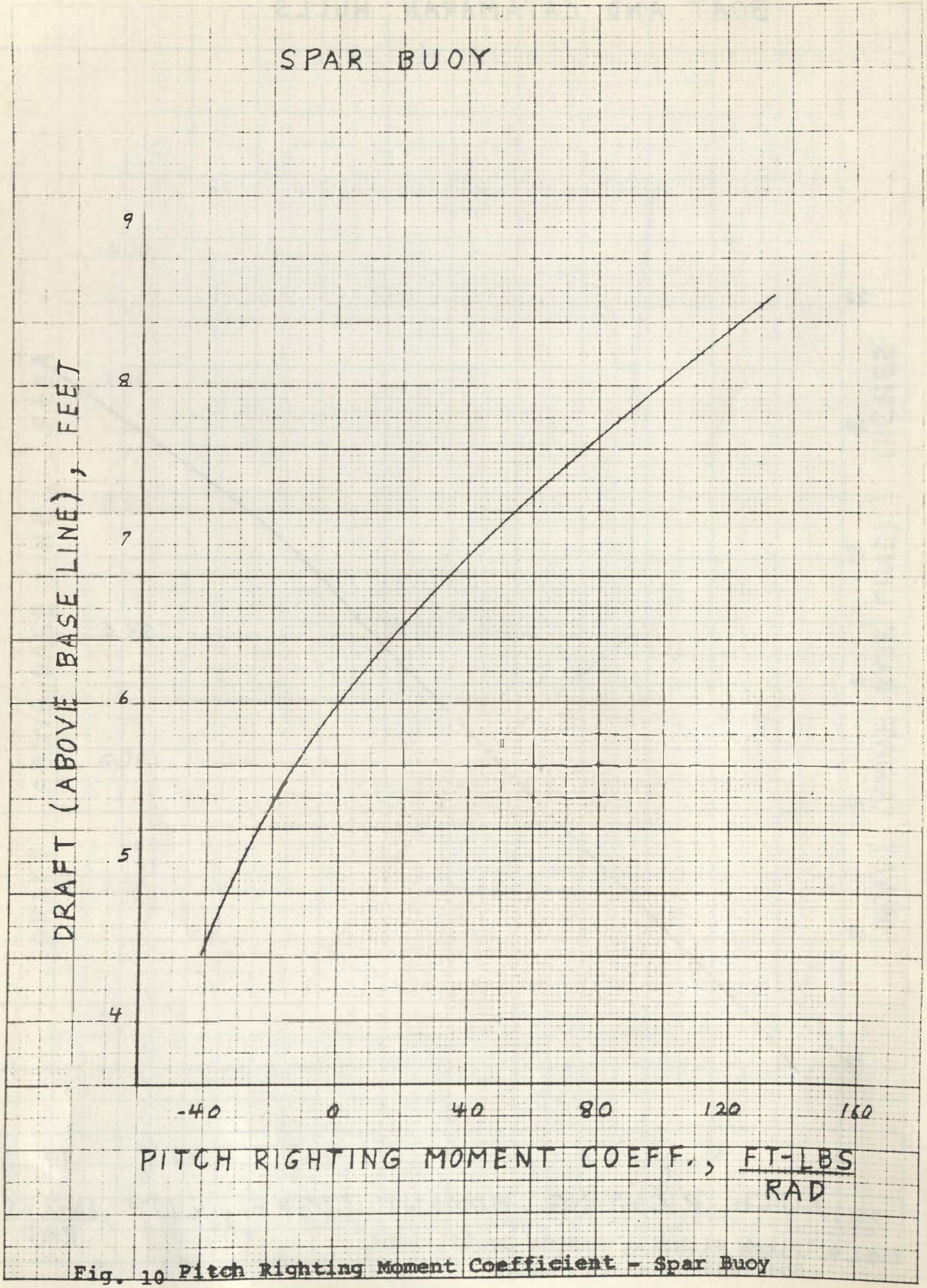

Fig. 10 Pitch Righting Moment Coefficient - Spar Buoy

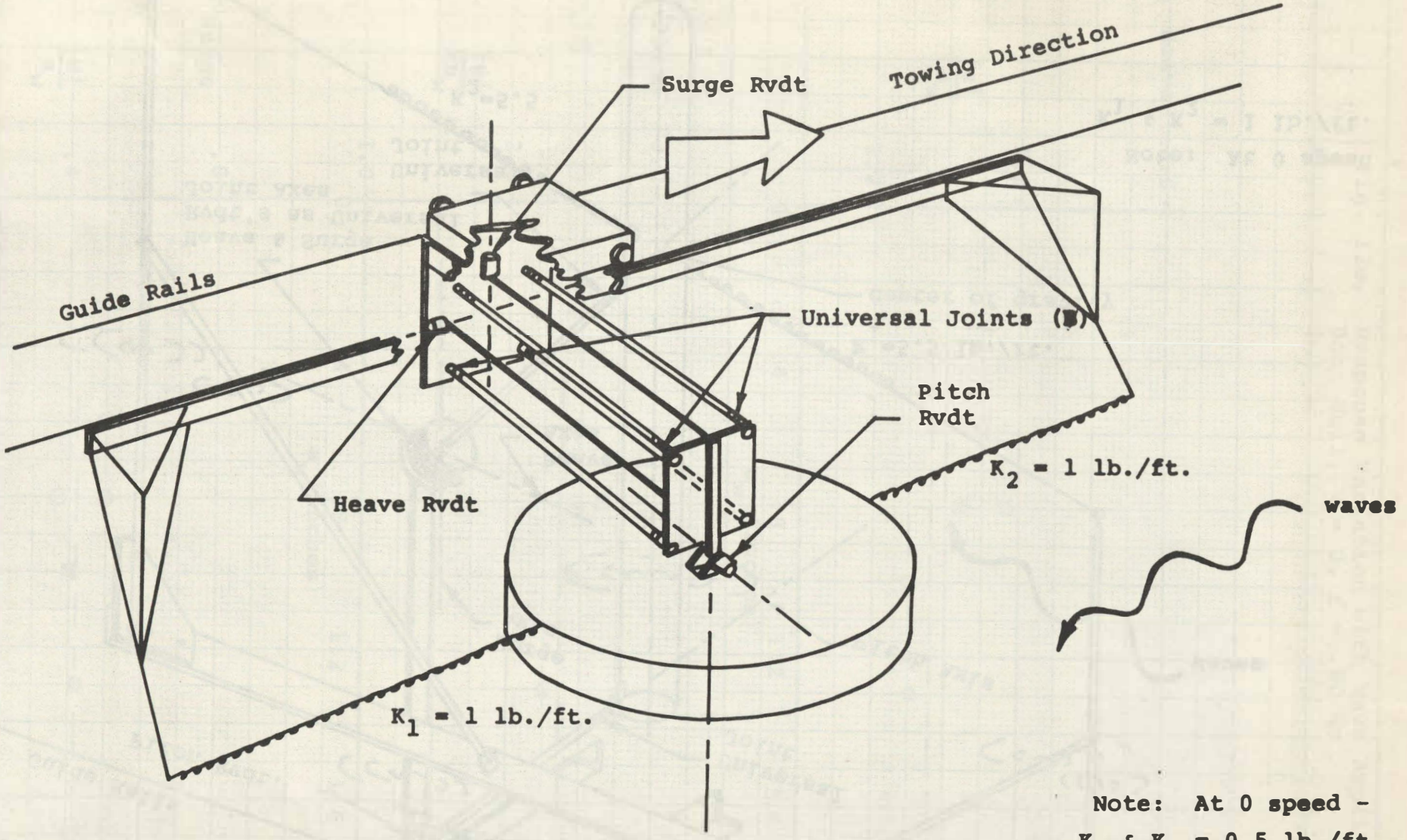

Figure 11a. Instrumentation System for Boat, Catamaran and Disc Hulls

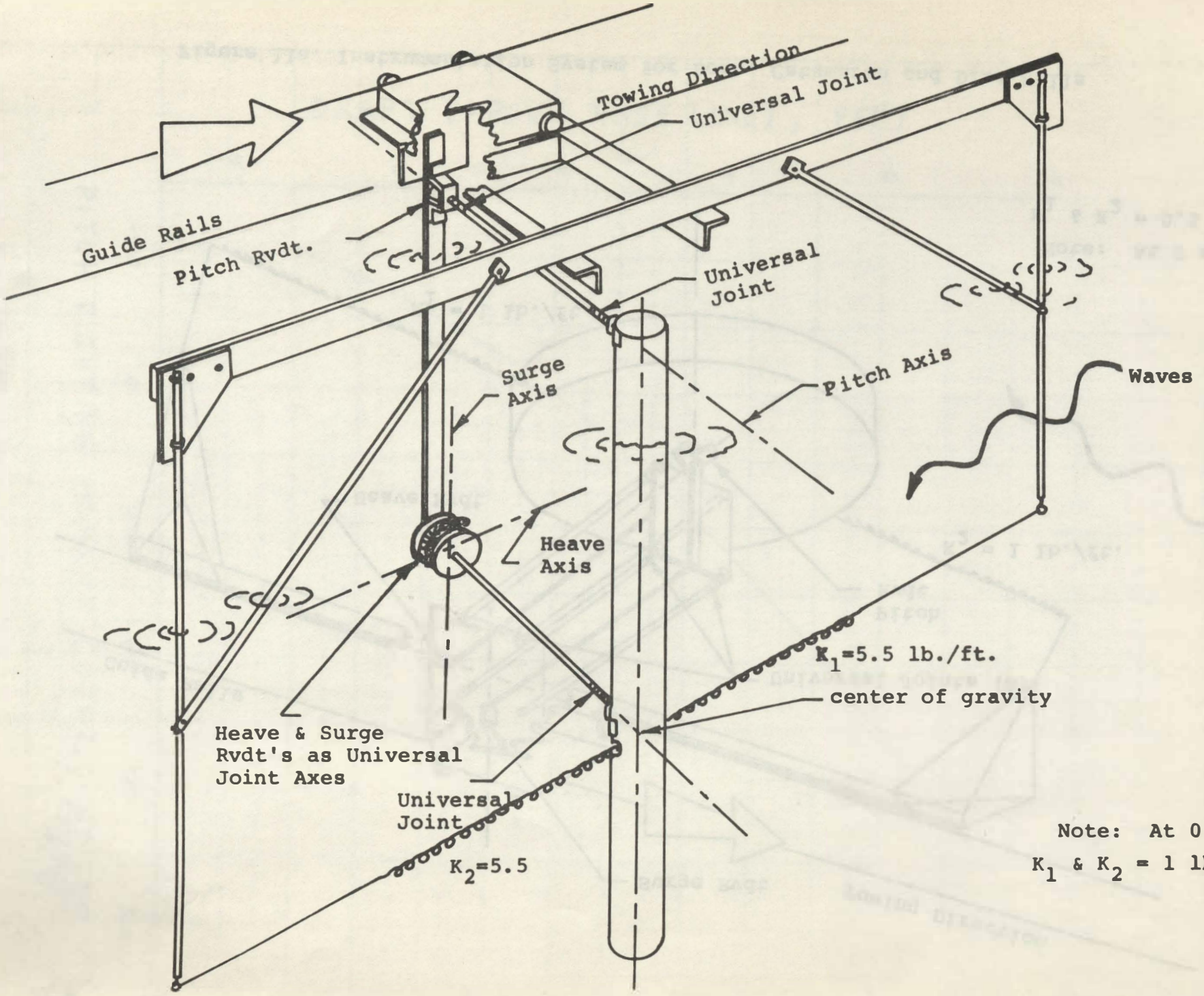

Figure 11b. Instrumentation System for Spar Buoy

Fig. 12a. Response Variation with Wave Amplitude
Boat Hull, V = 0, f = .80 Hz

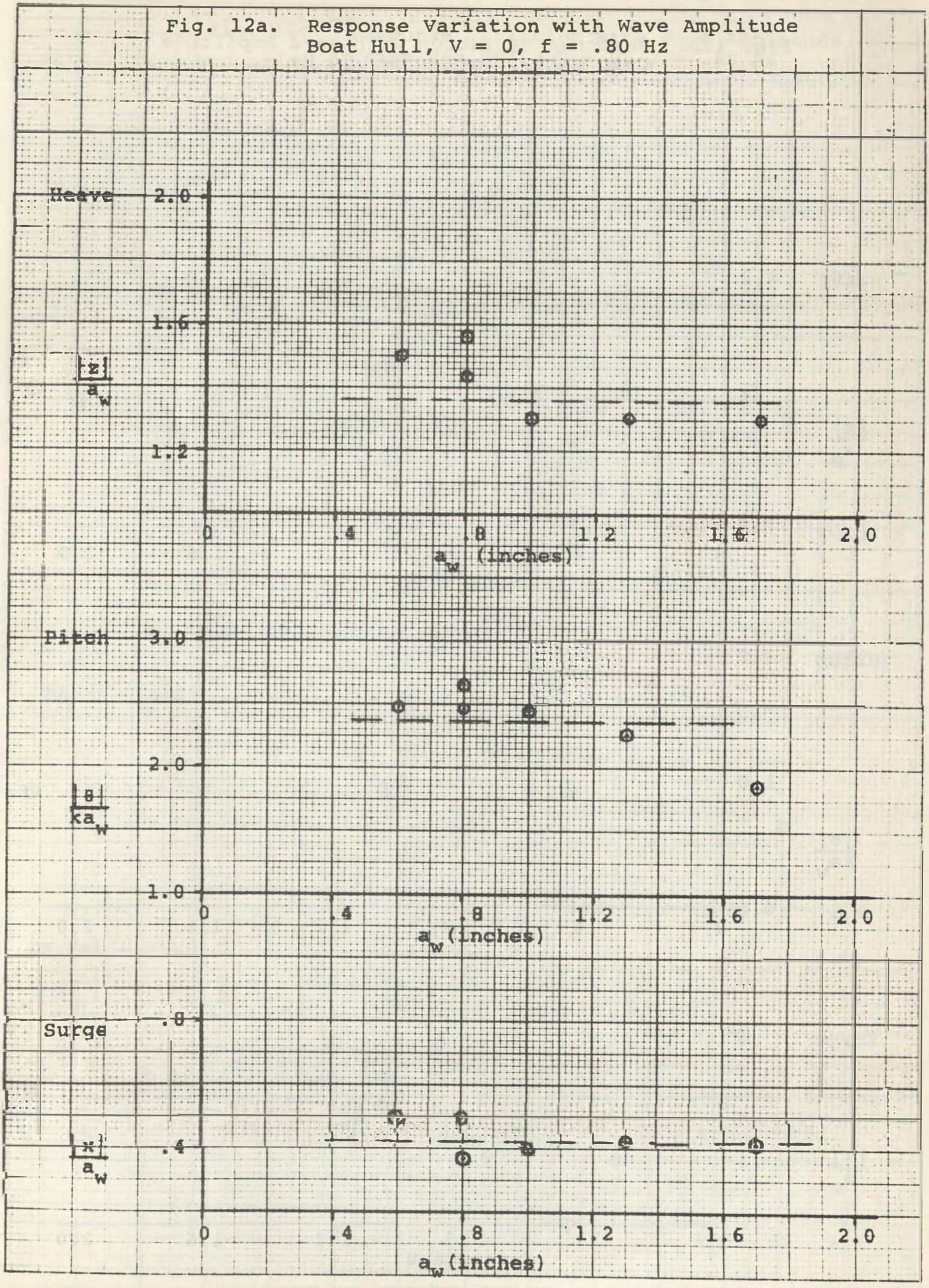

Fig. 12b. Response Variation with Wave Amplitude
Disc Hull, V = 0, f = .70 Hz

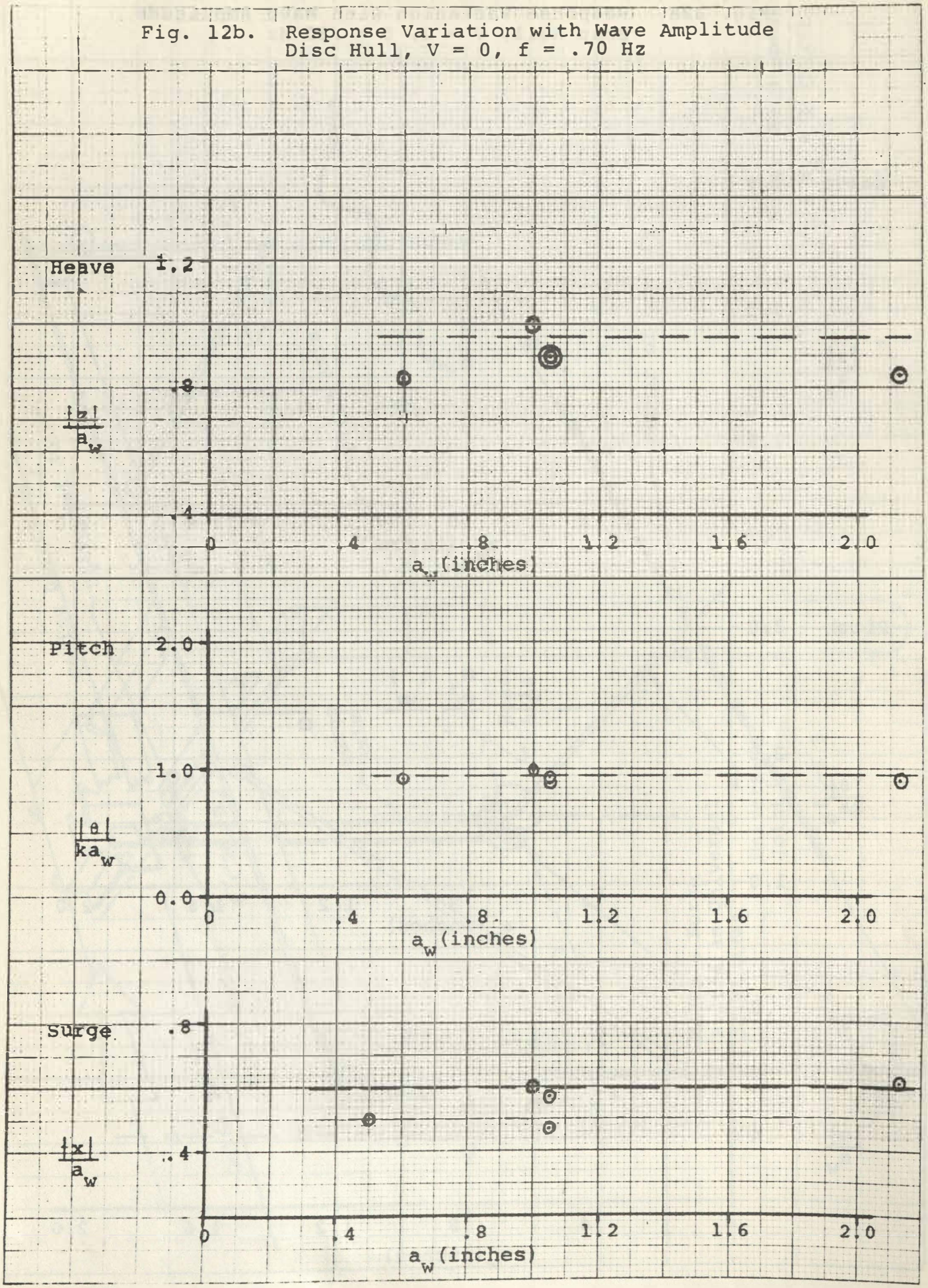

Fig. 12c. Response Variation with Wave Amplitude
Catamaran Hull, V = 0, f = .80 Hz

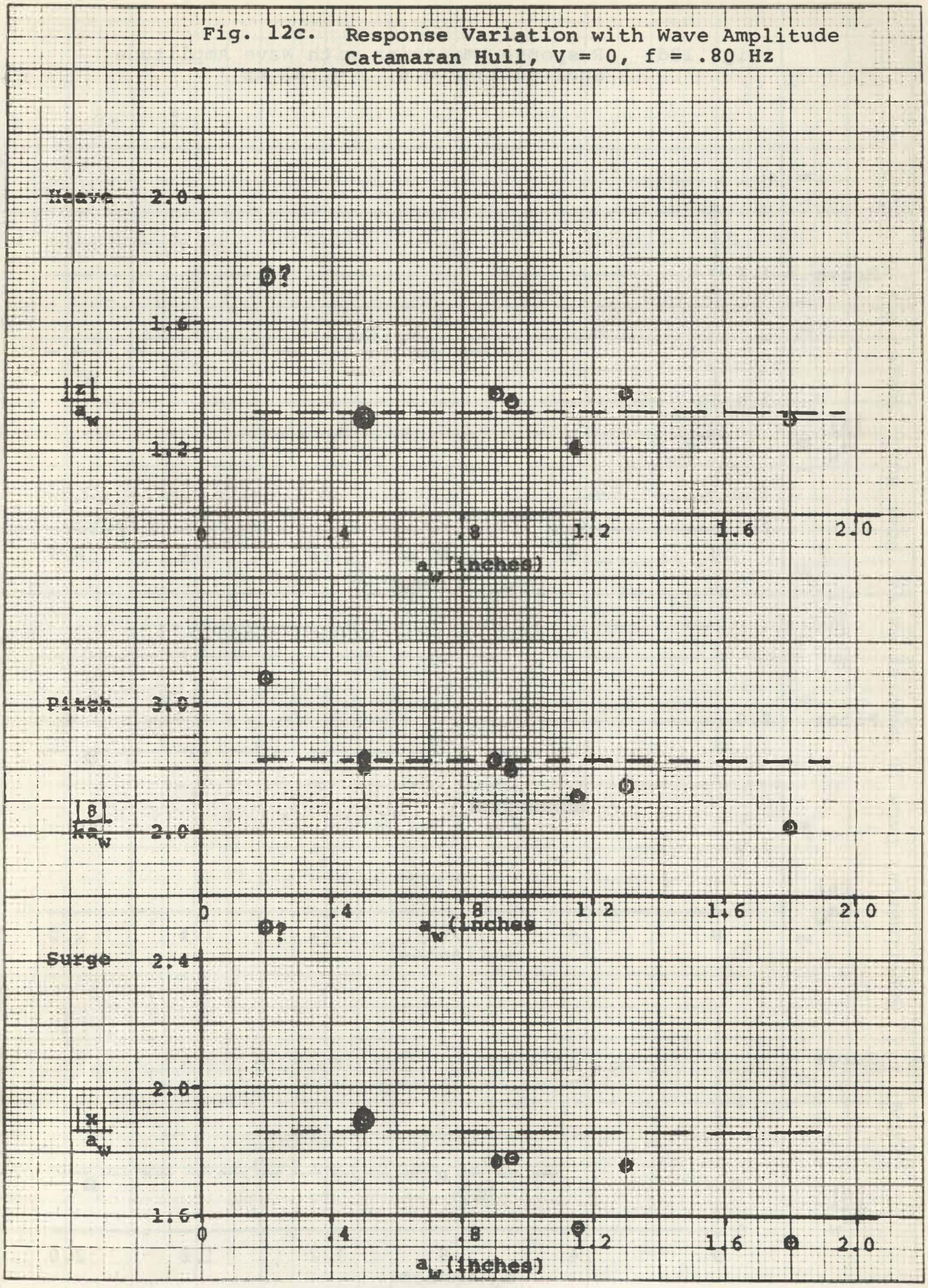

Fig. 12d. Response Variation with Wave Amplitude
Spar Hull, V = 0, f = .37 Hz

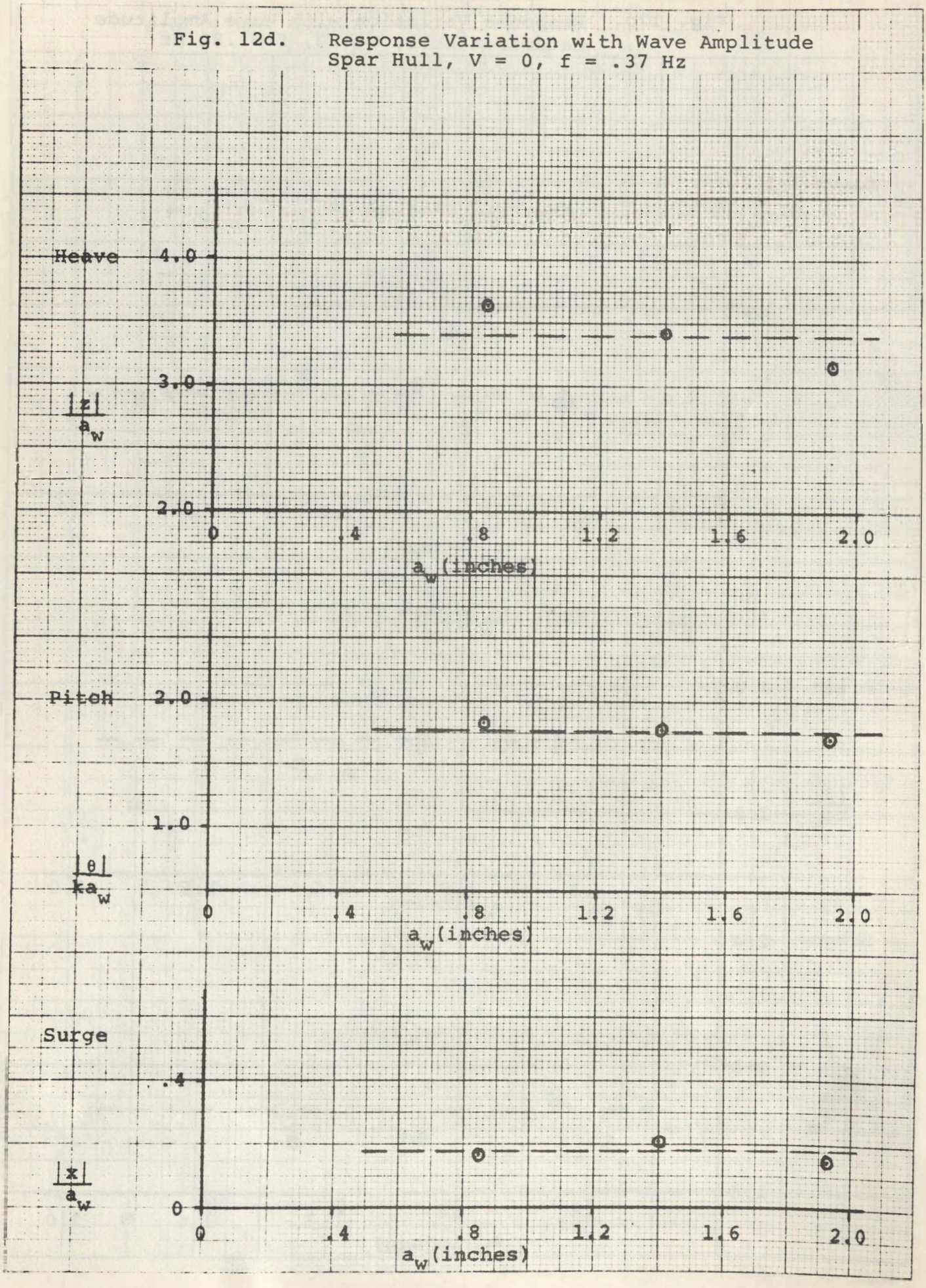

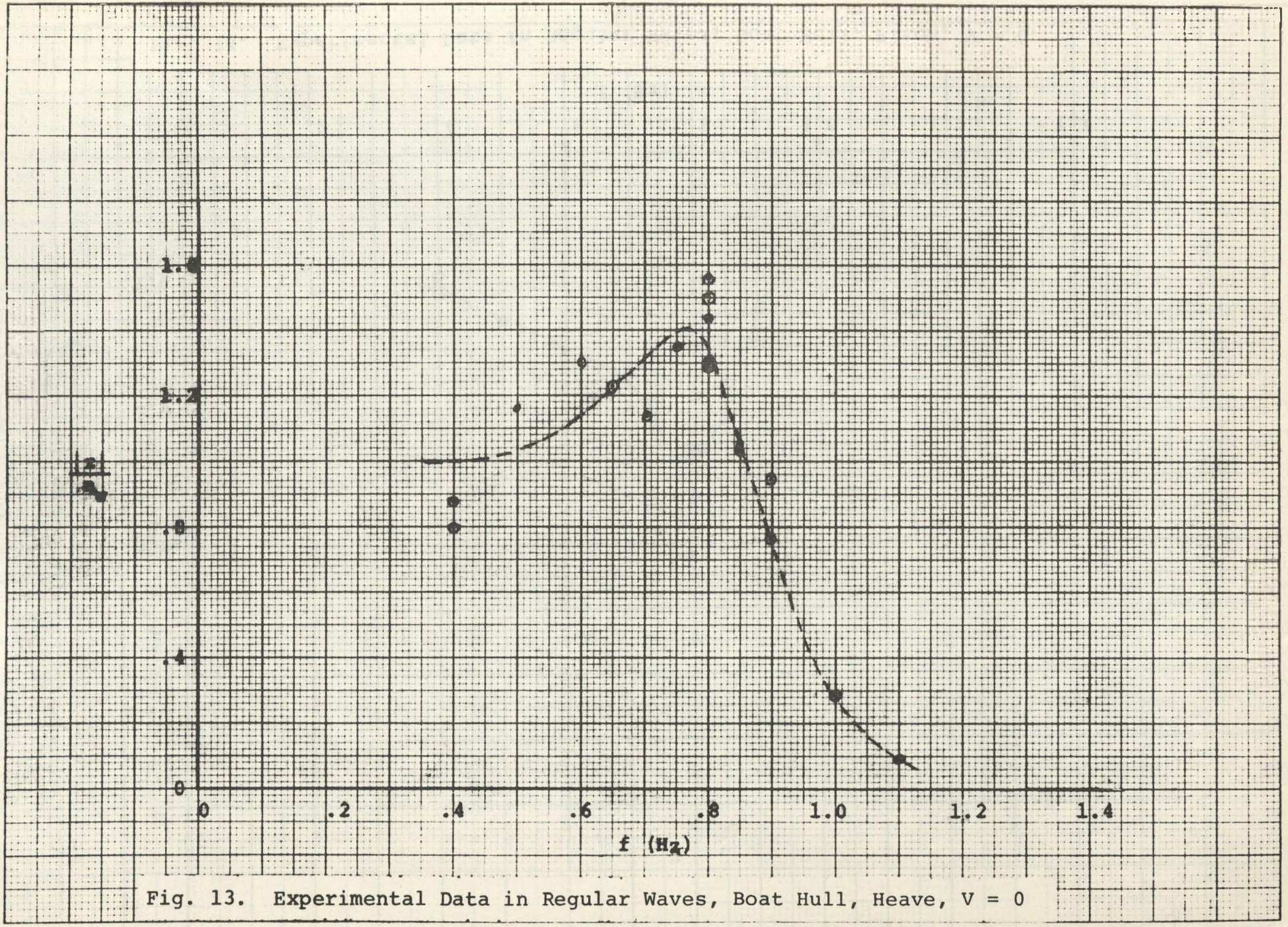

Fig. 13. Experimental Data in Regular Waves, Boat Hull, Heave, V = 0

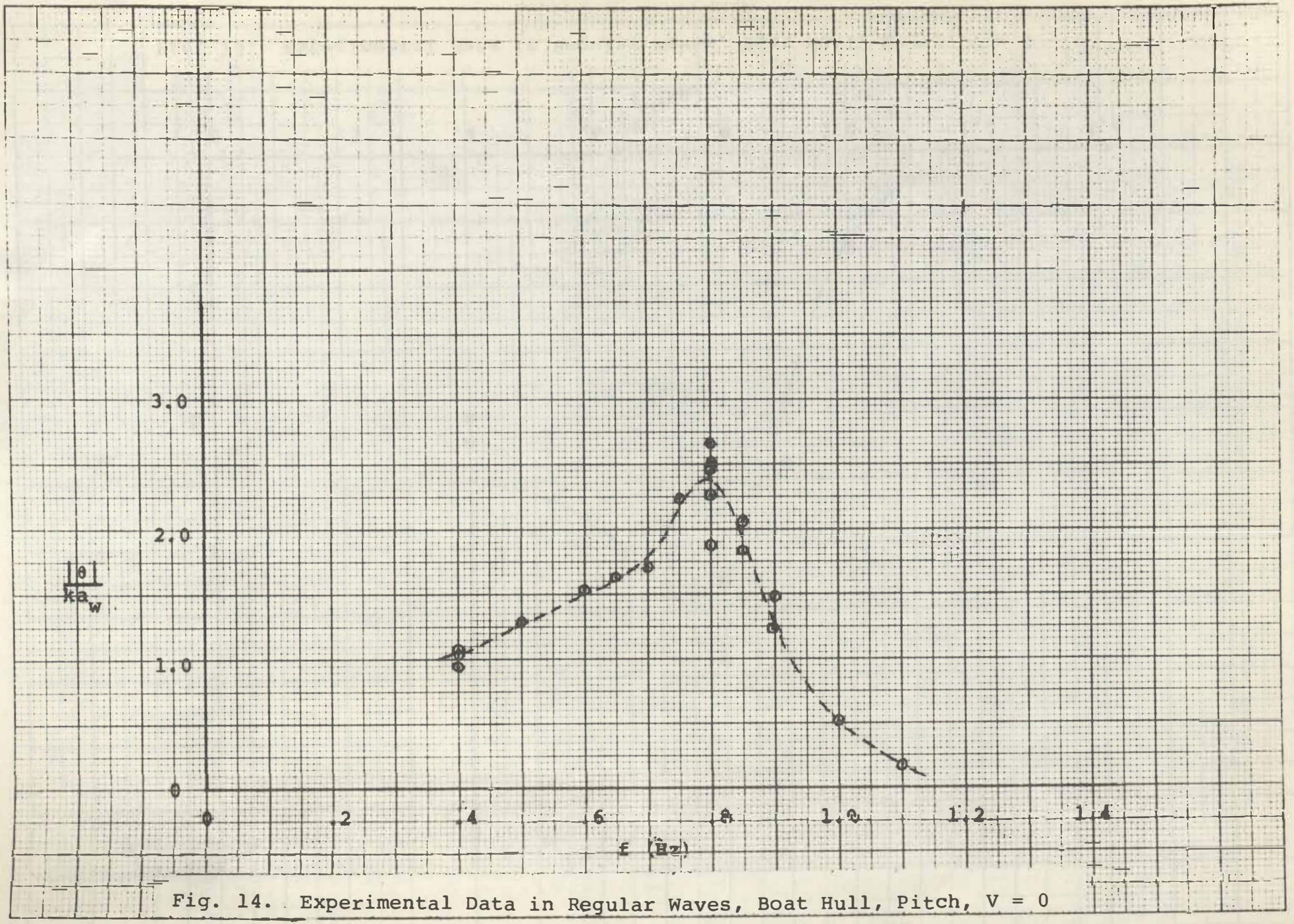

Fig. 14. Experimental Data in Regular Waves, Boat Hull, Pitch, V = 0

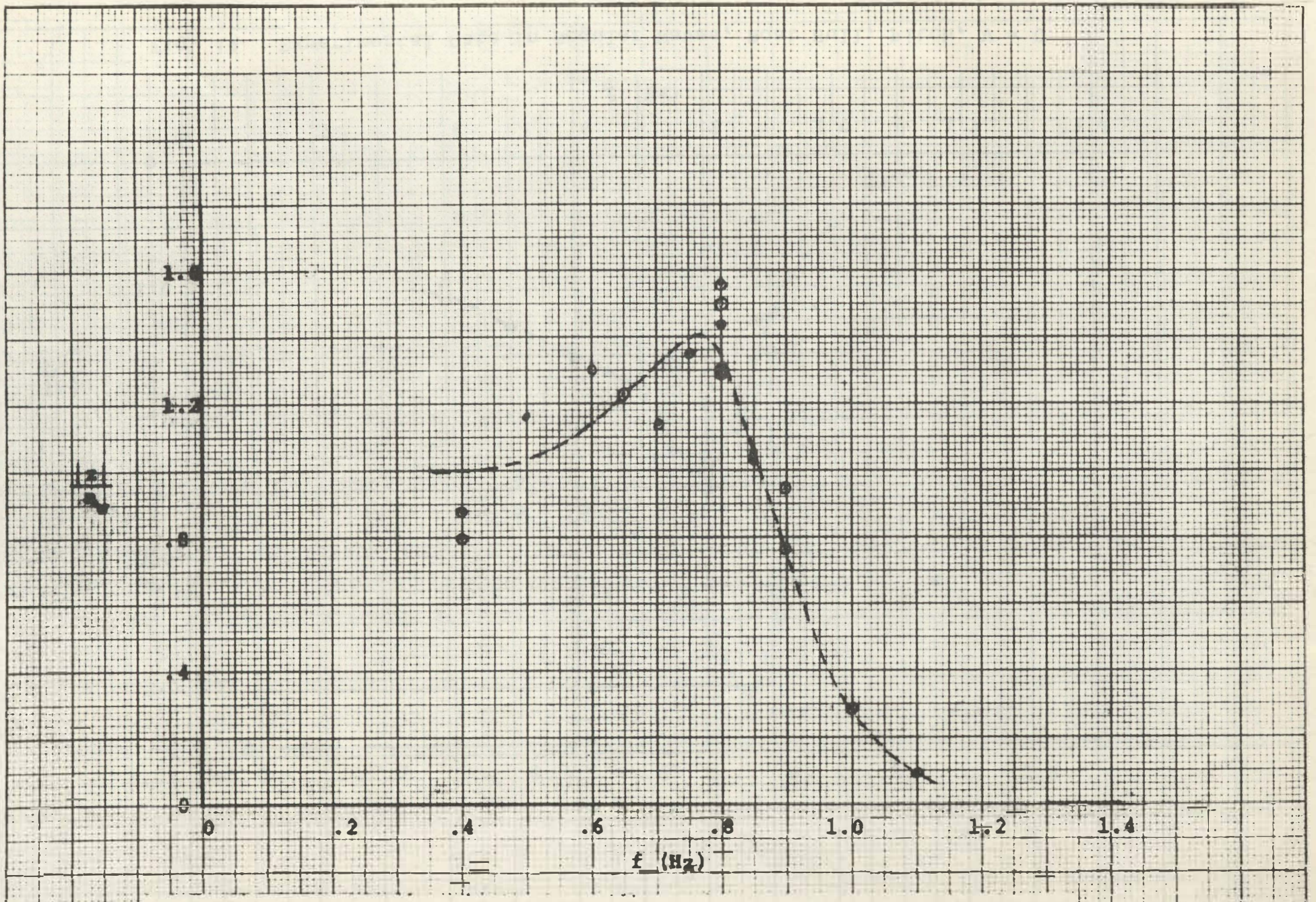

Fig. 13. Experimental Data in Regular Waves, Boat Hull, Heave, V = 0

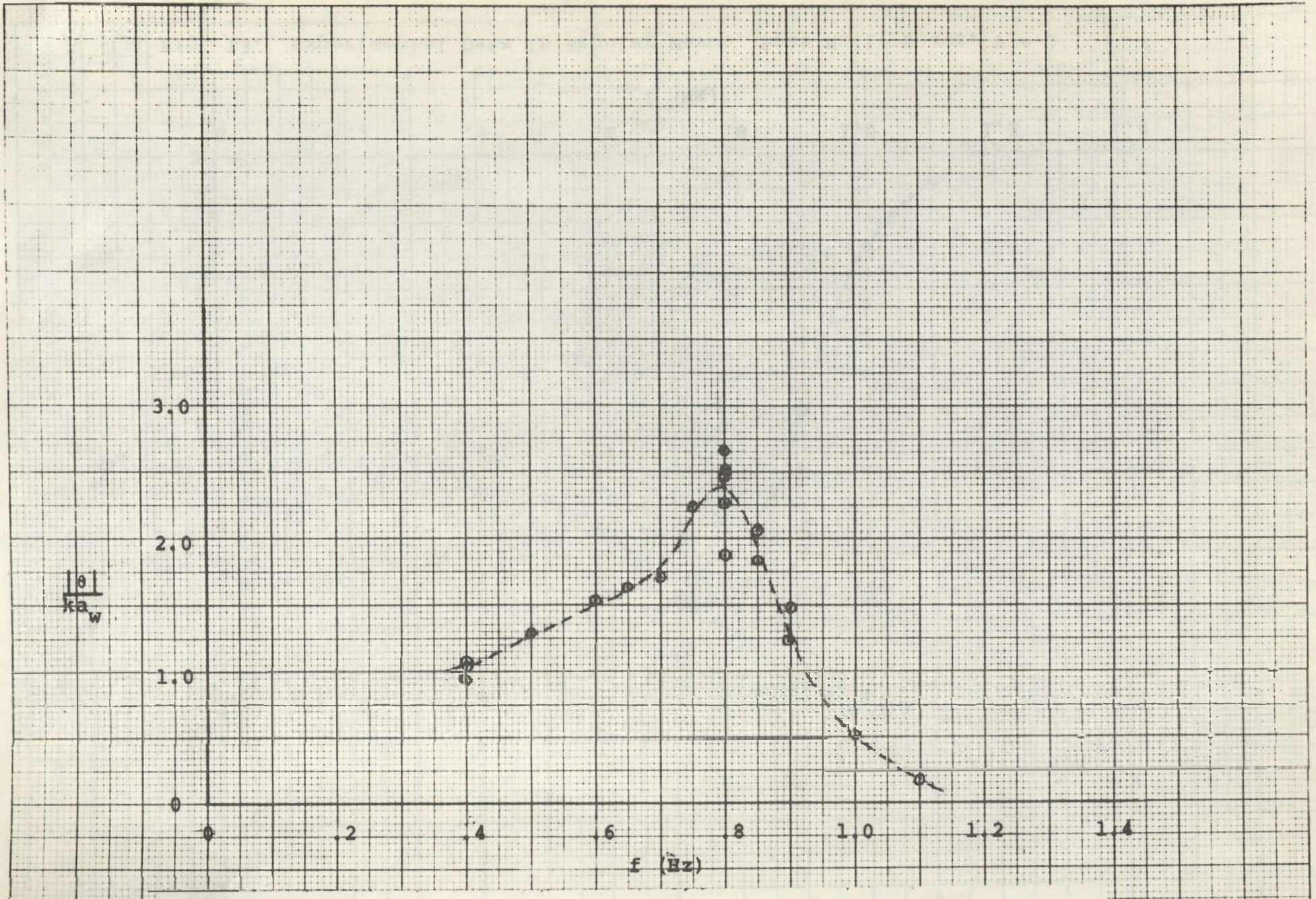

Fig. 14. Experimental Data in Regular Waves, Boat Hull, Pitch, V = 0

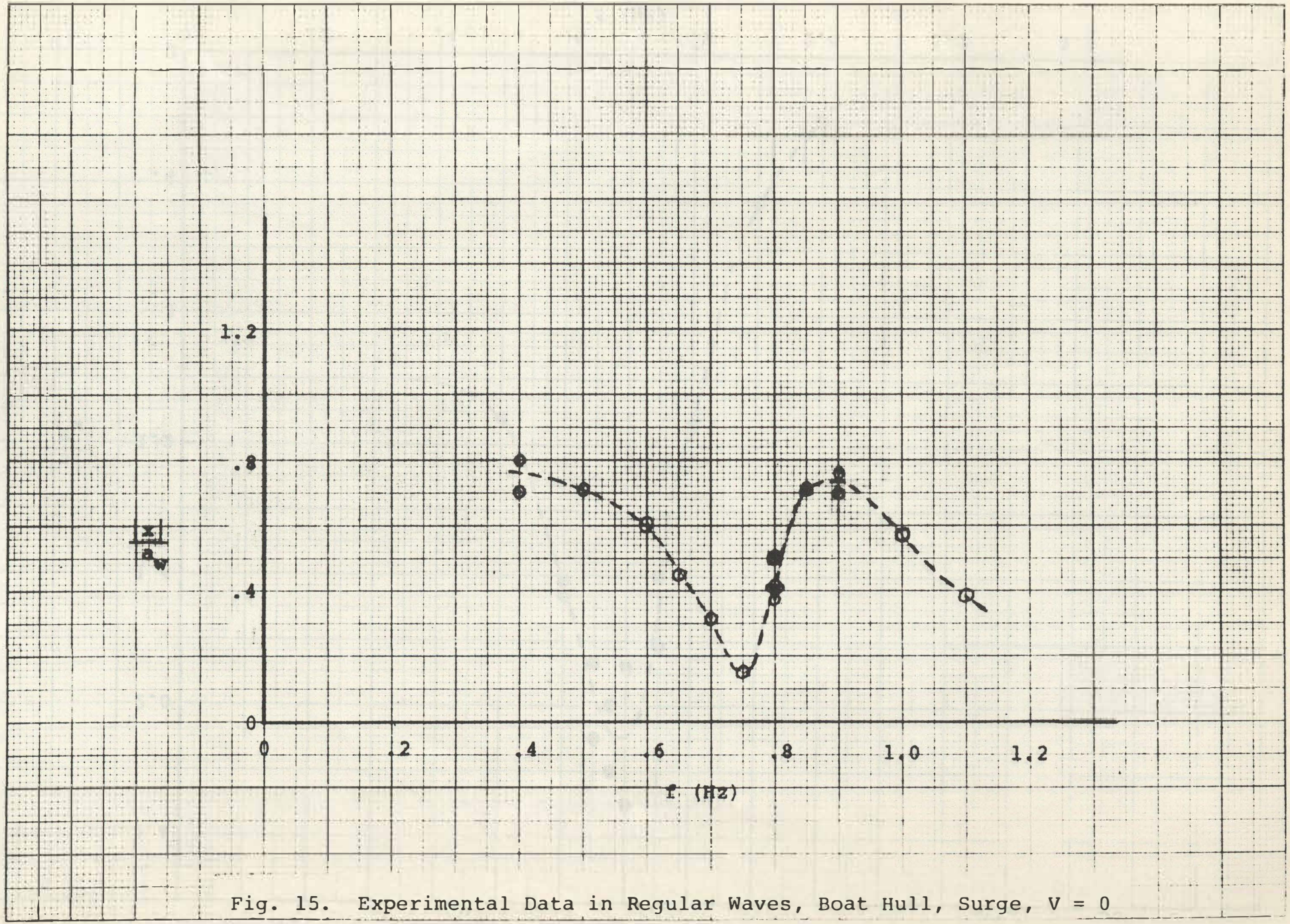

Fig. 15. Experimental Data in Regular Waves, Boat Hull, Surge, V = 0

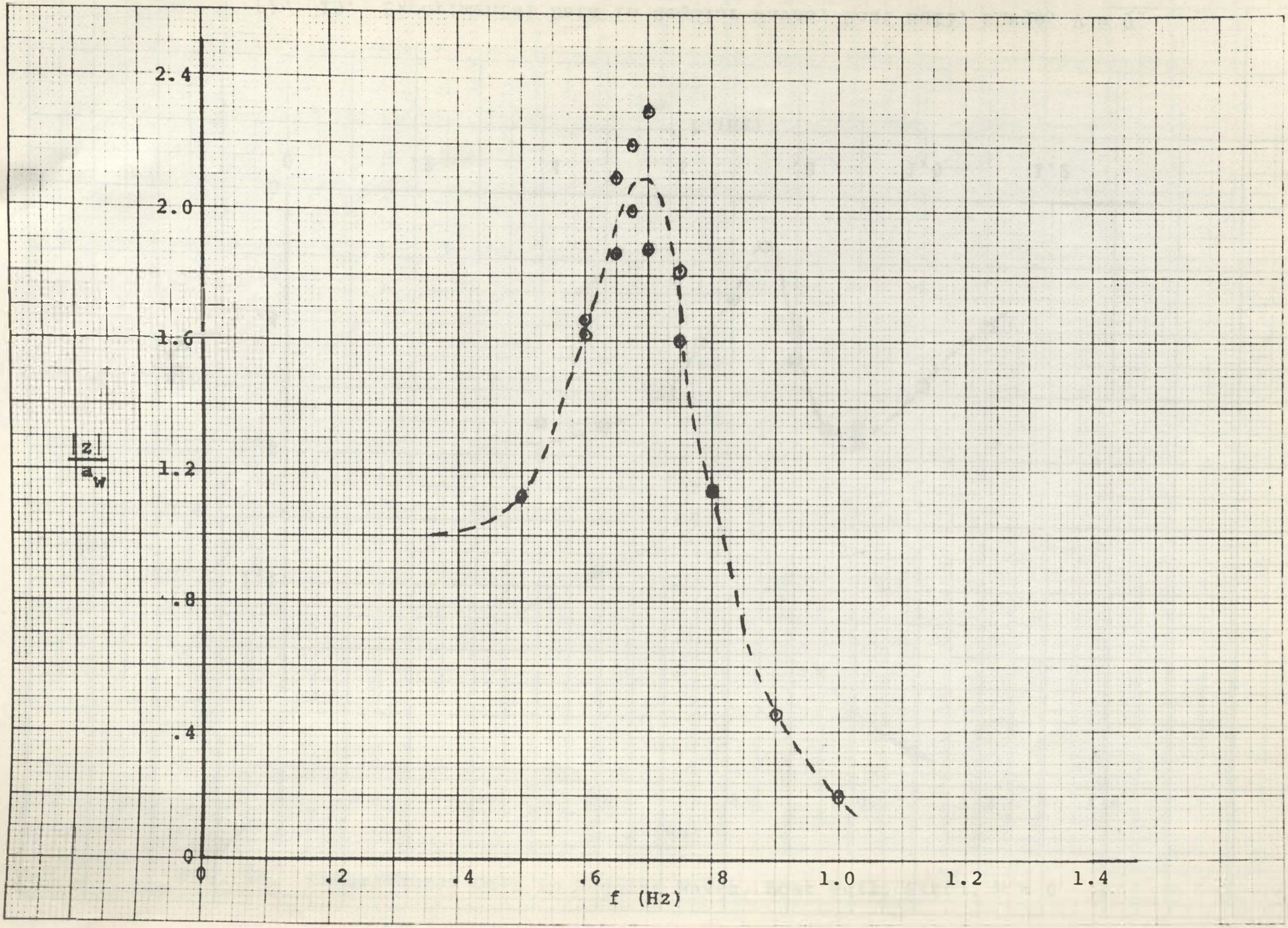

Fig. 16. Experimental Data in Regular Waves, Boat Hull, Heave, V = 1.96 fps

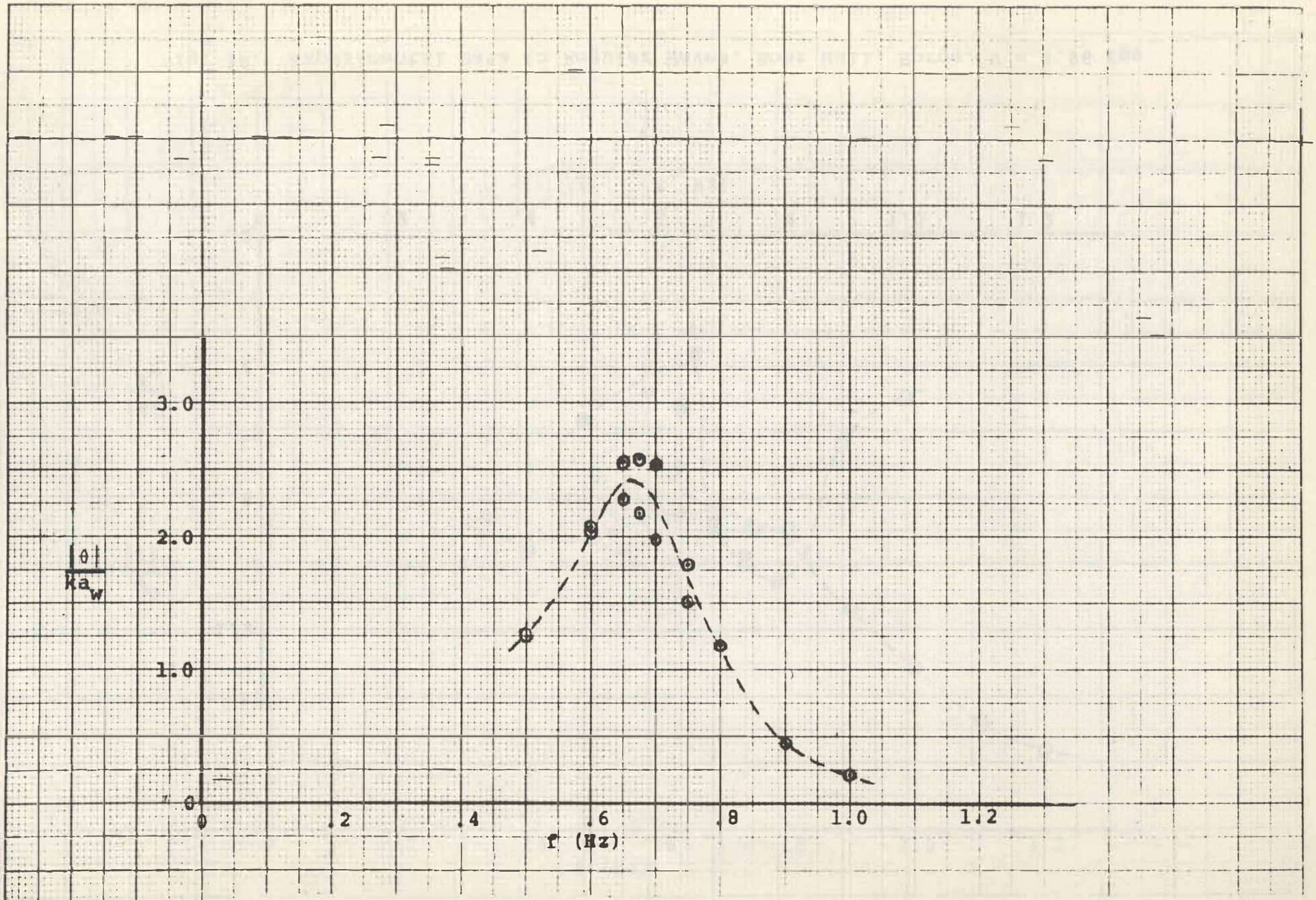

Fig. 17. Experimental Data in Regular Waves, Boat Hull, Pitch, V = 1.96 fps

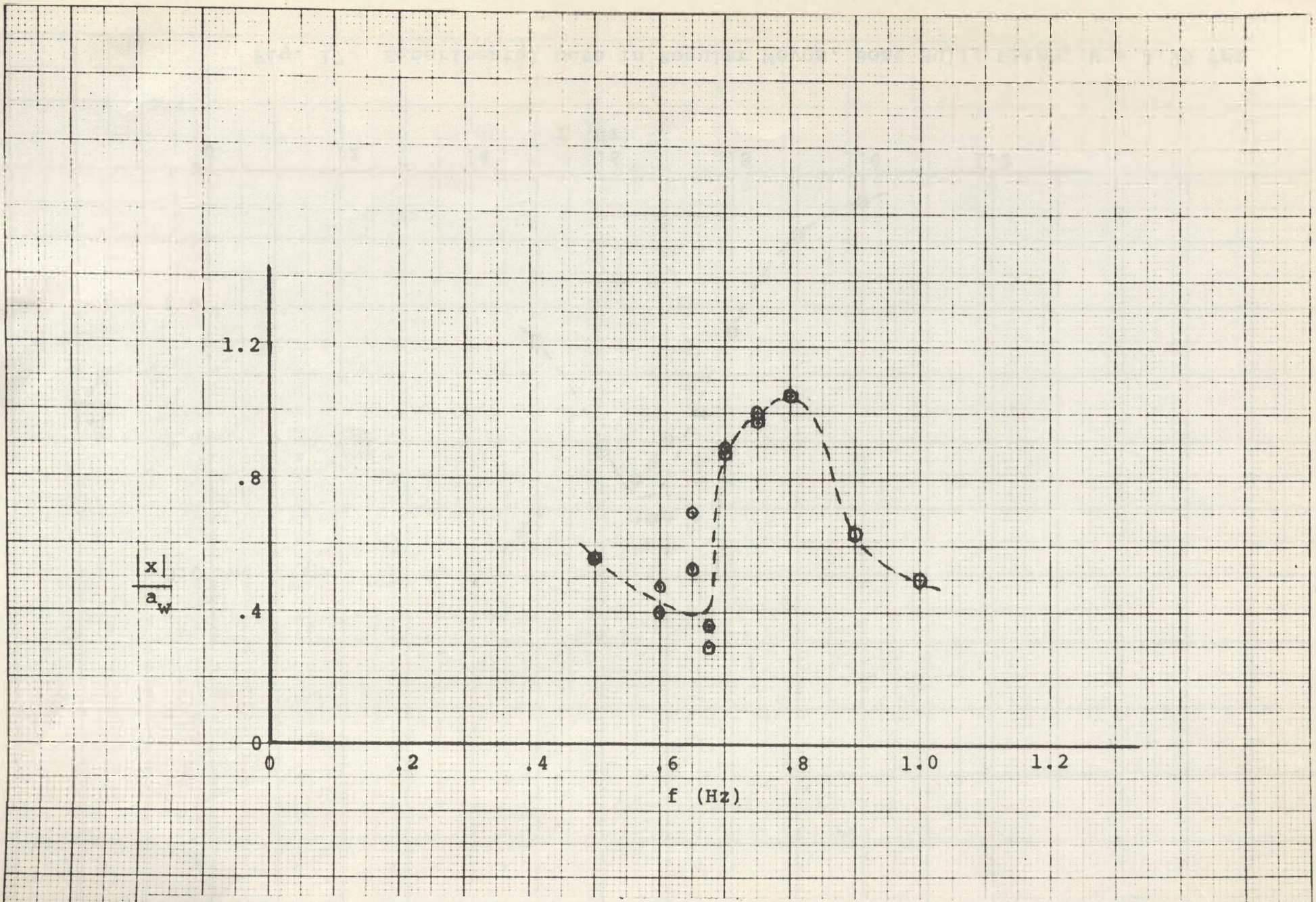

Fig. 18. Experimental Data in Regular Waves, Boat Hull, Surge, V = 1.96 fps

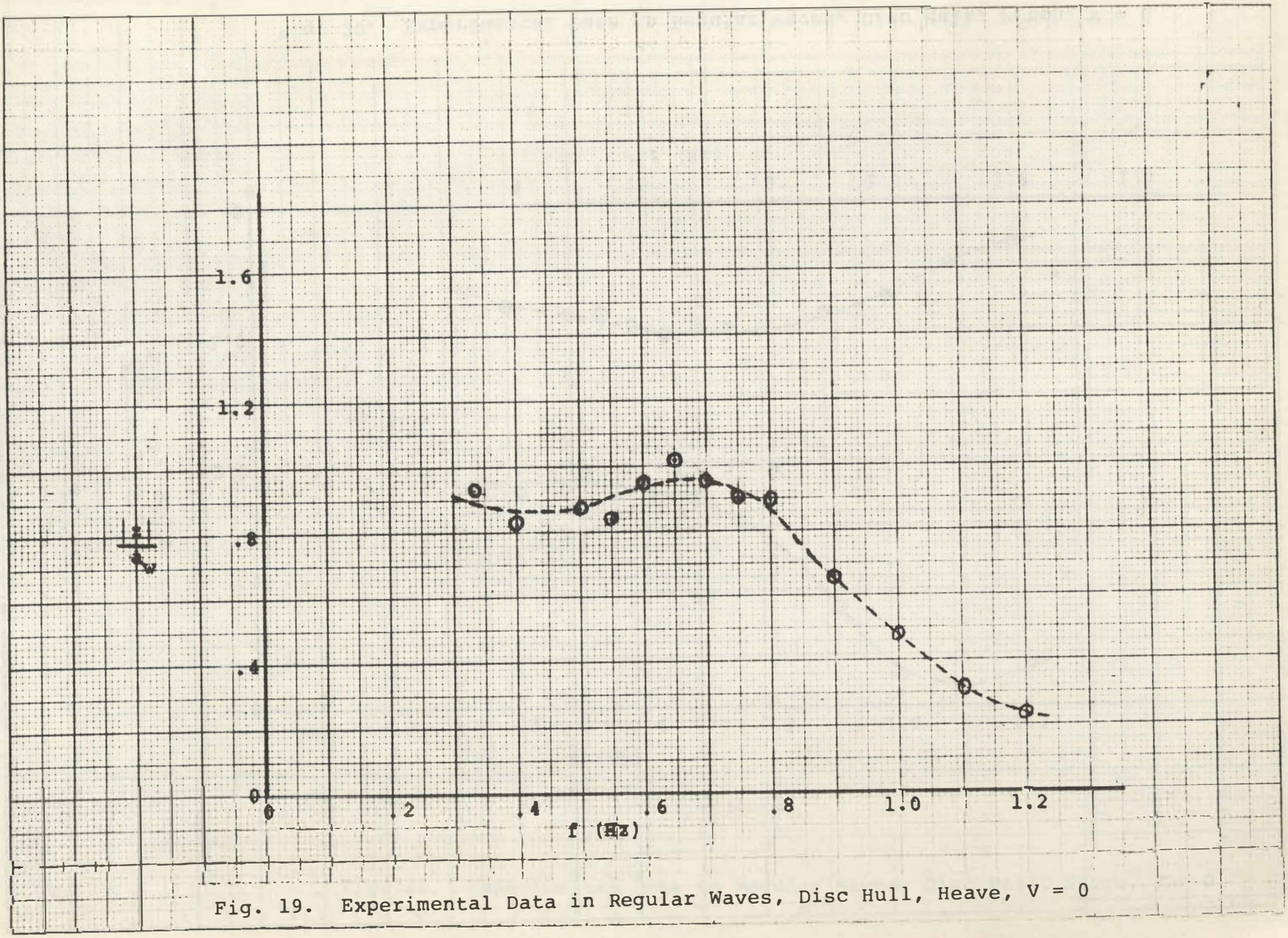

Fig. 19. Experimental Data in Regular Waves, Disc Hull, Heave, V = 0

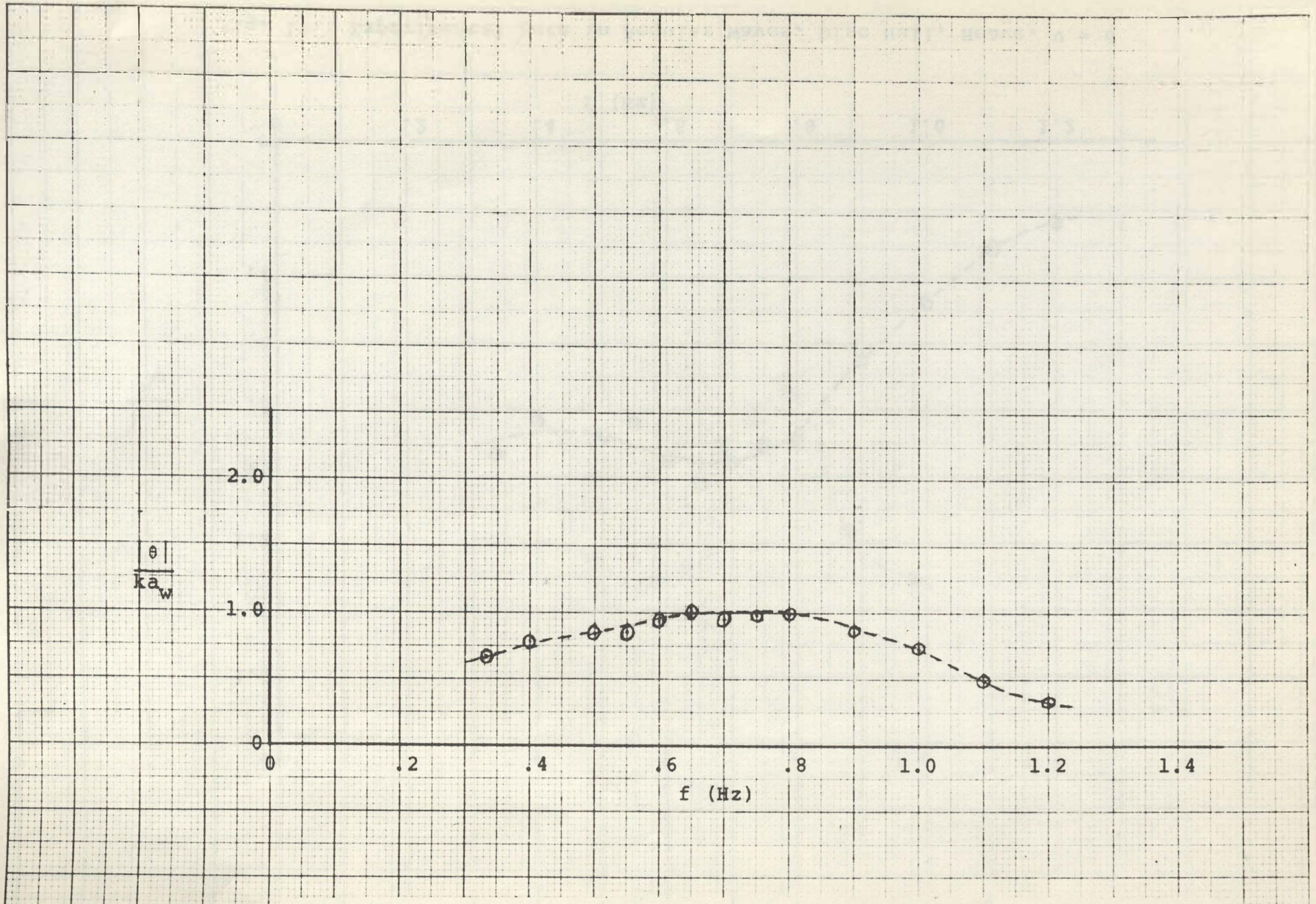

Fig. 20. Experimental Data in Regular Waves, Disc Hull, Pitch, V = 0

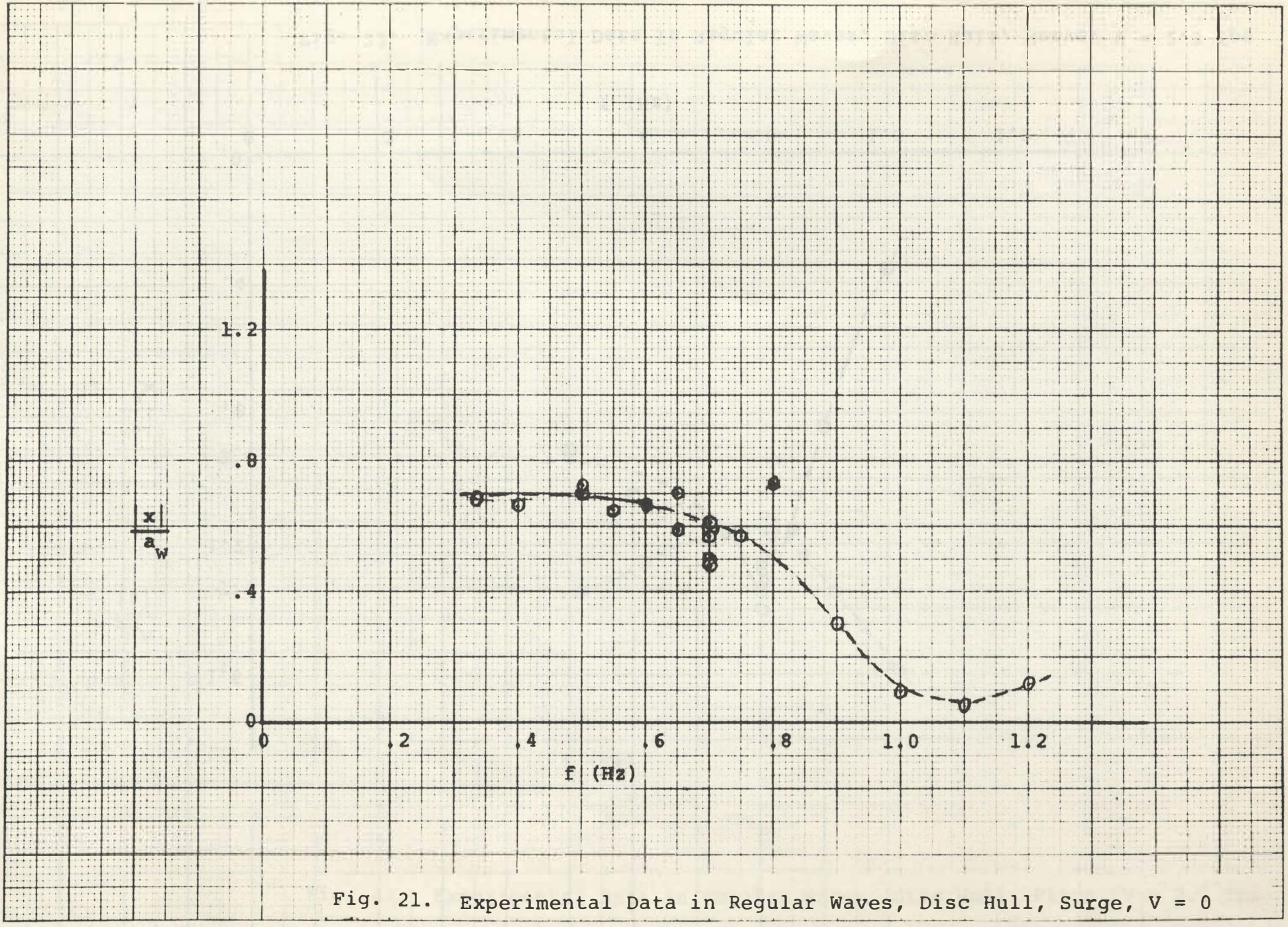

Fig. 21. Experimental Data in Regular Waves, Disc Hull, Surge, V = 0

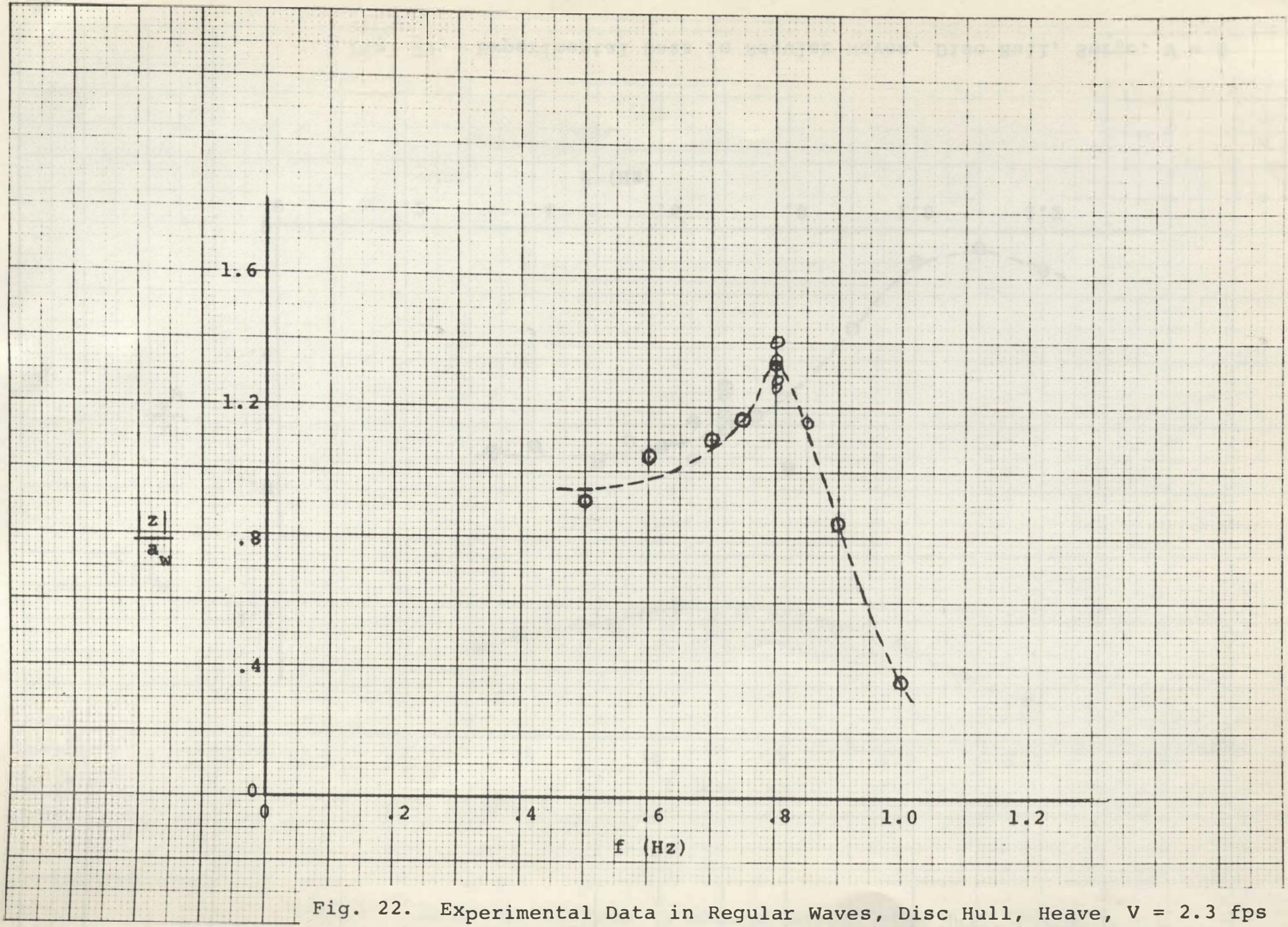

Fig. 22. Experimental Data in Regular Waves, Disc Hull, Heave, V = 2.3 fps

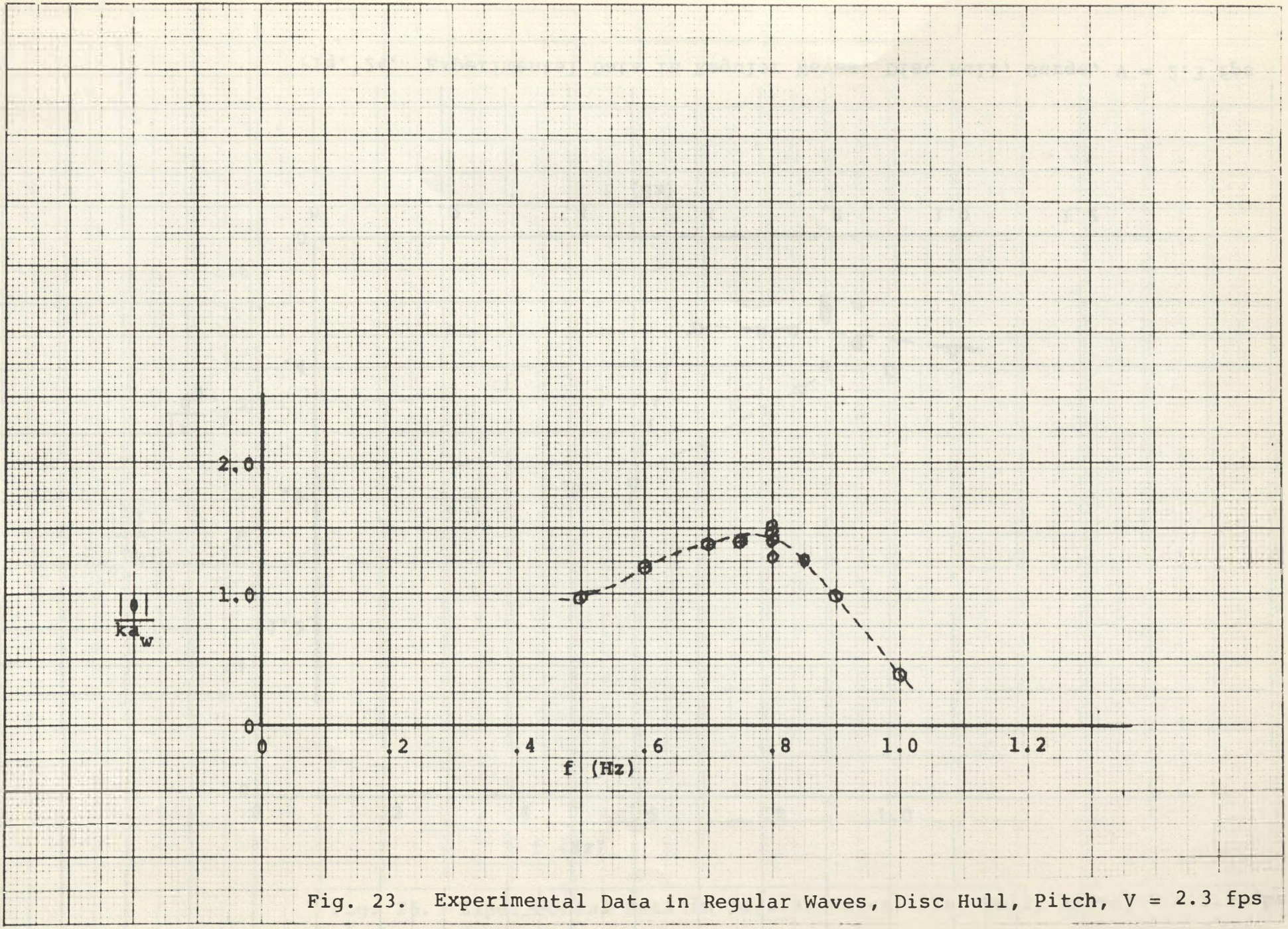

Fig. 23. Experimental Data in Regular Waves, Disc Hull, Pitch, V = 2.3 fps

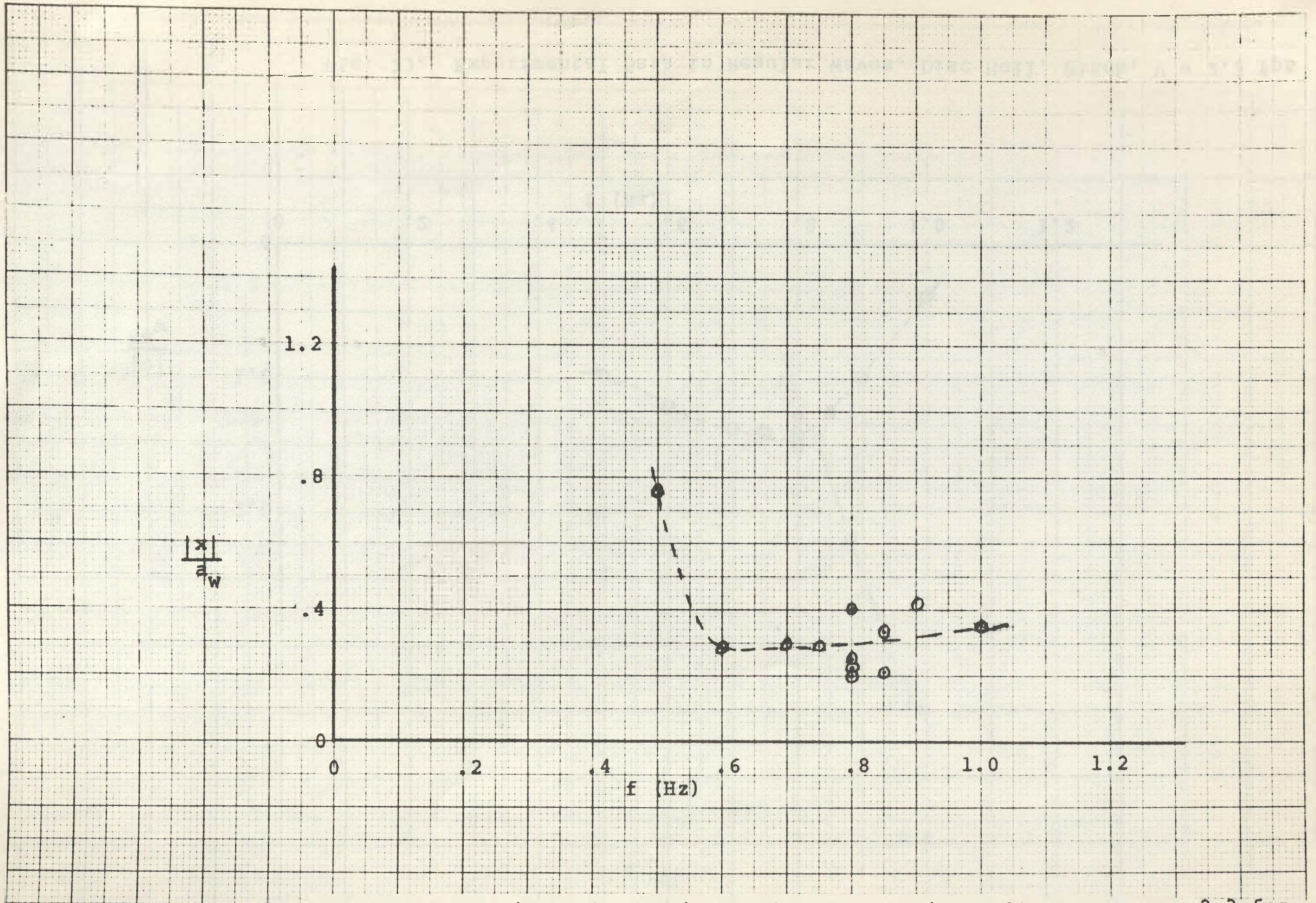

Fig. 24. Experimental Data in Regular Waves, Disc Hull, Surge, V = 2.3 fps

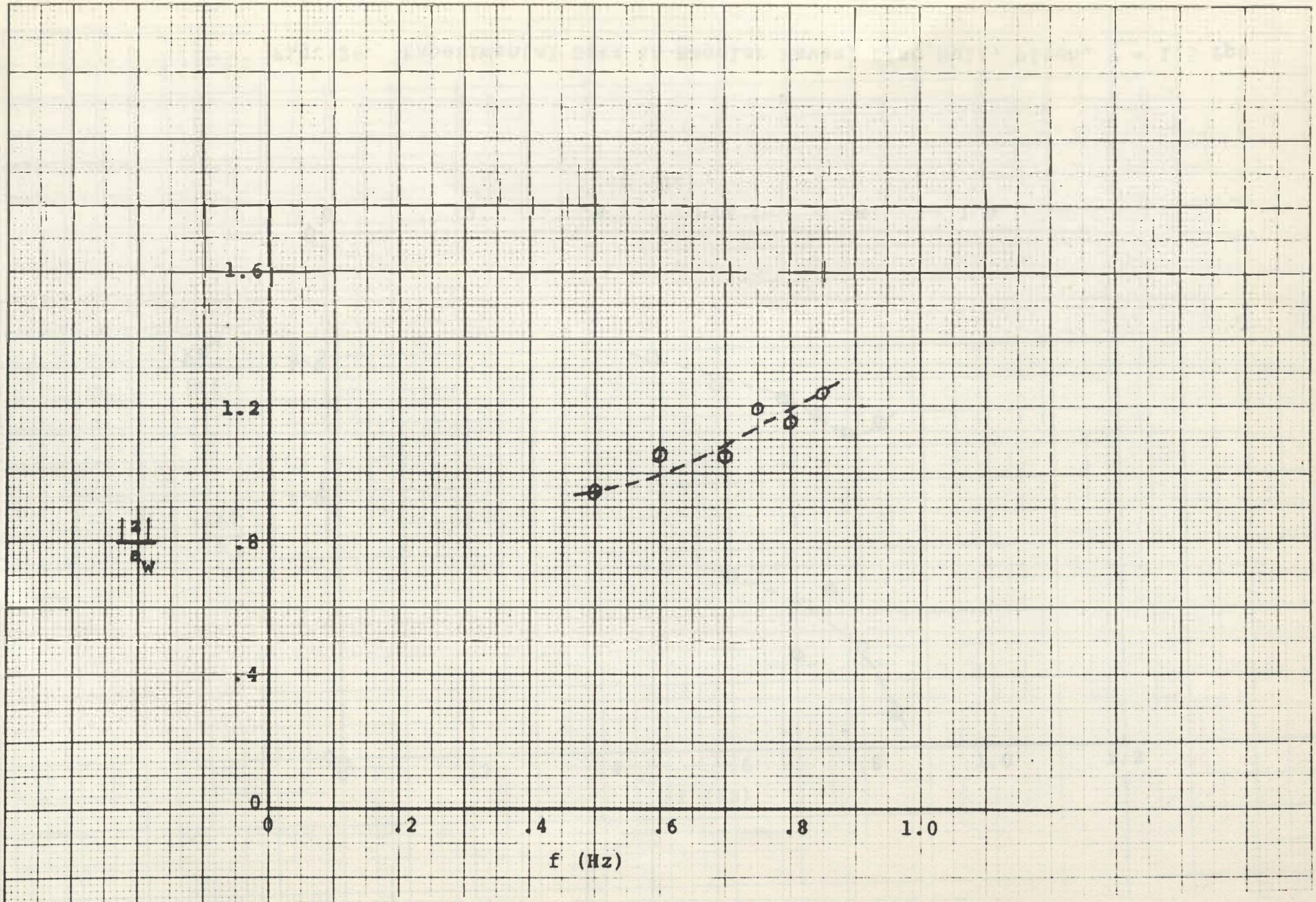

Fig. 25. Experimental Data in Regular Waves, Disc Hull, Heave, V = 1.5 fps

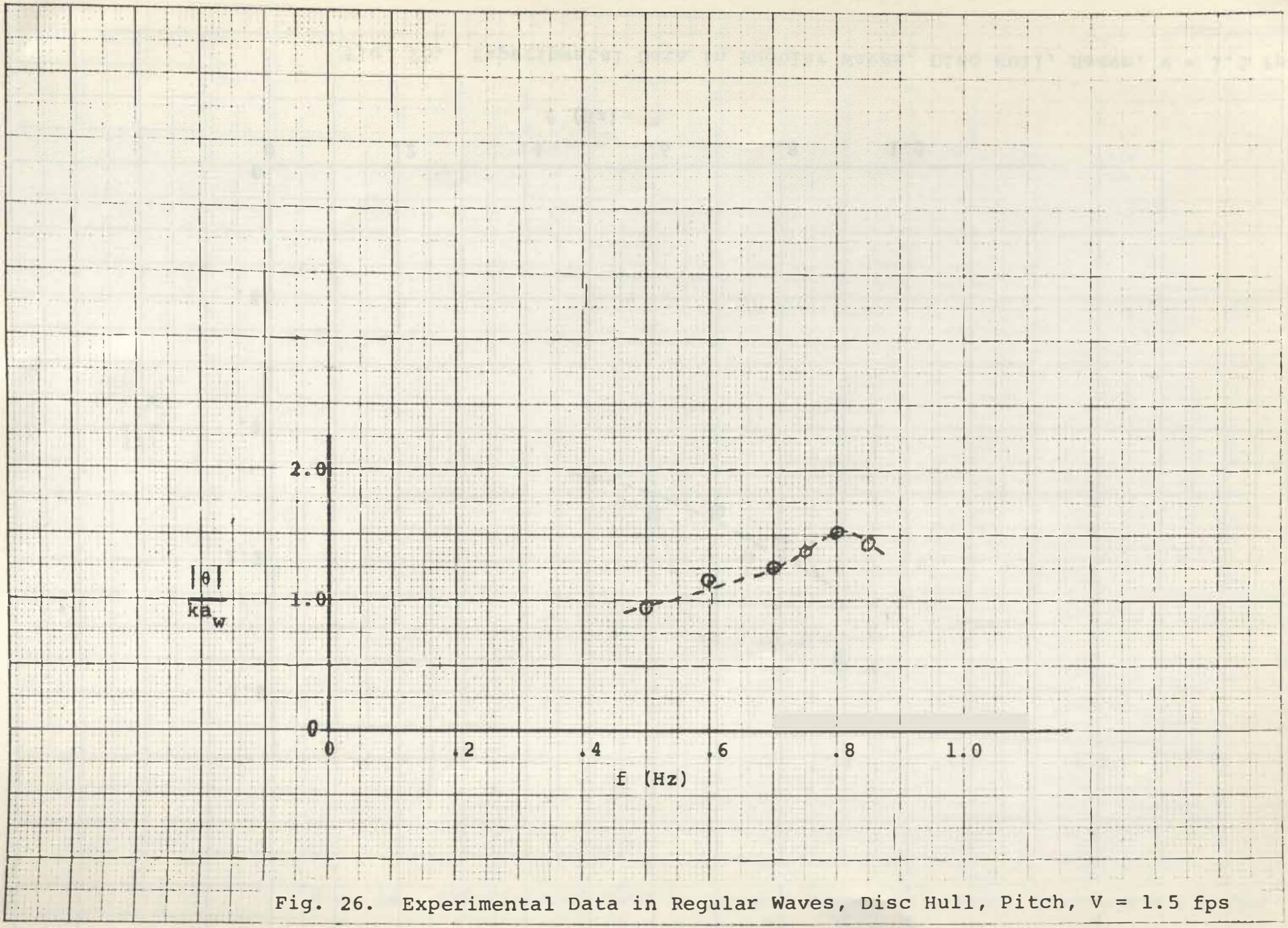

Fig. 26. Experimental Data in Regular Waves, Disc Hull, Pitch, V = 1.5 fps

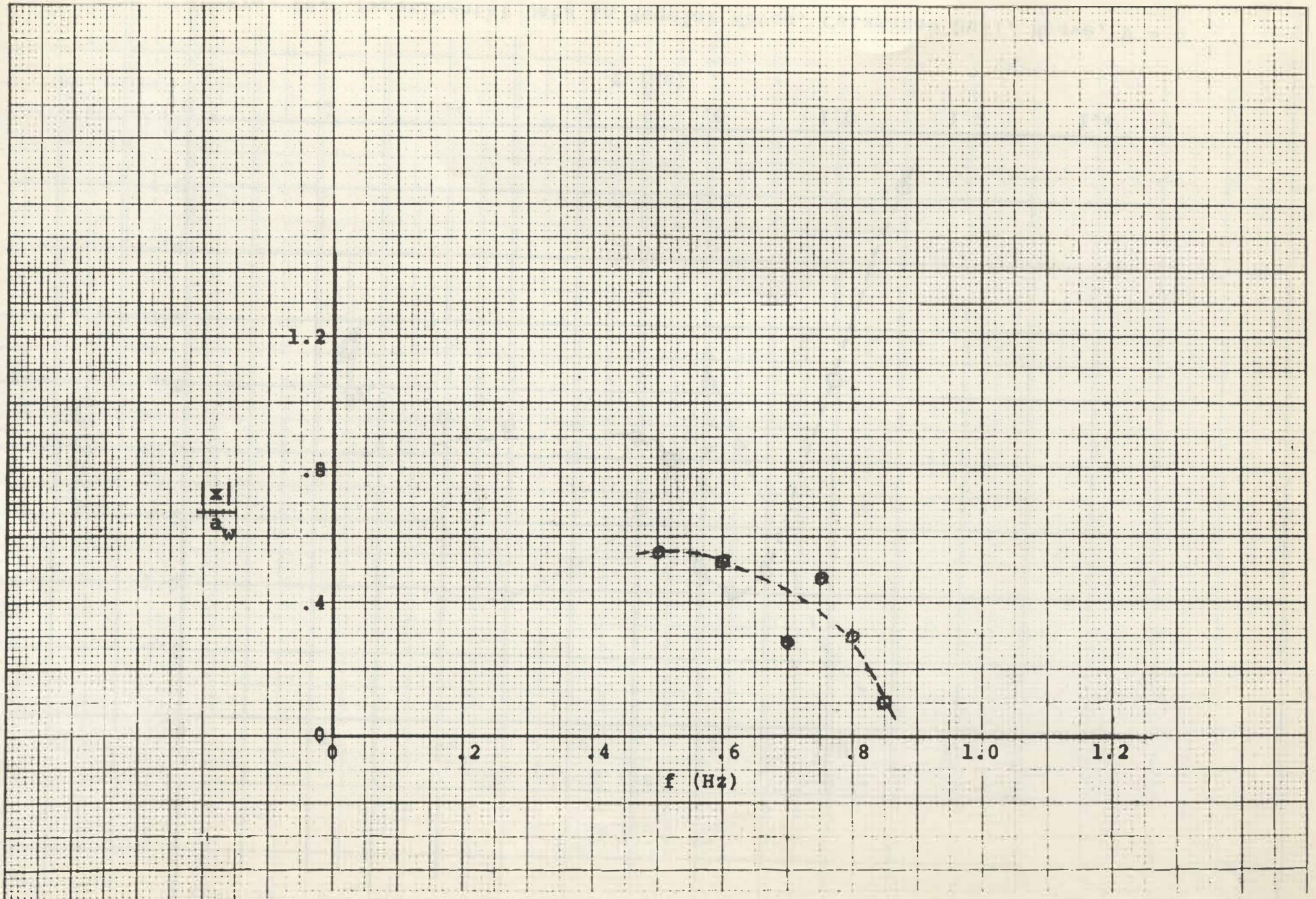

Fig. 27. Experimental Data in Regular Waves, Disc Hull, Surge, V = 1.5 fps

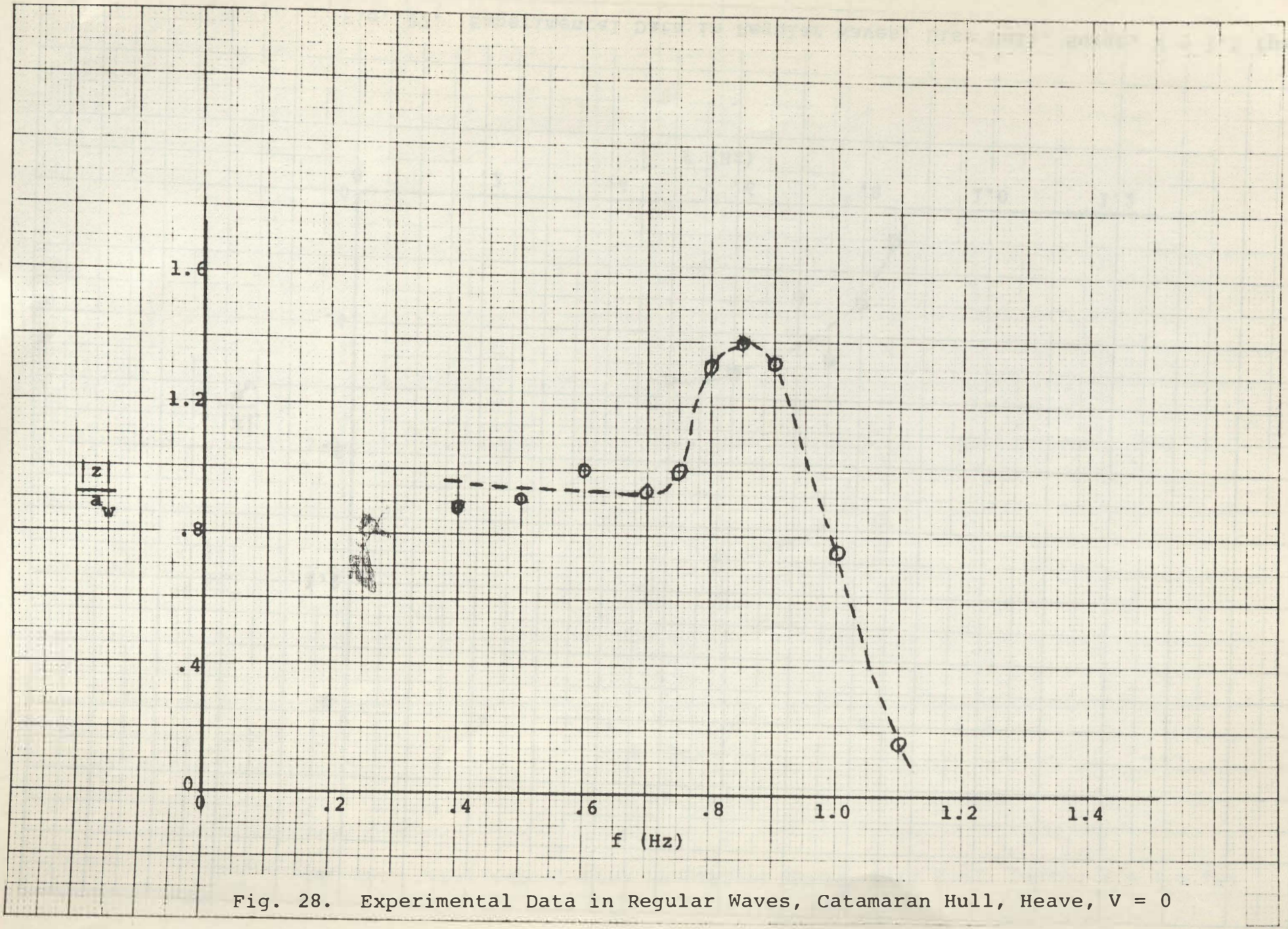

Fig. 28. Experimental Data in Regular Waves, Catamaran Hull, Heave, V = 0

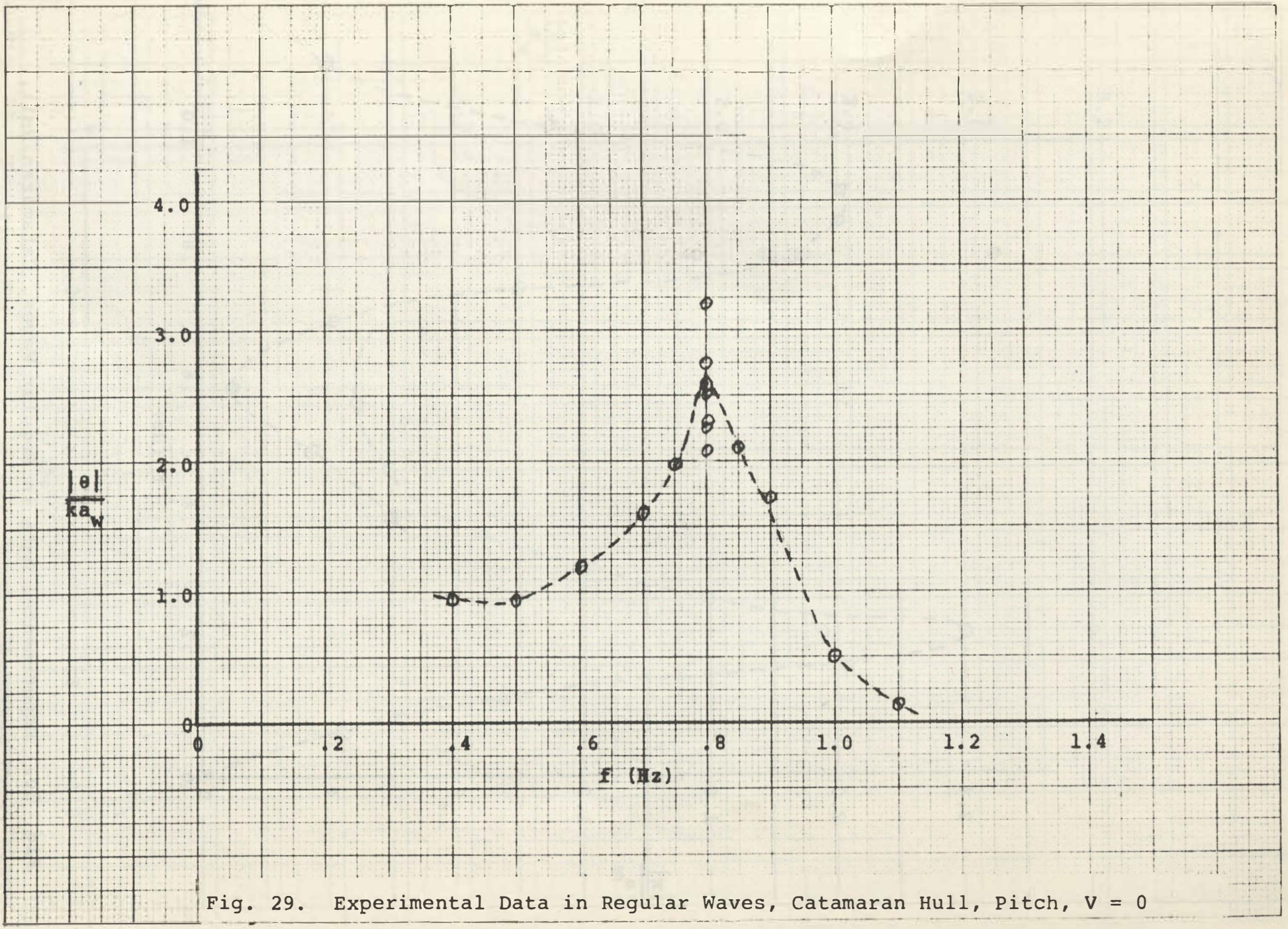

Fig. 29. Experimental Data in Regular Waves, Catamaran Hull, Pitch, V = 0

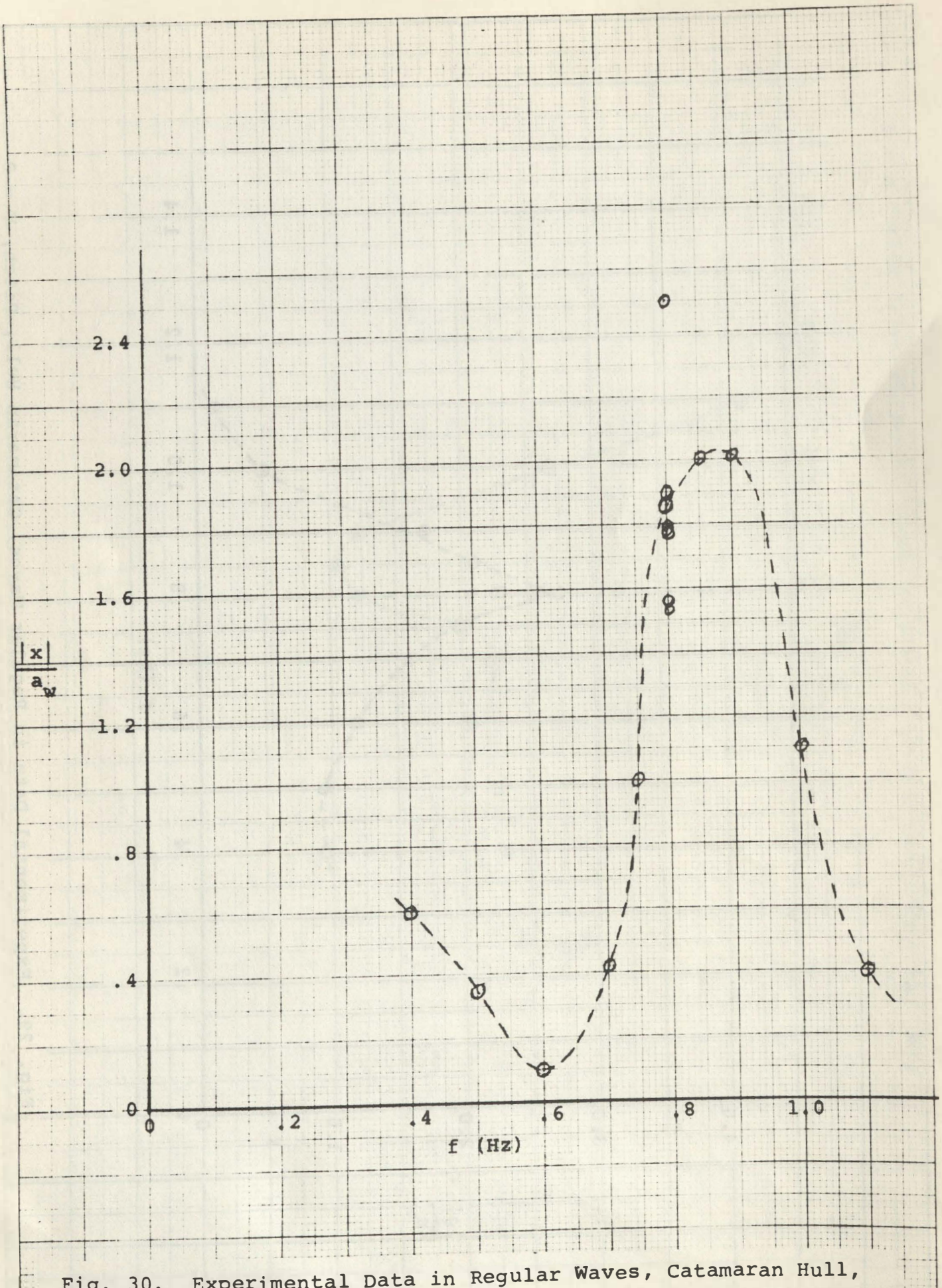

Fig. 30. Experimental Data in Regular Waves, Catamaran Hull, Surge, V = 0

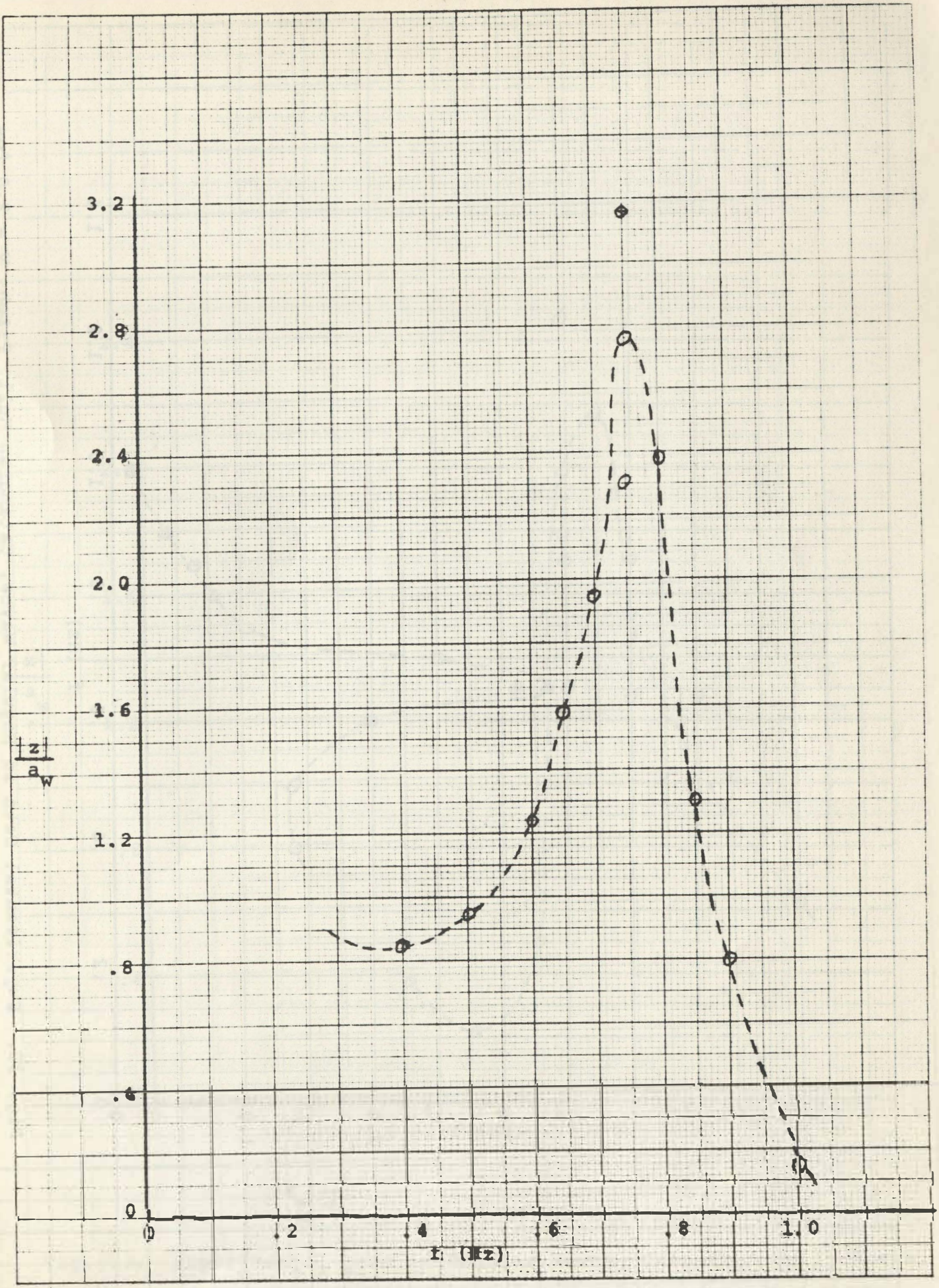

Fig. 31. Experimental Data in Regular Waves, Catamaran Hull, Heave, V = 2.0 fps

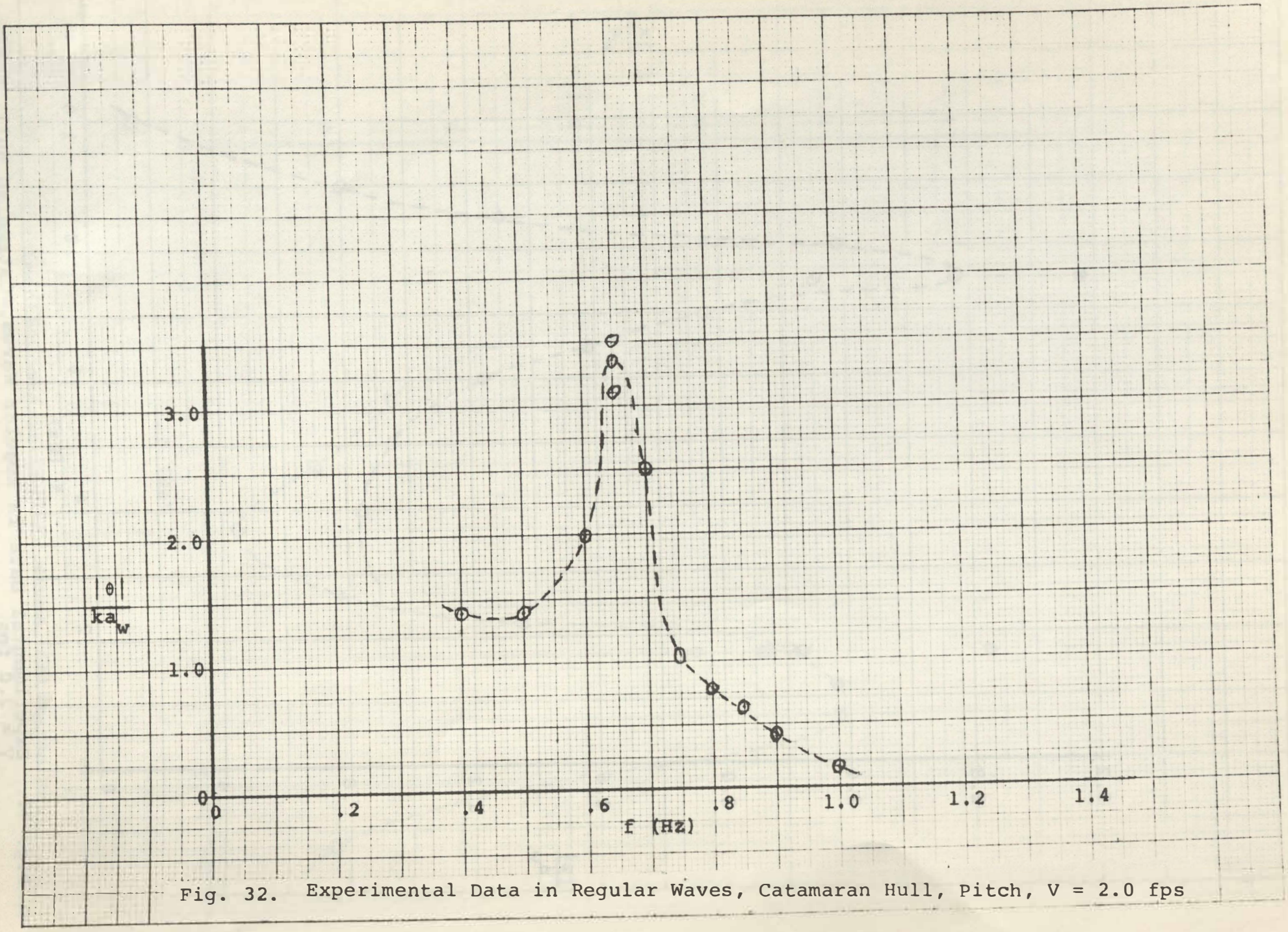

Fig. 32. Experimental Data in Regular Waves, Catamaran Hull, Pitch, V = 2.0 fps

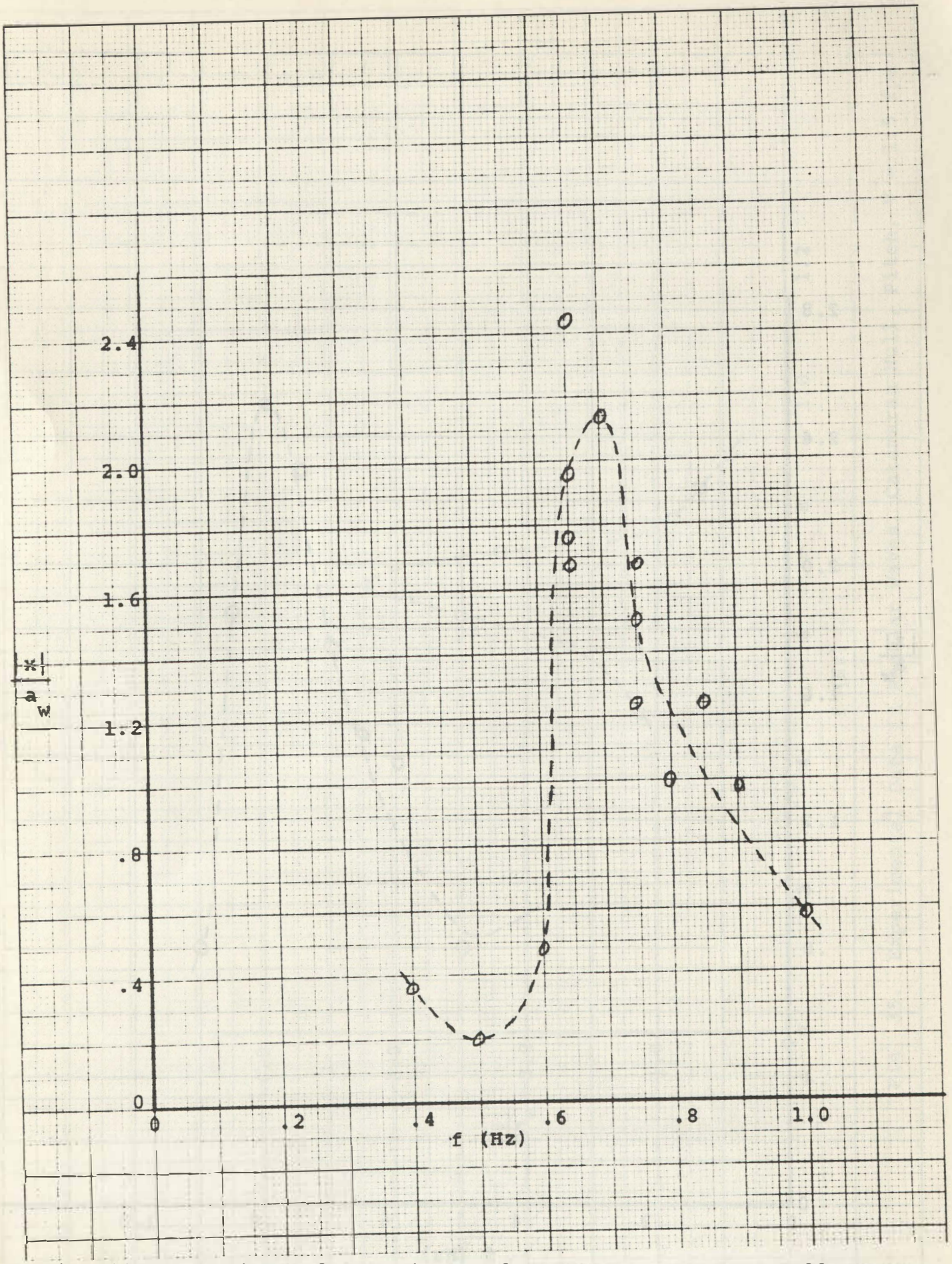

Fig. 33. Experimental Data in Regular Waves, Catamaran Hull, Surge, V = 2.0 fps

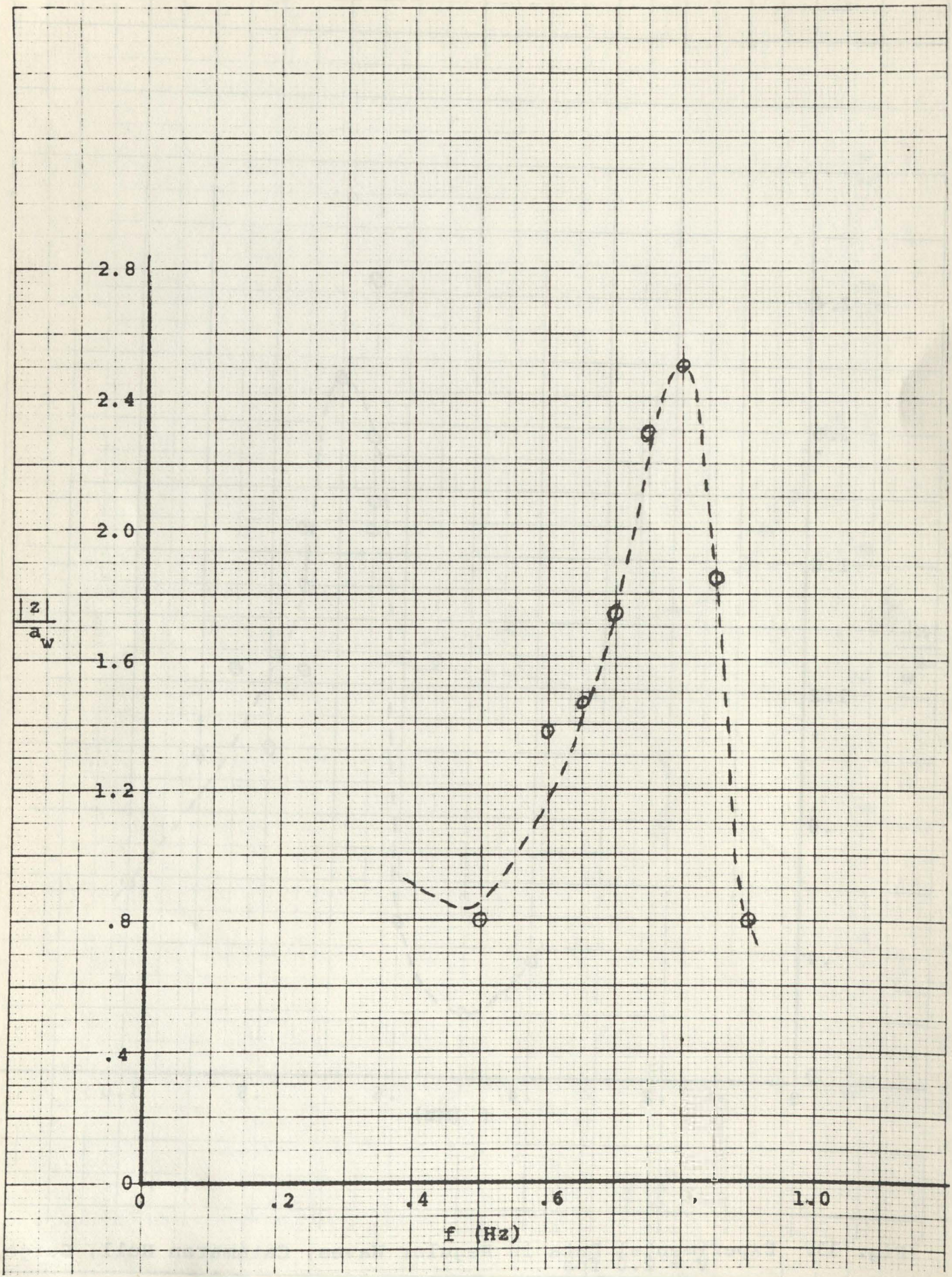

Fig. 34. Experimental Data in Regular Waves, Catamaran Hull, Heave, V=1.5 fps

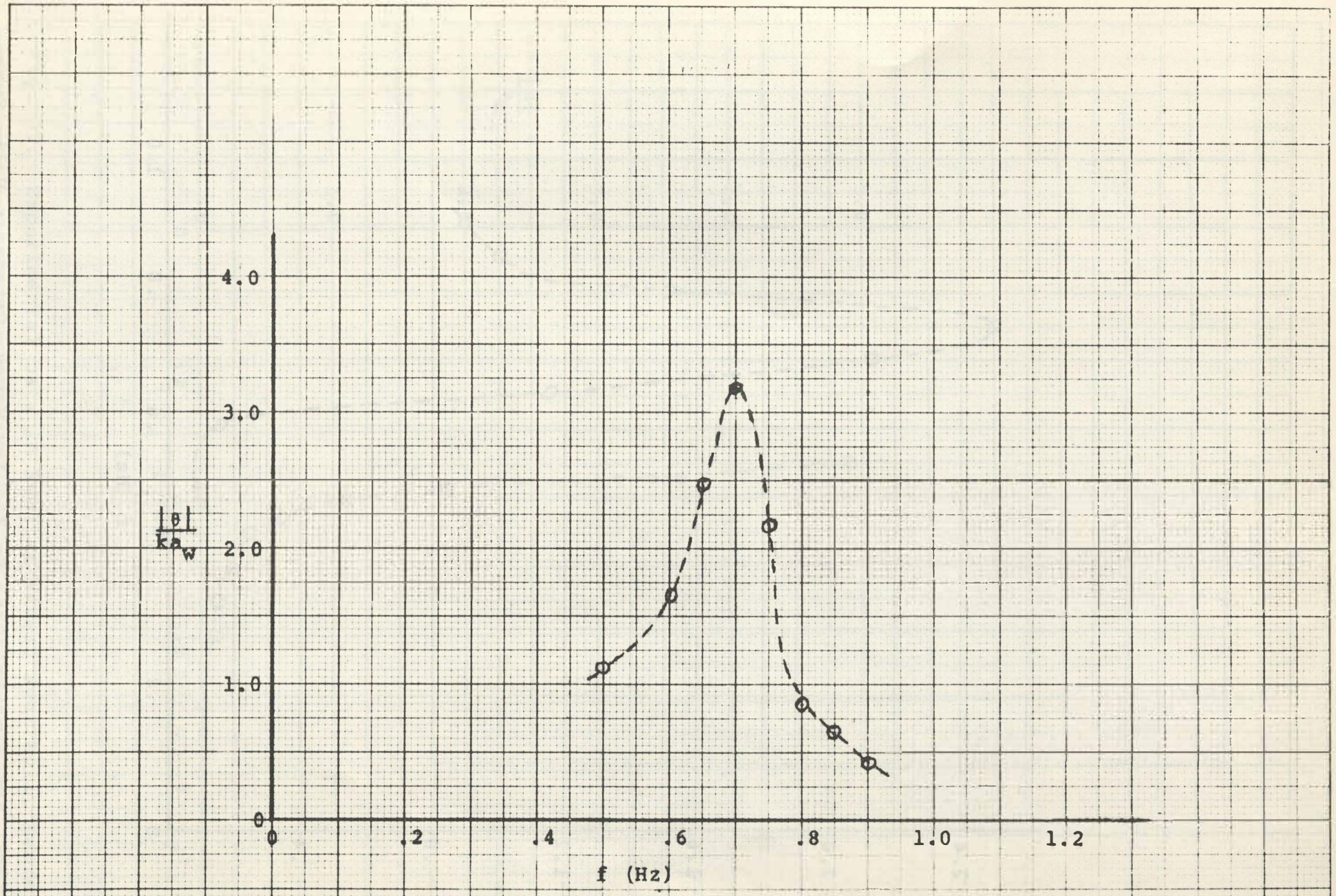

Fig. 35. Experimental Data in Regular Waves, Catamaran Hull, Pitch, V = 1.5 fps

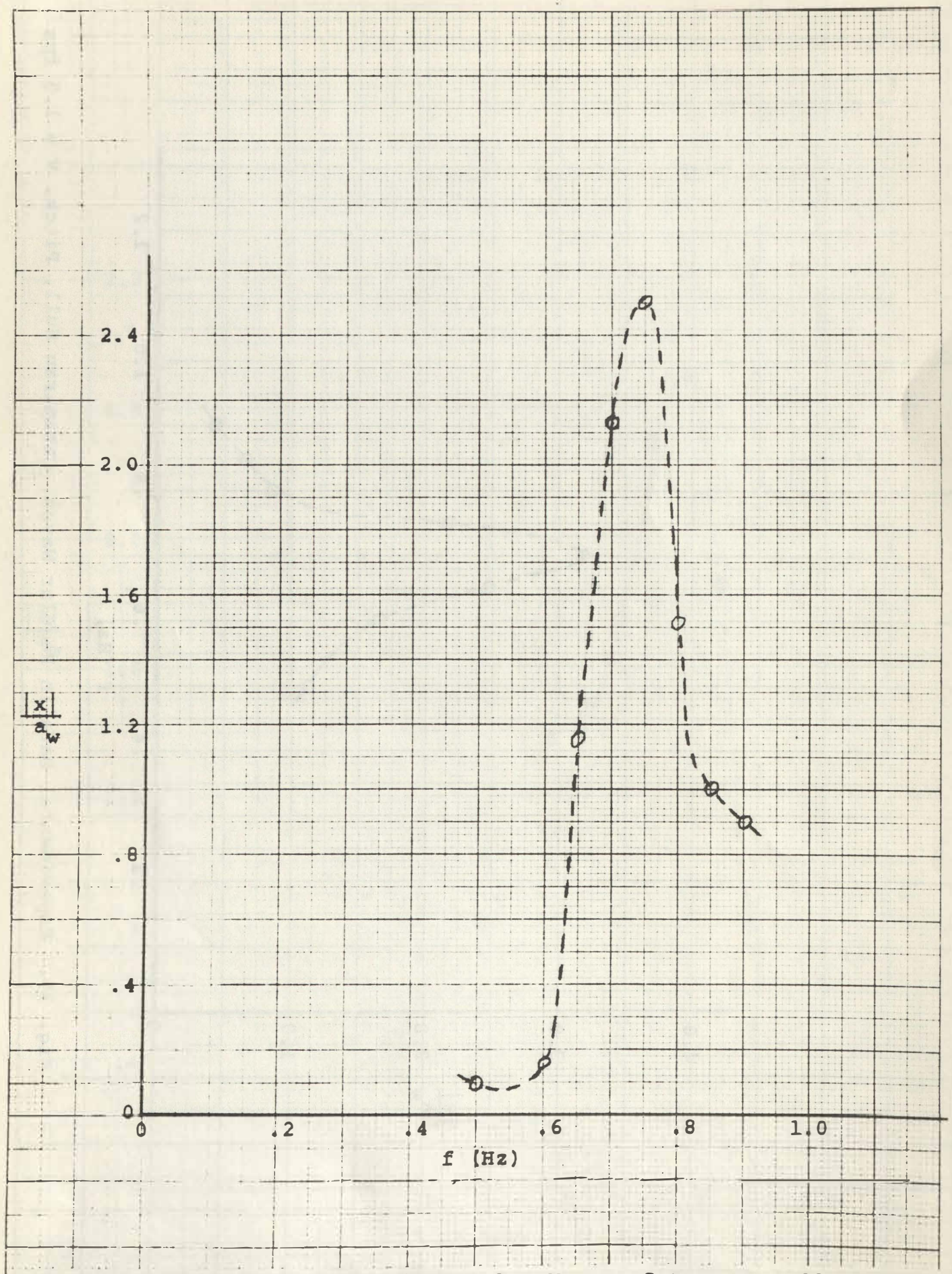

Fig. 36. Experimental Data in Regular Waves, Catamaran Hull, Surge, V = 1.5 fps

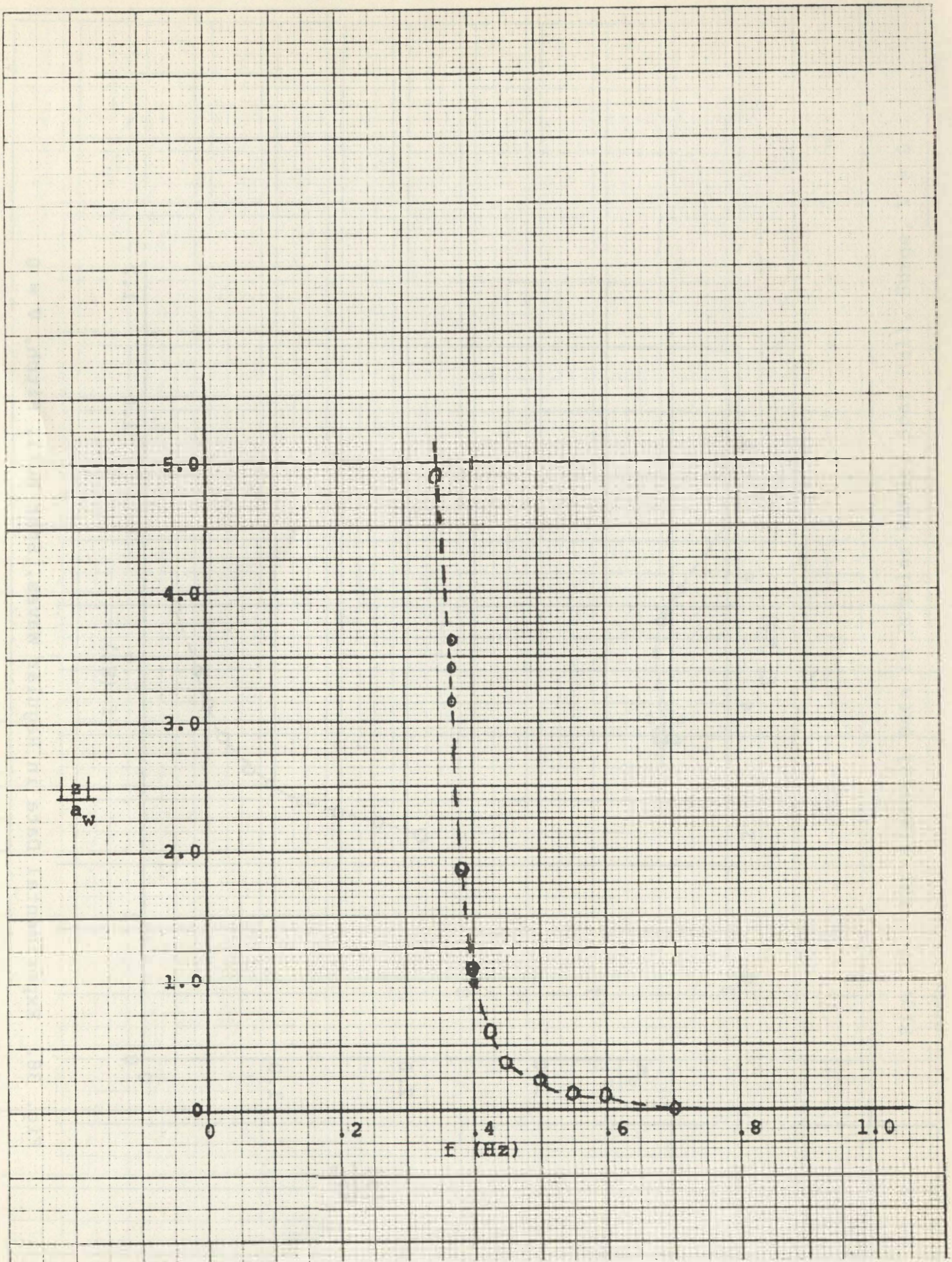

Fig. 37. Experimental Data in Regular Waves, Spar Hull, Heave, V = 0

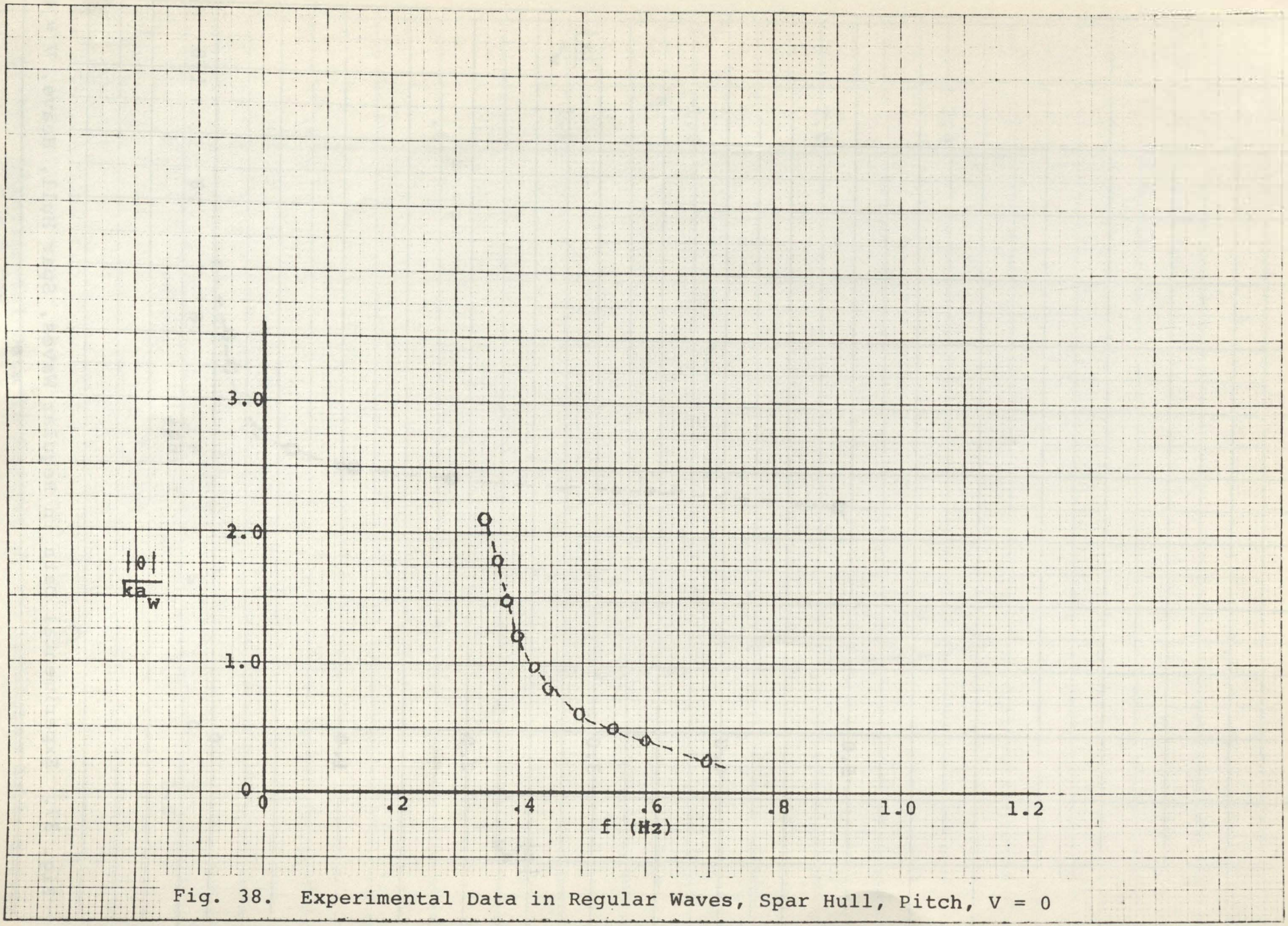

Fig. 38. Experimental Data in Regular Waves, Spar Hull, Pitch, V = 0

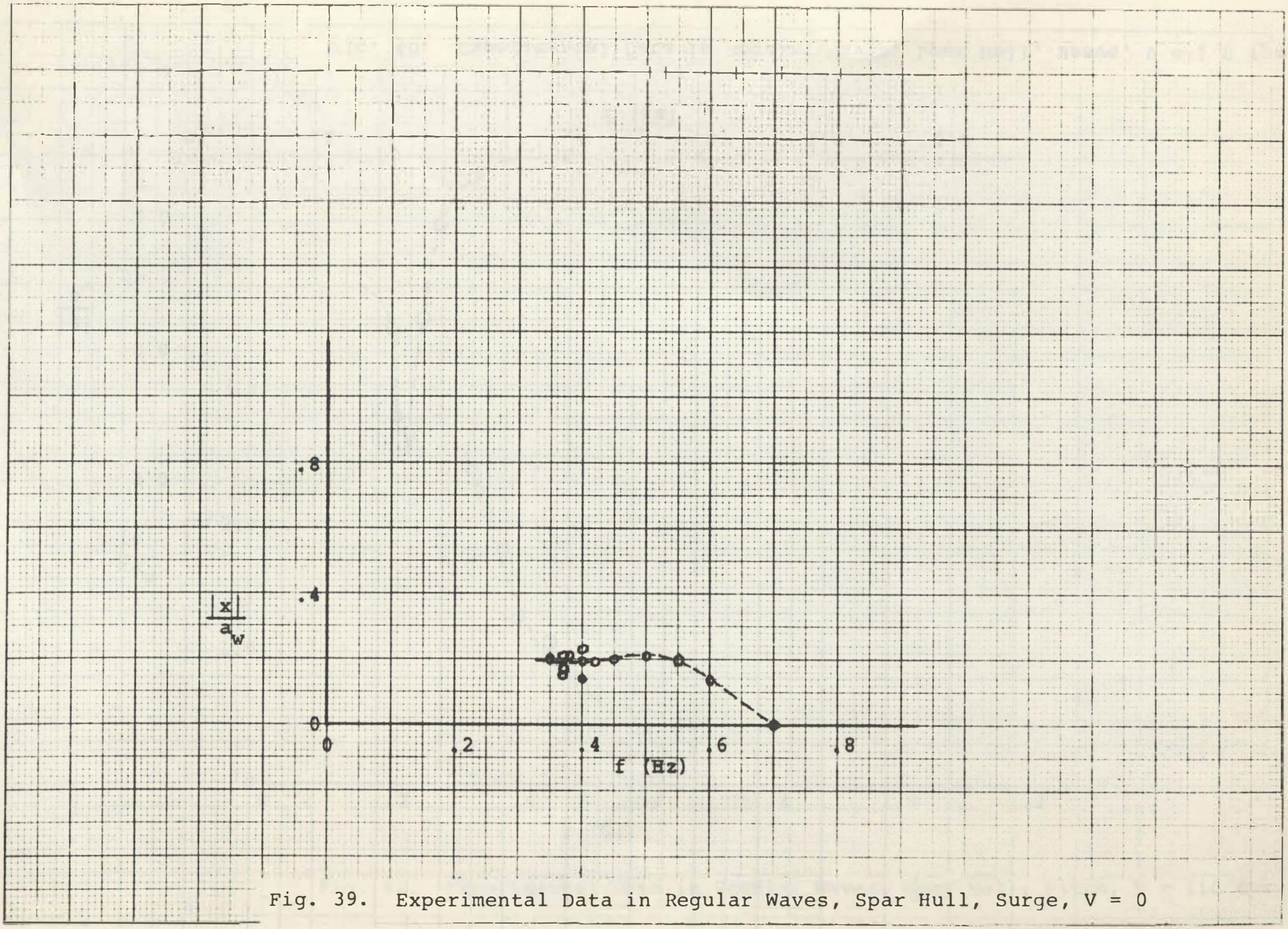

Fig. 39. Experimental Data in Regular Waves, Spar Hull, Surge, V = 0

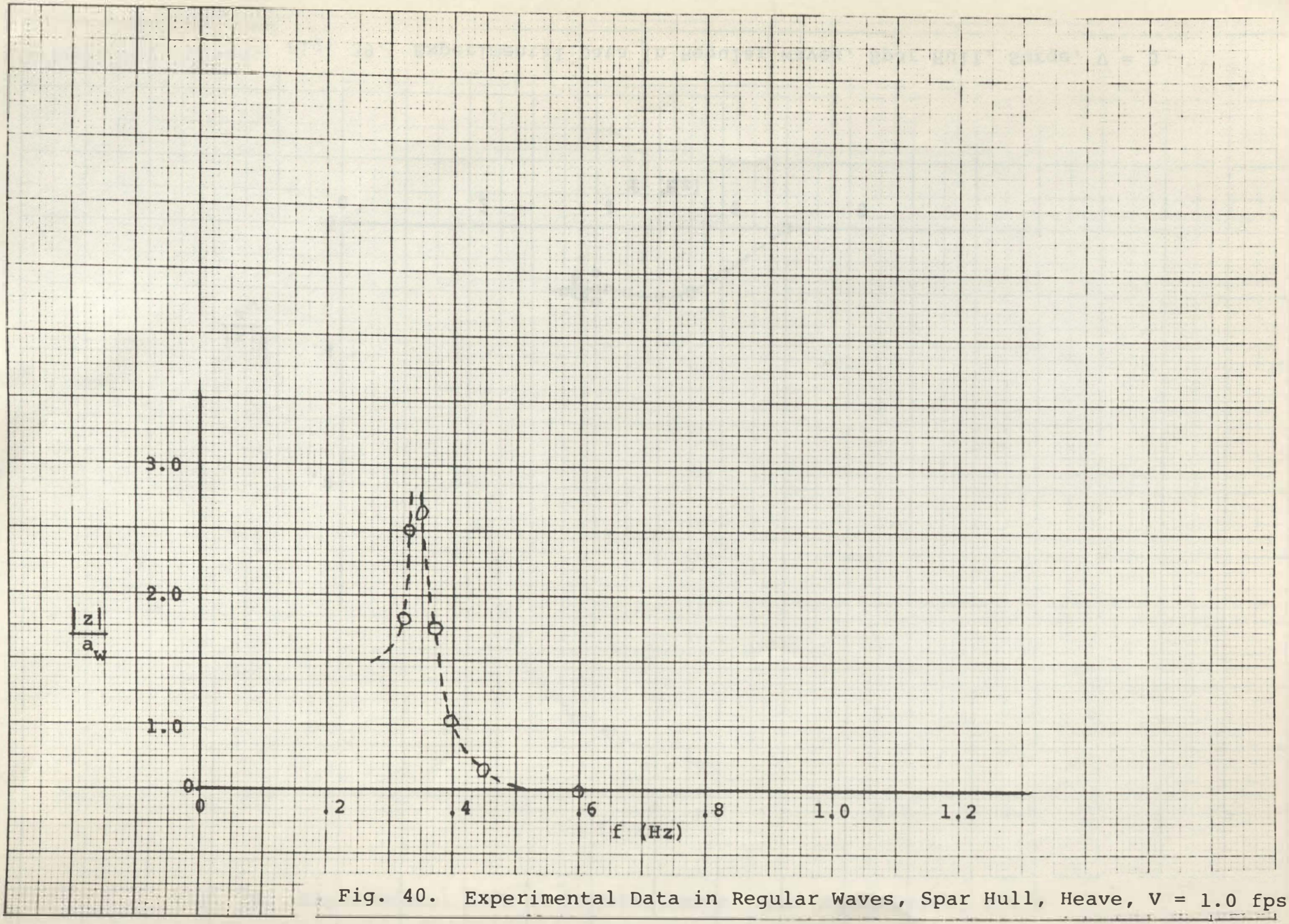

Fig. 40. Experimental Data in Regular Waves, Spar Hull, Heave, V = 1.0 fps

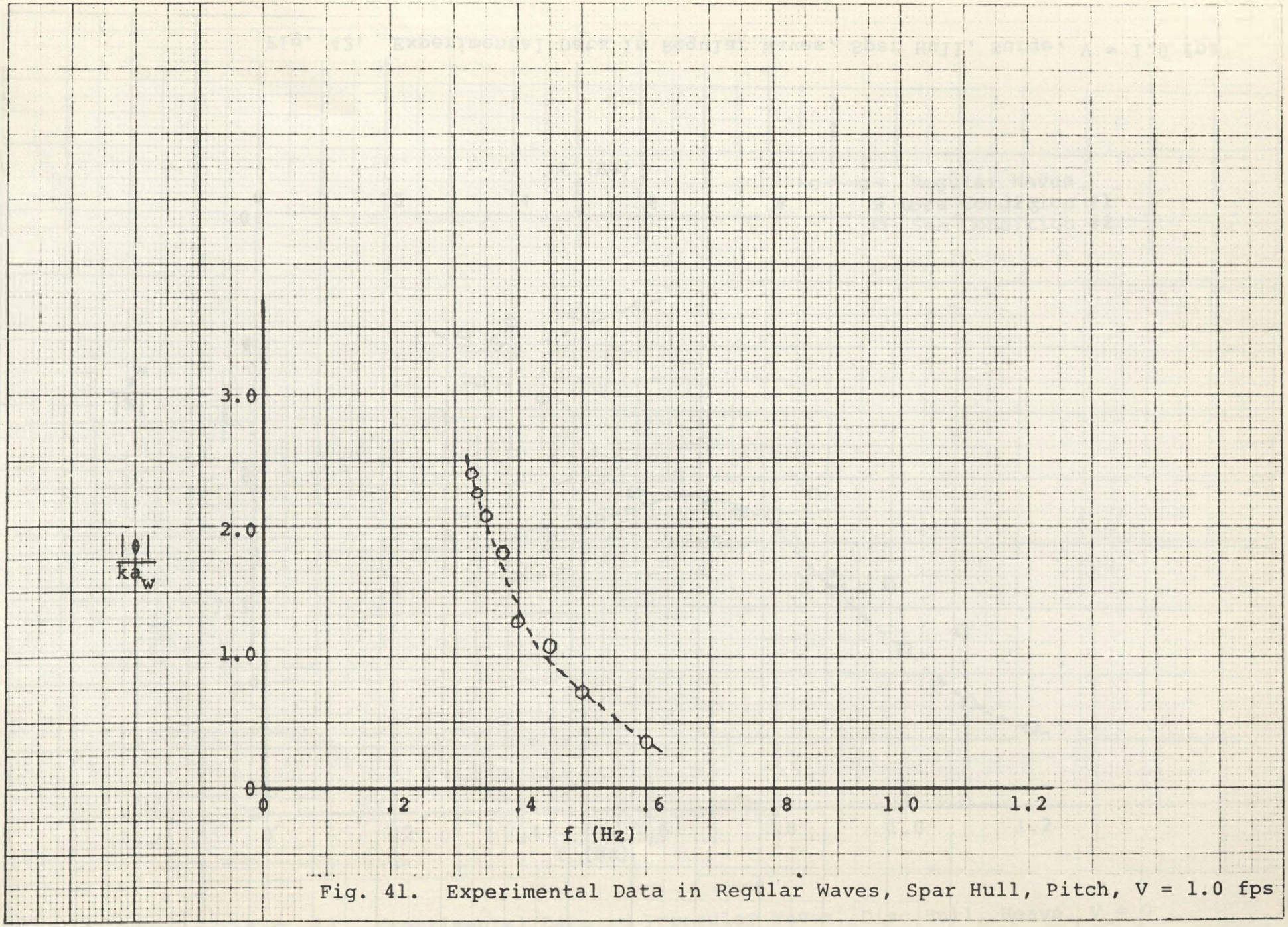

Fig. 41. Experimental Data in Regular Waves, Spar Hull, Pitch, V = 1.0 fps

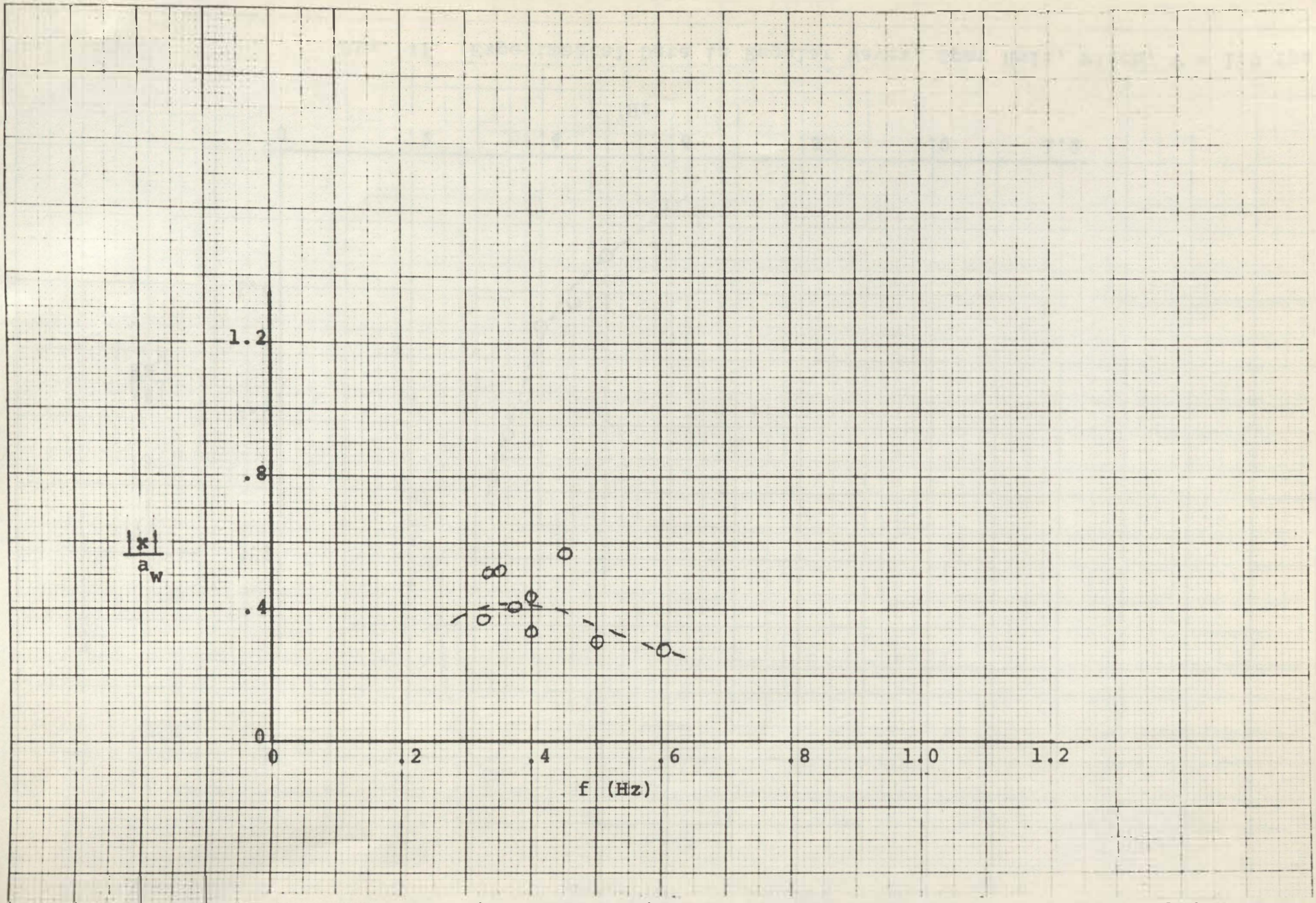

Fig. 42. Experimental Data in Regular Waves, Spar Hull, Surge, V = 1.0 fps

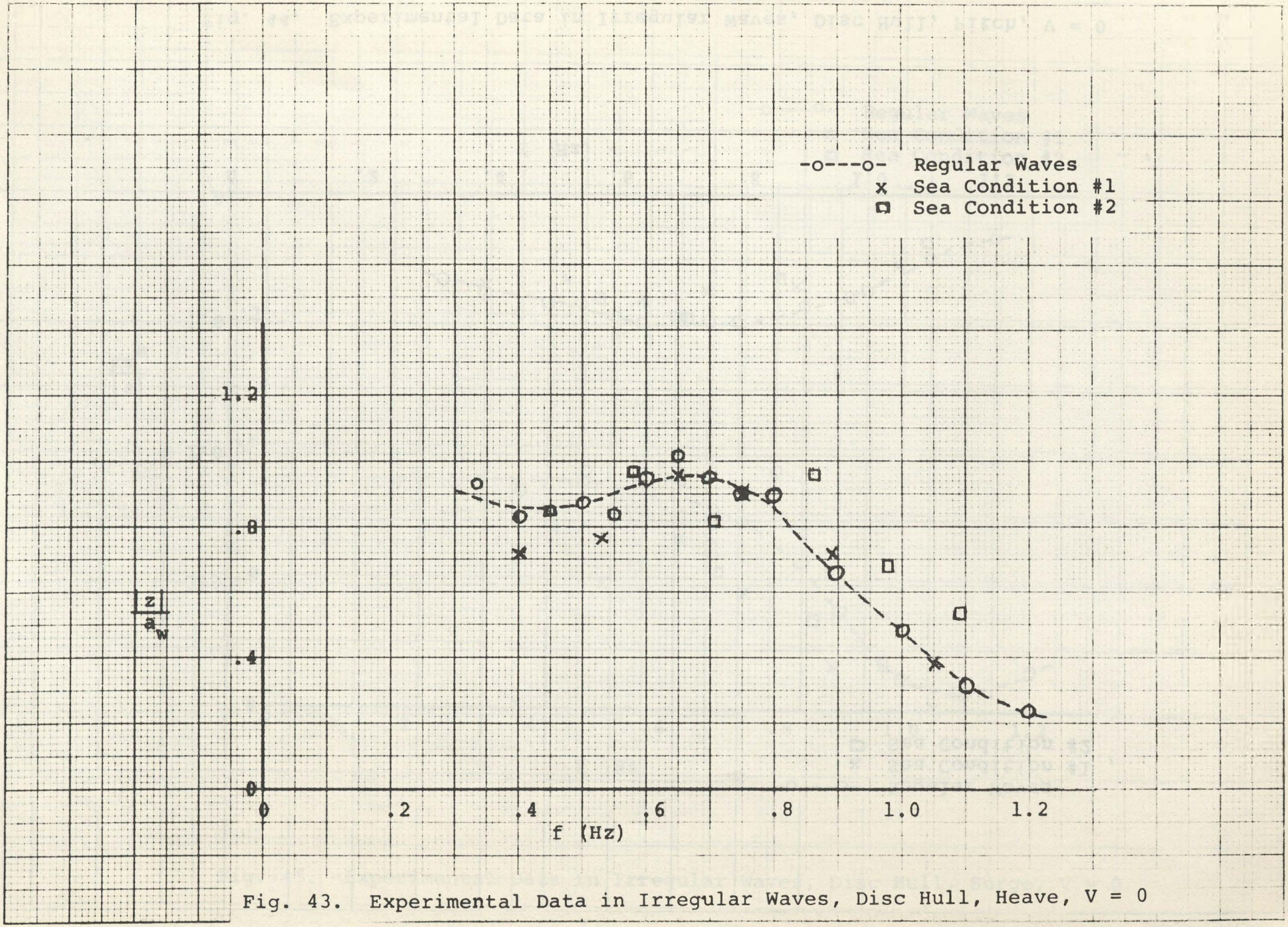

Fig. 43. Experimental Data in Irregular Waves, Disc Hull, Heave, V = 0

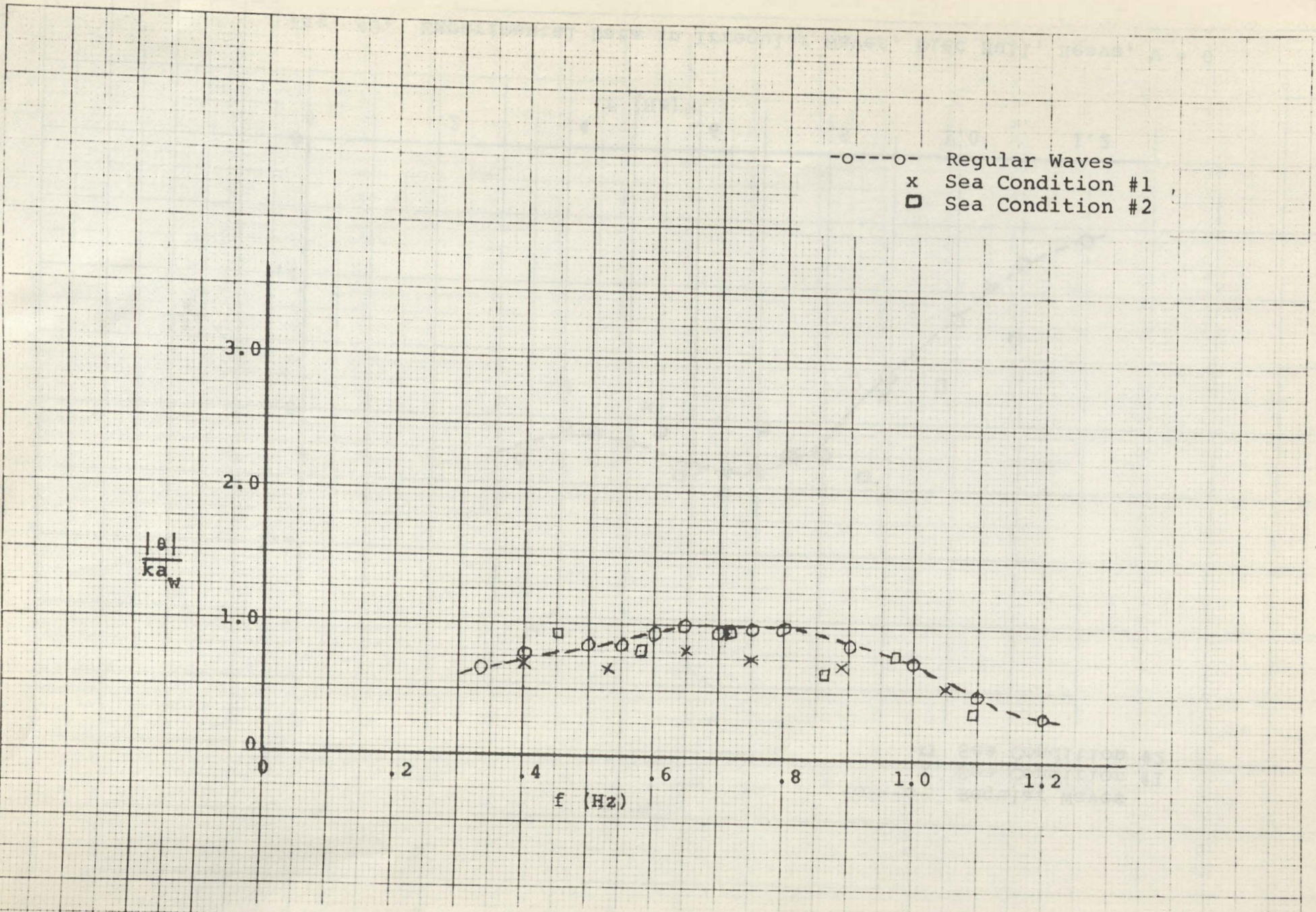

Fig. 44. Experimental Data in Irregular Waves, Disc Hull, Pitch, V = 0

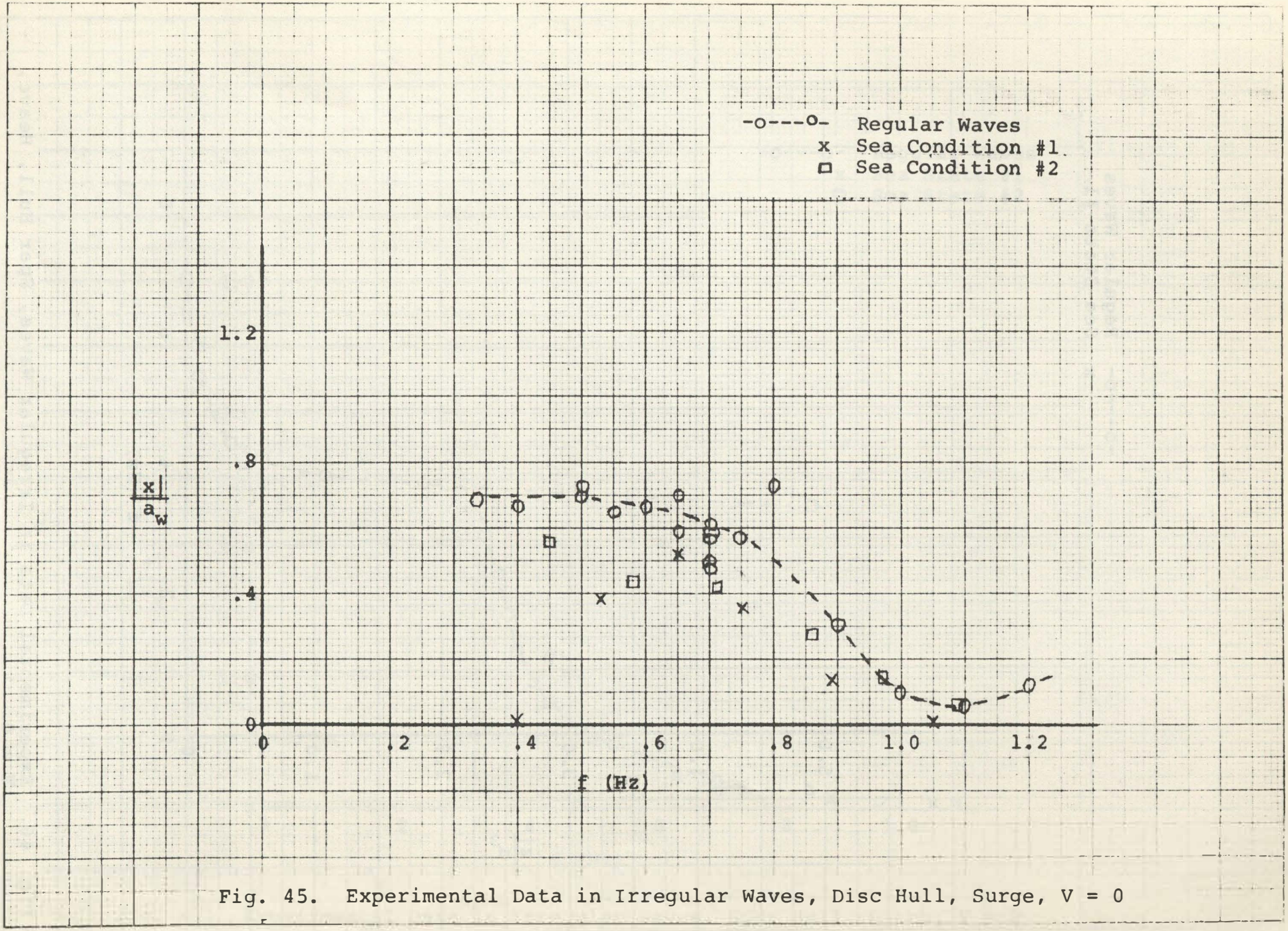

Fig. 45. Experimental Data in Irregular Waves, Disc Hull, Surge, V = 0

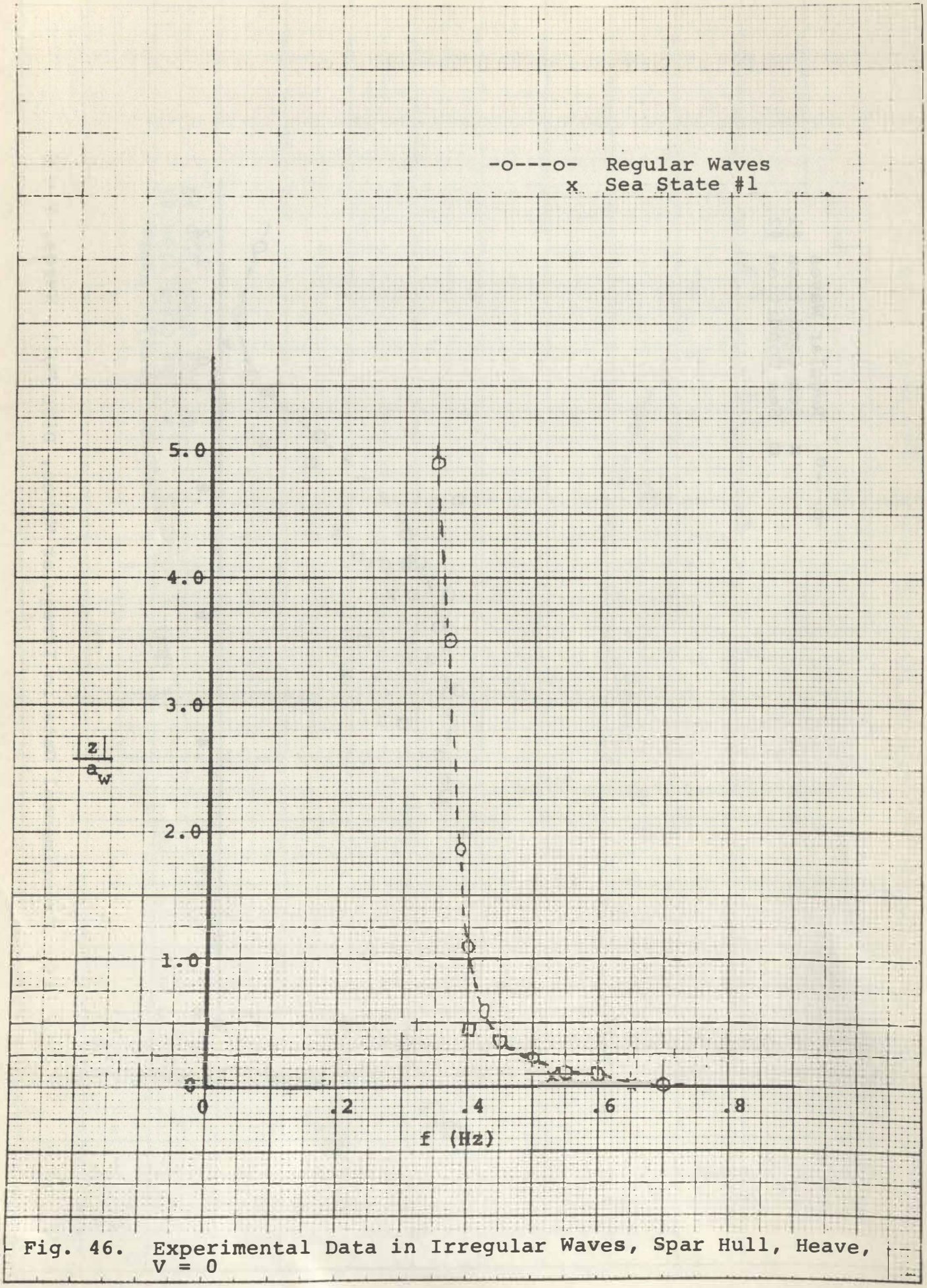

Fig. 46. Experimental Data in Irregular Waves, Spar Hull, Heave, V = 0

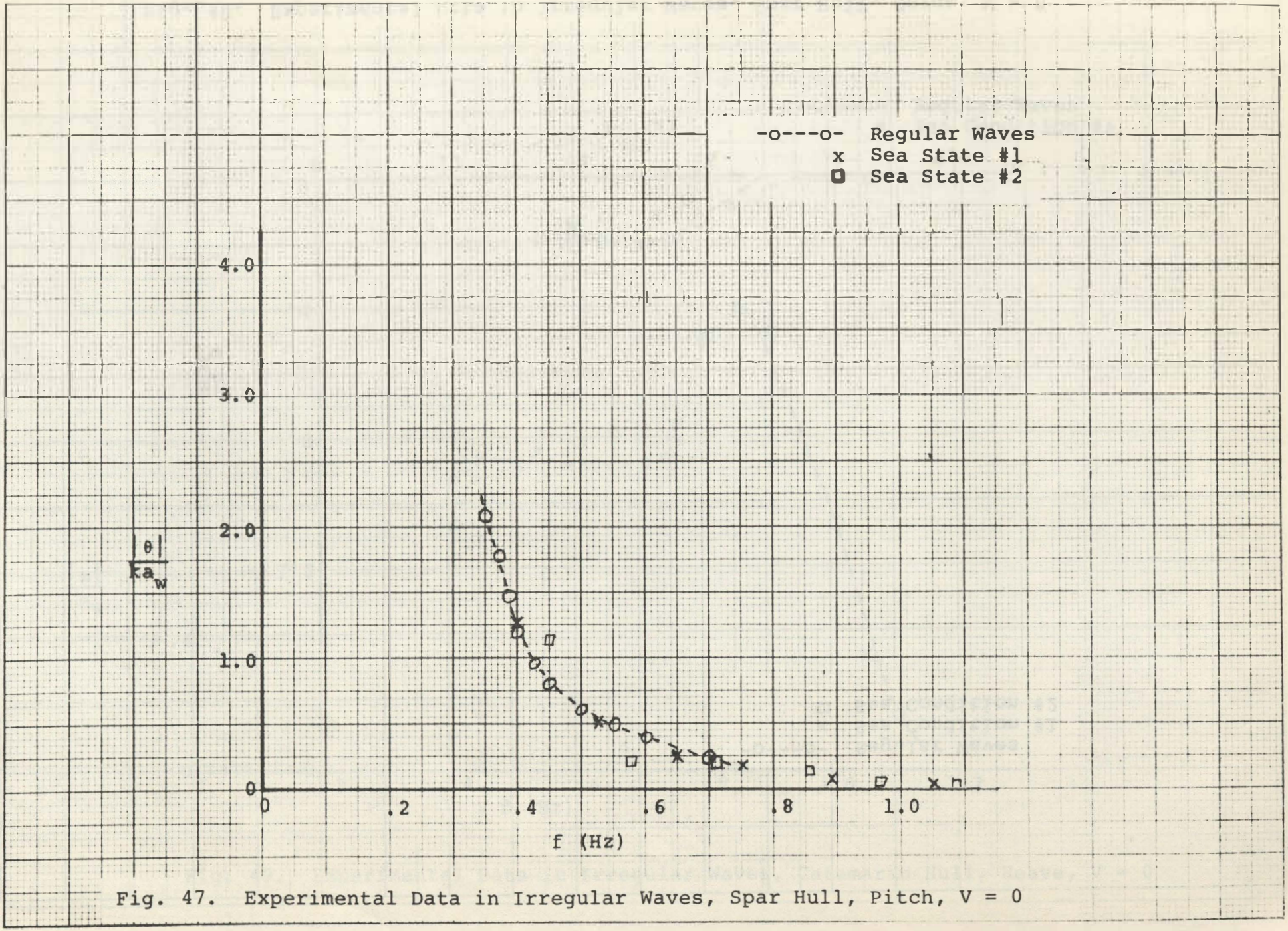

Fig. 47. Experimental Data in Irregular Waves, Spar Hull, Pitch, V = 0

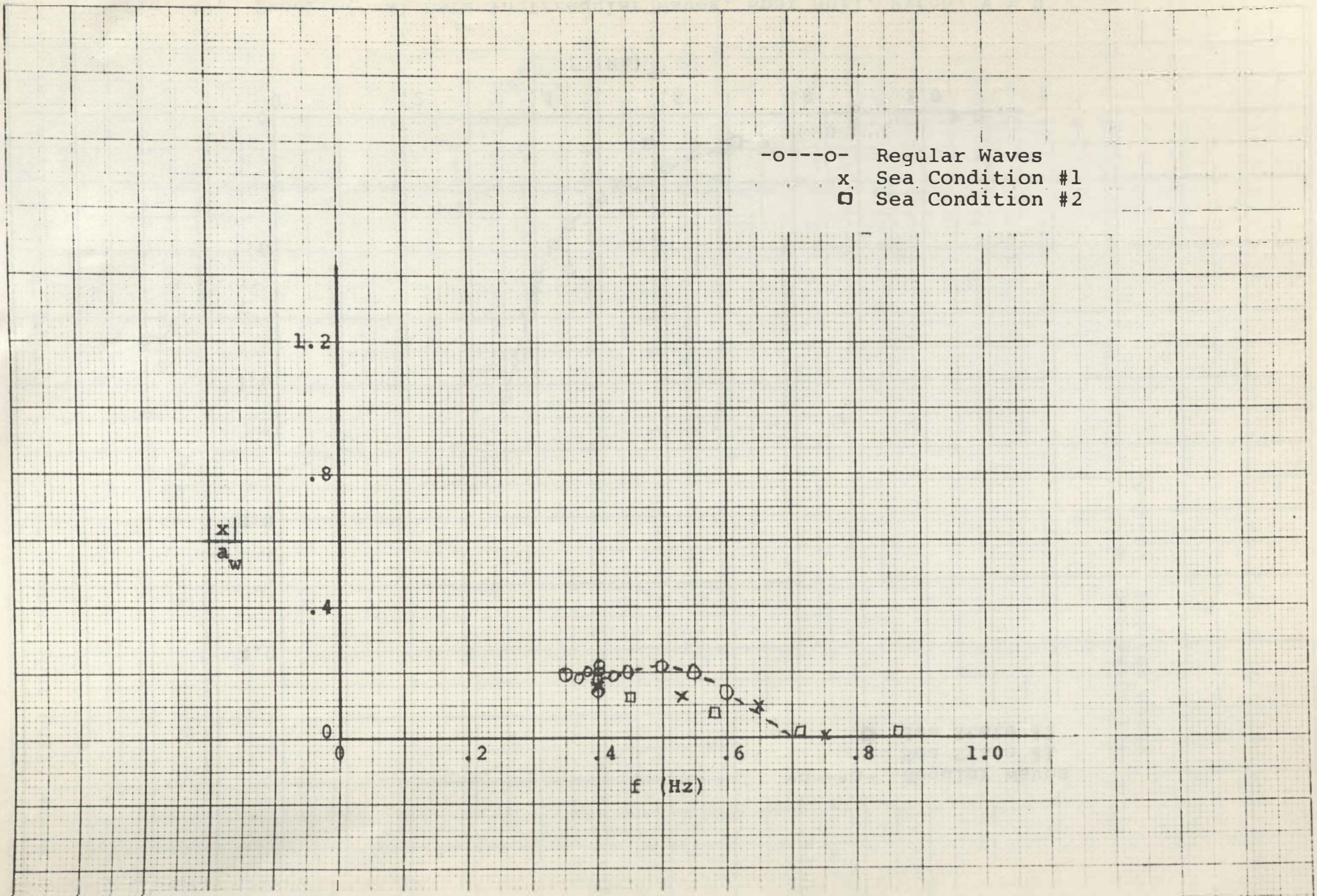

Fig. 48. Experimental Data in Irregular Waves, Spar Hull, Surge, V = 0

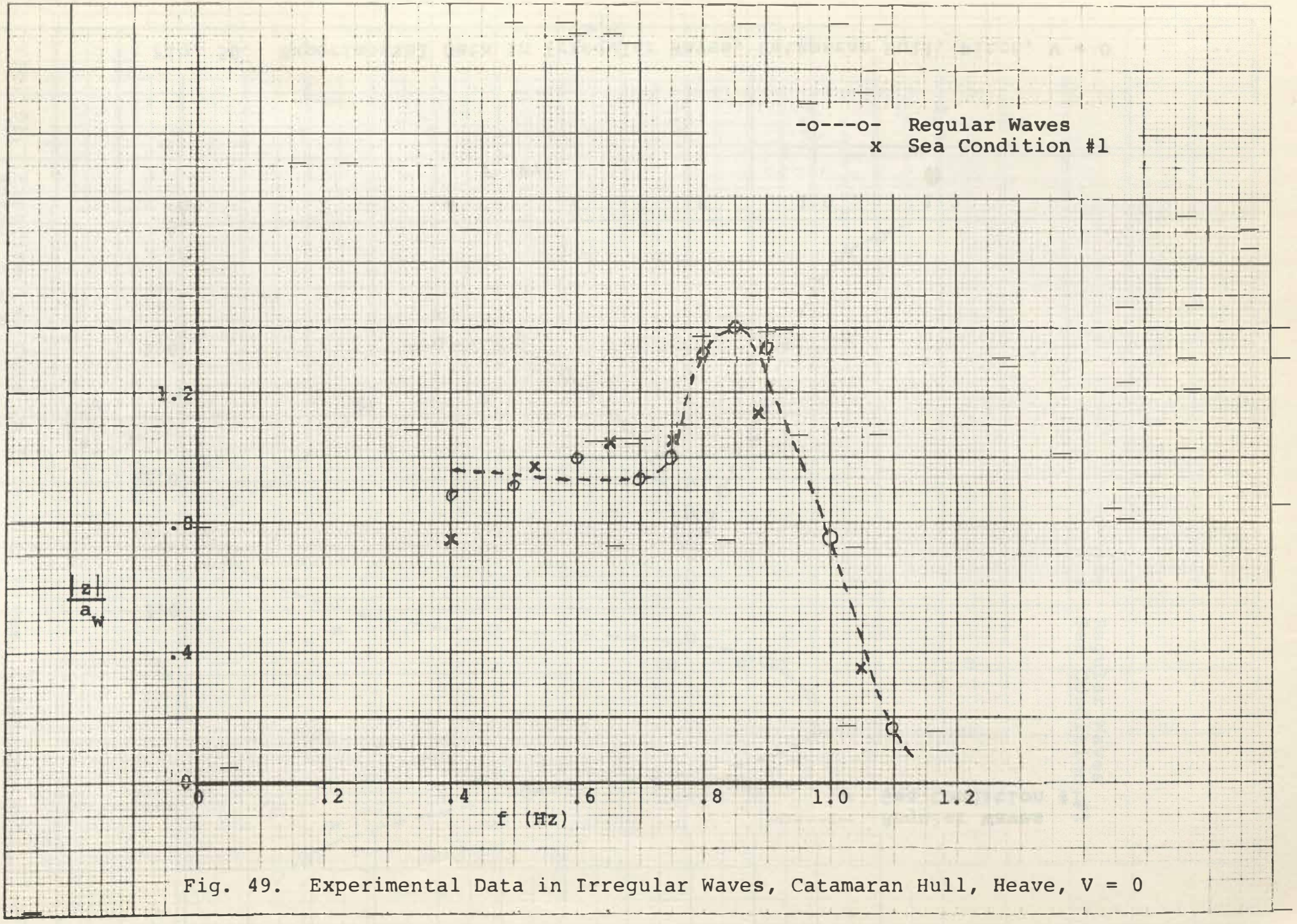

Fig. 49. Experimental Data in Irregular Waves, Catamaran Hull, Heave, V = 0

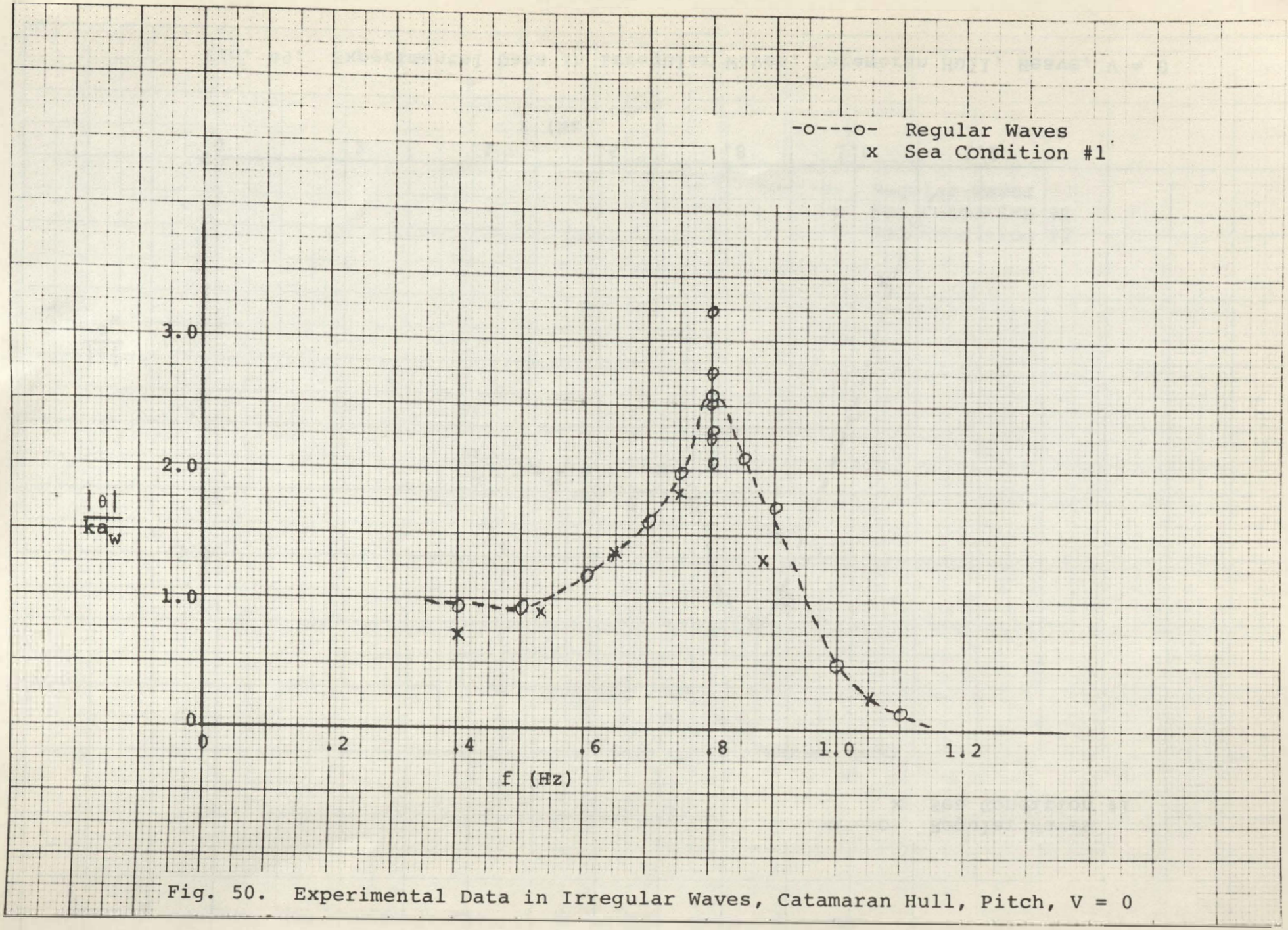

Fig. 50. Experimental Data in Irregular Waves, Catamaran Hull, Pitch, V = 0

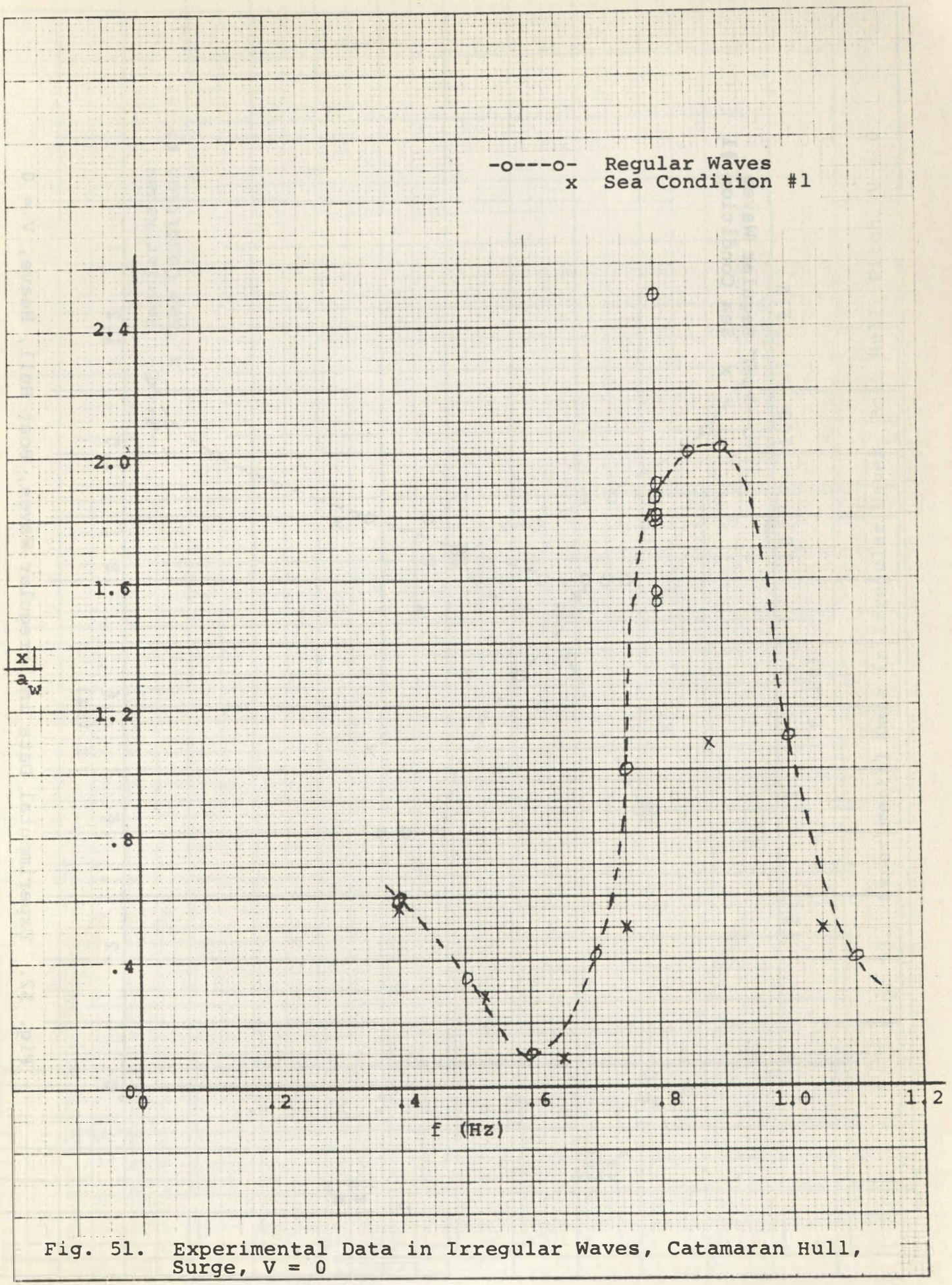

Fig. 51. Experimental Data in Irregular Waves, Catamaran Hull, Surge, V = 0

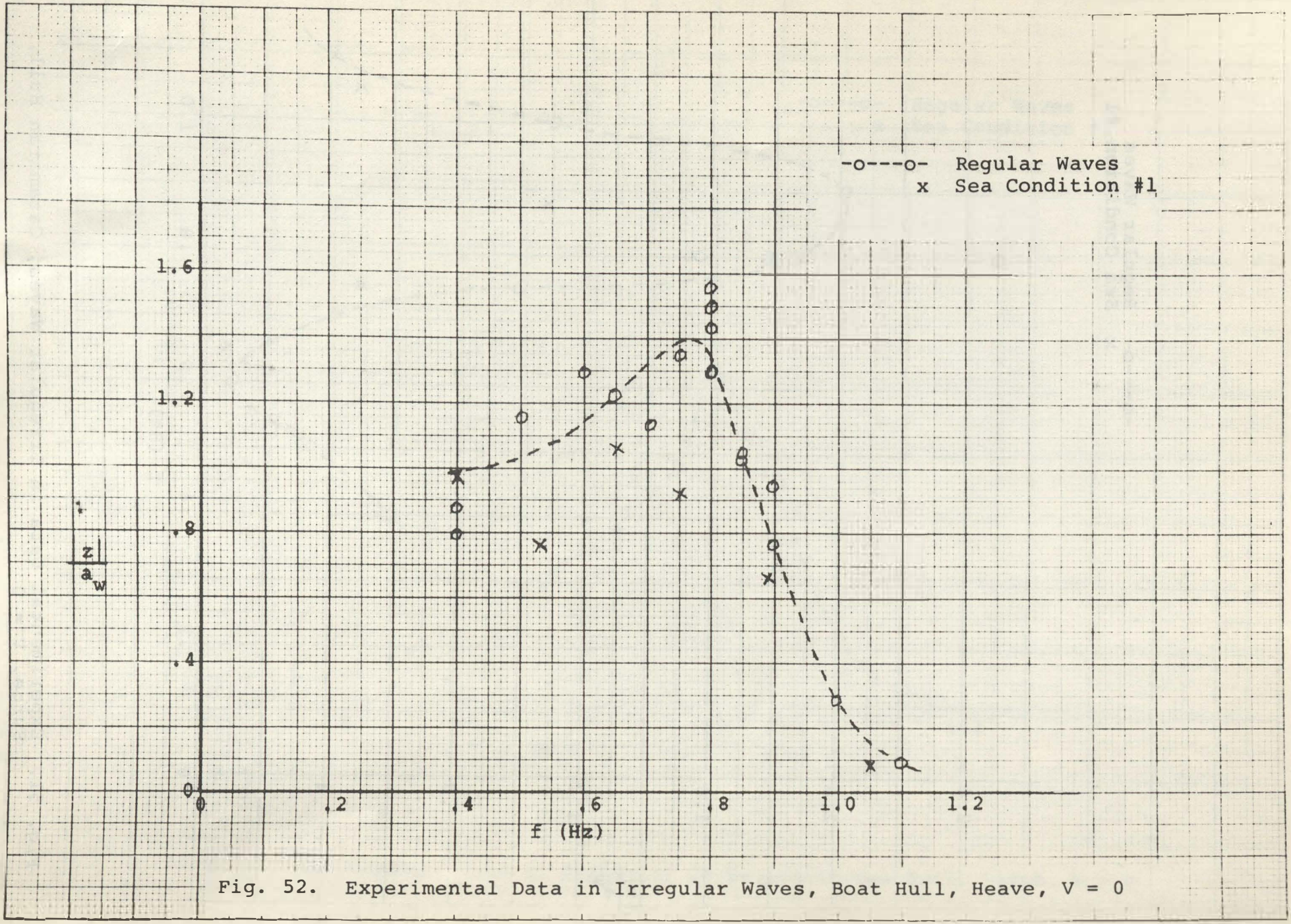

Fig. 52. Experimental Data in Irregular Waves, Boat Hull, Heave, V = 0

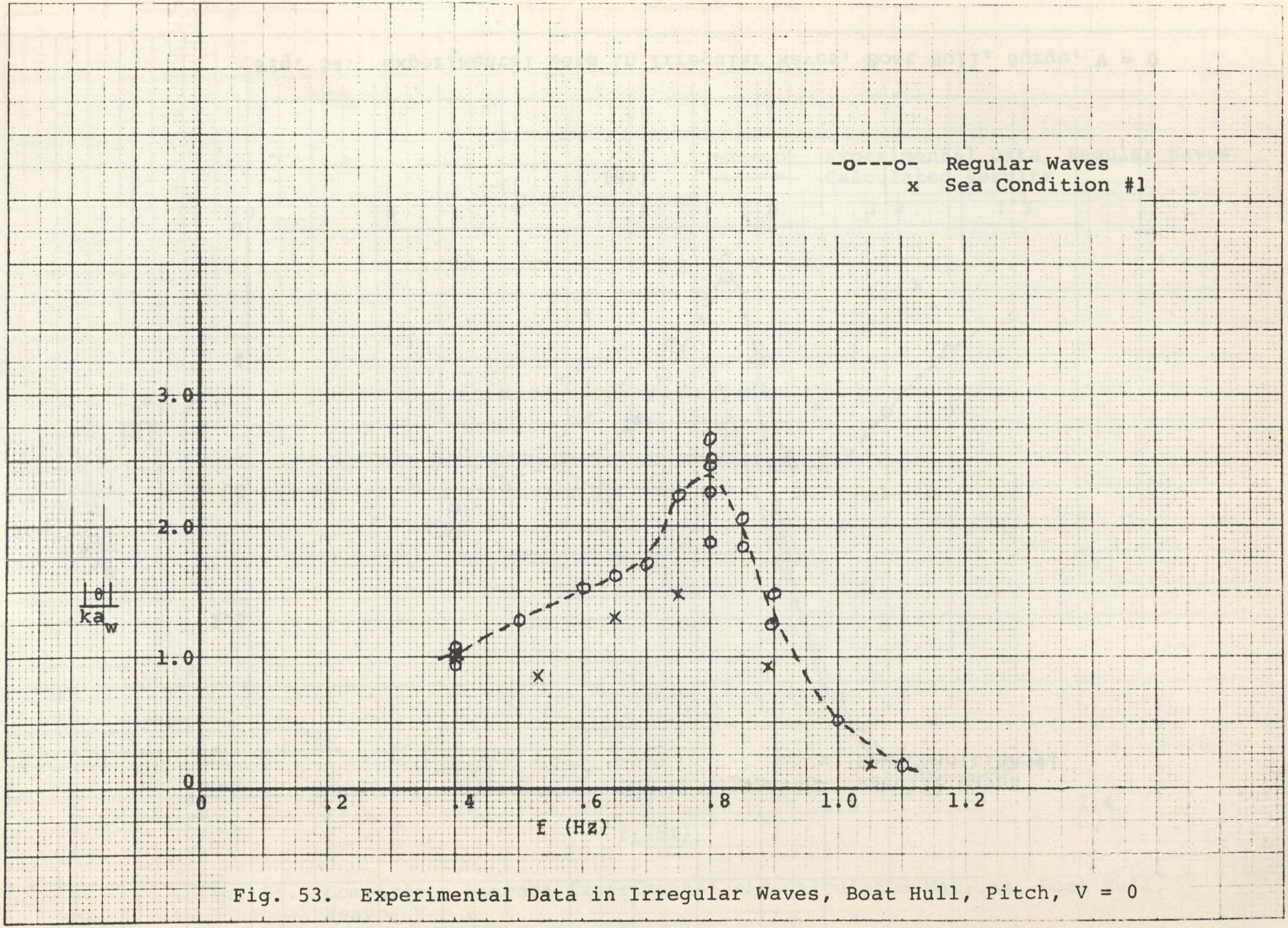

Fig. 53. Experimental Data in Irregular Waves, Boat Hull, Pitch, V = 0

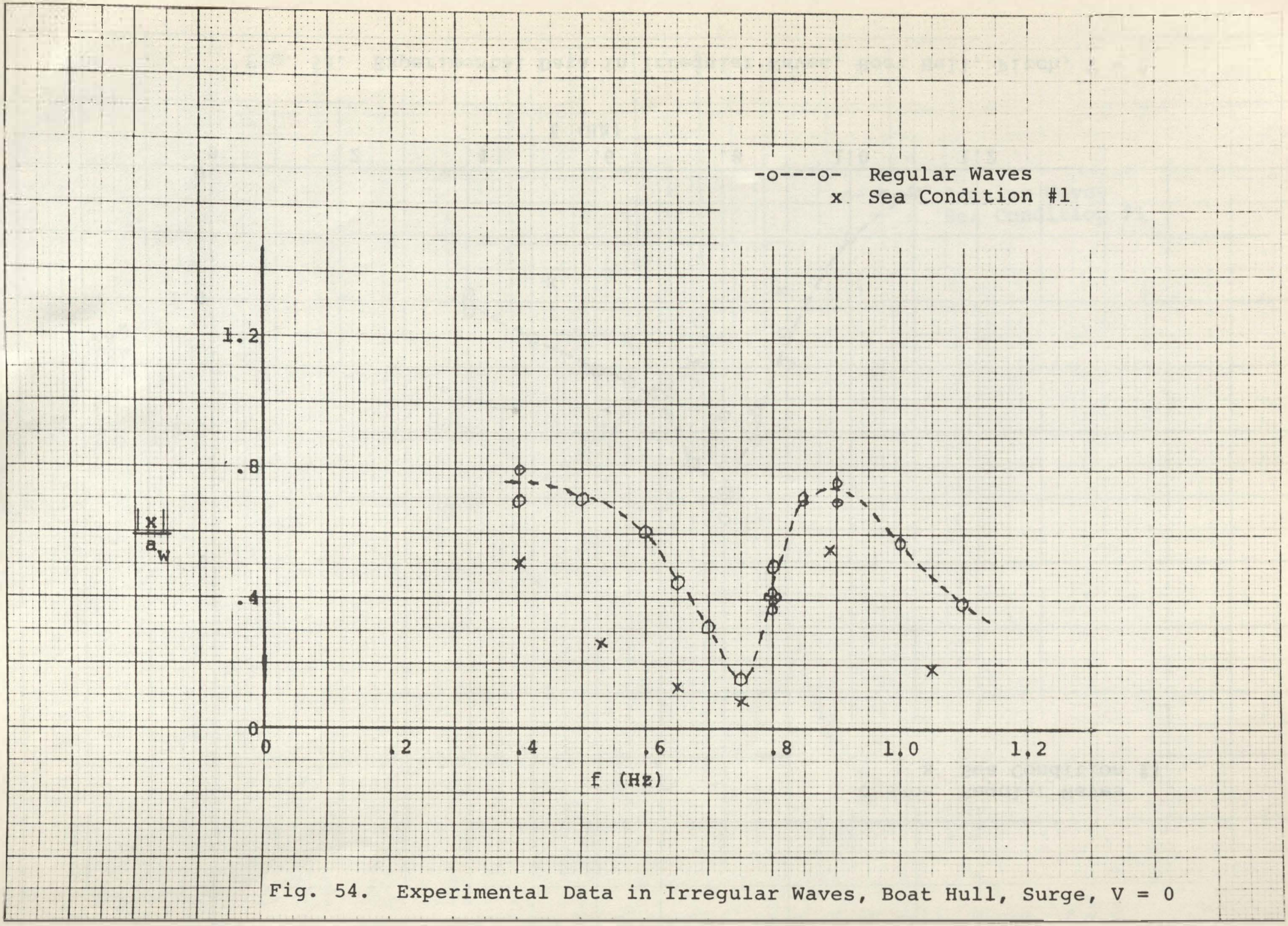

Fig. 54. Experimental Data in Irregular Waves, Boat Hull, Surge, V = 0

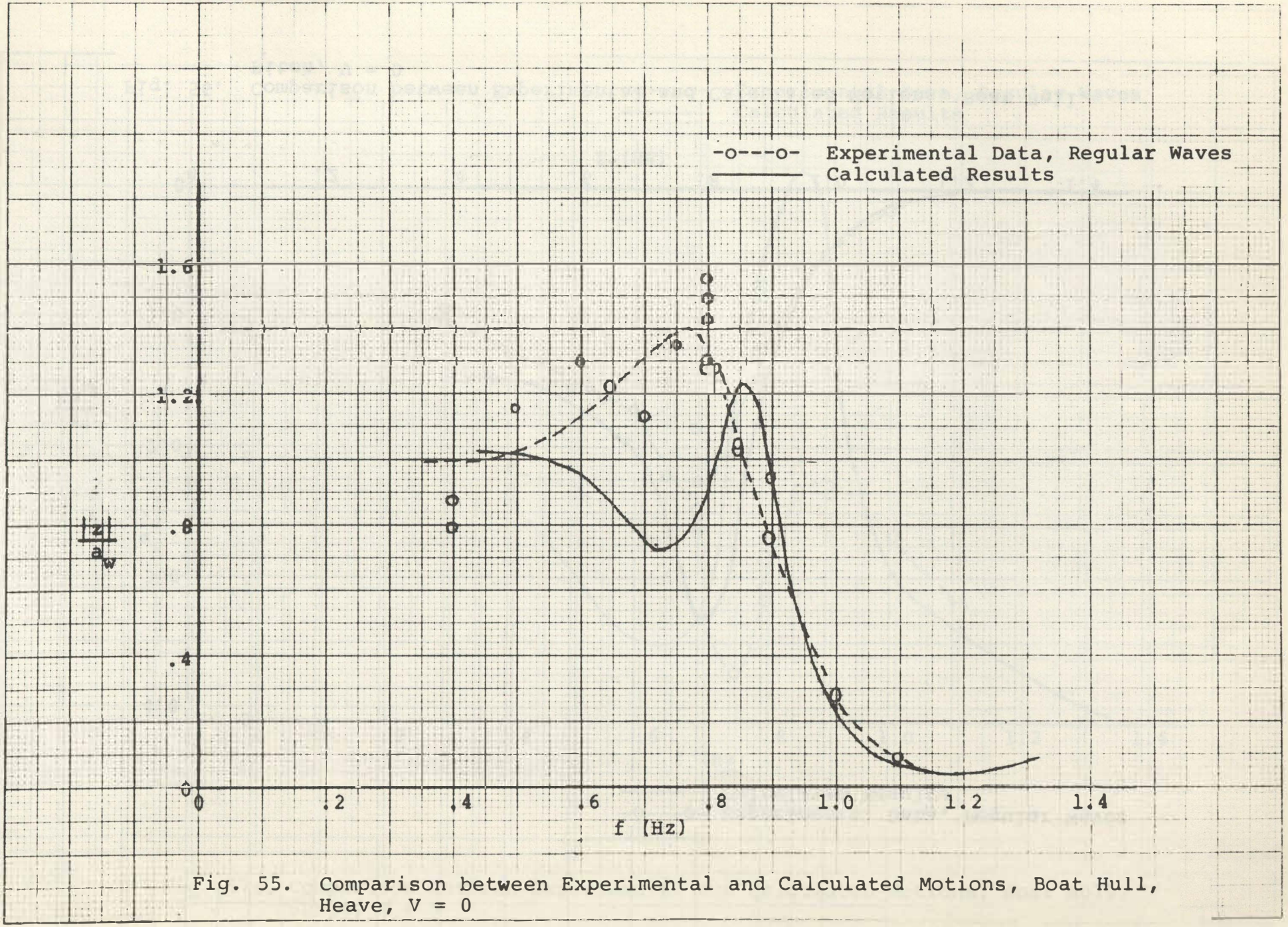

Fig. 55. Comparison between Experimental and Calculated Motions, Boat Hull, Heave, V = 0

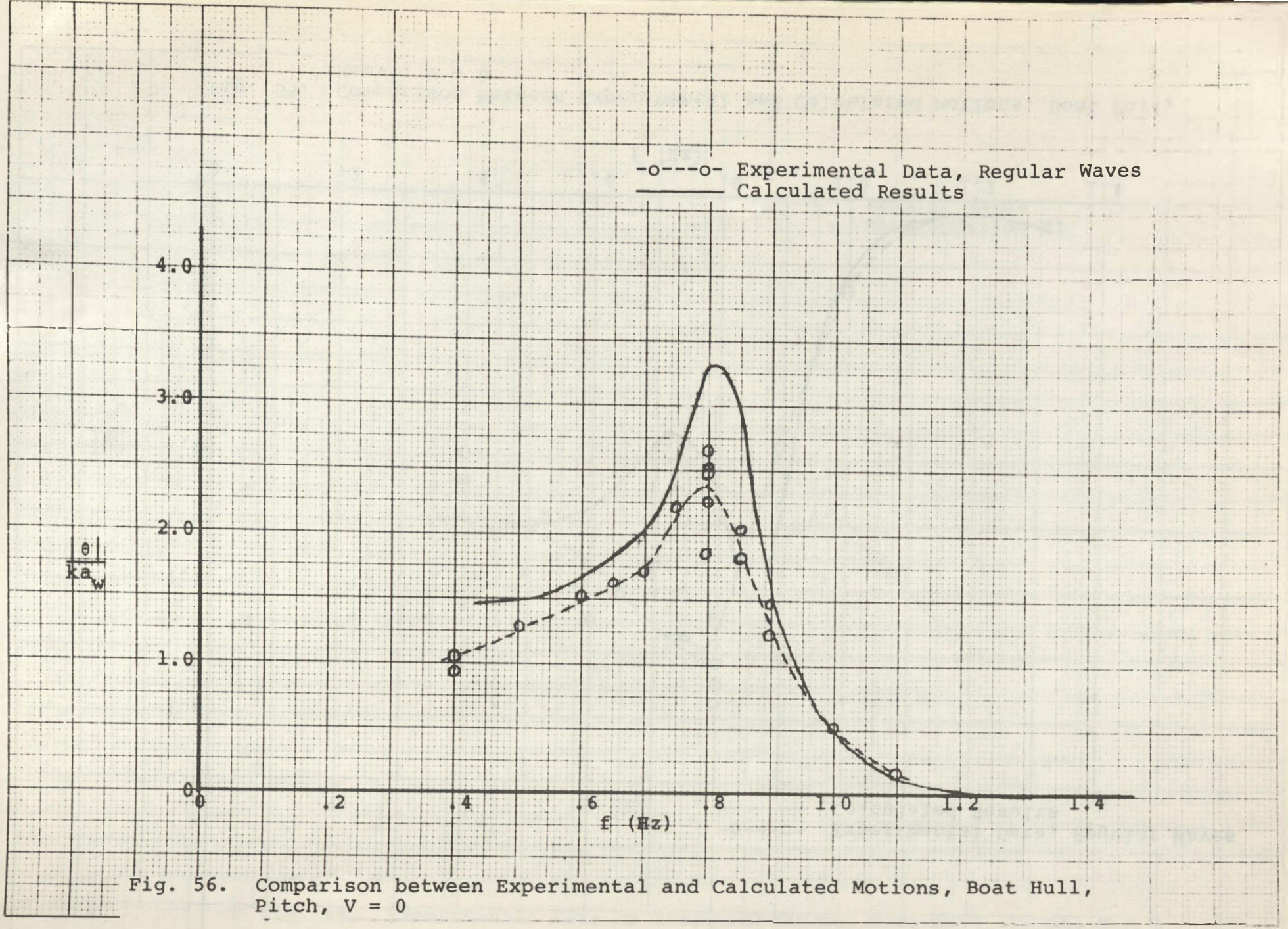

Fig. 56. Comparison between Experimental and Calculated Motions, Boat Hull, Pitch, V = 0

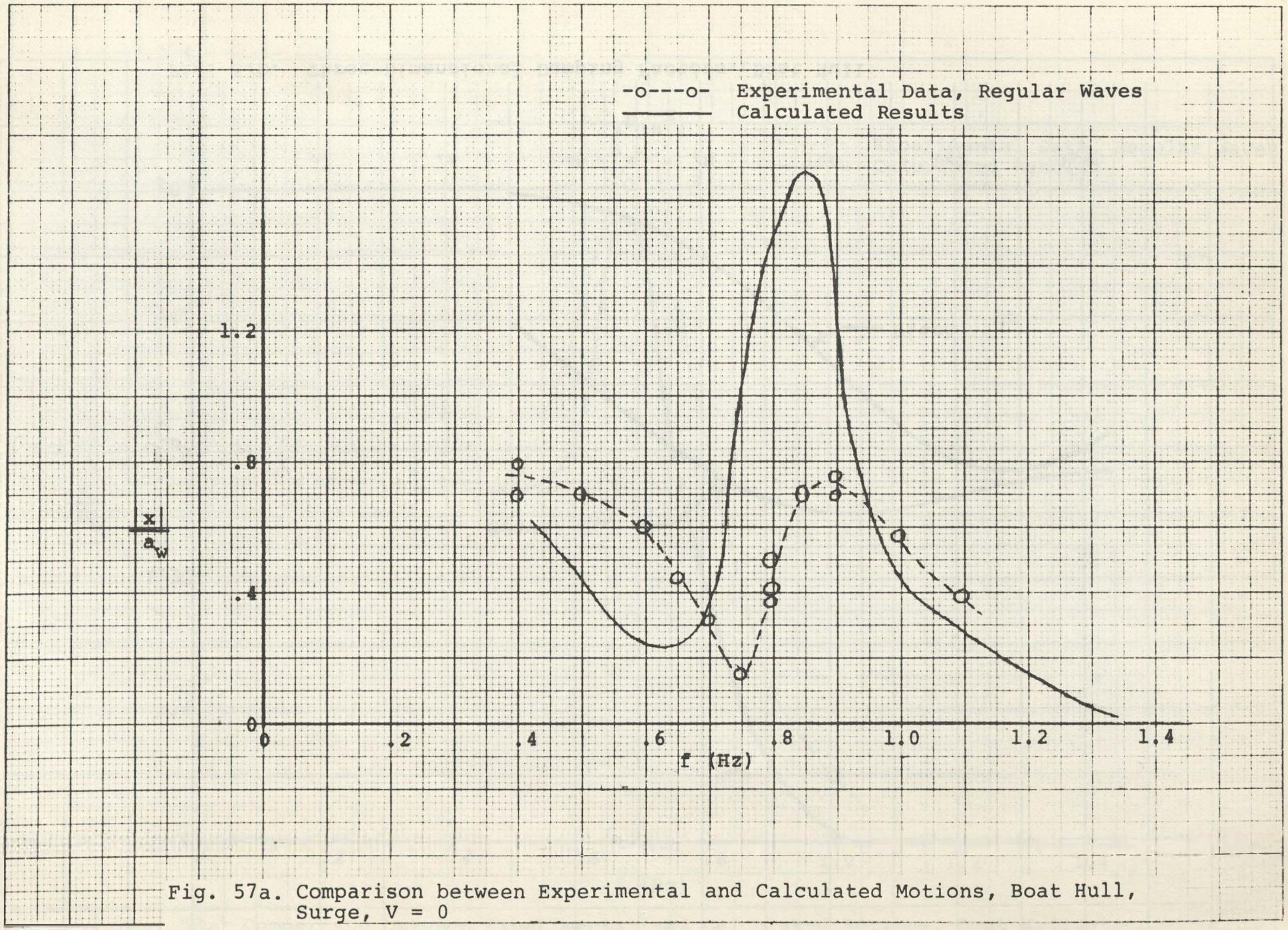

Fig. 57a. Comparison between Experimental and Calculated Motions, Boat Hull, Surge, V = 0

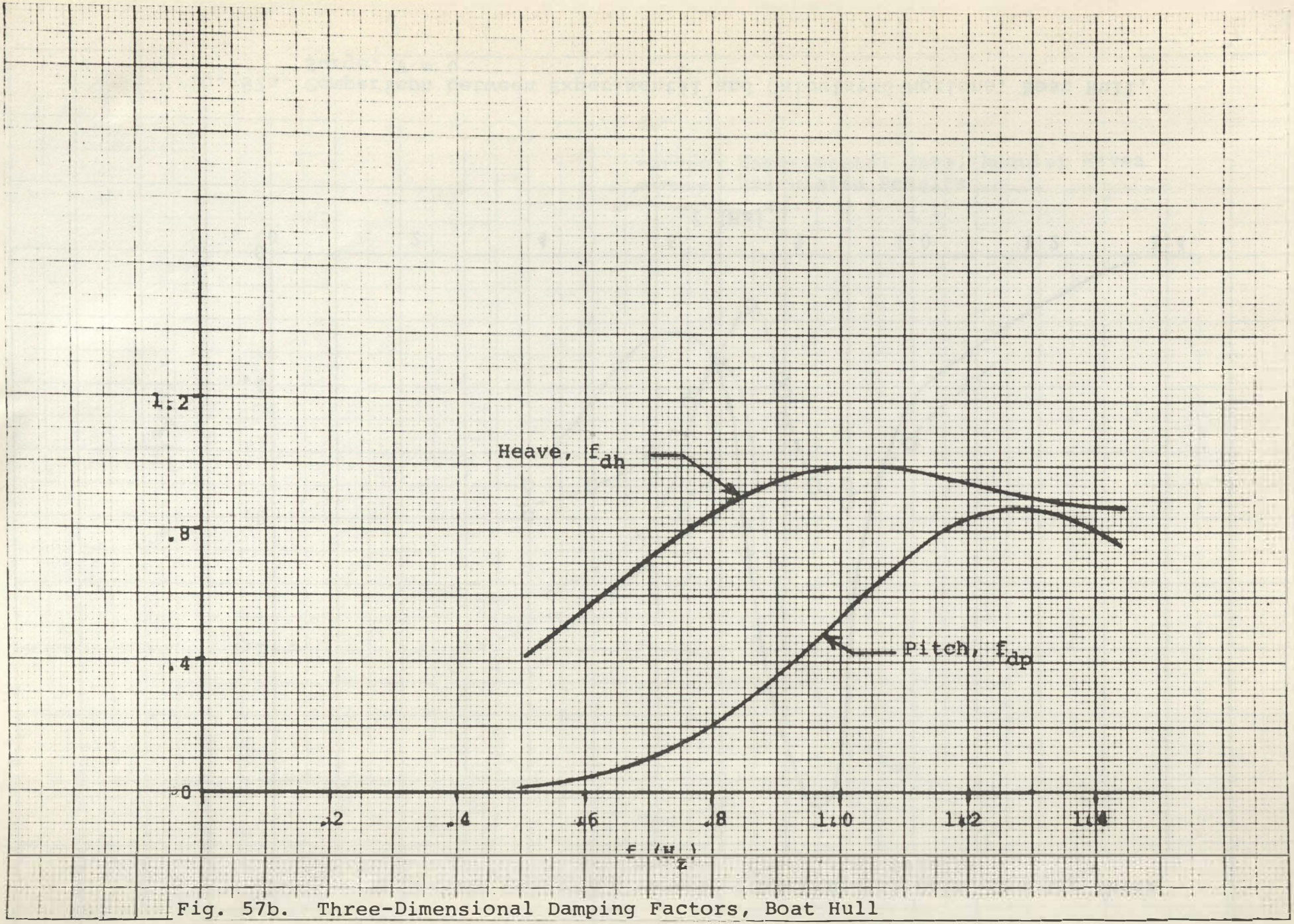

Fig. 57b. Three-Dimensional Damping Factors, Boat Hull

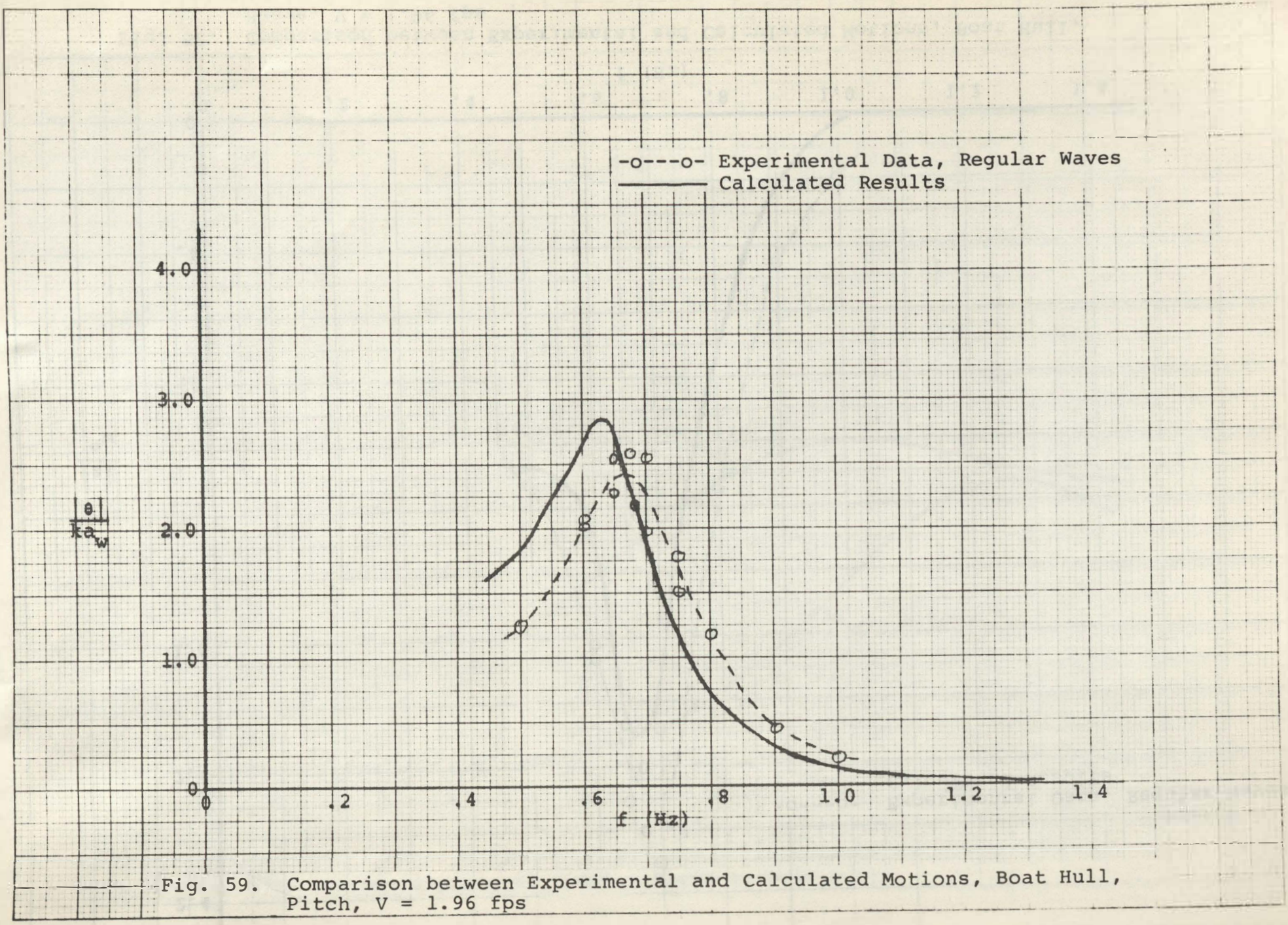

Fig. 59. Comparison between Experimental and Calculated Motions, Boat Hull, Pitch, V = 1.96 fps

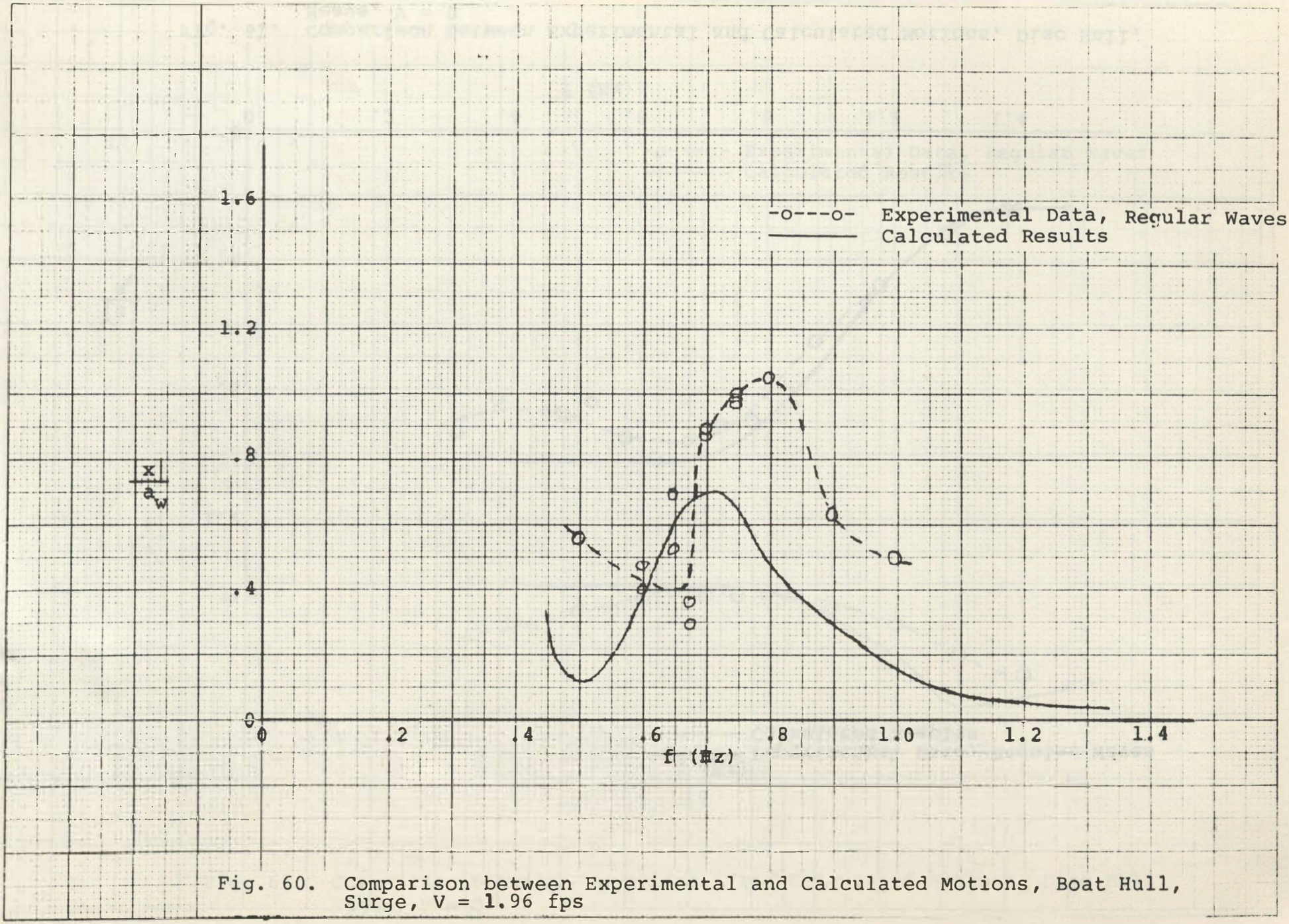

Fig. 60. Comparison between Experimental and Calculated Motions, Boat Hull, Surge, V = 1.96 fps

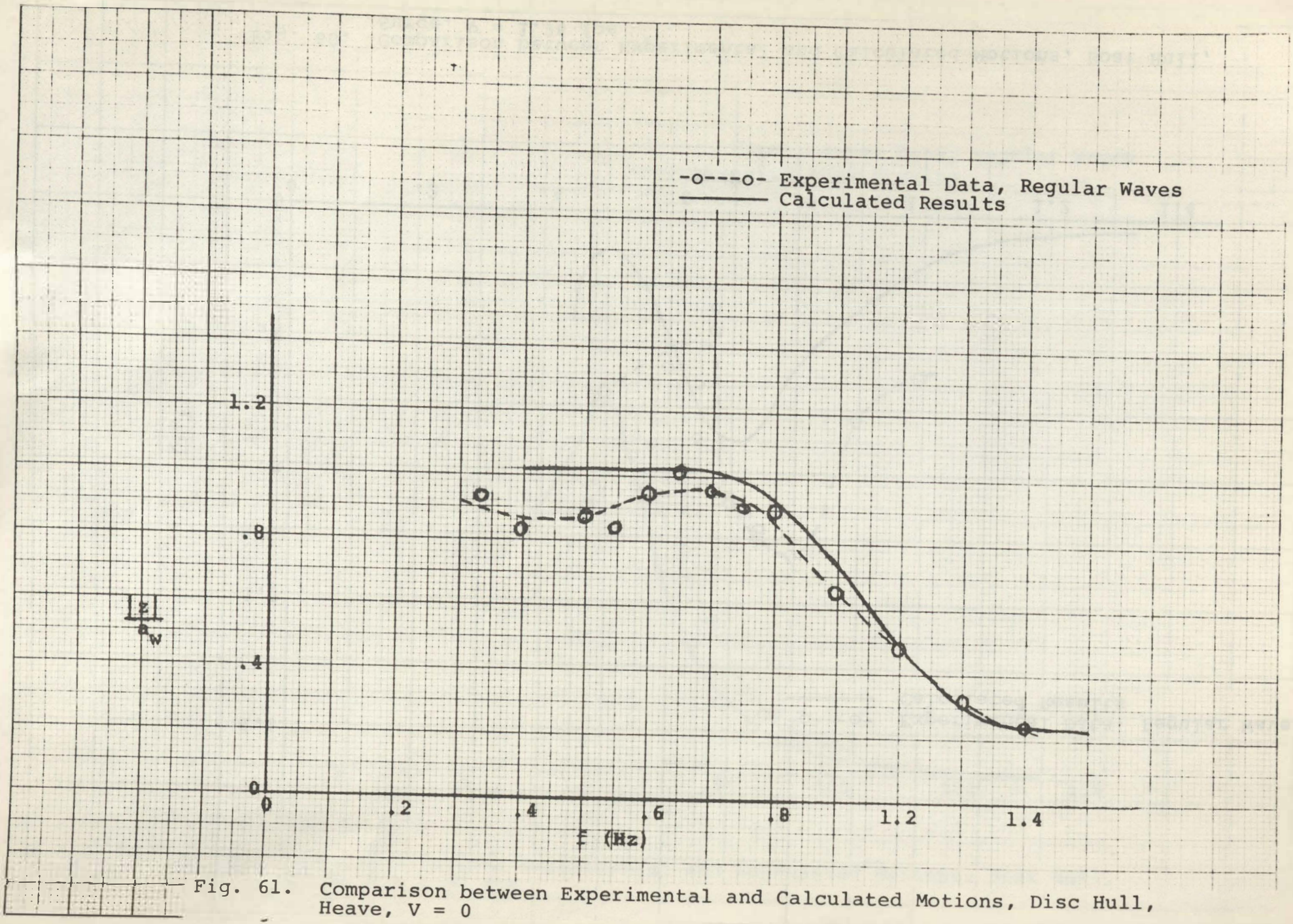

Fig. 61. Comparison between Experimental and Calculated Motions, Disc Hull, Heave, V = 0

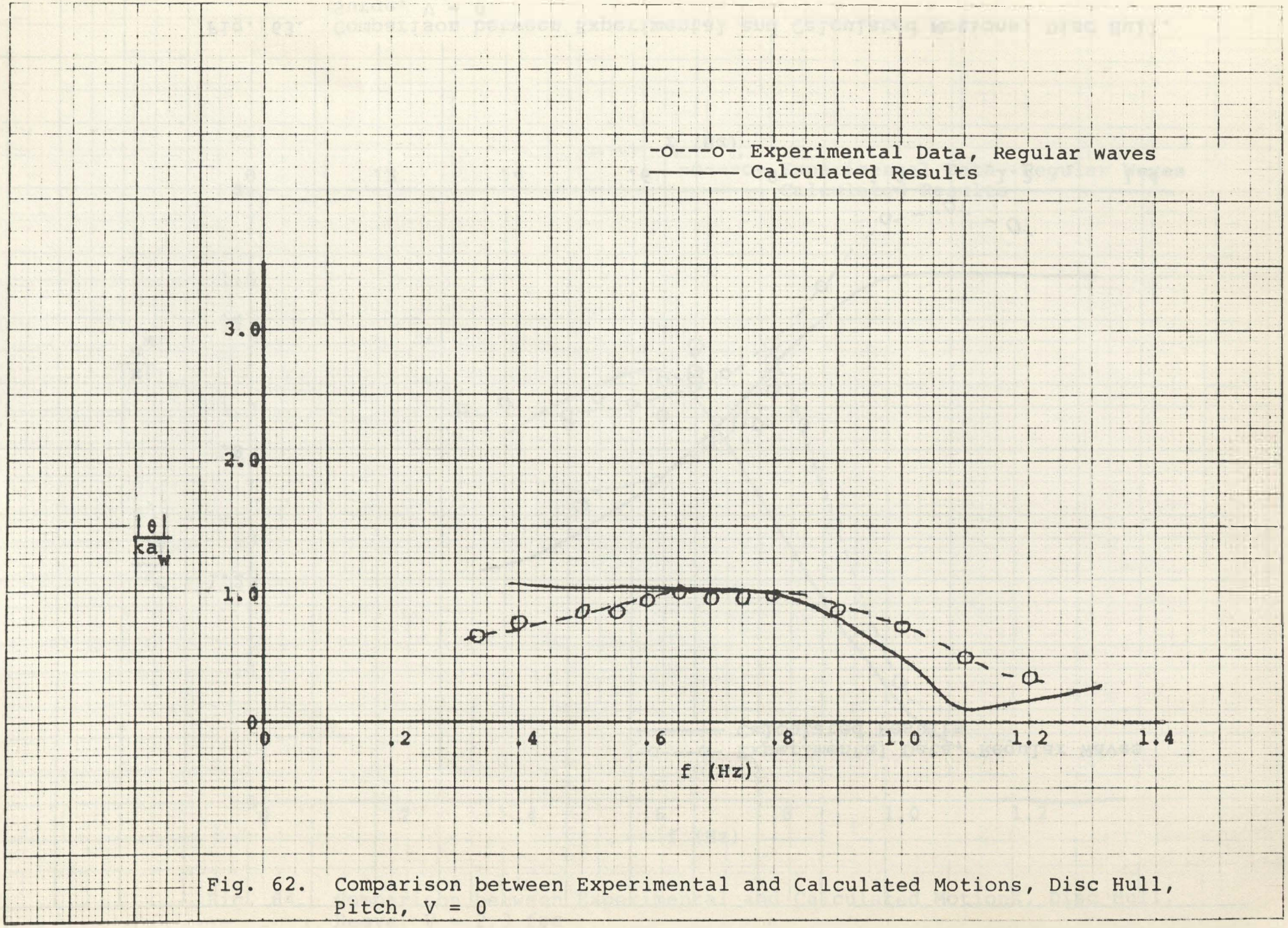

Fig. 62. Comparison between Experimental and Calculated Motions, Disc Hull, Pitch, V = 0

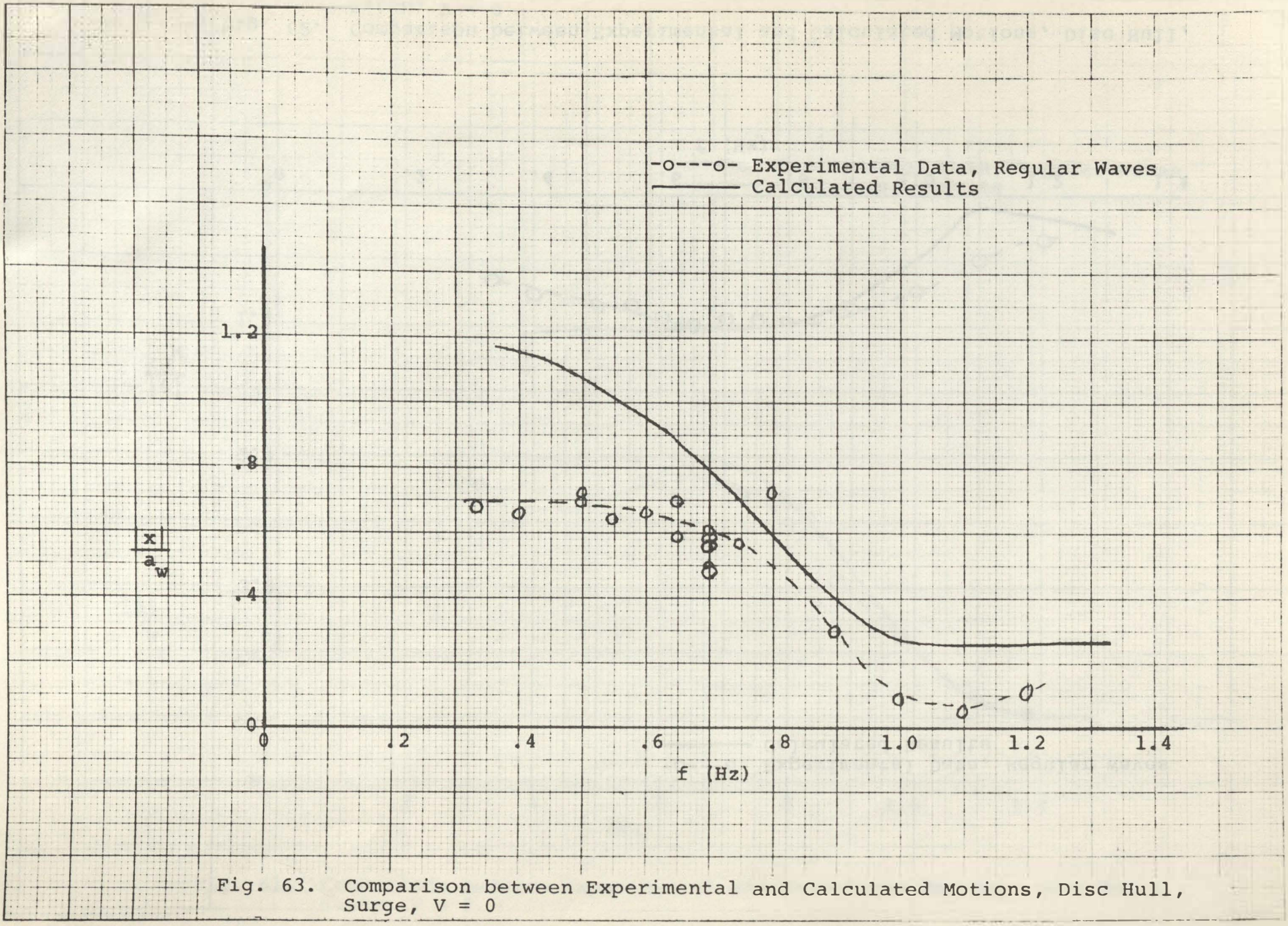

Fig. 63. Comparison between Experimental and Calculated Motions, Disc Hull, Surge, V = 0

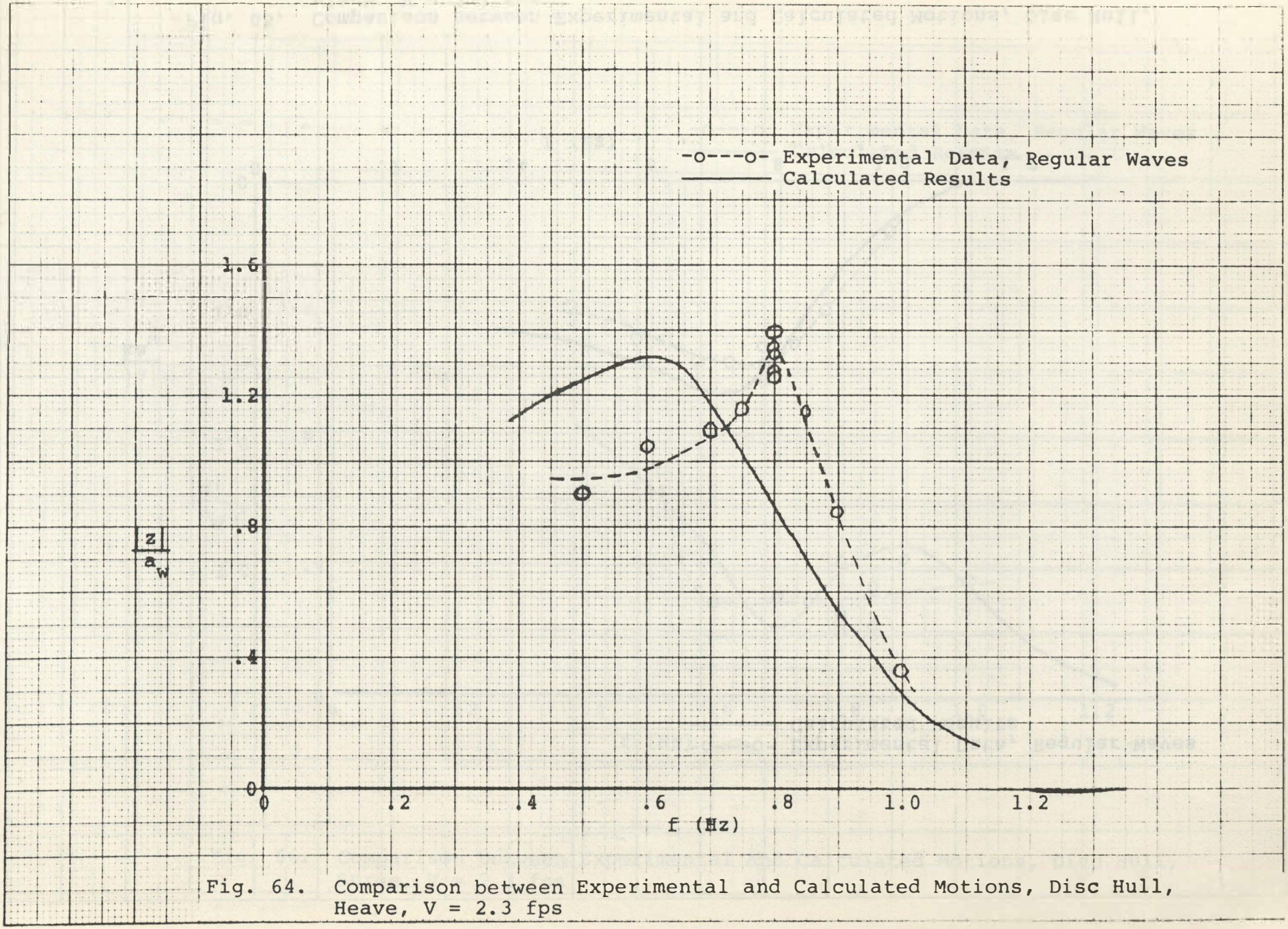

Fig. 64. Comparison between Experimental and Calculated Motions, Disc Hull, Heave, V = 2.3 fps

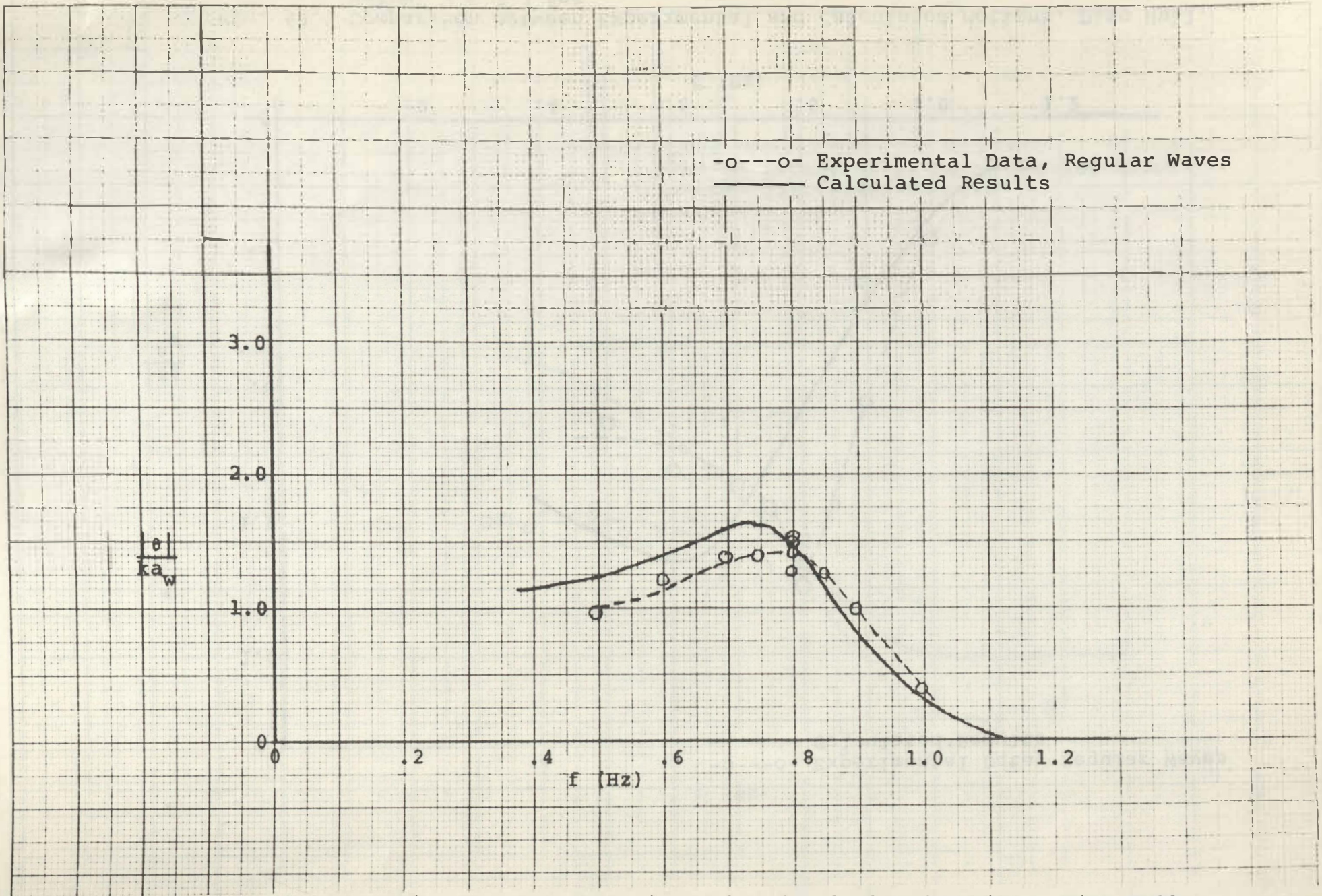

Fig. 65. Comparison between Experimental and Calculated Motions, Disc Hull, Pitch, V = 2.3 fps

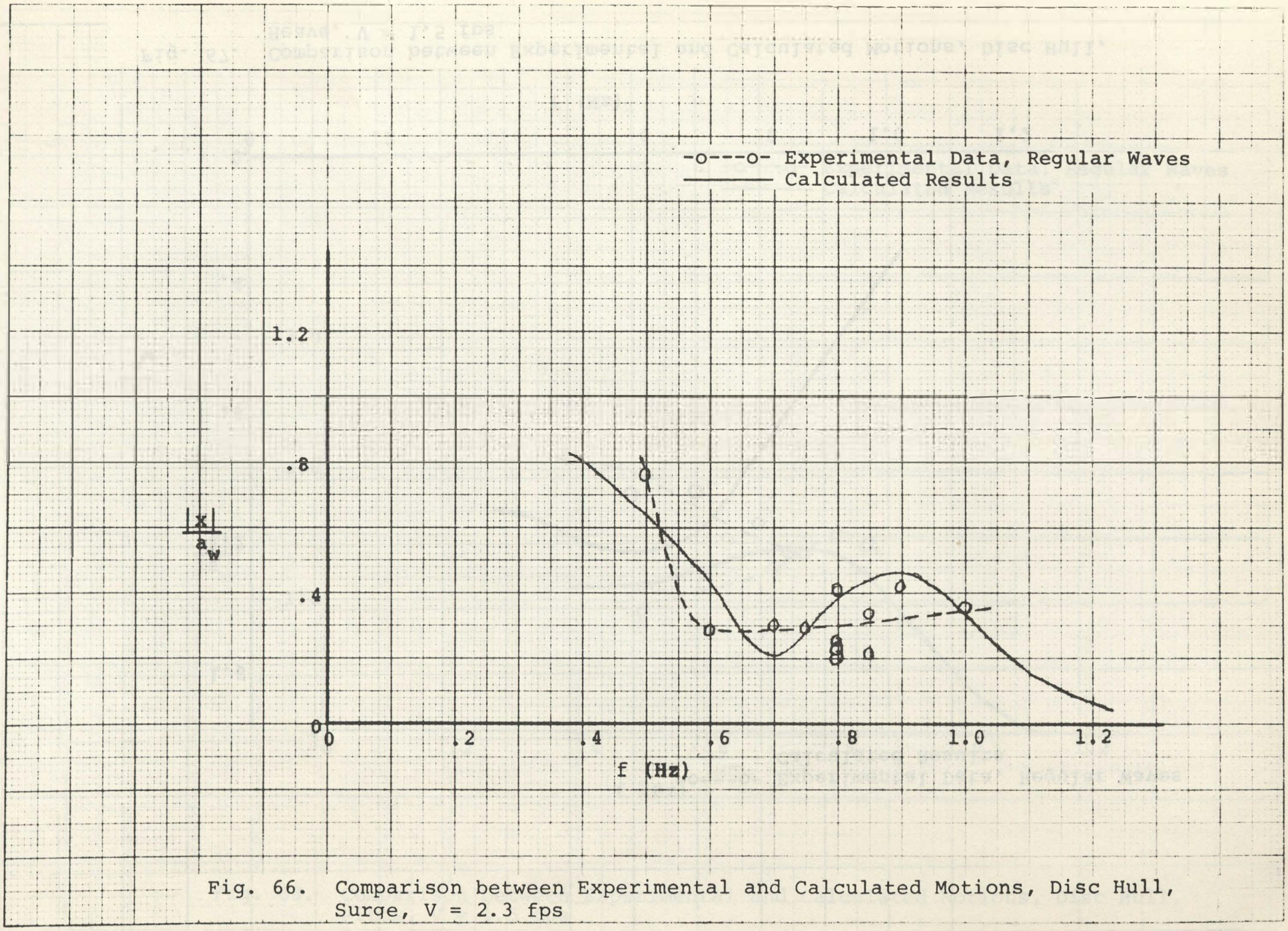

Fig. 66. Comparison between Experimental and Calculated Motions, Disc Hull, Surge, V = 2.3 fps

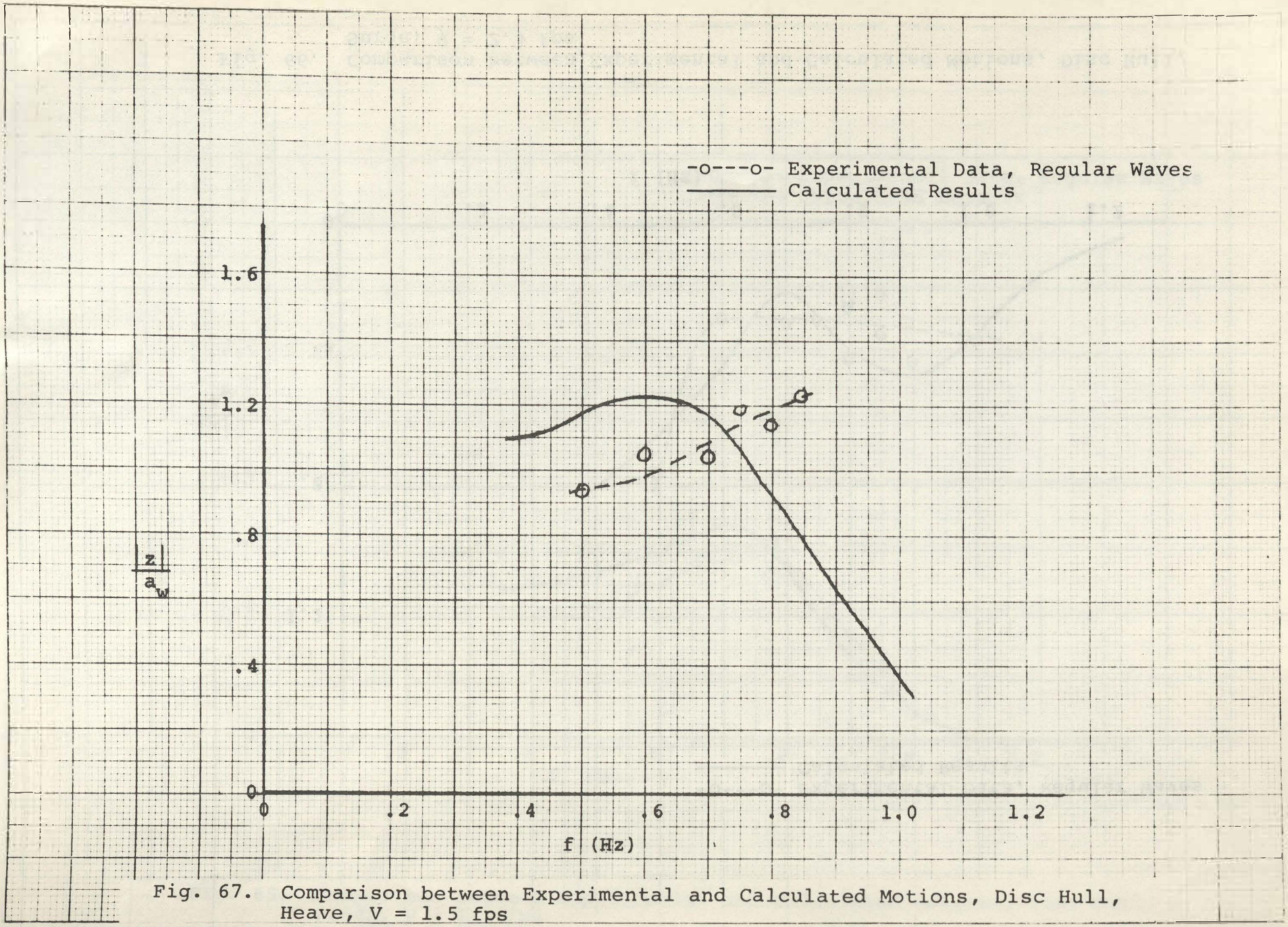

Fig. 67. Comparison between Experimental and Calculated Motions, Disc Hull, Heave, V = 1.5 fps

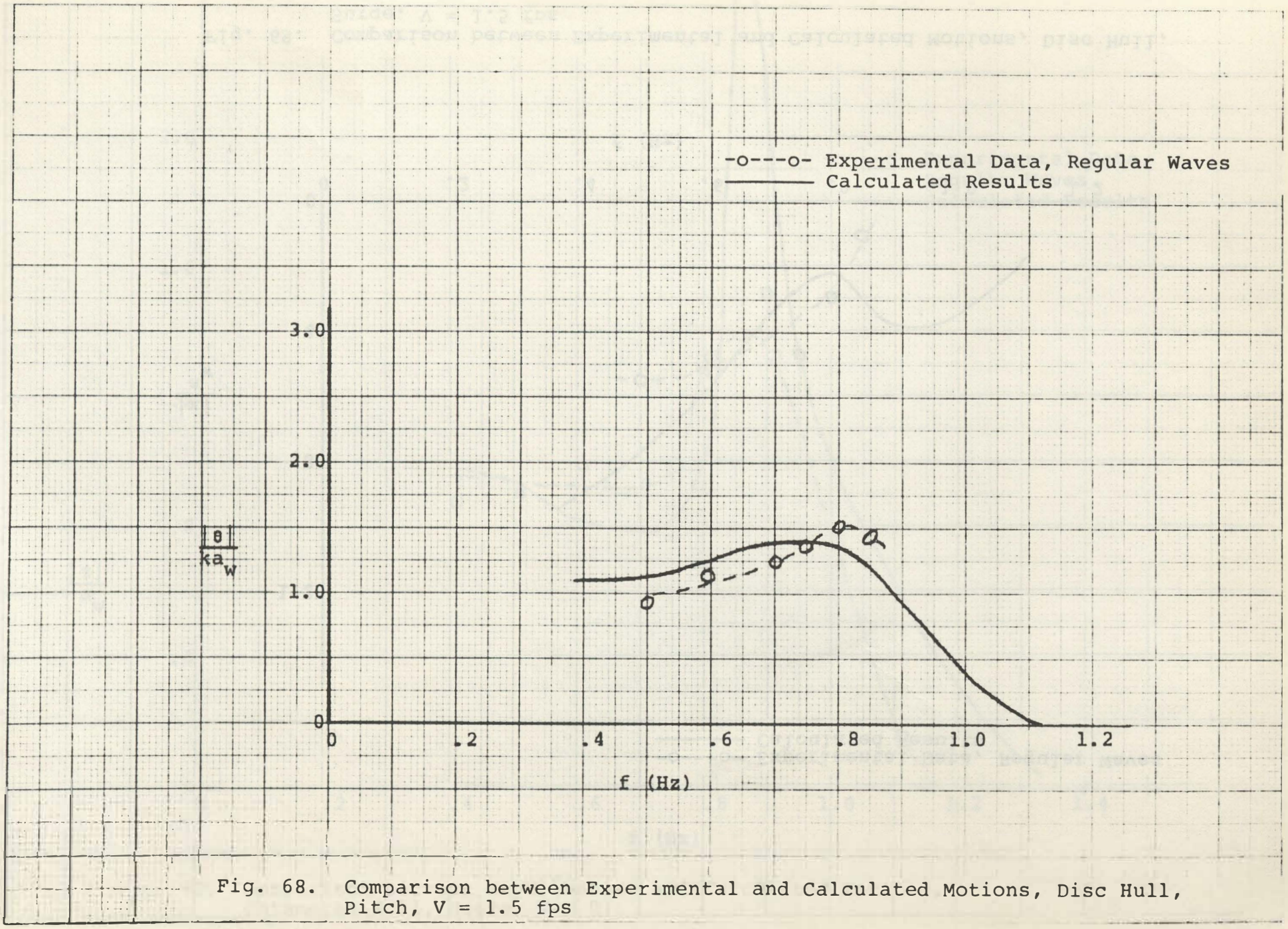

Fig. 68. Comparison between Experimental and Calculated Motions, Disc Hull, Pitch, V = 1.5 fps

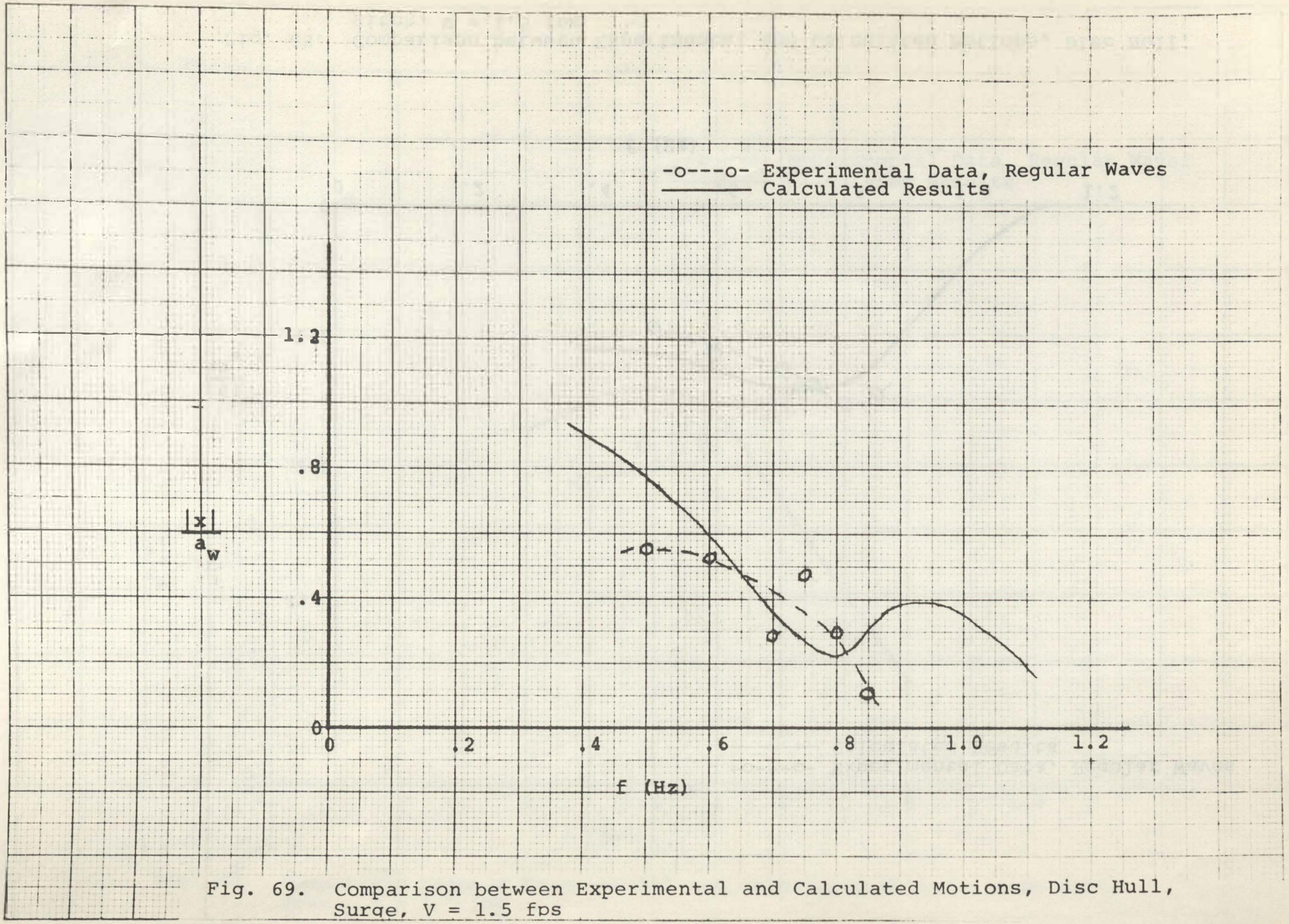

Fig. 69. Comparison between Experimental and Calculated Motions, Disc Hull, Surge, V = 1.5 fps

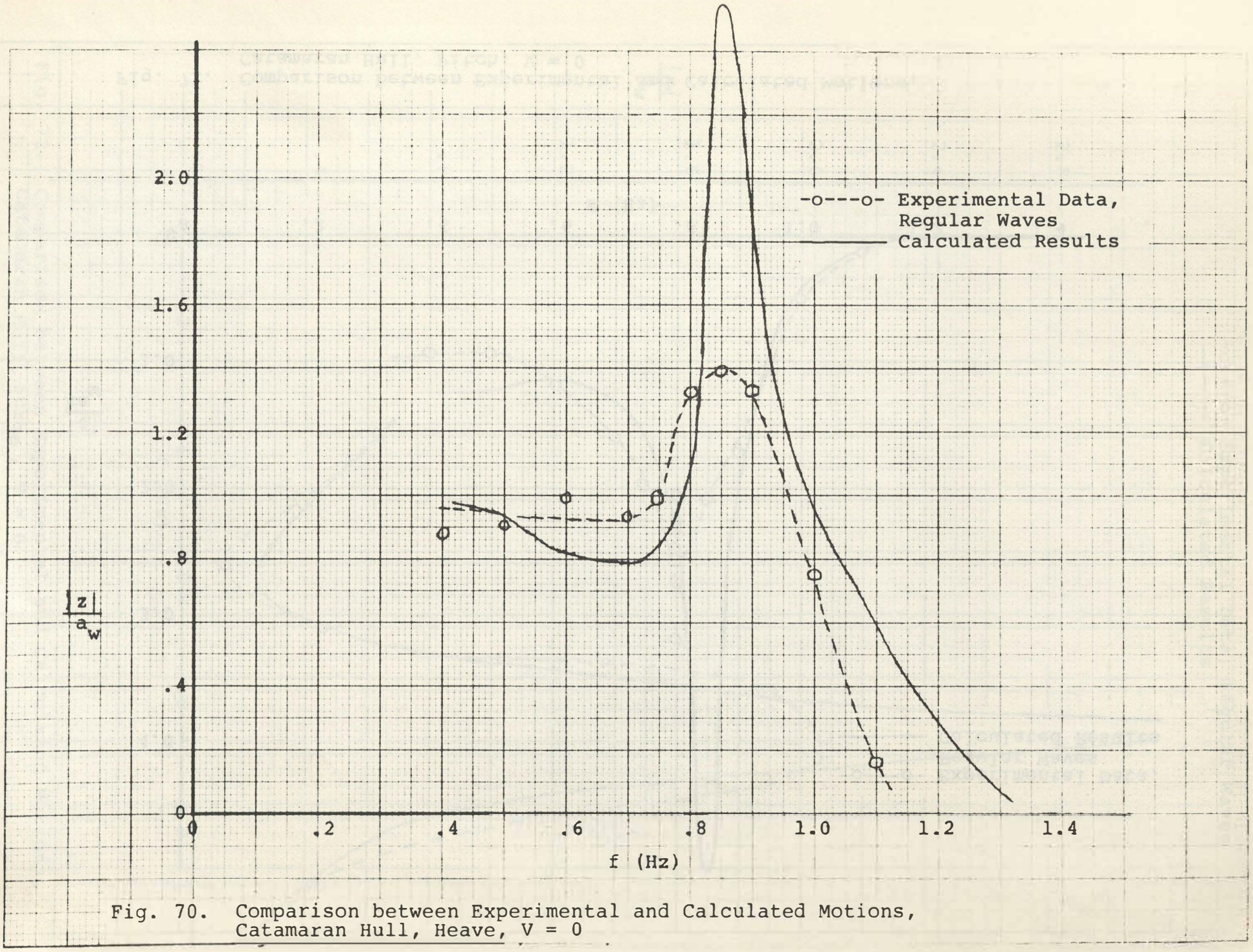

Fig. 70. Comparison between Experimental and Calculated Motions, Catamaran Hull, Heave, V = 0

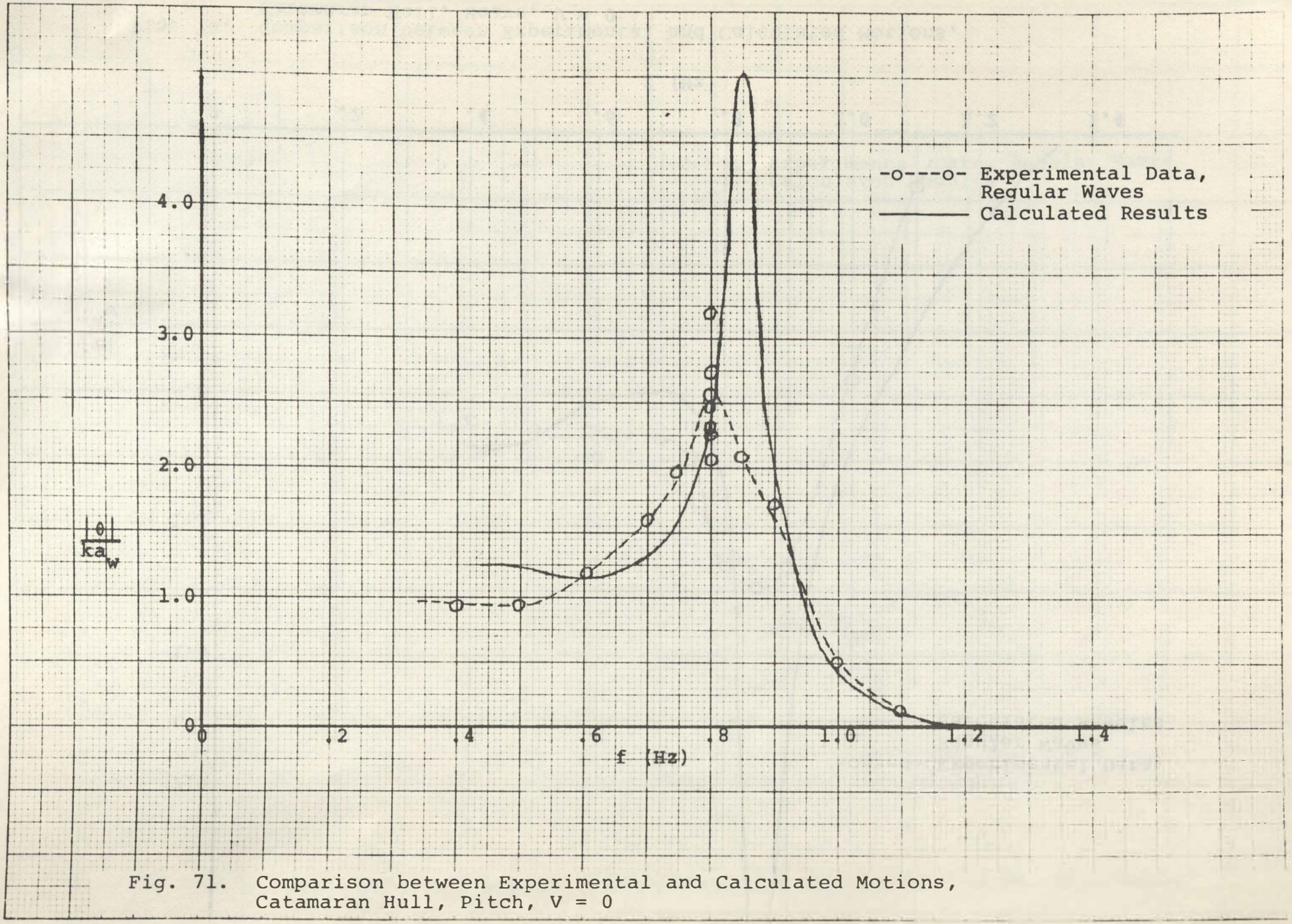

Fig. 71. Comparison between Experimental and Calculated Motions, Catamaran Hull, Pitch, V = 0

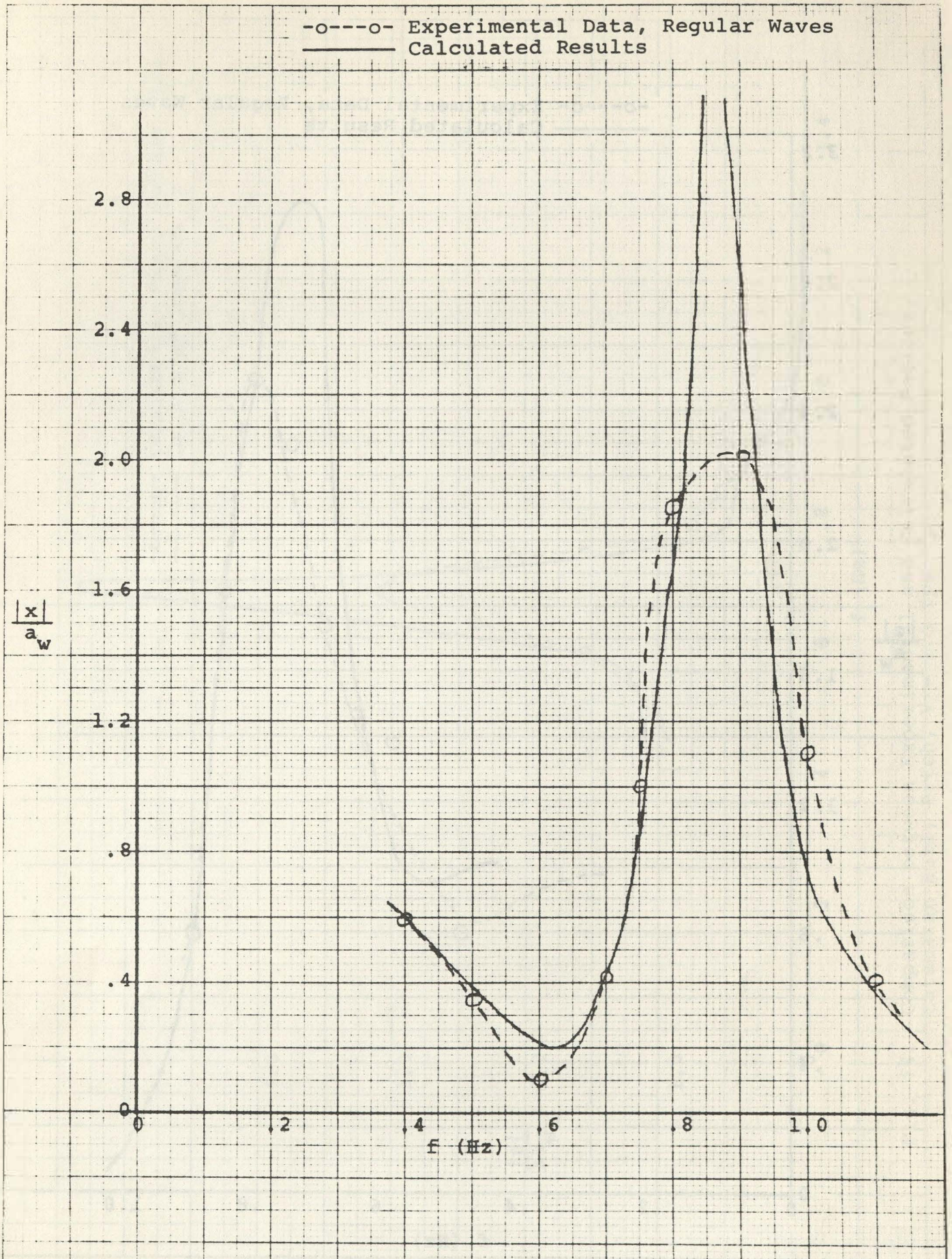

Fig. 72. Comparison between Experimental and Calculated Motions, Catamaran Hull, Surge, V = 0

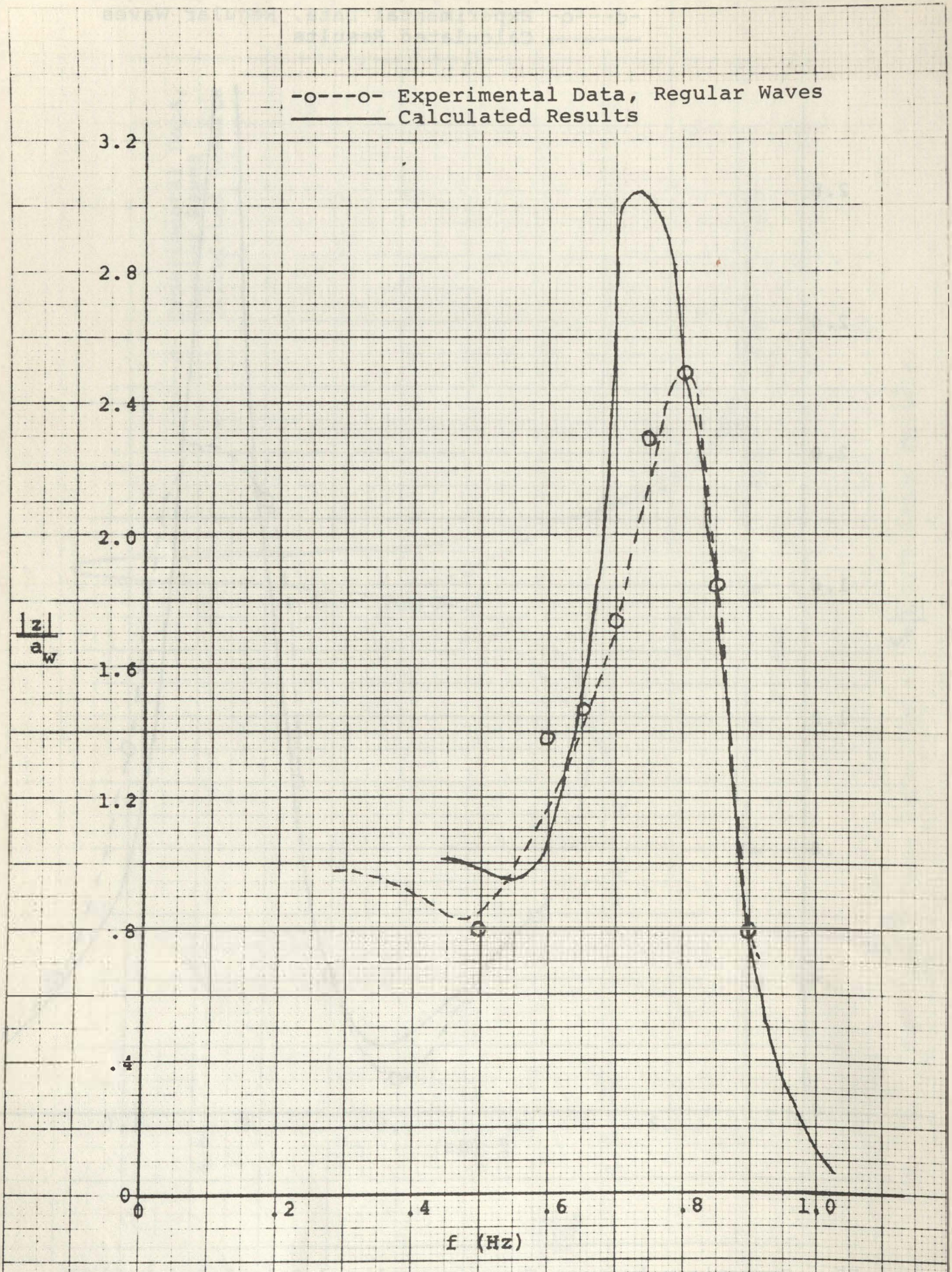

Fig. 73. Comparison between Experimental and Calculated Motions, Catamaran Hull, Heave, V = 1.5 fps

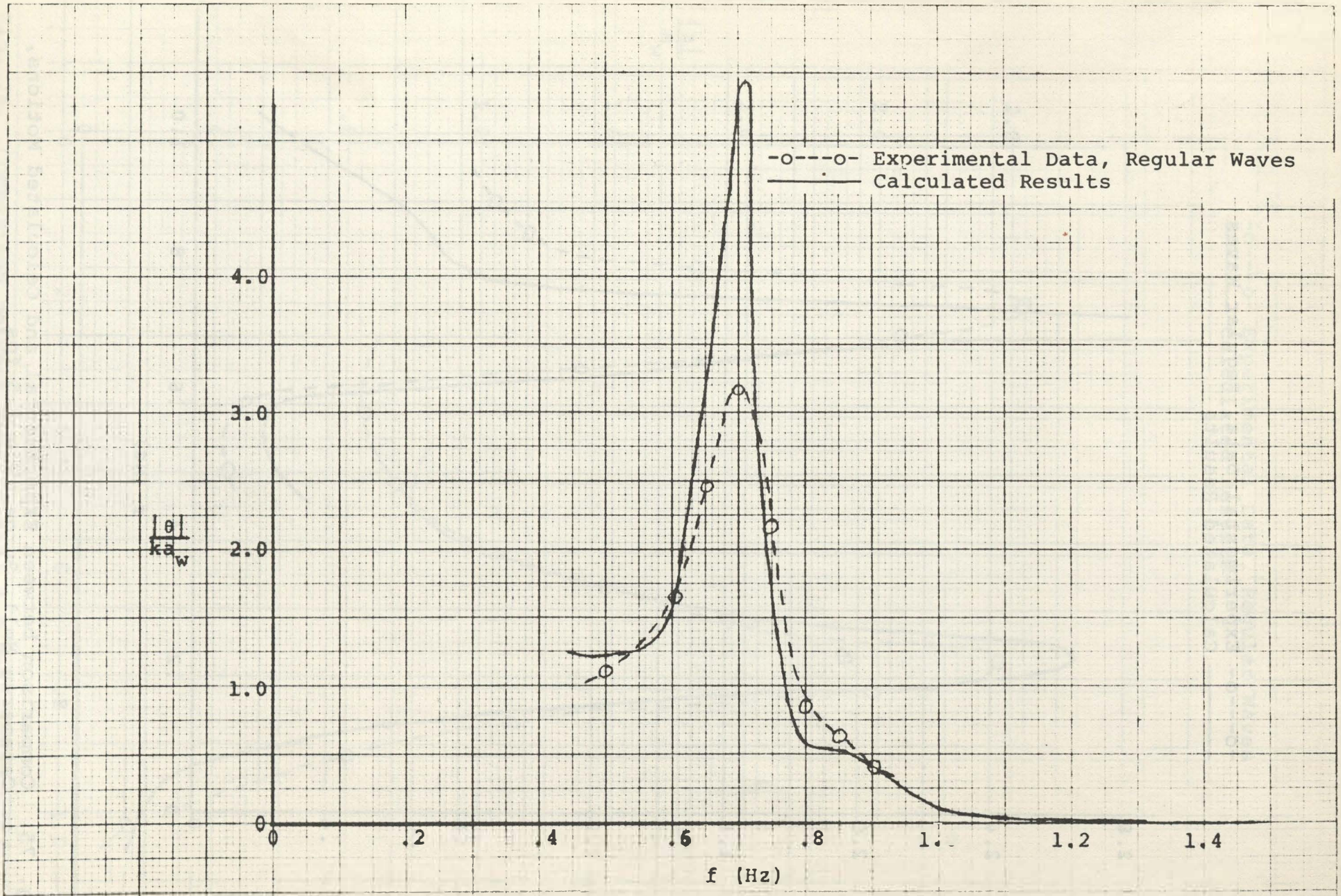

Fig. 74. Comparison between Experimental and Calculated Motions, Catamaran Hull, Pitch, V = 1.5 fps

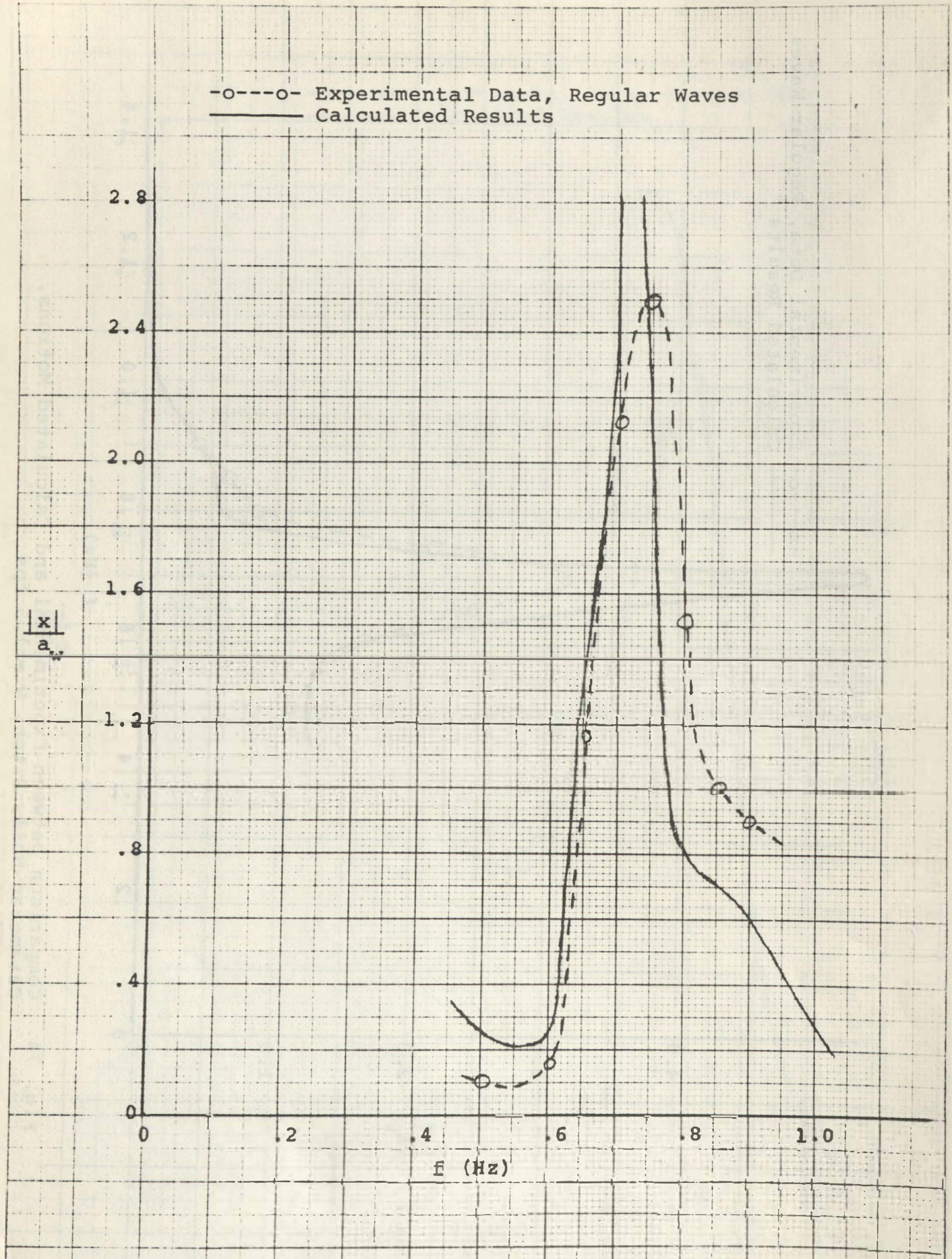

Fig. 75. Comparison between Experimental and Calculated Motions, Catamaran Hull, Surge, V = 1.5 fps

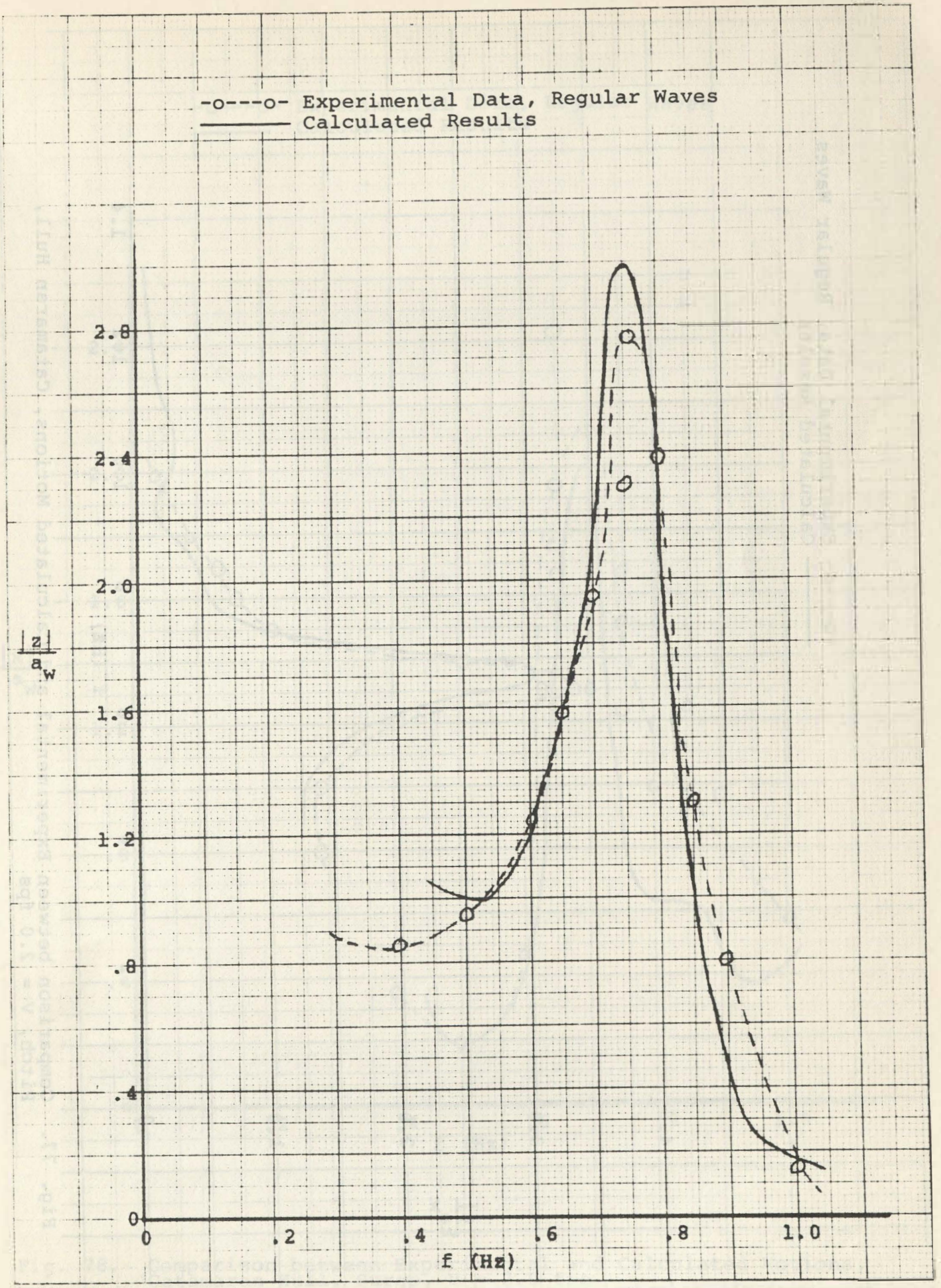

Fig. 76. Comparison between Experimental and Calculated Motions, Catamaran Hull, Heave, V = 2.0 fps

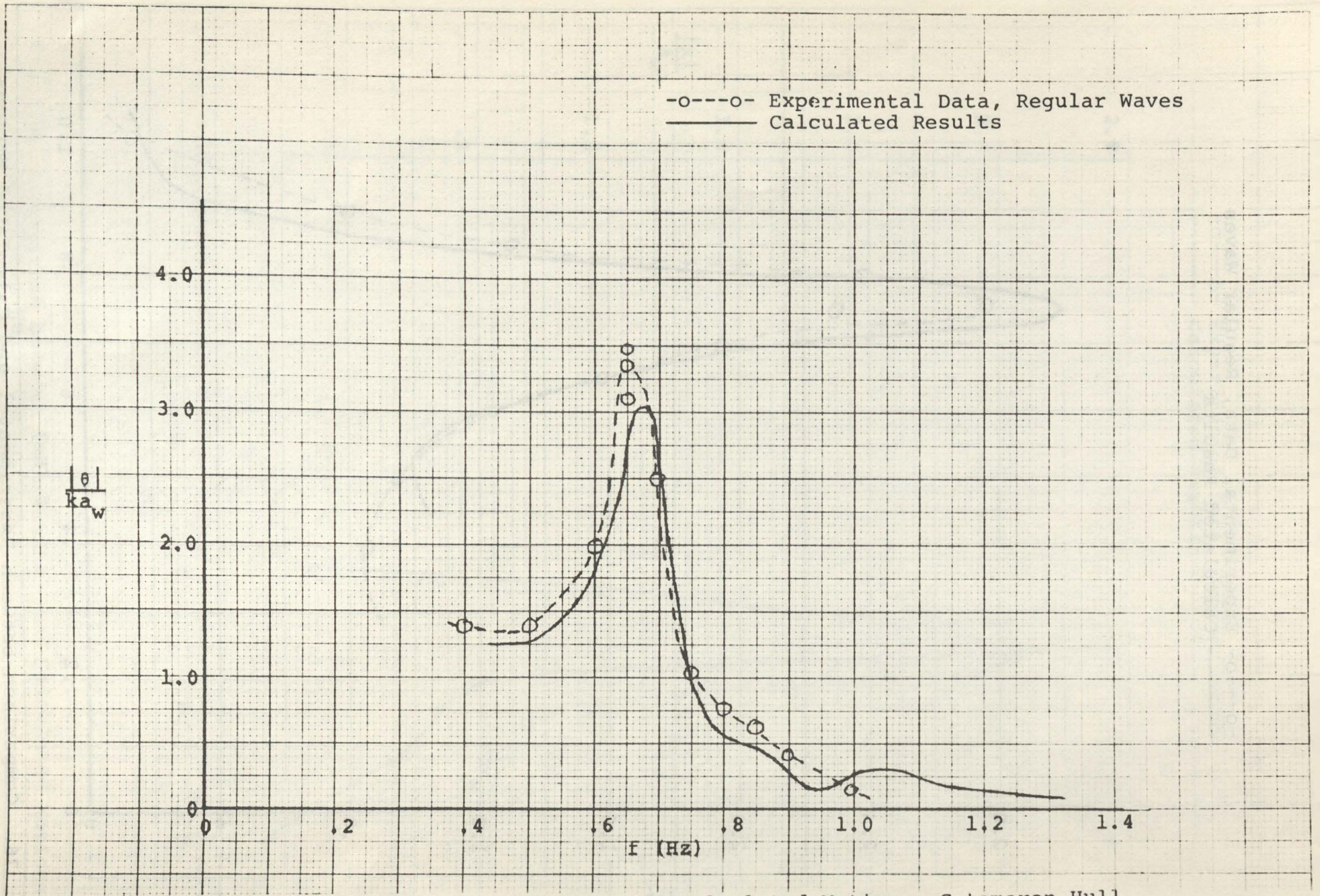

Fig. 77. Comparison between Experimental and Calculated Motions, Catamaran Hull, Pitch, V = 2.0 fps

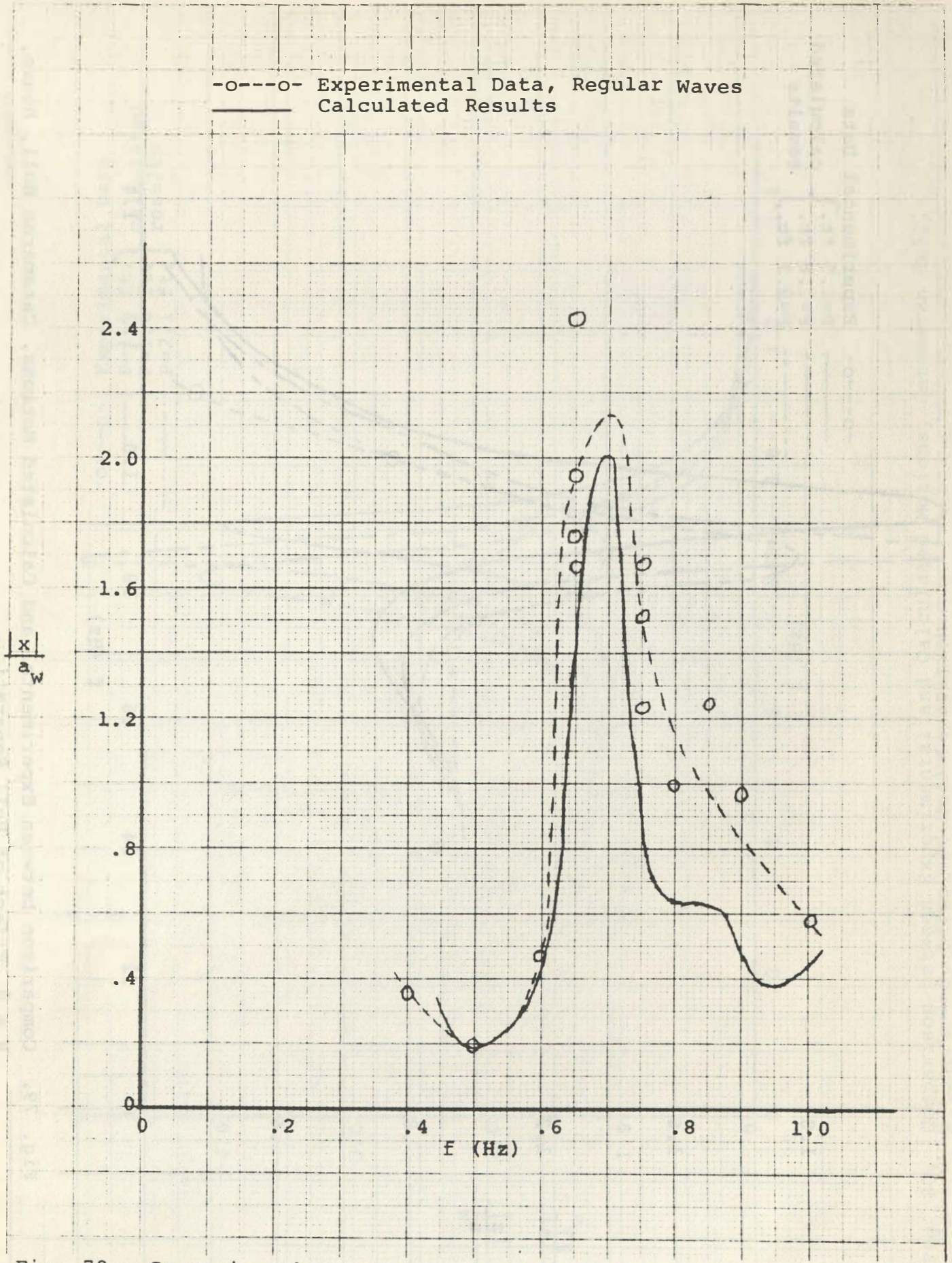

Fig. 78. Comparison between Experimental and Calculated Motions, Catamaran Hull, Surge, V = 2.0 fps

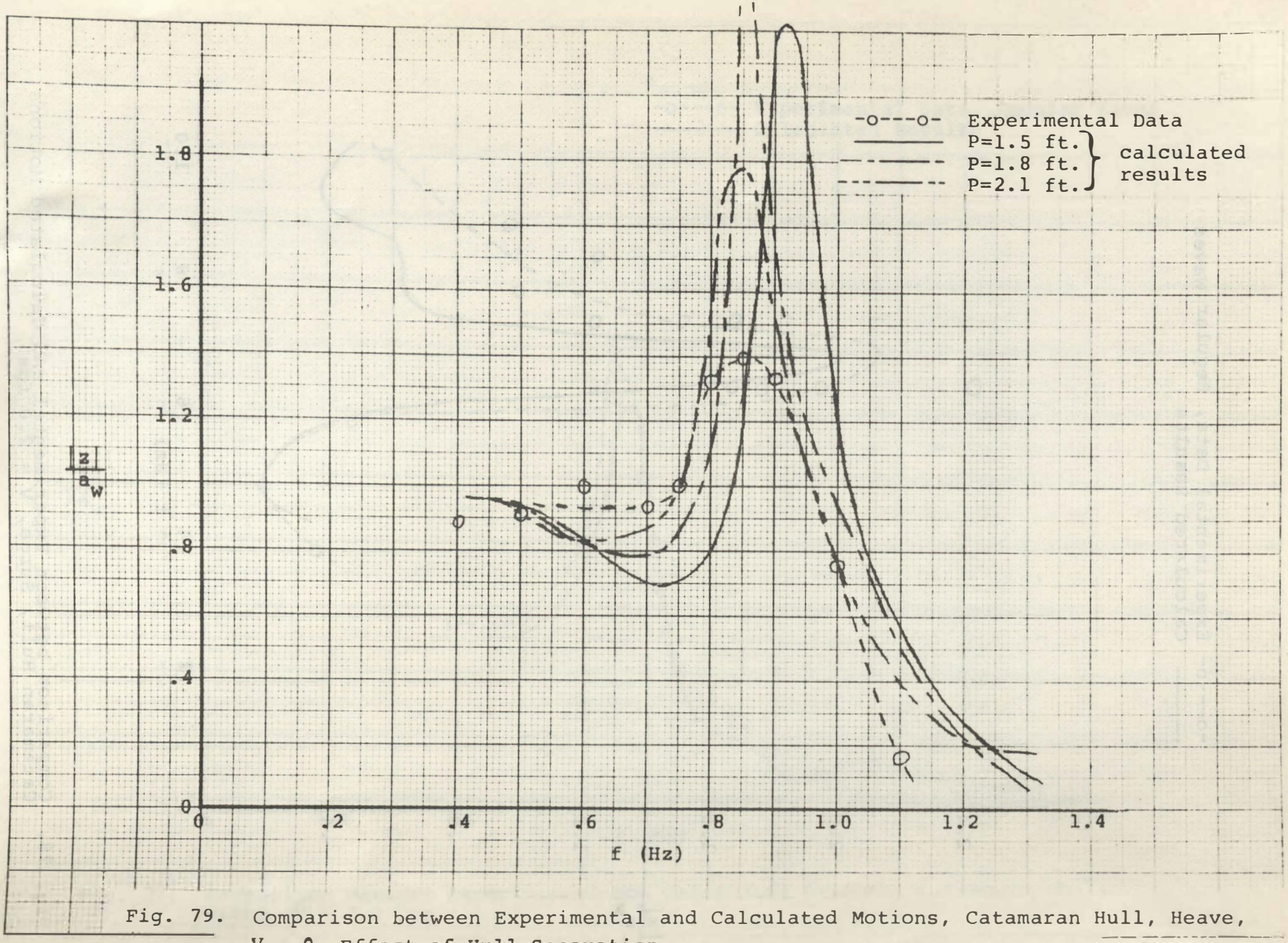

Fig. 79. Comparison between Experimental and Calculated Motions, Catamaran Hull, Heave, V = 0, Effect of Hull Separation

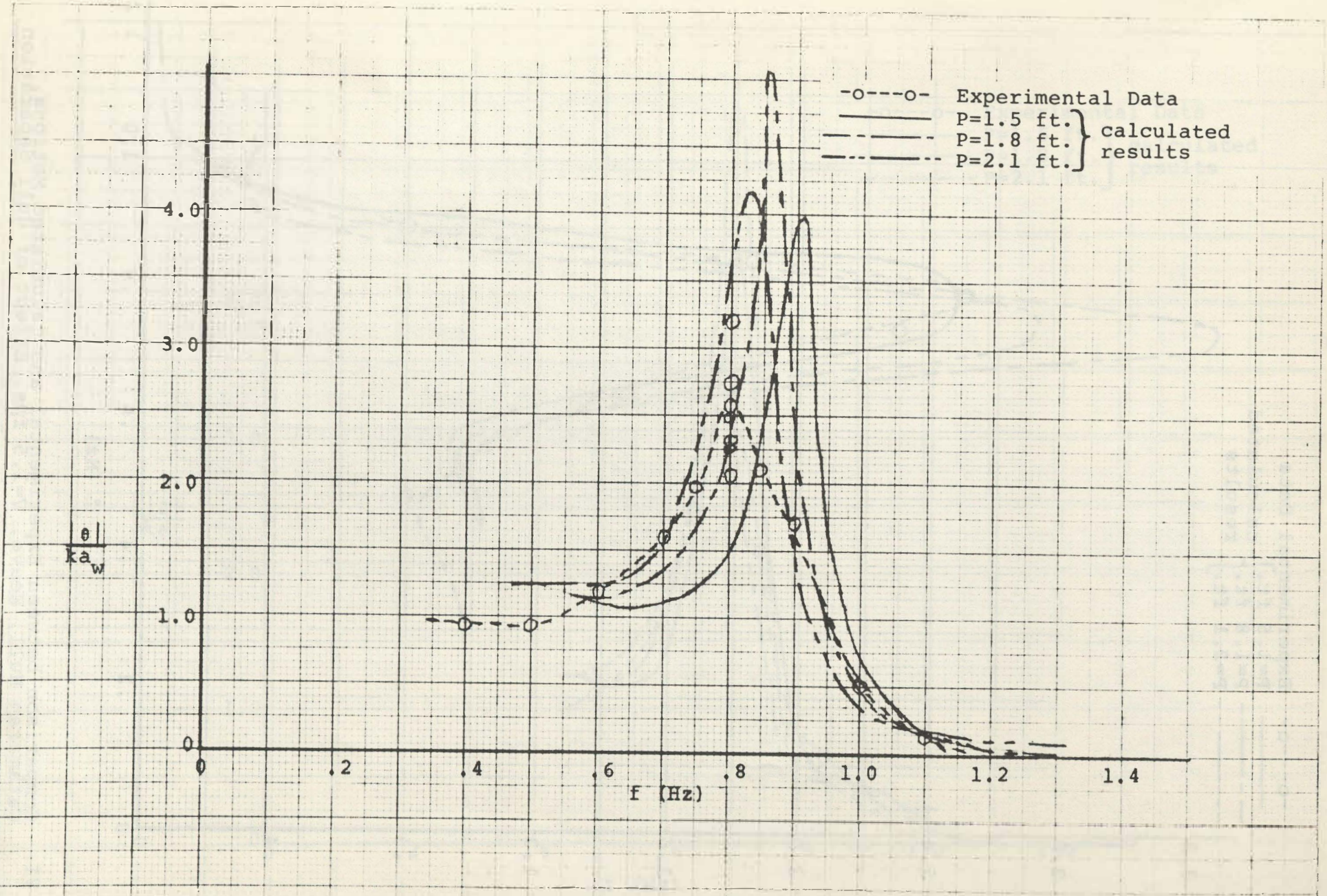

Fig. 80. Comparison between Experimental and Calculated Motions, Catamaran Hull, Pitch, V = 0, Effect of Hull Separation

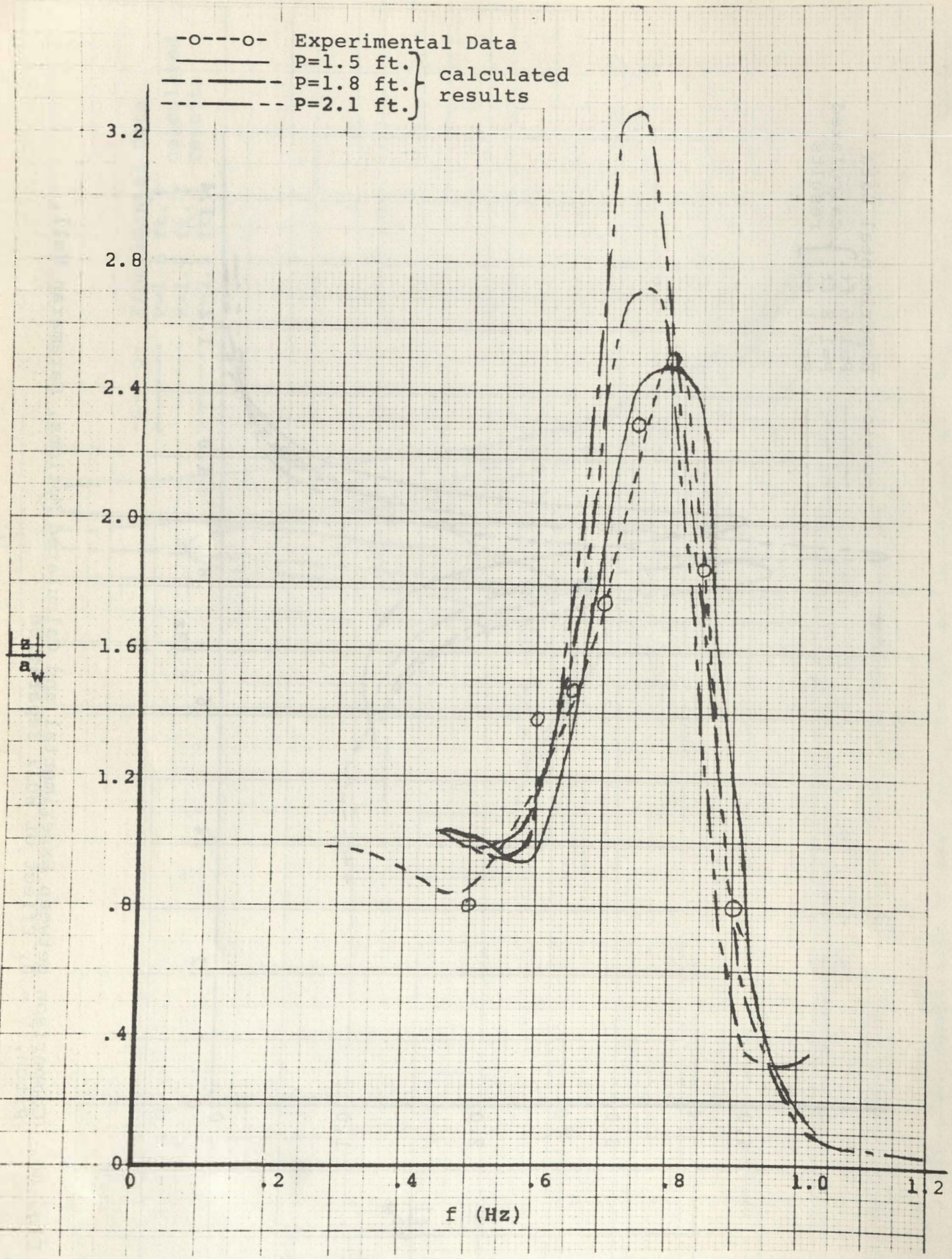

Fig. 81. Comparison between Experimental and Calculated Motions, Catamaran Hull, Heave, V=1.5 fps, Effect of Hull Separation

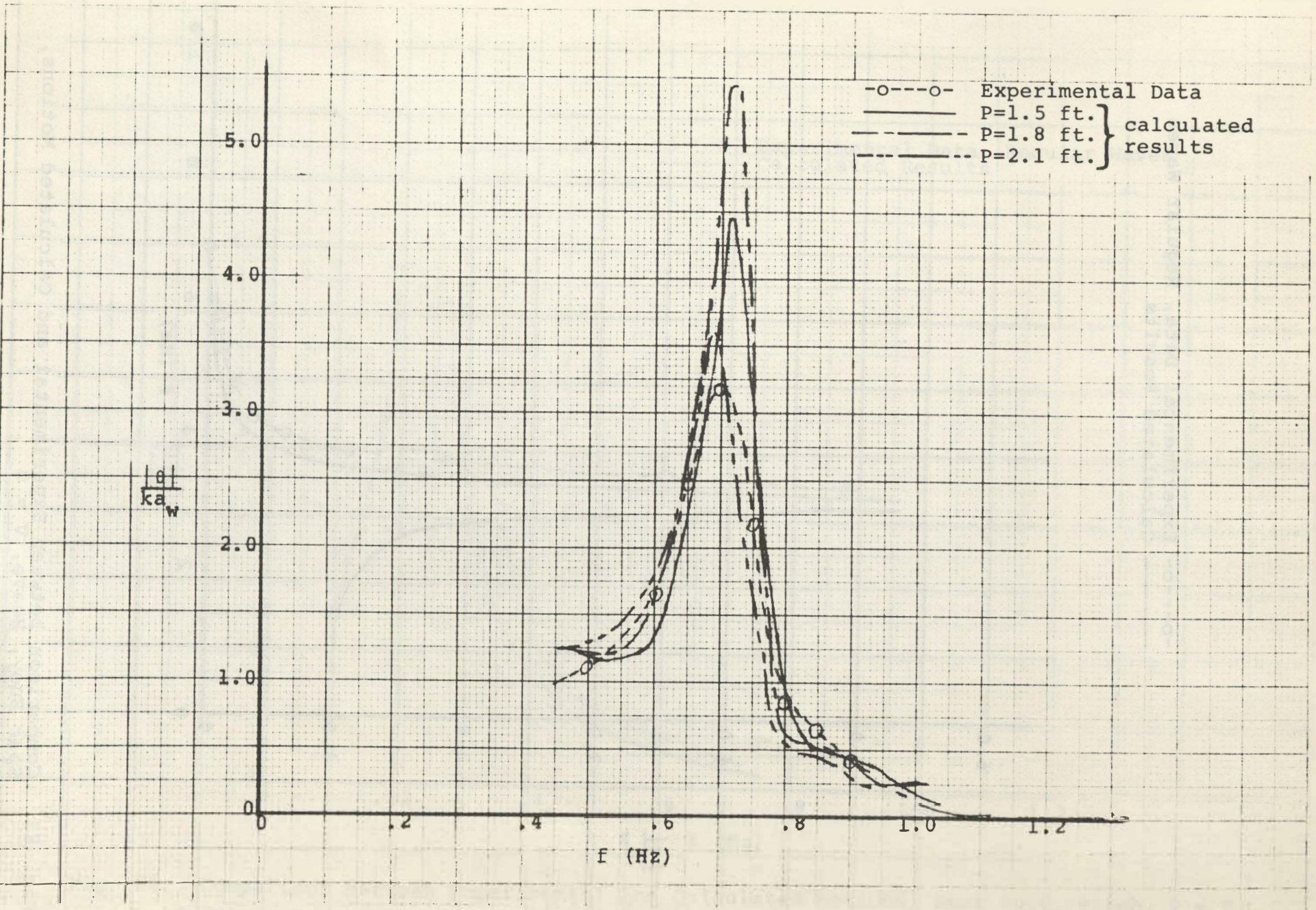

Fig. 82. Comparison between Experimental and Calculated Motions, Catamaran Hull, Pitch, V=1.5 fps, Effect of Hull Separation

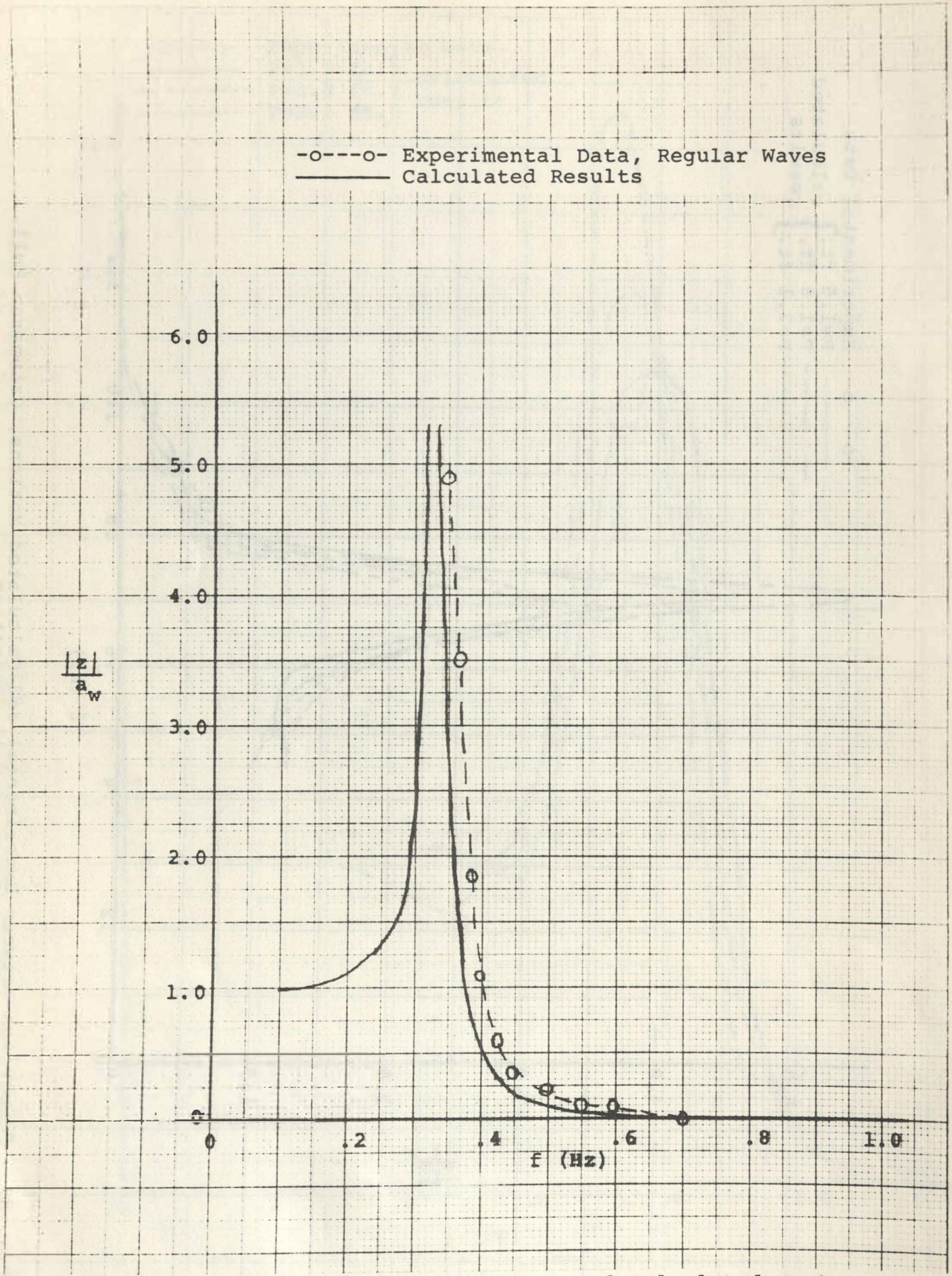

Fig. 83. Comparison between Experimental and Calculated Motions, Spar Buoy, Heave, V = 0

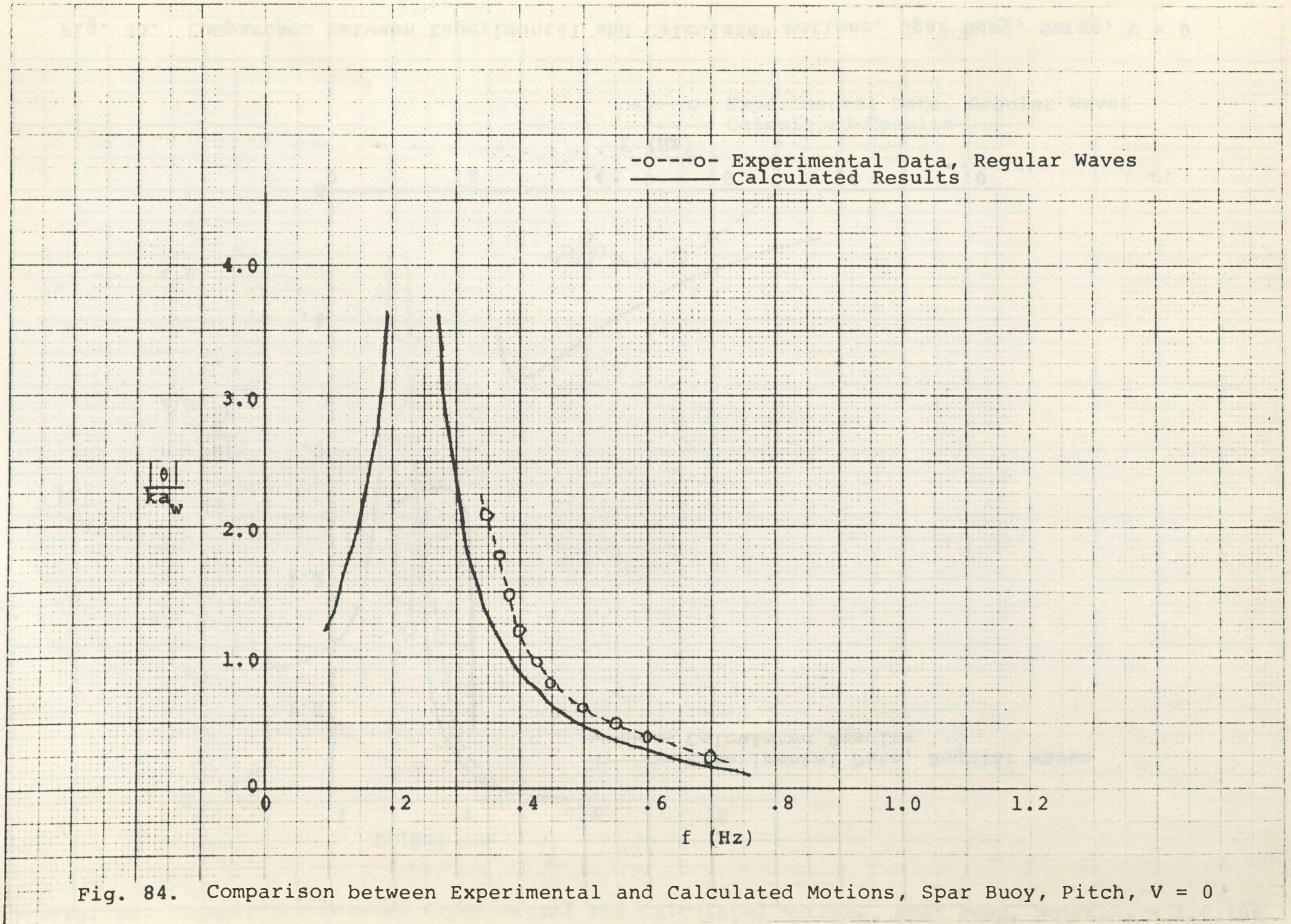

Fig. 84. Comparison between Experimental and Calculated Motions, Spar Buoy, Pitch, V = 0

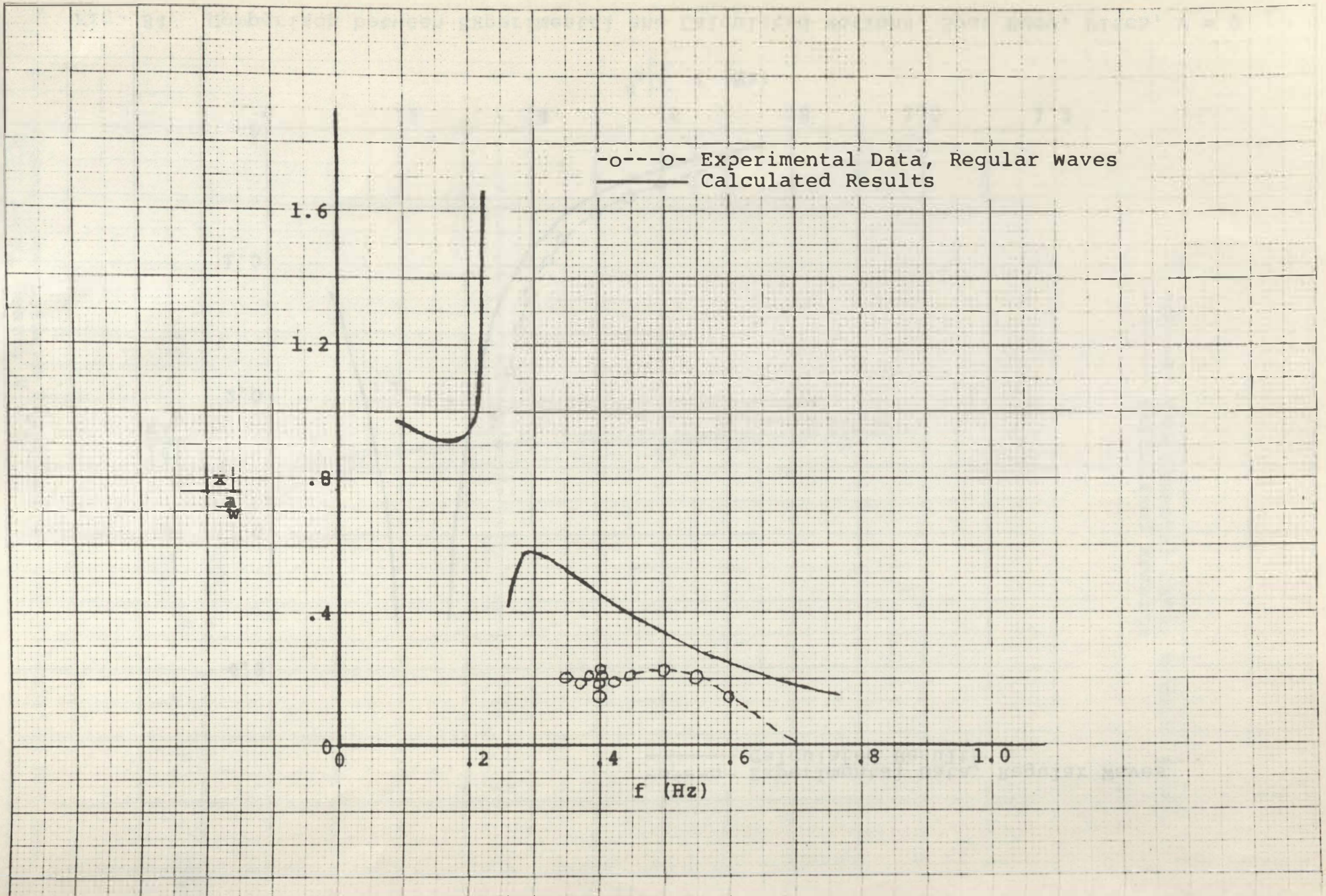

Fig. 85. Comparison between Experimental and Calculated Motions, Spar Buoy, Surge, V = 0

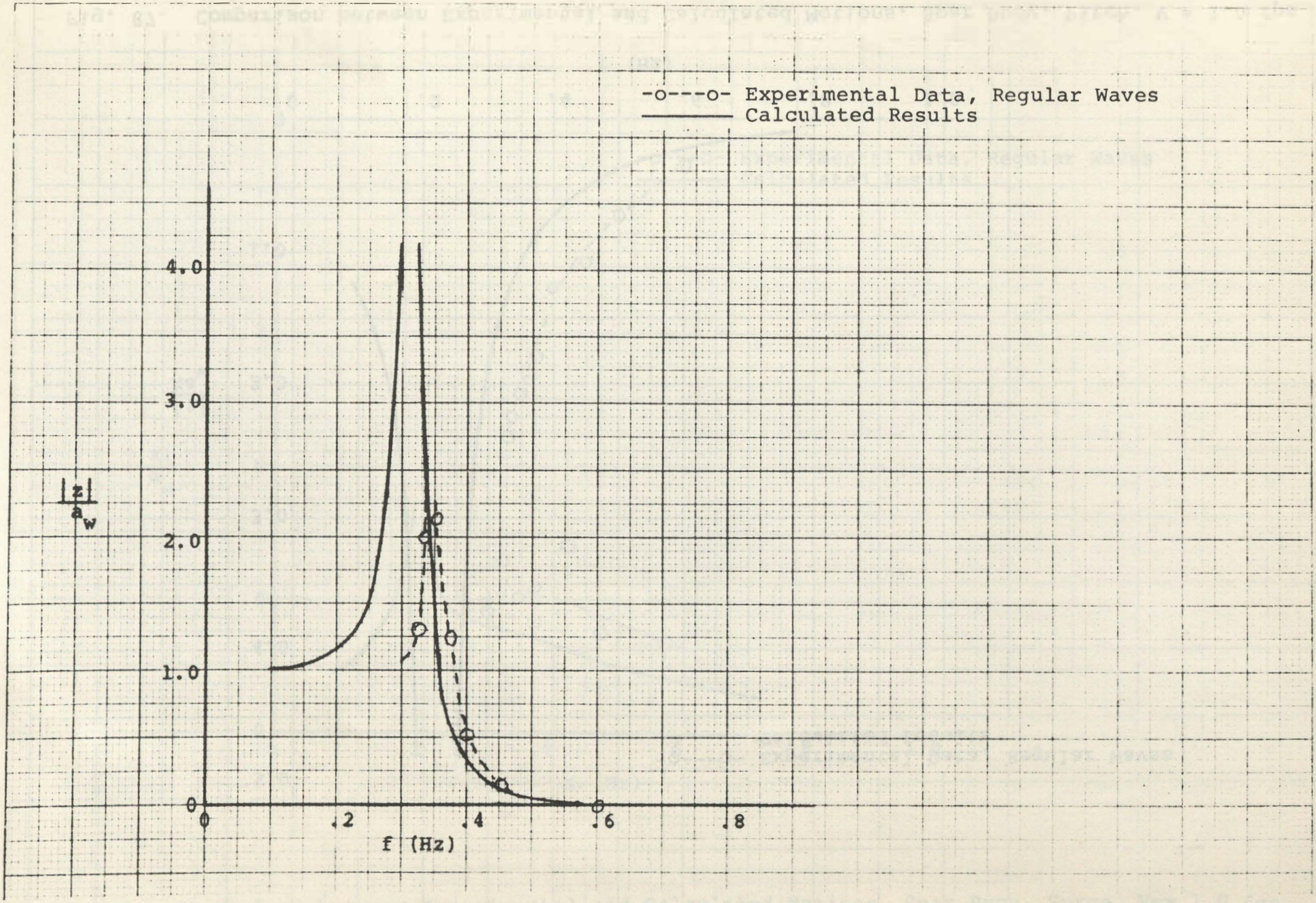

Fig. 86. Comparison between Experimental and Calculated Motions, Spar Buoy, Heave, V = 1.0 fps

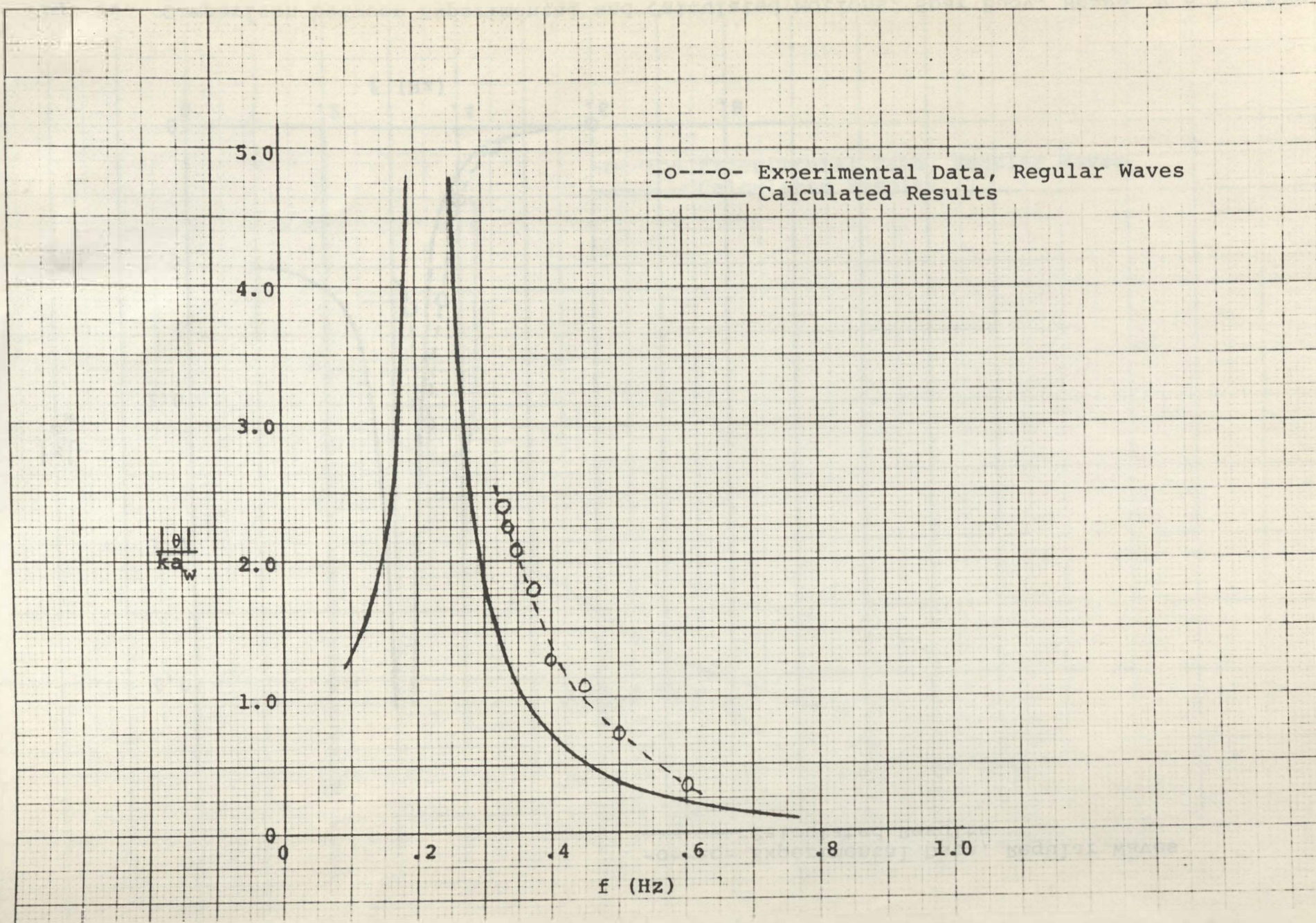

Fig. 87. Comparison between Experimental and Calculated Motions, Spar Buoy, Pitch, V = 1.0 fps

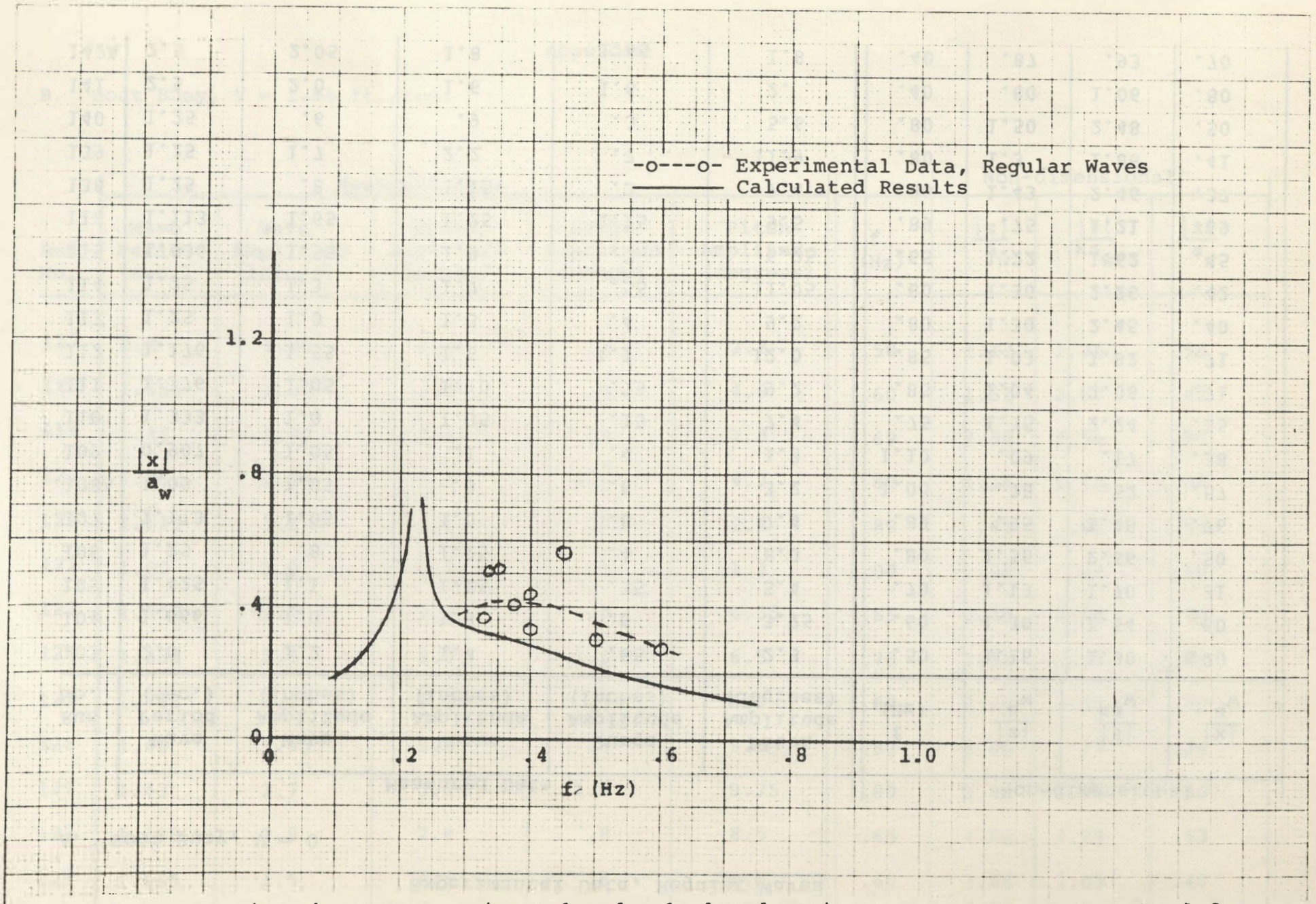

Fig. 88. Comparison between Experimental and Calculated Motions, Spar Buoy, Surge, V= 1.0 fps

Appendix

Experimental Data, Regular Waves

A. Boat Buoy, V = 0

Run No.	Measured Data: Wave Period (sec.)	Wave Amplitude (inches)	Heave Amplitude (inches)	Surge Amplitude (inches)	Pitch Amplitude (degrees)	f (Hz)	Non-dimensional: $\frac{\lvert z \rvert}{a_w}$	$\frac{\lvert \theta \rvert}{ka_w}$	$\frac{\lvert x \rvert}{a_w}$
103	2.0	1.2	1.4	.85	2.3	.50	1.16	1.30	.70
104	1.666	1.0	1.3	.6	3.25	.60	1.30	1.54	.60
105	1.425	1.1	1.25	.35	5.4	.70	1.13	1.70	.31
106	1.25	.8	1.25	.4	8.0	.80	1.56	2.66	.50
107	1.113	1.05	1.0	.8	7.4	.89	.95	1.48	.76
108A	1.00	1.05	.3	.6	3.2	1.00	.28	.52	.57
109	0.907	1.05	.1	.4	1.3	1.10	.09	.17	.38
110	1.333	1.0	1.35	.15	7.4	.75	1.35	2.24	.15
111	1.176	1.05	1.10	.75	9.2	.85	1.04	2.06	.71
112	1.176	1.55	1.6	1.1	12.0	.85	1.03	1.82	.71
113	1.25	1.0	1.3	.4	9.2	.80	1.30	2.45	.40
114	1.25	1.3	1.7	.55	11.05	.80	1.30	2.26	.42
115	1.536	1.55	1.9	.7	6.25	.65	1.22	1.62	.45
116	1.113	1.65	1.25	1.15	9.5	.89	.75	1.21	.69
138	1.25	.8	1.15	.3	7.4	.80	1.43	2.46	.37
139	1.25	1.7	2.2	.7	11.9	.80	1.3	1.86	.41
140	1.25	.6	.9	.3	5.6	.80	1.50	2.48	.50
141	2.5	2.0	1.6	1.6	2.	.40	.80	1.06	.80
142A	2.5	2.05	1.8	1.45	1.8	.40	.87	.93	.70

Appendix

B. Boat Buoy, V = 1.96 ft./sec.

Run No.	Measured Data: Wave Period (sec.)	Wave Amplitude (inches)	Heave Amplitude (inches)	Surge Amplitude (inches)	Pitch Amplitude (degrees)	f (Hz)	Non-dimensional: $\frac{\lvert z \rvert}{a_w}$	$\frac{\lvert \theta \rvert}{k a_w}$	$\frac{\lvert x \rvert}{a_w}$
117	2.0	1.25	1.4	.7	2.3	.50	1.12	1.25	.56
118	1.665	1.05	1.7	.5	4.6	.60	1.61	2.07	.47
119	1.43	1.00	2.3	.9	7.3	.69	2.30	2.54	.90
120	1.25	1.05	1.2	1.1	4.7	.80	1.14	1.19	1.04
121	1.112	1.1	0.5	.7	2.4	.89	.45	.46	.63
122	1.00	1.0	0.2	.5	1.3	1.00	.20	.22	.50
123	1.537	1.0	2.1	.7	6.35	.65	2.10	2.56	.70
124	1.333	1.1	2.0	1.1	6.5	.75	1.81	1.79	1.00
125	1.482	1.0	2.2	.3	6.9	.67	2.20	2.58	.30
126	1.48	1.65	3.3	.6	9.6	.67	2.00	2.17	.36
127	1.43	1.7	3.2	1.5	9.75	.69	1.88	1.99	.88
128	1.538	1.5	2.8	.8	8.5	.65	1.86	2.29	.53
129	1.665	1.5	2.5	.6	6.5	.60	1.66	2.05	.40
130	1.333	1.75	2.8	1.7	8.7	.75	1.60	1.50	.97

C. Disc Buoy, V = 0

Run No.	Measured Data: Wave Period (sec.)	Wave Amplitude (inches)	Heave Amplitude (inches)	Surge Amplitude (inches)	Pitch Amplitude (degrees)	f (Hz)	Non-dimensional: $\frac{\lvert z \rvert}{a_w}$	$\frac{\lvert \theta \rvert}{ka_w}$	$\frac{\lvert x \rvert}{a_w}$
203B	2.0	1.1	1.0	.8	1.45	.50	.90	.90	.72
204	1.666	1.05	1.0	.7	2.10	.60	.95	.94	.66
205	1.428	1.05	0.95	.6	2.8	.70	.90	.93	.57
206	1.25	.95	.85	.7	3.5	.80	.89	.98	.73
207	1.111	1.0	.65	.3	4.1	.90	.65	.86	.30
208	1.00	1.05	.5	.1	4.5	1.00	.47	.73	.09
209	.909	.95	.3	.05	3.3	1.10	.31	.49	.05
210A	.834	.85	.2	.1	2.3	1.19	.23	.32	.11
211	1.538	1.0	1.05	.7	2.6	.65	1.05	1.05	.70
212	1.333	1.05	.95	.6	3.4	.75	.90	.98	.57
213	1.428	1.05	.95	.5	2.7	.70	.90	.89	.47
214	1.428	2.13	1.8	1.3	5.55	.70	.84	.91	.61
215	1.538	2.10	2.05	1.25	5.0	.65	.97	.96	.59
216	1.818	1.075	.9	.7	1.6	.55	.83	.83	.65
217	1.818	2.15	1.8	1.4	3.25	.55	.83	.85	.65
218A	2.5	2.05	1.7	1.35	1.5	.40	.82	.78	.65
219	3.0	2.05	1.9	1.4	.9	.33	.92	.67	.68
220	1.428	.6	.5	.3	1.6	.70	.83	.92	.50
232	1.428	1.0	1.0	.6	2.85	.70	1.00	.99	.60
233	2.0	.85	.7	.6	1.0	.50	.82	.80	.70

Appendix

D. Disc Buoy, V = 1.5 ft./sec.

Run No.	Measured Data: Wave Period (sec.)	Wave Amplitude (inches)	Heave Amplitude (inches)	Surge Amplitude (inches)	Pitch Amplitude (degrees)	f (Hz)	Non-dimensional: $\frac{\lvert z \rvert}{a_w}$	$\frac{\lvert \theta \rvert}{ka_w}$	$\frac{\lvert x \rvert}{a_w}$
234	2.0	.9	.85	.5	1.25	.50	.94	.94	.55
235	1.667	.95	1.0	.5	2.3	.60	1.05	1.15	.52
236	1.428	1.05	1.1	.3	3.75	.70	1.04	1.24	.28
237A	1.25	1.00	1.15	.3	5.7	.80	1.15	1.52	.30
238	1.333	1.05	1.25	.5	4.75	.75	1.19	1.37	.47
239	1.176	.975	1.2	.1	5.95	.85	1.23	1.44	.10

E. Disc Buoy, V = 2.3 ft./sec.

Run No.	Measured Data						Non-dimensional		
	Wave Period (sec.)	Wave Amplitude (inches)	Heave Amplitude (inches)	Surge Amplitude (inches)	Pitch Amplitude (degrees)	f (Hz)	$\frac{\lvert z \rvert}{a_w}$	$\frac{\lvert \theta \rvert}{ka_w}$	$\frac{\lvert x \rvert}{a_w}$
221	2.00	1.05	.95	.8	1.5	.50	.90	.97	.76
222	1.667	1.05	1.1	.3	2.65	.60	1.04	1.19	.28
223	1.428	1.0	1.1	.3	3.95	.70	1.10	1.37	.30
224	1.25	1.0	1.35	.25	5.7	.80	1.35	1.52	.25
225	1.111	.95	.8	.4	4.4	.90	.84	.97	.42
226	1.0	1.125	.4	.4	2.55	1.00	.35	.38	.35
227	1.176	1.35	1.5	.45	6.35	.85	1.11	1.11	.33
228	1.333	1.2	1.40	.35	5.5	.75	1.16	1.39	.29
229	1.25	.9	1.15	.2	5.1	.80	1.27	1.51	.22
230	1.25	2.25	2.85	.45	10.9	.80	1.26	1.29	.20
231	1.25	.5	.7	.2	2.65	.80	1.40	1.41	.40
240	1.176	.95	1.2	.2	5.7	.85	1.26	1.41	.21

Appendix

F. Catamaran Buoy, V = 0

Run No.	Measured Data: Wave Period (sec.)	Wave Amplitude (inches)	Heave Amplitude (inches)	Surge Amplitude (inches)	Pitch Amplitude (degrees)	f (Hz)	Non-dimensional: $\frac{\lvert z \rvert}{a_w}$	$\frac{\lvert \theta \rvert}{ka_w}$	$\frac{\lvert x \rvert}{a_w}$
303	2.0	.875	.8	.3	1.2	.50	.91	.93	.34
304	1.667	1.0	1.0	.1	2.5	.60	1.00	1.18	.10
305	1.428	1.075	1.0	.45	4.9	.70	.93	1.58	.41
306	1.25	.9	1.25	1.6	8.7	.80	1.38	2.57	1.77
307	1.111	1.05	1.4	2.25	8.6	.90	1.33	1.72	2.14
308A	1.0	1.0	.75	1.1	3.0	1.00	.75	.51	1.10
309	.91	1.25	.2	.5	1.2	1.09	.16	.13	.40
310	1.176	1.075	1.5	2.2	9.6	.85	1.39	2.11	2.04
311	1.333	1.1	1.1	1.1	7.15	.75	1.00	1.97	1.00
312	2.5	1.35	1.2	.8	1.2	.40	.88	.94	.59
313	1.25	1.15	1.4	1.8	9.9	.80	1.21	2.29	1.56
314	1.25	1.3	1.8	2.3	11.6	.80	1.38	2.37	1.76
315A	1.25	.5	.65	.95	4.7	.80	1.30	2.50	1.90
316	1.25	1.8	2.35	2.75	13.9	.80	1.30	2.05	1.52
317	1.25	.95	1.3	1.7	8.9	.80	1.36	2.49	1.78
318	1.25	.2	.35	.5	2.4	.80	1.75	3.20	2.5
319	1.25	.5	.65	.95	4.85	.80	1.30	2.58	1.9

Appendix

G. Catamaran Buoy, V = 1.5 ft./sec.

	Measured Data						Non-dimensional		
Run No.	Wave Period (sec.)	Wave Amplitude (inches)	Heave Amplitude (inches)	Surge Amplitude (inches)	Pitch Amplitude (degrees)	f (Hz)	$\frac{\lvert z \rvert}{a_w}$	$\frac{\lvert \theta \rvert}{ka_w}$	$\frac{\lvert x \rvert}{a_w}$
335	2.00	1.0	.8	.1	1.65	.5	.80	1.12	.10
336	1.667	.975	1.35	.15	3.4	.6	1.38	1.65	.15
337	1.536	.95	1.4	1.1	5.8	.65	1.47	2.47	1.15
338	1.427	1.125	1.75	2.5	10.05	.7	1.56	3.11	2.22
339	1.333	1.0	2.3	2.5	7.15	.75	2.30	2.17	2.5
340	1.428	1.1	2.1	2.25	10.3	.70	1.91	3.26	2.04
341	1.250	.9	2.3	1.3	2.55	.80	2.56	.75	1.44
342	1.111	1.0	.8	.9	2.05	.90	.80	.43	.90
343	1.25	.95	2.3	1.5	3.25	.8	2.42	.91	1.57
344	1.176	1.0	1.85	1.0	2.7	.85	1.85	.63	1.0

Appendix

H. Catamaran Buoy, V = 2.0 ft./sec.

Run No.	Measured Data: Wave Period (sec.)	Wave Amplitude (inches)	Heave Amplitude (inches)	Surge Amplitude (inches)	Pitch Amplitude (degrees)	f (Hz)	Non-dimensional: $\frac{\lvert z \rvert}{a_w}$	$\frac{\lvert \theta \rvert}{k a_w}$	$\frac{\lvert x \rvert}{a_w}$
320	2.000	1.0	.95	.2	2.05	.50	.95	1.39	.20
321	1.667	1.05	1.3	.5	4.4	.60	1.23	1.98	.47
322	1.428	1.075	2.1	2.3	7.7	.70	1.95	2.50	2.14
323	1.25	1.05	2.5	1.05	3.15	.80	2.38	.79	1.0
324A	1.111	1.125	.90	1.1	2.3	.90	.80	.43	.97
325	1.0	1.025	.15	.6	.9	1.00	.14	.15	.58
326	1.176	1.0	1.3	1.25	2.7	.85	1.30	.63	1.25
327	1.333	1.05	2.9	1.6	3.35	.75	2.76	.96	1.52
328	1.538	.95	1.5	1.6	8.2	.65	1.57	3.48	1.68
329	1.538	1.425	2.3	2.5	11.0	.65	1.61	3.11	1.75
331	1.538	.45	.7	1.1	3.9	.65	1.55	3.50	2.44
332A	1.333	1.65	3.8	2.05	5.0	.75	2.30	.91	1.24
333	1.333	.475	1.5	.8	2.0	.75	3.15	1.27	1.68
334	2.5	1.375	1.15	.5	1.7	.40	.83	1.31	.36

Appendix

I. Spar Buoy, V = 0

Run No.	Measured Data: Wave Period (sec.)	Wave Amplitude (inches)	Heave Amplitude (inches)	Surge Amplitude (inches)	Pitch Amplitude (degrees)	f (Hz)	Non-dimensional: $\frac{\lvert z \rvert}{a_w}$	$\frac{\lvert \theta \rvert}{ka_w}$	$\frac{\lvert x \rvert}{a_w}$
403	1.667	1.4	.1	.2	1.2	.60	.07	.40	.14
404	1.818	1.5	.15	.3	1.3	.55	.10	.48	.20
405	2.0	1.4	.3	.3	1.25	.50	.21	.61	.21
406	2.222	1.45	.5	.3	1.4	.45	.34	.81	.20
407	2.5	1.475	1.6	.35	1.8	.40	1.08	1.32	.23
408A	2.70	1.4	4.8	.3	2.0	.37	3.42	1.78	.21
409	2.597	1.4	2.6	.3	1.8	.38	1.85	1.48	.21
410	2.353	1.575	.9	.3	1.6	.42	.57	.96	.19
411	2.702	.85	3.1	.15	1.25	.37	3.64	1.83	.17
412A	2.702	1.925	6.1	.3	2.65	.37	3.16	1.71	.15
413	2.857	.5	2.45	.1	.75	.35	4.90	2.08	.2
414	2.5	1.025	1.1	.15	1.1	.40	1.07	1.14	.14
415	2.5	2.1	2.1	.4	2.15	.40	1.00	1.09	.19
416	1.428	1.65	0	.1	1.2	.70	0	.25	0

Appendix

J. Spar Buoy, V = 1.0 ft./sec.

Run No.	Measured Data						Non-dimensional		
	Wave Period (sec.)	Wave Amplitude (inches)	Heave Amplitude (inches)	Surge Amplitude (inches)	Pitch Amplitude (degrees)	f (Hz)	$\frac{\lvert z \rvert}{a_w}$	$\frac{\lvert \theta \rvert}{ka_w}$	$\frac{\lvert x \rvert}{a_w}$
423	1.667	1.45	0	.4	1.1	.60	0	.36	.27
424	2.000	1.5	0	.45	1.6	.50	0	.72	.30
425	2.5	1.55	.8	.35	1.8	.40	.51	1.23	.22
426	2.222	1.575	.25	.9	2.0	.45	.15	1.08	.57
427	2.857	1.35	2.9	.7	2.0	.35	2.14	2.06	.51
428	2.667	1.35	1.7	.55	2.0	.37	1.25	1.79	.40
430	3.077	1.35	1.8	.5	2.0	.32	1.33	2.39	.37
432	2.985	1.35	2.7	.7	2	.33	2.00	2.25	.51
433	2.50	2.075	1.25	.95	2.6	.40	.60	1.33	.45